

# Long chain soaps and alkyl sulfates in aqueous solutions at room temperature



## Dissertation

zur Erlangung des Doktorgrades der Naturwissenschaften (Dr. rer. nat.)  
der Fakultät Chemie und Pharmazie  
der Universität Regensburg

vorgelegt von  
**Stefan Wolfrum**  
aus Bayreuth  
2017



Official Registration:	30.08.2017
Defense:	25.10.2017
Ph. D. Supervisor:	Prof. Dr. Werner Kunz
Adjudicators:	Prof. Dr. Werner Kunz Prof. Dr. Hubert Motschmann Prof. Dr. Arno Pfitzner
Chair:	Prof. Dr. Henri Brunner



# Preface

This thesis is based on the research carried out between October 2013 and August 2017 at the Institute of Physical and Theoretical Chemistry (Faculty of Natural Sciences IV) at the University of Regensburg.

This work would not have been possible without the help and support of many people to whom I would like to express my honest gratitude.

First of all, I would like to express my sincere thank to Prof. Dr. Werner Kunz for giving me the opportunity to work independently at his institute, for the very interesting topic, for the financial support and at last for the numerous and informative scientific discussions.

I am very grateful to Dr Didier Touraud for his innovative ideas, for his continuous interest in the progress of this work, for the countless scientific discussions as well as for always having some helpful advice.

In addition, I want to thank Prof. Dr. Reinhard Rachel (Center of electron microscopy, University of Regensburg) for performing electron microscopy studies on several samples and his expertise during evaluation of the pictures. I am likewise thankful to Dr. Harald Huber (Institute for biochemistry, genetics and microbiology, University of Regensburg) for providing his light microscope for several times.

Many gratitude to all my colleagues at the institute for the pleasant atmosphere and their helpfulness, the uncountable nice (barbecue) evenings as well as other free-time activities. In particular, I want to thank my two office mates Theresa and Lydia for the enjoyable way of working and laughing together.

Infinite thanks to my family, my parents, Bernd and Marina, and my brother Michael for encouraging me in any respect throughout my whole life and for enabling me to reach my aims.

Last but not least, heartfelt thanks to my wife Eva for her mental support, understanding and encouraging me all the time.

Stefan Wolfrum



# Table of contents

<b>Chapter 1</b>	<b>Introduction and motivation .....</b>	<b>1</b>
1.1	Literature .....	5
<b>Chapter 2</b>	<b>Fundamental information.....</b>	<b>9</b>
2.1	Surfactants.....	9
2.1.1	Structure and classification of surfactants.....	11
2.1.1.1	Classification by the polar head group .....	11
2.1.1.2	Classification by the origin of the raw materials.....	13
2.1.2	Toxicity and biodegradability of surfactants .....	16
2.1.2.1	Toxicity .....	16
2.1.2.1.1	Biological functions of surfactants.....	16
2.1.2.1.2	Local toxic effects .....	17
2.1.2.1.3	Systemic toxic effects .....	18
2.1.2.2	Biodegradability and ecotoxicity .....	19
2.1.2.2.1	European legislation and test methods.....	20
2.1.2.2.2	Biodegradability .....	21
2.1.2.2.3	Ecotoxicity .....	23
2.1.2.2.4	Ecological assessment and Environmental risk assessment....	24
2.1.3	Future requirements for surfactants in industry.....	25
2.1.4	Adsorption of surfactants to liquid surfaces/interfaces.....	27
2.1.4.1	Surface and interfacial tensions .....	27
2.1.4.2	Surfactant adsorption and reduction of the surface/interfacial tension .....	28
2.1.4.2.1	Efficiency and effectiveness of surfactant surface tension reduction .....	28
2.1.4.2.2	Adsorption theory - the Gibbs adsorption isotherm .....	30
2.1.5	Self-assembly of surfactants in aqueous solutions .....	32
2.1.5.1	Critical micellar concentration and general structure of micelles .	32
2.1.5.2	Thermodynamics and kinetics of micelle formation .....	36

2.1.5.3	Surfactant solubility and Krafft temperature .....	37
2.1.6	Application in laundry detergency .....	40
<b>2.2</b>	<b>Specific ion effects and Collins' concept .....</b>	<b>44</b>
<b>2.3</b>	<b>Choline - a vital amine.....</b>	<b>51</b>
2.3.1	Choline in food and recommended adequate intake .....	52
2.3.2	Biological functions of choline .....	52
2.3.3	Effects of choline on health and brain development.....	53
2.3.4	Choline derivatives used in this work.....	54
<b>2.4</b>	<b>Soaps in aqueous systems .....</b>	<b>56</b>
2.4.1	History of soaps.....	56
2.4.2	Water solubility and "Krafft temperature" of soaps .....	59
2.4.3	Salt sensitivity of soaps.....	64
2.4.4	pH sensitivity and acid-base titration curves of soaps.....	65
<b>2.5</b>	<b>Literature .....</b>	<b>72</b>
<b>Chapter 3</b>	<b>Highly translucent and stable solutions of NaOI and RebA at neutral pH and room temperature .....</b>	<b>83</b>
<b>3.1</b>	<b>Abstract .....</b>	<b>83</b>
<b>3.2</b>	<b>Introduction .....</b>	<b>83</b>
<b>3.3</b>	<b>Results and discussion .....</b>	<b>86</b>
3.3.1	Aqueous solubility and cmc of RebA .....	87
3.3.2	Phase behavior of aqueous NaOI solutions at different neutralization states .....	90
3.3.3	Influence of RebA on aqueous NaOI solutions at different neutralization states .....	93
3.3.4	Phase behavior of mixtures containing NaOI and RebA at different neutralization states .....	96
3.3.4.1	Macroscopic phase behavior .....	97
3.3.4.2	Microscopic phase behavior .....	103
3.3.4.3	Important parameters of stable systems and tentative phase diagram .....	107
3.3.4.4	Possible mode of action of RebA within the mixed systems.....	112

3.3.4.5	Time dependent phase behavior of the system 1 wt% NaOl/0.8 wt% RebA .....	114
3.3.5	Influence of RebA on aqueous sodium dodecanoate solutions at different neutralization states .....	116
3.3.6	Stable and highly translucent solutions of $\omega$ -3-fatty acids .....	120
<b>3.4</b>	<b>Conclusion and "green" strategies to overcome problems with soaps in application .....</b>	<b>122</b>
<b>3.5</b>	<b>Experimental .....</b>	<b>126</b>
3.5.1	Chemicals .....	126
3.5.2	Sample preparation.....	126
3.5.3	Cmc measurements.....	127
3.5.4	Turbidity measurements .....	127
3.5.5	pH measurements.....	128
3.5.6	Phase contrast microscopy.....	128
3.5.7	Freeze fracture transmission electron microscopy .....	128
3.5.8	Dynamic light scattering.....	129
<b>3.6</b>	<b>Literature .....</b>	<b>129</b>
<b>Chapter 4</b>	<b>Choline and beta-methylcholine as counter ion for long chain alkyl sulfates .....</b>	<b>135</b>
<b>4.1</b>	<b>Abstract .....</b>	<b>135</b>
<b>4.2</b>	<b>Introduction.....</b>	<b>135</b>
<b>4.3</b>	<b>Results and discussion .....</b>	<b>138</b>
4.3.1	Krafft temperature .....	138
4.3.2	Critical micellar concentration (cmc).....	139
4.3.3	Other physico-chemical properties derived from cmc measurements ( $\Gamma$ , A, $pC_{20}$ , $\gamma_{cmc}$ ).....	142
4.3.4	Differences in phase behavior between NaS18 and ChS18/MeChS18 .....	144
<b>4.4</b>	<b>Conclusion .....</b>	<b>149</b>
<b>4.5</b>	<b>Experimental .....</b>	<b>150</b>
4.5.1	Chemicals .....	150

4.5.2	Surfactant synthesis .....	150
4.5.3	Determination of $T_{Kr}$ .....	153
4.5.4	Surface tension measurements .....	153
4.5.5	Conductivity measurements .....	155
<b>4.6</b>	<b>Literature .....</b>	<b>157</b>
<b>Chapter 5 Choline and beta-methylcholine salts to reduce <math>T_{Kr}</math> of long chain sodium alkyl sulfates - the "2 in 1"-builder-concept.....</b>		
<b>5.1</b>	<b>Abstract .....</b>	<b>161</b>
<b>5.2</b>	<b>Introduction .....</b>	<b>162</b>
<b>5.3</b>	<b>Results and discussion .....</b>	<b>163</b>
5.3.1	Experiments in millipore water .....	164
5.3.1.1	Influence of Ch salt on $T_{Kr}$ of ChS18 and Na salt on $T_{Kr}$ of NaS16 and NaS18.....	164
5.3.1.2	Influence of Na salt on $T_{Kr}$ of ChS18 .....	164
5.3.1.3	Influence of Ch, MeCh salts on $T_{Kr}$ of NaS16 and NaS18 .....	165
5.3.1.4	Effect of nonionic alcohol ehoxylate on $T_{Kr}$ of ChS18 and NaS18....	171
5.3.2	Experiments in hard water .....	173
5.3.2.1	NaS16 plus additional builder .....	175
5.3.2.1.1	Ch <sub>4</sub> EDTA/Na <sub>4</sub> EDTA.....	175
5.3.2.1.2	Ch <sub>3</sub> Cit/Na <sub>3</sub> Cit .....	179
5.3.2.2	NaS18 plus LutAO7 and builder .....	181
5.3.2.2.1	Ch <sub>4</sub> EDTA/Na <sub>4</sub> EDTA.....	181
5.3.2.2.2	Ch <sub>3</sub> Cit/Na <sub>3</sub> Cit .....	184
<b>5.4</b>	<b>Conclusion .....</b>	<b>185</b>
<b>5.5</b>	<b>Experimental .....</b>	<b>187</b>
5.5.1	Chemicals.....	187
5.5.2	Sample preparation .....	187
5.5.3	Determination of $T_{Kr}$ .....	188
<b>5.6</b>	<b>Literature .....</b>	<b>188</b>

<b>Chapter 6</b>	<b>Ethoxylated choline derivatives as counter ions for long chain alkyl sulfates and soaps .....</b>	<b>191</b>
<b>6.1</b>	<b>Abstract .....</b>	<b>191</b>
<b>6.2</b>	<b>Introduction.....</b>	<b>192</b>
<b>6.3</b>	<b>Results and discussion .....</b>	<b>194</b>
6.3.1	Physico-chemical properties of ChEO <sub>m</sub> S18 .....	194
6.3.1.1	Solubility behavior and T <sub>Kr</sub> .....	194
6.3.1.2	Cmc and other physico-chemical parameters derived from cmc measurements .....	196
6.3.2	Influence of ChEO <sub>m</sub> salts on T <sub>Kr</sub> of NaS16 and NaS18.....	198
6.3.3	ChEO <sub>m</sub> as counter ion of stearate .....	201
6.3.3.1	T <sub>Kr</sub> and macroscopic appearance.....	201
6.3.3.2	Complex phase behavior in dilute soap solutions and the importance of the counter ion .....	207
6.3.4	Foaming properties of aqueous ChEO <sub>m</sub> C18 solutions.....	212
6.3.4.1	Visual observations and dependence of foam stability on the ratio organic base to C18.....	213
6.3.4.2	Time dependent surface tension measurements and a possible mechanism for the formation of stable foams .....	216
<b>6.4</b>	<b>Conclusion .....</b>	<b>220</b>
<b>6.5</b>	<b>Experimental .....</b>	<b>222</b>
6.5.1	Chemicals .....	222
6.5.2	Surfactant synthesis.....	223
6.5.3	Sample preparation.....	224
6.5.4	Determination of T <sub>Kr</sub> .....	224
6.5.5	Surface tension measurements.....	225
6.5.5.1	Du Noüy ring technique .....	225
6.5.5.2	Pendant drop technique .....	225
6.5.6	Foaming tests.....	226
<b>6.6</b>	<b>Literature .....</b>	<b>226</b>

<b>Chapter 7</b>	<b>Laundry detergency tests at room temperature .....</b>	<b>231</b>
7.1	Abstract .....	231
7.2	Introduction .....	232
7.3	Experimental .....	234
7.3.1	Preparation of the detergent solutions .....	234
7.3.2	Detergency tests .....	239
7.3.2.1	Setup and procedure .....	239
7.3.2.2	Evaluation by photometric .....	239
7.3.2.3	Soiled textiles .....	240
7.4	Results and discussion .....	242
7.4.1	Macroscopic appearance of the detergent solutions .....	242
7.4.2	Detergency tests on cotton at room temperature .....	243
7.4.2.1	WfK 10D .....	243
7.4.2.2	Swissatest cotton soiled with palmitic acid/Sudan Black B.....	245
7.5	Conclusion .....	252
7.6	Literature .....	253
<b>Chapter 8</b>	<b>Summary .....</b>	<b>255</b>
	<b>List of figures.....</b>	<b>261</b>
	<b>List of tables .....</b>	<b>275</b>
	<b>List of publications.....</b>	<b>279</b>
	<b>List of poster presentations.....</b>	<b>281</b>
	<b>Eidesstattliche Erklärung.....</b>	<b>283</b>

## **Chapter 1 Introduction and motivation**

This thesis can be divided into two main parts, which both deal with the improvement of the solubility of long chain surfactants in aqueous solutions at room temperature. In the first part, the problem of instability of aqueous solutions of long chain soaps at neutral pH values is addressed. The second part is about the improvement of solubility, respectively the reduction of the Krafft temperature ( $T_{Kr}$ ) of long chain alkyl sulfates and soaps by variation of the counter ion.

The experiments and results belonging to the first part of the thesis are presented in Chapter 3. It is a self-contained study, that was already published in the peer-reviewed journal *Advances in Colloid and Interface Science*.

The work and results, which can be assigned to part two, can be found in Chapter 4 to Chapter 7. Although each of these chapters is written to be (part of) a draft for an article (or patent), the chapters build on each other and should be read in the presented order.

A complete list of publications and poster presentations at national and international conferences is attached at the end of the thesis.

Now, two questions arise. First, why the focus is on soaps and alkyl sulfates, and secondly why it is desired to increase the solubility of long chain surfactants under certain conditions at room temperature.

The answer to the first question is given by the inherent features of soaps and alkyl sulfates. Surfactants are a major class of chemical substances and their extensive and increasing use in detergents, cosmetics and in industrial processes leads to a significant discharge of surfactants into the environment.<sup>1, 2</sup> Therefore, high biodegradability and low ecotoxicity of the surfactant are very important. Further, in the last decades, there is a "green movement" in surfactant industry to replace petrochemical products by surfactants based on natural raw materials.<sup>3, 4</sup> Both soaps and alkyl sulfates fulfill these criteria and are readily biodegradable, exhibit low ecotoxicity and are fully synthesized from renewable starting material.<sup>2, 5, 6</sup>

The answer to the second question is a bit more elaborate. Although both parts of the thesis deal with the increase of the solubility of long chain surfactants at room temperature, the motivation for the two projects was slightly different and will be specified for each part in the following:

*Part 1 (Chapter 3):* Soaps are the oldest and perhaps most natural surfactants. Nevertheless, they lost much of their importance since “technical surfactants”, usually based on sulfates or sulfonates, have been developed over the last fifty years.<sup>7, 8</sup> Indeed, soaps are pH- and salt-sensitive<sup>9, 10</sup>, they are irritant<sup>11</sup> and saturated long chain soaps exhibit high Krafft temperatures.<sup>12</sup> These problems are addressed in detail in a review part in section 2.4. However, it should be possible to solve most or perhaps all of these problems with modern formulation approaches.

In this first part of the work, the focus is on the pH sensitivity of aqueous long chain soaps solutions. Such solutions are only clear and macroscopically stable above a certain pH value ( $> 9$ ) and become turbid and unstable at lower pH values, where lamellar, crystalline or oil-like phases are formed. This effect is not compatible with the formulation of aqueous formulations being stable at neutral or even acidic pH values. This behavior of aqueous soap solutions is well-known and has been intensively studied.<sup>13-19</sup> The aim of the experiments presented in chapter 3 was to overcome this macroscopic instability at pH values close to neutral and to prepare highly stable aqueous solutions of long chain fatty acids at neutral pH and at room temperature. Such systems would allow the use of long chain soaps in aqueous formulations, in which a certain pH value may not be exceeded due to specific application conditions. This could be for example in cosmetics or food, where too high pH values can cause irritancy problems. Solving this problem would expand the range of possible applications of aqueous soap solutions and could possibly lead to the replacement of some synthetic surfactants by simple soap.

The starting point for the experiments was an earlier study of our group<sup>20</sup>, in which we could show that Rebaudioside A (RebA) lowers significantly the apparent pKa (apKa) value of sodium oleate (NaOI) in a beverage microemulsion. Further, it is able to lower its clearing temperature being defined as the temperature, from which on the solution is highly translucent and macroscopically singel-phase. RebA is a natural, non-caloric high efficiency sweetener which is extracted from the plant *Stevia rebaudiana* and known in high purity under the name Rebiana.<sup>21-23</sup>

Now, the effect of RebA on the apKa and the macroscopic and microscopic phase behavior of simple aqueous NaOI solutions at different pH values was investigated. For certain initial mass ratios of RebA to NaOI, it was possible to prepare macroscopically stable and highly translucent aqueous solution at nearly neutral pH values and at room temperatures. A possible mode of action of RebA in the mixed systems was suggested and the time dependent stability of the curves was investigated. These findings were applied to make aqueous solutions of omega-3-fatty acid salts at neutral pH. Similar experiments were also carried out with sodium

dodecanoate. In addition, the critical micellar concentration (cmc) of RebA was determined.

At the end of Chapter 3, some general "green strategies" are presented to overcome the well-known drawbacks of simple long chain soaps in aqueous solutions discussed in section 2.4.

*Part 2 (Chapter 4 to Chapter 7):* Longer chain ionic surfactants are most desirable surfactants, since an increase in the hydrophobic chain length leads to increased surface activity and solubilization power as well as lower cmc values and better detergency.<sup>6, 24-27</sup> Simply spoken, a longer chain surfactant is generally more efficient. Unfortunately, the solubility in water of an ionic surfactant decreases with increasing hydrophobic chain length and the Krafft temperature ( $T_{Kr}$ ) increases.<sup>6, 12, 28</sup> For both sodium alkyl sulfates and sodium soaps, homologues with more than 12 C-atoms in the straight hydrocarbon chain exhibit  $T_{Kr}$  values higher than 25 °C and are only sparingly soluble at room temperature.<sup>6, 12</sup> Common strategies to improve the solubility of longer chain homologues is usually aimed at making the free energy of the surfactant's solid state less favorable by chemical modification of the surfactant. This can be achieved by introducing a methyl group or some other branching in the alkyl chain or by introducing a polar segment between the alkyl chain and the ionic group.<sup>28</sup> These modifications can greatly affect the biodegradability or the performance of the surfactant in certain applications. Another possibility to increase the solubility of long chain surfactants is the addition of co-surfactants, like alcohols or other polar organic compounds.<sup>28-30</sup> These mixed systems (surfactant plus co-surfactant) can also behave markedly different than the simple surfactant solution. The main aim of this part was to render chemically unmodified long chain alkyl sulfates and long chain soaps water soluble at room temperature, e.g. reduce  $T_{Kr}$  below 25 °C. This should be achieved by using unsymmetrical and bulky counter ions, since this can also greatly affect the free energy of the surfactant's solid crystalline state.

The experiments in this part are based on the work of Klein<sup>31</sup> and Rengstl<sup>32</sup>, who synthesized and investigated choline (Ch) soaps up to a chain length of 18 C atoms and choline alkyl sulfates up to a chain length of 16 C atoms. Choline is a quaternary ammonium ion of biological origin, which acts as a precursor for many important molecules in the human metabolism.<sup>33</sup> They found that  $T_{Kr}$  of Ch soaps and alkyl sulfates is below room temperature up to a chain length of 16 C-atoms. For Ch stearate (ChC18), the measured  $T_{Kr}$  value was above room temperature (40 °C). Further, both choline alkyl sulfates and choline soaps were found to be readily

biodegradable and exhibited a low cytotoxicity similar to their sodium equivalents. The huge decrease in  $T_{Kr}$  compared to the sodium surfactants was explained by the unsymmetrical and bulky structure of the choline ion. Further, it was shown for dodecyl sulfate (S12) and dodecanoate (C12) that the addition of choline ions to the respective sodium surfactant can markedly reduce  $T_{Kr}$  of the system.

The experiments and results presented in chapter 4 to chapter 7 were all based on the strategy to increase the solubility of the chemically unmodified long chain surfactant by using a bulky and unsymmetrical counter ion. The more bulky and unsymmetrical the counter ion, the higher the free energy of the surfactant's solid state and the lower  $T_{Kr}$  should be. Therefore, beta-methylcholine (MeCh) and ethoxylated choline ( $\text{ChEO}_m$ ) derivatives were used as counter ions, since they are more bulky than simple Ch. MeCh exhibits an additional methyl group compared to Ch and exhibits some further features which render it an interesting counter ion. Like Ch, it can be assumed to be much less toxic than common TAAs, since it was identified in some rats and flies as the decarboxylation product of carnitine.<sup>34</sup> Moreover, it is already commercially available in large scale, since it is an intermediate in Methacholine (acetyl-beta-methylcholine) synthesis.<sup>35</sup>  $\text{ChEO}_m$  ions were synthesized by BASF and are Ch derivatives with additional oxyethylene (EO) groups between the quaternary N ion and the ethanol moiety. From a structural point of view, these molecules are very interesting as counter ions to long chain surfactants. They combine a very unsymmetrical and bulky structure with the flexibility of an ethoxylated moiety in one molecule.<sup>36, 37</sup> This should render these molecules very promising candidates as counter ions for long chain anionic surfactants to reach very low  $T_{Kr}$  values. Many experiments are also based on the observation that the addition of tetraalkyl ammonium ions (like choline) to sodium alkyl sulfates or soaps can also lead to considerably reduced  $T_{Kr}$  values of these aqueous solutions.

Determination of the solubility and physico-chemical properties of dodecyl sulfate (S12), hexadecyl sulfate (S16) and octadecyl sulfate (S18) surfactants with choline and beta-methylcholine (MeCh) as counter ion shown in Chapter 4 was part of a first cooperation with TAMINCO. The introduced "2 in 1"-builder-concept, which is stepwise developed in Chapter 5, was also part of this project.

Similar experiments with  $\text{ChEO}_m$ S18, respectively NaS16 and NaS18 plus  $\text{ChEO}_m$  salt, as well as ChC18 and  $\text{ChEO}_m$ C18 discussed in Chapter 6 were part of a second cooperation with BASF. The detergency tests on cotton textile at room temperature presented in Chapter 7 were also part of this cooperation.

## 1.1 Literature

1. Huber, L.; Nitschke, L., Environmental Aspects of Surfactants. In *Handbook of Applied Surface and Colloid Chemistry (Volume 1)*, Holmberg, K., Ed. Wiley: 2002; pp 509-536.
2. Scott, M. J.; Jones, M. N., *Biochim Biophys Acta - Biomembranes* **2000**, 1508 (1-2), 235-251.
3. Foley, P.; Kermanshahi pour, A.; Beach, E. S.; Zimmerman, J. B., *Chem Soc Rev* **2012**, 41 (4), 1499-1518.
4. Svensson, M., Surfactants Based on Natural Fatty Acids. In *Surfactants from Renewable Resources*, Kjellin, M.; Johansson, I., Eds. John Wiley & Sons, Ltd: 2010; pp 1-19.
5. Schmalstieg, A.; Wasow, G. W., Anionic surfactants. In *Handbook of Applied Surface and Colloid Chemistry (Volume 1)*, Holmberg, K., Ed. Wiley: 2002; pp 271-292.
6. Domingo, X., Alcohol and Alcohol Ether Sulfates. In *Anionic Surfactants: Organic Chemistry*, Stache, H., Ed. Marcel Dekker: 1996; pp 223-312.
7. Myers, D., An Overview of Surfactant Science and Technology. In *Surfactant Science and Technology*, John Wiley & Sons, Inc.: 2005; pp 1-28.
8. Smulders, E.; Rähse, W.; von Rybinski, W.; Steber, J.; Sung, E.; Wiebel, F., Historical Review. In *Laundry Detergents*, Wiley-VCH Verlag GmbH & Co. KGaA: 2003; pp 1-6.
9. Myers, D., The Organic Chemistry of Surfactants. In *Surfactant Science and Technology*, John Wiley & Sons, Inc.: 2005; pp 29-79.
10. Rosen, M. J., Characteristic Features of Surfactants. In *Surfactants and Interfacial Phenomena*, John Wiley & Sons, Inc.: 2004; pp 1-33.
11. Landeck, L.; Baden, L.; John, S.-M., Detergents. In *Kanerva's Occupational Dermatology*, Rustemeyer, T.; Elsner, P.; John, S.-M.; Maibach, H., Eds. Springer Berlin Heidelberg: 2012; pp 847-857.
12. Lin, B.; McCormick, A. V.; Davis, H. T.; Strey, R., *J Colloid Interface Sci* **2005**, 291 (2), 543-549.
13. Hirai, A.; Kawasaki, H.; Tanaka, S.; Nemoto, N.; Suzuki, M.; Maeda, H., *Colloid Polym Sci* **2006**, 284 (5), 520-528.
14. Kaibara, K.; Ogawa, T.; Kawasaki, H.; Suzuki, M.; Maeda, H., *Colloid Polym Sci* **2003**, 281 (3), 220-228.
15. Apel, C. L.; Deamer, D. W.; Mautner, M. N., *Biochim Biophys Acta - Biomembranes* **2002**, 1559 (1), 1-9.
16. Edwards, K.; Silvander, M.; Karlsson, G., *Langmuir* **1995**, 11 (7), 2429-2434.

17. Cistola, D. P.; Hamilton, J. A.; Jackson, D.; Small, D. M., *Biochemistry* **1988**, 27 (6), 1881-1888.
18. Hargreaves, W. R.; Deamer, D. W., *Biochemistry* **1978**, 17 (18), 3759-3768.
19. Rosano, H. L.; Breindel, K.; Schulman, J. H.; Eydt, A. J., *J Colloid Interface Sci* **1966**, 22 (1), 58-67.
20. Marcus, J.; Wolfrum, S.; Touraud, D.; Kunz, W., *J Colloid Interface Sci* **2015**, 460, 105-112.
21. Prakash, I.; Dubois, G. E.; King, G. A.; Upreti, M. Rebaudioside A composition and method for purifying rebaudioside A. US Patent No. 8,791,253, 2014.
22. Prakash, I.; DuBois, G. E.; Clos, J. F.; Wilkens, K. L.; Fosdick, L. E., *Food Chem Toxicol* **2008**, 46 (7, Supplement), 75-82.
23. Carakostas, M. C.; Curry, L. L.; Boileau, A. C.; Brusick, D. J., *Food Chem Toxicol* **2008**, 46 (7, Supplement), 1-10.
24. Rosen, M. J., Detergency and Its Modification by Surfactants. In *Surfactants and Interfacial Phenomena*, John Wiley & Sons, Inc.: 2004; pp 353-378.
25. Rosen, M. J., Solubilization by Solutions of Surfactants: Micellar Catalysis. In *Surfactants and Interfacial Phenomena*, John Wiley & Sons, Inc.: 2004; pp 178-207.
26. Rosen, M. J., Reduction of Surface and Interfacial Tension by Surfactants. In *Surfactants and Interfacial Phenomena*, John Wiley & Sons, Inc.: 2004; pp 208-242.
27. Smulders, E.; Rähse, W.; von Rybinski, W.; Steber, J.; Sung, E.; Wiebel, F., Detergent Ingredients. In *Laundry Detergents*, Wiley-VCH Verlag GmbH & Co. KGaA: 2003; pp 38-98.
28. Lindman, B., Physico-Chemical Properties of Surfactants. In *Handbook of Applied Surface and Colloid Chemistry (Volume 1)*, Holmberg, K., Ed. Wiley: 2002; pp 421-443.
29. Kaneshina, S.; Kamaya, H.; Ueda, I., *J Colloid Interface Sci* **1981**, 83 (2), 589-598.
30. Nakayama, H.; Shinoda, K.; Hutchinson, E., *J Phys Chem* **1966**, 70 (11), 3502-3504.
31. Klein, R., Dissertation. Universität Regensburg: 2011.
32. Rengstl, D., Dissertation. Universität Regensburg: 2013.
33. Blusztajn, J. K., *Science* **1998**, 281 (5378), 794-795.
34. Khairallah, E. A.; Wolf, G., *J Biol Chem* **1967**, 242 (1), 32-39.
35. Vardanyan, R. S.; Hruby, V. J., Cholinomimetics. In *Synthesis of Essential Drugs*, Elsevier: Amsterdam, 2006; pp 179-193.

36. Klein, R.; Zech, O.; Maurer, E.; Kellermeier, M.; Kunz, W., *J Phys Chem B* **2011**, *115* (29), 8961-8969.

37. Zech, O.; Hunger, J.; Sangoro, J. R.; Iacob, C.; Kremer, F.; Kunz, W.; Buchner, R., *Phys Chem Chem Phys* **2010**, *12* (42), 14341-14350.



## Chapter 2 Fundamental information

### 2.1 Surfactants

Surfactants are ubiquitous and indispensable in daily life. They can be found in many household products, like personal care and cleaning/washing products, or as emulsifiers in food. Moreover, they are very important in a lot of industrial processes, like in paper industry, oil industry, agricultural industry or in pharmacy.<sup>1, 2</sup>

Surfactants are surface-active molecules, which readily adsorb at interfaces or surfaces with an accompanied reduction of the interfacial or surface tension. Moreover, in aqueous solution, they exhibit many interesting physico-chemical properties like the critical micellar concentration (cmc, see section 2.1.5.1) or the Krafft temperature ( $T_{Kr}$ , see section 2.1.5.3).<sup>3-6</sup>

Soap was the first **surface active agent** made by mankind and already used in consumer products for several hundred years<sup>2, 7, 8</sup>, and it is still the predominant surfactant in the world.<sup>9</sup> In the last century, synthetic (nonsoap) or partially synthetic surfactants became more and more important, since they proved to be superior with regard to common problems with classical soaps (e.g. salt- or pH-sensitivity). Moreover, they can be tailor made for more specialized application fields. This development was strongly supported by new material feedstock from modern petrochemical industry and improved process technology.<sup>2, 8, 10-12</sup>

Nowadays, surfactant industry possesses a huge market which has a value of several billion dollars. In 2013, the global surfactant market was worth about 30 billion dollars<sup>13</sup> and it is expected to reach almost 40 billion dollars in 2021<sup>14</sup>. This constant increase at a rate in excess of population growth can be explained by an improved economic situation, by generally improved living conditions (above all in less developed countries) and manufacturing process development in less industrialized countries.<sup>2, 15</sup>

The predominant share in the world surfactant market is made up by anionic surfactants (see also **Figure 2-1**). This is due to their excellent application properties, ease and low costs of manufacture and good ecotoxicological data.<sup>3, 11, 12</sup>

Excluding soap, in 2013, the world surfactant consumption was about 15 million metric tons and was distributed over the three major application areas as follows: household (cleaning) products (52%), personal care products (13 %) and industrial use (35 %).<sup>13</sup> In the same year, in Western Europe 1450 kilotons nonionic

surfactants, 1197 kilotons anionic surfactants, 229 kilotons cationic surfactants and 107 kilotons amphoteric surfactants were produced.<sup>16</sup>

**Figure 2-1** shows the global surfactant demand for six of the major surfactants in 2015 as well as an outlook for 2025.<sup>17</sup> These data underline the previously mentioned supremacy of anionic surfactants as well as the marked growth of the surfactant market in the future.

Outlook on global surfactant demand (in kt)		
	2015	2025
LABS	4450	5780
MES	230	425
AS	600	840
FES	2200	3650
AE	1850	3080
APE	515	400

**Figure 2-1:** Outlook on global surfactant demand taken from reference 17. Abbreviations: LABS: linear alkylbenzene sulfonate, MES: methyl ester sulfonate, AS: fatty alcohol sulfate, FES: fatty alcohol ether sulfate, AE: alcohol ethoxylate, APE: alkylphenol ethoxylate.

In the last decades, like in many other parts of the chemical industry, there is a "green movement" in surfactant industry. "Green" surfactants have to be readily biodegradable, exhibit a low (aquatic) toxicity and should be made of renewable raw materials.<sup>2, 3, 18, 19</sup>

## 2.1.1 Structure and classification of surfactants

Surfactants are amphiphilic molecules that consist of a lyophobic part ("lyophobic tail") and a lyophilic part ("lyophilic head"). In most applications, the solvent is water and lyophobic/lyophilic turns into hydrophobic/hydrophilic. The hydrophobic part of a surfactant usually consists of a linear or branched alkyl chain of at least 8 carbon atoms. However, short polymeric, fluoroalkyl or siloxane chains are also possible. The hydrophilic part can either be a water-soluble nonionic or ionic/zwitterionic group. For ionic surfactants, a counter ion, which can have a great influence on the surfactant's physico-chemical properties, is necessary.

As a result of this basic composition, surfactants exhibit a certain solubility in water as well as an affinity to hydrophobic environments. This behavior leads to interfacial/surface activity as well as to many physico-chemical properties, for which this class of chemicals is well-known.<sup>3, 11, 20</sup>

The schematic composition of a surfactant is illustrated by the ionic surfactant choline hexadecyl sulfate in **Figure 2-2**.

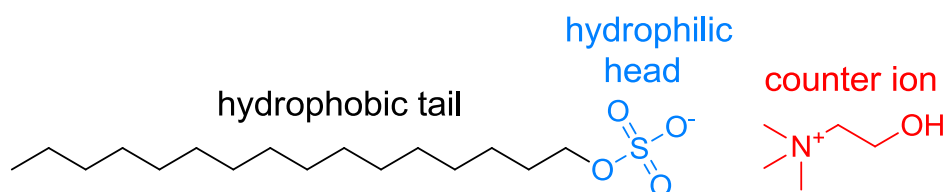


**Figure 2-2:** The ionic surfactant choline hexadecyl sulfate as an example for the general structure of a surfactant.

### 2.1.1.1 Classification by the polar head group

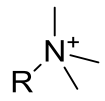
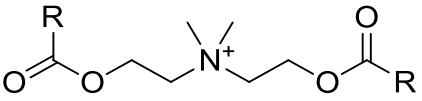
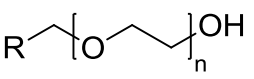
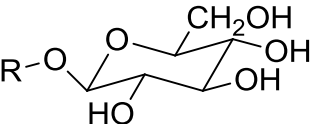
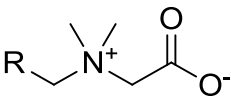
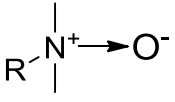
Commonly, surfactants are classified by their polar head group into four classes: anionic, cationic, nonionic and zwitterionic surfactants.<sup>3, 11, 20</sup> The structure of a few important head groups for each surfactant class can be found in **Table 2-1**. In the following listing some important facts about each group are given<sup>3</sup>:

- anionic:
  - the head group bears a negative charge (e.g. sulfates, carboxylates)
  - the largest surfactant class
  - generally not compatible with cationics
  - in general sensitive to hard water
  - their physico-chemical properties are heavily affected by electrolytes

## Surfactants

- cationic:
  - head group bears a positive charge (e.g. quaternary amin)
  - third largest surfactant class
  - generally not compatible with anionics
  - adsorb strongly to most surfaces
  - their physico-chemical properties are heavily affected by electrolytes
  
- nonionic:
  - head group bears no charge (e.g. alcohol ethoxylates)
  - second largest surfactant class
  - usually compatible with all other surfactant types
  - insensitive to hard water
  - their physico-chemical properties are not markedly affected by electrolytes
  - ethoxylated compounds can be tailor-made by the degree of ethoxylation
  - physico chemical properties of ethoxylated compounds are strongly temperature dependent and water solubility decreases with temperature
  
- zwitterionic:
  - head group bears a positive and a negative charge (e.g. betaine)
  - smallest surfactant class
  - compatible with all other surfactant types
  - insensitive to hard water
  - most types exhibit very low eye and skin irritation and thus well suited for use in personal care products.

Class of surfactant	examples
Anionic	<div style="display: flex; justify-content: space-around; align-items: center;"> <div style="text-align: center;"> <math display="block">\text{R}-\text{C}(=\text{O})\text{O}^-</math>           alkyl carboxylate         </div> <div style="text-align: center;"> <math display="block">\text{R}-\text{O}-\text{S}(=\text{O})_2\text{O}^-</math>           alkyl sulfate         </div> <div style="text-align: center;"> <math display="block">\text{R}-\text{CH}_2-\text{CH}(\text{C}_6\text{H}_4\text{SO}_3^-)-\text{CH}_2\text{R}</math>           alkyl benzenesulfonate         </div> </div>

<b>Cationic</b>	 alkyl quat  alkyl ester quat
<b>Nonionic</b>	 alcohol ethoxylate  alkyl glucoside
<b>Zwitterionic</b>	 alkyl betaine  alkyl amine oxide

**Table 2-1:** Structures of some important ionic, nonionic and zwitterionic head groups.

### 2.1.1.2 Classification by the origin of the raw materials

Apart from structural and functional groups, surfactants can be classified by the origin of their starting materials.

On the one hand, oleochemical-based "natural" surfactants. They are synthesized from fatty acid methyl esters, fatty alcohols or other building blocks, which are derived from natural oils (e.g. coconut oil or palm kernel oil) or animal fats (see **Figure 2-3**). On the other hand, petrochemical-based "synthetic" surfactants derived from modified petroleum distillates.<sup>2, 3, 10</sup>

Excluding soap, in the first decade of the 21<sup>st</sup> century around 50 % of the surfactants were derived from renewable raw materials and nearly the same amount from fossil raw materials.<sup>2, 21, 22</sup> However, a significant difference is observed with regard to place of surfactant manufacturing. In 2013, in Asia and South America nearly 100 % of the fatty alcohols used for surfactant production were derived from natural resources. In Europe the share was about 65 % and in North America only about 25 %. In Africa, the fatty alcohols were solely petrochemical-based.<sup>23</sup>

In the last decades, surfactant industry turned its attention more and more to renewable resources to replace petrochemical products.<sup>19</sup> Considering alcohol-based surfactants, the share of oleochemical-based starting material increased from 40 up to 71 % during the last 35 years.<sup>21, 23</sup> This development can partly be explained by increased prices for petroleum-based starting materials as well as their limited stock, an increased supply of vegetable oils, advances in oleochemistry process chemistry and customer's increased demand for "natural"

products/ingredients.<sup>24</sup> Moreover, surfactant manufacturing based on renewable raw materials is preferred from the carbon dioxide cycle point of view.<sup>3, 25</sup>

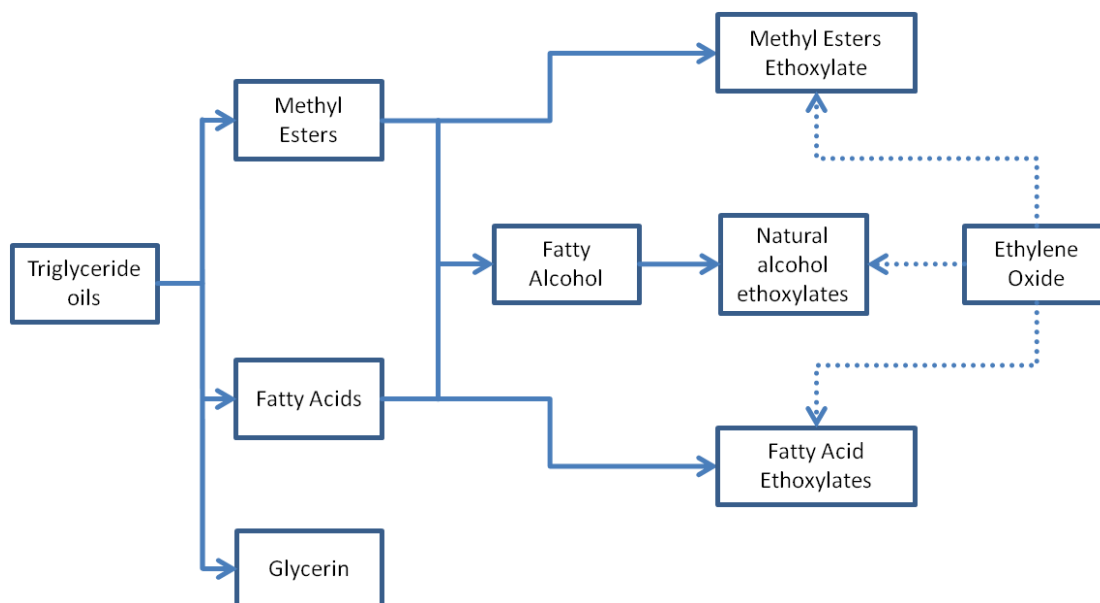


**Figure 2-3:** Simple scheme of the production of nonionic and anionic surfactants derived from natural oils. The figure is based on reference 10.

There has been a great debate on the pros and cons of "natural" and "synthetic" surfactants. The popular opinion that "natural" products are better for the environment than "synthetic" products as well as the limited stock of petrochemicals has led to the suggestion that petrochemical-based surfactants should be replaced by oleochemical-based ones. However, this is quite a limited view. There are important reasons why it will neither be possible nor desirable to substitute all petrochemical-based surfactants by oleochemical-based ones.

At the moment, it would be very difficult to achieve the functional characteristic of surfactants in many applications by using only renewable raw materials. There is also always the pressure to keep costs as low as possible. Furthermore, the focus may not only be on the production of the surfactant, but also on its performance in practice. Petrochemical-based surfactants with outstanding application qualities compared to oleochemical-based ones can save a lot of energy. For example, reduced process temperatures (e.g. cold machine washing), what would lead to reduced air emissions and conservation of petroleum stocks by saving energy. Moreover, there is no measurable difference in environmental impact of oleochemical-based or petrochemical-based surfactants. Consequently, research should be carried out with oleochemical-based and petrochemical-based surfactants, since not all "theoretical" promising surfactants can both be prepared from fossil and

renewable resources. In the end, costs and performance will decide whether a surfactant technology becomes successful.<sup>2</sup>

## 2.1.2 Toxicity and biodegradability of surfactants

The presence of surfactants in industrial processes and many household products, like in cleaning agents, detergents or personal care products, leads inevitably to exposure of humans and the environment to surfactants.

For humans, this can be direct contact with skin or eyes as well as oral uptake. For this reason, toxicology studies on surfactants are indispensable to ensure the safety and health of humans using such products.

Moreover, surfactants can be released into the environment via domestic or industrial waste water. Thus, their good biodegradability and low ecotoxicity, above all to aquatic organisms, are important.

### 2.1.2.1 Toxicity

There are many possible toxicity tests that can be performed with a single chemical substance and many data can be generated. However, for surfactants these studies are usually focused on local effects (e.g. skin/eye irritation, skin penetration, sensitization) and systemic effects (e.g. acute/chronic, carcinogenicity).<sup>26, 27</sup>

Herein, at first, a short overview of the biological functions of surfactants which cause toxicity is given and afterwards some general findings concerning toxicity of surfactants are presented.

#### 2.1.2.1.1 Biological functions of surfactants

Most of the biological properties of surfactants result from the interactions that take place between surfactant molecules and fundamental biological structures like membranes, enzymes and proteins. Depending on surfactant type and concentration, these interactions can cause serious damage to living cells and the function of enzymes.

At low surfactant concentrations, surfactant interactions with the (cell) membrane lead to a change in membrane permeability followed by undesired material transport. With increasing concentration, cell lysis takes place and even complete solubilization of the membrane is possible.

Moreover, surfactants can form adsorption complexes with proteins. A precondition seems to be polar interactions between the charged sites of a protein and the surfactant's charged head group. However, hydrophobic interactions can also play an important role. Such complex formation can lead to denaturation of the protein and in the case of an enzyme to deactivation and a change in metabolic function.

Due to the absence of a charged head group, nonionic surfactants rarely cause protein denaturation.<sup>26-28</sup>

#### 2.1.2.1.2 Local toxic effects

The main application of surfactants are laundry detergency, cleaning agents and personal care products. In all these applications local contact to skin or eye is unavoidable. Some examples would be: contact to hands during dish washing, contact to skin and eye by using a shower gel/shampoo during showering or skin contact by surfactant residues on clothes after laundry detergency.

The test methods for physiological effects of surfactants on skin are numerous. They comprise methods for the effect of surfactants on the skin surface up to methods which determine the penetration of surfactants through the skin.<sup>3, 27</sup>

Results show that the penetration of ionic surfactants through skin is quite low. Nonionic surfactants show a greater tendency to penetrate the skin, but the amount of substance entering the organism is still so low that it may not be regarded as a potential hazard.<sup>26, 27</sup>

The toxic effect of surfactants on the skin can be explained by the ability of surfactants to emulsify lipids. As a consequence, the skin is defatted and its barrier function is decreased. This leads to a loss of moisture and an increased permeability of the skin for chemical substances. The damage of surfactants to the skin can be expressed by dryness, roughness, scaling or symptoms of inflammation. In severe cases complete destruction of the tissue can occur.<sup>26, 27</sup>

In general, it can be stated that all commercially relevant surfactants are well-tolerated at typical use levels.<sup>26, 27</sup> Some further general results of skin toxicology tests are listed below:

- although skin tolerance to surfactants varies widely among the surfactants of each group one can generalize: nonionic > anionic > cationic.<sup>26</sup>
- irritancy potential of a surfactant strongly increases with its concentration.<sup>27</sup>
- zwitterionic surfactants (e.g. betaines), polyol surfactants (e.g. alkyl glucosides) and isethionates are generally known to be mild to the skin and are therefore often used in cosmetic formulations.<sup>3</sup>
- for anionic surfactants with a saturated linear alkyl chain the highest potential of damage is found for a chain length of 10 to 12 C atoms.<sup>26, 27</sup>
- alkyl ether sulfates show lower irritancy potential than alkyl sulfates.<sup>3, 29</sup>

Due to structural differences from mucus membranes to normal skin, like the absence of keratin, the eye is much more sensitive to damage by surfactants. The extent of eye irritancy depends heavily on the surfactant concentration in solution. In general, at normal use levels only minimal irritation is caused that quickly passes off. Comparison of test results with regard to surfactant class and surfactant structure show that the same statements are true as listed above for skin irritancy.<sup>26, 27, 29</sup>

Based on many investigation and the long experience with surfactants in consumer products, it is well established that surfactants do not increase the risk of allergy for the consumer. For some individual cases, in which surfactants were indicted to cause allergic reactions, it could be shown that these reactions were caused by some impurities and not by the surfactant molecules.<sup>3, 26, 27</sup>

#### **2.1.2.1.3 Systemic toxic effects**

Next to local toxic effects, it is also important to know the effects caused by a surfactant which is absorbed by the organism. Resorption of surfactants by the organism through the skin as well as by oral ingestion of surfactants have to be mainly considered. While surfactant resorption through the skin is quite low (see 2.1.2.1.2), surfactants can easily orally enter the body. This can happen via food because of surfactant traces on dishes, during showering or brushing the teeth or by accidental swallowing of products containing surfactants.<sup>27</sup>

Test results show a low acute oral toxicity for well-established surfactants. LD<sub>50</sub> values in animal tests are usually between several hundred and several thousand milligrams per kilogram body weight. This is in the same order of magnitude as for table salt or sodium bicarbonate.

The most detrimental effect of surfactants is damaging the mucus membrane of the gastrointestinal tract. Higher doses can lead to vomiting and diarrhea. Although anionic and nonionic surfactants are readily resorbed through the gastrointestinal tract, there was never found a significant accumulation of surfactants in the body. This is due to their rapid metabolism, by mainly  $\beta$ - and  $\omega$ -oxidation of the alkyl chains. The elimination of the metabolites is primarily carried out by the bile and the urine.<sup>26, 27, 29</sup>

Investigation on chronic toxicity was intensely studied with surfactants from all classes. Many experiments with animals over periods up to two years and dosage ranges of from 0.1 to 1 % surfactants in feed did not show any observable effects. Moreover, some studies with humans exist. Volunteers consumed considerable

amounts of nonionic and anionic surfactants for a long time without any serious side effects.<sup>26, 27, 29</sup>

The high LD<sub>50</sub> value for acute oral toxicity of surfactants suggests that is nearly impossible, even by accidental swallowing, to cause severe poisoning with products containing surfactants. This is confirmed by statistics of poison centers, too. The estimated oral intake of surfactants during a normal day is 0.3 - 3 mg for one person. Even if a small amount, usually less than by oral intake, of surfactants is resorbed by the skin, these amounts can be regarded as negligible.<sup>27</sup>

Compounds of each class of surfactants have been tested on carcinogenicity, mutagenicity and teratogenicity. The studies show that surfactants do not possess carcinogenic activity, pose only a negligibly small risk of genetic damage and do not act teratogenic.<sup>26, 27</sup>

#### **2.1.2.2 Biodegradability and ecotoxicity**

The extensive and increasing use of surfactants in detergents, cosmetics and in industrial processes leads to a significant discharge of surfactants into the environment. Basically, this can happen on three ways: by discharging into the aquatic system via effluents of waste water treatment plants or industry, via direct discharge or via the use of sewage sludge on land.<sup>30, 31</sup>

Historically, the fact that surfactants can have strong impact on the environment was realized after World War II by the change from mainly soap-based detergents to mainly synthetic surfactant based detergents. The synthetic surfactant of choice was tetrapropylenebenzene sulfonate (branched alkylbenzene sulfonate, BABS) because of its low manufacturing costs and excellent performance. In the late 1950s, BABS made up 65 % of the total synthetic surfactant demand in the Western world. Its impact on environment became clearly visible in the following years. Considerably amounts of foam were present in waste-water treatment plants and rivers. Another newly introduced synthetic surfactant, alkylphenol ethoxylate (APE), supported that process. Before these observations, no one had sought about how to deal with surfactants after their application.

It was quickly found out that low biodegradability of some anionic (BABS) and nonionic (APE) surfactants, which could not be sufficiently removed by modern waste water treatment plants, was responsible for their accumulation in rivers and the resulting foam. As a consequence, already in the early 1960s, first laws concerning the minimum biodegradability of surfactants were passed. Moreover,

research in suitable chemical methods for analysis and biological test methods to determine biodegradability as well ecotoxicity was started.<sup>8, 30, 31</sup>

#### **2.1.2.2.1 European legislation and test methods**

The development of surfactant specific legislation was mainly focused on detergent industry.

In 1961, the first legal actions by European Governments were taken to control the environmental impact of surfactants and detergents. From then until now, the European legislation concerning surfactants and detergents was continuously adapted and improved. The European Economic Community (EEC) elaborated many directives that were transformed into detergent laws by the member states. These directives contain exact specifications on the minimum primary biodegradability of surfactants contained in detergents and on the approved test procedures. There are many standardized [Organization for Economic Co-operation and Development (OECD) and International Organization for Standardization (ISO)] test methods to determine the primary or ultimate biodegradation as well as the ecotoxicity of surfactants. The results of these tests are also important parameters for the environmental risk assessment of surfactants, which is also guided by directives of the EEC. Surfactants that passed these primary and ultimate biodegradability tests are classified as "primary biodegradable", respectively "ready biodegradable".<sup>30, 32, 33</sup>

In 2004, the Detergents Regulation (648/2004/EC) was published that replaced all the other detergent specific legislation. It entered into force on the 8th of October 2005.<sup>34</sup> The scope of the new legislation is much more prescriptive and inclusive than the previous legislation. The regulation contains an exact definition of surfactants and a comprehensive list of what is considered a detergent application. It is not retrospective and applies to all products that were placed on the market after it had come into effect. The goal of this Detergents Regulation is to protect the aquatic environment by ensuring only "ready biodegradable" surfactants are used in common detergent applications. In previous legislation, only primary biodegradability was addressed.<sup>32</sup> With time, there have been some amendments to the Detergents Regulation. For example, the 2012 amendment (259/2012/EC) prescribes a limitation for phosphates and other phosphorus compounds in consumer laundry detergents und consumer automatic dishwasher detergents to fight "eutrophication".<sup>35</sup>

A detailed overview on the development in European legislation concerning surfactants with all its strengths and weaknesses is provided in reference 32.

### 2.1.2.2.2 Biodegradability

Biodegradation is the destruction of chemical compounds by the biological action of microorganisms. It is the most important mechanism for the complete removal of organic compounds from the environment. For surfactants, biodegradation is usually divided into primary and ultimate degradation. Primary degradation refers to the state of biodegradation when the surfactant has lost its surfactant properties. Ultimate degradation refers to the state when the surfactant molecule has been converted to  $\text{CO}_2$ ,  $\text{H}_2\text{O}$ , inorganic ions and biomass (see left side **Figure 2-4**).<sup>30, 31</sup>

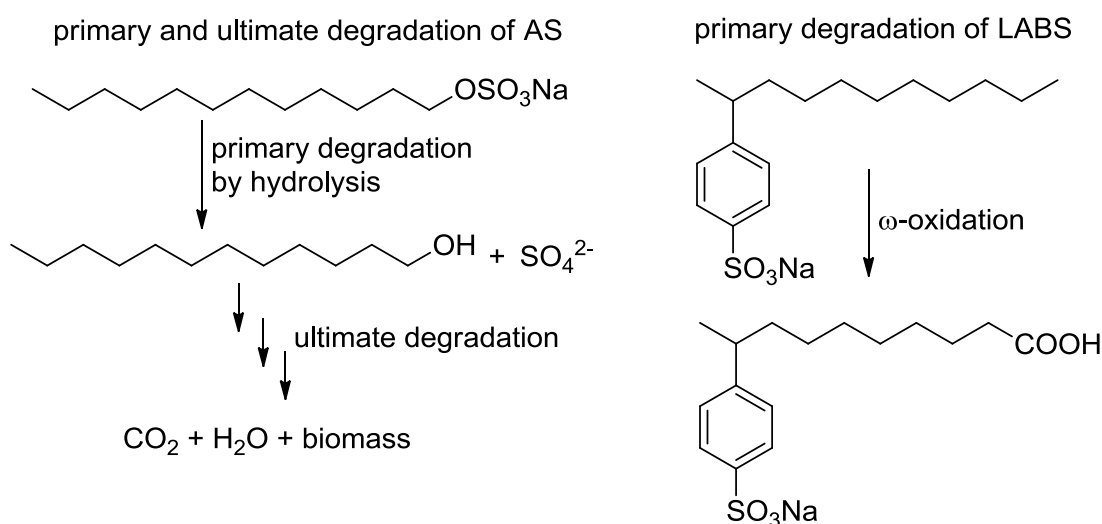


**Figure 2-4:** left: primary and ultimate biodegradation of linear alkyl sulfate; right: primary degradation step for linear alkylbenzene sulfonate. Based on schemes from reference 30.

Primary degradation only removes undesired properties from surfactants and ensures that foaming ability as well as their aquatic toxicity decrease. Ultimate degradation, however, is necessary to completely remove the surfactant and its degradation intermediates from the environment.<sup>26, 36</sup> Moreover, one has to differentiate between aerobic and anaerobic biodegradation.

In waste-water treatment plants both routes are important. Some amount of the surfactant can already be removed from the waste water in the mechanical stage of the plant by adsorption to resident particulate matter or precipitation with divalent metal ions. This particulate matter, relatively rich in surfactants, is commonly removed to primary settling tanks, where usually anaerobic digestion takes place. The addition of this anaerobically treated sewage sludge to agricultural land is a potential source of exposure of badly anaerobic degradable surfactants to the environment. The aerobic way is the important one during the biological step in the plant as well as in the environment.<sup>30, 31</sup>

Microorganisms mainly use two pathways for surfactant biodegradation. One way is to cleave the surfactant between the hydrophilic and the hydrophobic group, which is further oxidatively degraded. The other way is by oxidizing the hydrophobic part while it is still bound to the hydrophilic one. Both mechanisms lead to a loss of the surfactant structure.<sup>37, 38</sup> The difference is illustrated in **Figure 2-4** for the suggested primary degradation of an alkyl sulfate and a linear alkylbenzene sulfonate.

By comparison of many biodegradation tests of similar surfactants, which only vary slightly in their hydrophobic chain or their hydrophilic head group, some general relation between surfactant structure and rate of biodegradation can be drawn.

A review on surfactant biodegradability by Swisher<sup>38</sup> points out that:

- biodegradability increases with increased linearity of the hydrophobic group and decreases for isomeric substances by branching of the chain (see BABS and LABS). A single methyl branch does not change biodegradability, but additional ones do.
- in isomeric alkylbenzene and alkylphenol structures, biodegradation decreases when the aromatic group moves from the terminal position of the linear chain to a more central one.
- in ethoxylated nonionic surfactants, biodegradation slows down by an increased degree of ethoxylation. Secondary ethoxylates degrade more slowly than primary ones.
- for quaternary cationic surfactants, compounds with one alkyl chain attached to the nitrogen degrade faster than these with two alkyl chains, and these faster than those with three alkyl chains. Pyridinium compounds degrade much more slowly than the corresponding trimethyl ammonium compounds.

Many data of biodegradation for all surfactant classes are given in reference 30. Results for alkyl sulfates and alkyl ether sulfates indicate that these compounds are primarily and readily biodegradable under anaerobic and aerobic conditions. The same is true for soaps, linear alkyl ethoxylates and alkylpolyglycosides.<sup>30, 31, 33</sup>

Branched alkylbenzene sulfonates are poorly biodegradable and therefore banned from use in detergents in the EU and North America. Linear alkylbenzene sulfonates, however, are primarily and readily biodegradable under aerobic conditions. Poor biodegradation was found under anaerobic conditions. The discrepancy between the two surfactants can be explained by differences in the alkyl chain.<sup>30, 31, 33</sup>

Although alkylphenol ethoxylates are primarily biodegradable under anaerobic conditions, they are banned by law from detergents in Europe. This is due to the

formation of hazardous metabolites during aerobic and anaerobic biodegradation that are more toxic than the initial surfactant, namely nonylphenol and low ethoxylated nonylphenol compounds.<sup>30, 31, 33</sup>

Cationic alkylmethyl ammonium-type surfactants are poorly biodegradable under aerobic conditions and non-degradable under anaerobic ones. Esterquats however are primarily and readily biodegradable under aerobic and anaerobic conditions.<sup>30, 33</sup>

The zwitterionic cocamidopropyl betaine and disodium cocoamphodiacetate were found to be readily biodegradable under aerobic and anaerobic conditions.<sup>30</sup>

#### **2.1.2.2.3 Ecotoxicity**

Surfactants mainly reach the environment via discharges from waste water treatment plants and industry into fresh water or the use of sewage sludge on fields. Sometimes even direct discharge into the aquatic system takes place.<sup>30, 31</sup> Therefore, the most important subarea of surfactants' ecotoxicity, i.e. the toxicity to living organisms living in an environmental compartment, is the toxicity towards aquatic organisms.

There are many internationally accepted and standardized test systems to investigate aquatic toxicity of a surfactant. These tests cover the whole aquatic food chain and can be divided into acute and chronic or subchronic tests. Usually, the toxicity is tested towards algae as a plant representative, towards daphnia as plant feeding animals, towards fish as representative of higher trophic levels and finally towards bacteria which have to degrade organic matter.

The acute toxicity tests allow a first general evaluation. They last 24, 48 or 96 h and are usually expressed by the LC/EC (median lethal or effect concentration) values. Common are the EC/LC 0, 50 and 100 values, i.e. the highest concentration for which no organism is death/affected, the concentration which is expected to cause death/effects in 50 % of the organisms and the lowest concentration for which all organisms are death/affected.

Chronic/subchronic tests are more closely related to the practical situation. They last several weeks and their results are no observed effect concentrations (NOEC), i.e. the highest concentration for which no effect was observed compared to a benchmark.<sup>30, 33</sup>

Many data for acute and chronic toxicity of all surfactant classes can be found in reference 30.

#### 2.1.2.2.4 Ecological assessment and Environmental risk assessment

For the ecological assessment of surfactants, next to biodegradability and aquatic toxicity, which depict the main criteria, some other factors are relevant. These are for example bioaccumulation, toxicity in surfactant production, formation of hazardous degradation products or the effect on the function of sewage treatment plants.<sup>3, 30</sup>

In the European Union, the evaluation of the ecological risk of chemical substances is regulated in the risk assessment directives for new and existing chemicals. They were enacted to secure that chemical substances will have no adverse effect on living organisms in environmental compartments.

The basis of the environmental risk assessment of surfactants is to compare the predicted environmental concentration (PEC) of the surfactant to its predicted no-effect concentration (PNEC). The calculation/measurement of these values is a tiered process. Surfactants are regarded as safe and no risk for the environment is expected, if the PEC value is lower than PNEC value. If the ratio PEC/PNEC is larger than 1, risk measures have to be taken.

Biodegradability data, respectively the environmental fate of a chemical has an important effect on the PEC value. In the first tier of determining the PEC value of a surfactant a calculation model is used. This respects the per capita usage of the surfactant, per capita water consumption and an estimated elimination rate of the surfactant in waste water treatment plants based on the surfactant's physicochemical and biodegradability properties. This way, a theoretical concentration of the surfactant in the effluent of the waste water treatment plant is obtained. This concentration yields a first estimated PEC value by a division by 10. In the second tier, more reliable PEC values are obtained by taking into account exact data of the individual environmental situation. These can be elimination rates by waste water treatment plant simulation tests and exact information on the waste-water treatment and the river water situation. The highest and most reliable tier to determine a PEC value is by measuring real environmental concentrations, i.e. environmental-monitoring. Of course, this is only possible if the surfactant is already in use. The most common surfactants have been investigated by means of the multi-tiered approach. It could be shown that the calculated PEC values were higher than the data obtained by environmental-monitoring.

PNEC values can be obtained from the ecotoxicological data of a surfactant, either directly by chronic toxicity tests or by estimation from acute toxicity data by using an "application factor".<sup>30, 33</sup>

### 2.1.3 Future requirements for surfactants in industry

Nowadays, research in surfactants is indispensable. Next to the demand for "improved" surfactants in traditional surfactant application sectors by economic, environmental and social reasons, surfactants gain more and more importance in other industrial and technological areas. This is mainly caused by the overall technological progress and high-tech applications often need very special and tailor-made molecules. The required properties of surfactants (e.g. solubility, foaming properties, wetting...) vary significantly from one application to another, making a surfactant work well in one application but very badly in another one. There exists no "ultimate and universal" surfactant and such a molecule will surely never be found.<sup>2</sup>

There is a wide variety in possible hydrophobic and hydrophilic groups available for the design of new surfactants. Progress in synthetic technology and the development of new raw materials will even increase the number of theoretically and practically possible combinations of hydrophobic and hydrophilic groups in the future. Although the surfactant sector represents already a "mature" part of the chemical industry, these possibilities in the design of new tailor-made surfactants offer still large space for further research and growth.<sup>2</sup> Next to the development of new surfactants, research should also be carried out to improve existing process technologies in surfactant synthesis.<sup>39</sup>

However, despite this large playground for possible new surfactant structures, manufacturers are always restricted by economic and legal guidelines as well as social demands.

The market always demands lower-cost and higher-performing products.<sup>39</sup> Simultaneously, consumers show an increased demand for green products made of renewable raw materials and energy questions become more important with regard to the manufacture and application of surfactant containing products.<sup>2</sup> Additionally, legislation (e.g. (Eco)toxicity and biodegradability) concerning surfactants and surfactant containing products has to be considered.<sup>32, 40</sup> As a consequence, next to exhibiting an equal or increased performance, new surfactants should meet the following criteria: be easily and cheaply produced in large amounts, be low (eco)toxic and readily biodegradable, and be favorably produced from renewable raw materials. An example fulfilling these criteria are sophorolipids, which are the first bio-surfactants available on industrial scale and were recently commercialized by Evonik Industries.<sup>41, 42</sup>

With regard to these legal, environmental and economic requirements as well as social expectations for chemical products and technical processes, some possible areas of research could be:

- low toxic, natural/oleochemical-based and biodegradable surfactants that replace more toxic, petrochemical-based and less biodegradable ones at the same or higher functionality<sup>2</sup>
- surfactants that enable processes at lower temperatures to save energy (e.g. new surfactants that permit washing at lower temperatures)<sup>2</sup>
- multifunctional surfactants (e.g. detergent and fabric softener in one molecule) to save raw materials and costs<sup>2</sup>
- new strategies and technologies in present surfactant synthesis to save energy, reduce costs and decrease personal and environmental risks (e.g. improvement of existing manufacturing processes by new catalysts)<sup>39</sup>
- higher-performing surfactants that work at lower concentrations to save raw materials and costs<sup>39</sup>
- tailor-made surfactants for new (high-tech) applications

The experimental parts of this thesis are driven by some of these considerations.

First, only low toxic and "ready biodegradable" surfactants based on renewable raw materials are used.

The first main part (chapter 3), highly translucent and stable solutions of NaOI and RebA at neutral pH and room temperature, shows that natural long chain soaps can be the basis for aqueous formulations at neutral pH value. Maybe, these findings make it possible to replace some synthetic surfactants currently used in such applications by simple soaps.

The second main part (chapter 4 to chapter 7), which is about the reduction of the Krafft temperature of alkyl sulfates/soaps using choline derivatives as counter ion, is aimed at making more surface active and more efficient long chain surfactants water soluble at lower temperatures. Hopefully, this way, in some applications, the amount of surfactant can be reduced and/or energy can be saved.

## 2.1.4 Adsorption of surfactants to liquid surfaces/interfaces

The word surfactant is an abbreviation for surface active agent. The tendency of a surfactant to adsorb to surfaces or interfaces at low concentrations can be explained by its amphiphilic structure. Dissolving a surfactant in a solvent causes a distortion of the solvent structure by the lyophobic group of the amphiphile which leads to an increase of the overall free energy of the system ("hydrophobic effect", see 2.1.5.1). The free energy of the system can be reduced by "removing" the lyophobic part of the molecule from solution. This can be realized by adsorption of the surfactant molecules to surfaces/interfaces or by self-aggregation within the bulk phase in a way that the contact between the solvent and the lyophobic group is diminished.<sup>5, 43</sup>

### 2.1.4.1 Surface and interfacial tensions

A surface or an interface can be described as a boundary between two immiscible phases. In general, interfaces involving one vapor and one condensed phase (solid/vapor and liquid/vapor) are termed surfaces, while solid/solid, solid/liquid and liquid/liquid phase boundaries are termed interfaces.<sup>5, 43</sup>

The surface tension  $\gamma$  of liquids is related to attractive cohesive interactions (dispersion forces, dipole-dipole interactions, dipole-induced-dipole interactions and hydrogen bonding) that occur in a pure substance. Molecules in the bulk phase experience equal attractive forces in all directions. However, for molecules at the surface these attractive interactions are missing in one direction leading to a net force towards the bulk (see left side **Figure 2-5**). This asymmetry is the origin of the surface energy and is expressed as the surface tension. In other words, the surface tension or surface free energy is the minimum energy that is needed to expand a surface by a unit area.

The same is true for the interface between two immiscible fluids. Again, due to unequal attractive forces between the molecules in the bulk and at the interface, the potential free energy for the molecules in the bulk phases is lower than the potential free energy of the molecules facing each other at the interface (see right side **Figure 2-5**). The more dense structure of a liquid phase compared to a gas phase usually leads to less imbalanced forces acting on interfacial molecules (small attractive forces are better than none!). As a result, interfacial tension values are usually lower, even if the molecules are chemically very different.<sup>5, 44, 45</sup>

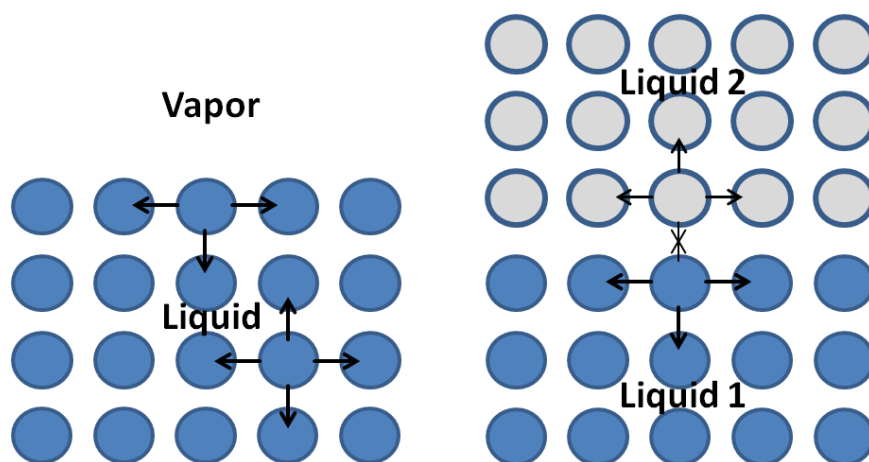


**Figure 2-5:** left: schematic illustration of the attractive forces acting on a molecule in the bulk and at the surface; right: schematic illustration of the different attractive forces leading to an interfacial tension between two liquids. The figures are based on reference 45.

#### 2.1.4.2 Surfactant adsorption and reduction of the surface/interfacial tension

As already mentioned, at low concentrations surfactants readily adsorb at surfaces or interfaces. This process is accompanied by a change in the surface/interfacial tension, respectively free energy.

##### 2.1.4.2.1 Efficiency and effectiveness of surfactant surface tension reduction

The surface tension of an aqueous solutions decreases with increasing concentration of surfactant in the aqueous phase until a more or less constant value is observed (see **Figure 2-6**). To compare the performance of surfactants in reducing the surface/interfacial tension, it is necessary to distinguish between the efficiency and the effectiveness of a surfactant.

The efficiency in surface tension reduction is determined by the concentration of surfactant in the bulk phase required to reduce the surface tension by a certain amount. Usually, the efficiency is expressed by the  $pC_{20}$  value, i.e. the log of the bulk surfactant concentration that is necessary to reduce the surface tension by 20 mN/m (see **Figure 2-6**). Generally, for surfactants in aqueous solutions, the efficiency to adsorb on surfaces increases with increasing hydrophobic character of the surfactant and can be related to the standard free energy of surfactant transfer from the bulk to the surface.

That means, an additional methylene group attached to a linear saturated hydrocarbon chain increases the efficiency, whereas branching or unsaturation of the hydrophobic chain at a constant number of C atoms decreases surfactant's efficiency. For ionic surfactants, addition of salt increases surfactant's efficiency due to its charge screening effect between the ionic groups at the interface. Accordingly, the replacement of an ionic head group by a nonionic one without varying the hydrophobic group also results in a strong increase in efficiency.<sup>5, 44</sup>

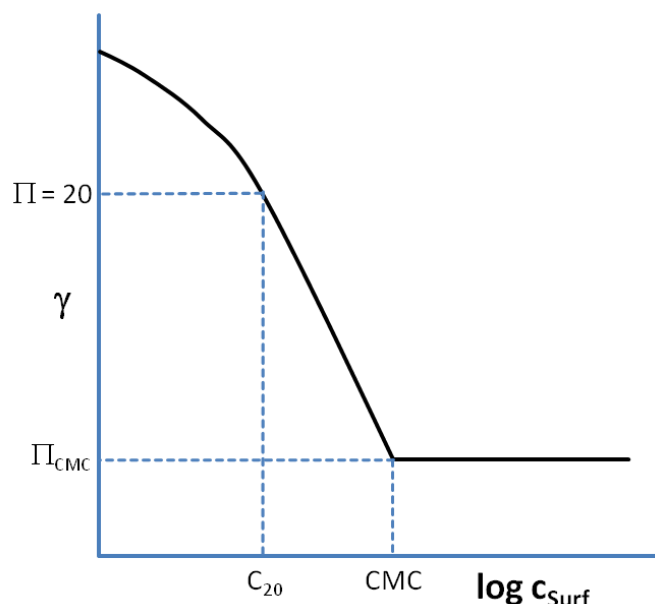


**Figure 2-6:** Schematic illustration of the general course of the surface tension  $\gamma$  of an aqueous solution vs.  $\log$  of the surfactant concentration in the bulk.  $C_{20}$  represents the surfactant concentration needed to decrease  $\gamma$  by 20 mN/m, CMC is the critical micellar concentration.

The effectiveness in surface tension reduction is determined by the maximum surface tension reduction that a surfactant can achieve independently of its bulk concentration. Usually, the effectiveness is expressed by the surface pressure  $\Pi_{\text{CMC}}$  ( $= \gamma_0 - \gamma_{\text{CMC}}$ ) measured at the critical micellar concentration, since the reduction of the surface tension beyond the cmc is negligible (see **Figure 2-6**). While the efficiency of a surfactant in surface tension reduction is mainly thermodynamically controlled by the structure of the hydrophobic moiety, the effectiveness is more related to the size of the hydrophobic and hydrophilic groups of the surfactant at the surface. The reduction of the surface tension is due to the substitution of solvent molecules by surfactant molecules at the surface. Therefore, the closer the surfactants can be packed at the surface, i.e. the smaller their effective surface areas, the lower the surface tension should be. Consequently, the higher the effectiveness of the surfactant in surface tension reduction should be.

This can be seen by the addition of salt to ionic surfactant solutions. The salt's screening effect leads to an increase in effectiveness, since the surfactant molecules can be packed more closely because of reduced repulsions between the charged head groups. The same is true for nonionic alcohol ethoxylates, where the effectiveness decreases with increasing number of EO groups (increasing head group size/effective surface area) for a given hydrophobic group. For both surfactant types, an increase in the linear saturated alkyl chain for a given head group has only little effect on the effectiveness of the surfactant. Moreover, for ionic surfactants, it is observed that branching in the hydrophobic alkyl chain leads to an increased effectiveness, although the effective surface area of the surfactant increases.<sup>5, 44</sup>

#### 2.1.4.2.2 Adsorption theory - the Gibbs adsorption isotherm

A general thermodynamic description of the adsorption phenomena explained on the foregoing pages can be given by the Gibbs adsorption isotherm.

The concept of the Gibbs treatment requires the division of the system into three phases: two bulk phases with defined volumes  $V_i$  and concentrations  $c_i$  for each compound, and an interface between them. As mentioned above, amphiphilic molecules reduce the surface tension by adsorption to interfaces. Therefore, a molar surface excess concentration of a component  $\Gamma_i$  can be defined as follows.<sup>46, 47</sup>

$$\Gamma_i = \frac{n_i^\gamma}{A} \quad (2-1)$$

where  $n_i^\gamma$  is the excess molar amount of a component in the interface and  $A$  is the area of the interface.

The fundamental interfacial thermodynamic equation for the Gibbs free energy can be given as:<sup>48</sup>

$$dG^\gamma = -S^\gamma dT + V^\gamma dp - Ad\gamma + \sum_i \mu_i dn_i^\gamma \quad (2-2)$$

where  $T$  is the temperature,  $S$  is the entropy,  $A$  is the area of the interface,  $\gamma$  is the interfacial tension,  $p$  is the pressure,  $V$  is the volume,  $\mu$  the chemical potential and  $n$  the amount of substance.

Further, the change in the interfacial Gibbs free energy  $dG^\gamma$  can also be written as:<sup>48</sup>

$$dG^\gamma = \sum \mu_i dn_i^\gamma + \sum n_i^\gamma d\mu_i \quad (2-3)$$

Comparison of equation 2-3 with equation 2-2 at constant pressure and temperature leads to the general form of the Gibbs adsorption isotherm:

$$-d\gamma = \sum_i \frac{n_i^\gamma}{A} d\mu_i = \sum_i \Gamma_i d\mu_i \quad (2-4)$$

The Gibbs adsorption isotherm relates the change in surface tension,  $d\gamma$ , to changes in the chemical potential in the bulk phase,  $d\mu_i$ , through the surface excess concentration  $\Gamma_i$ . Equation 2-4 is generally thermodynamically valid for adsorption processes.<sup>46, 47</sup>

For a binary liquid mixture, e.g. surfactant and water, reasonable locating of the dividing surface, so that the surface excess concentration of water  $\Gamma_1 = 0$  and  $d\mu_2 = RT d \ln c_2$  for low surfactant concentrations, the Gibbs adsorption isotherm is given as:<sup>46, 47</sup>

$$\Gamma_2 = - \frac{d\gamma}{RT d \ln c_2} \quad (2-5)$$

This term is true for uncharged species, for ionic species being able to dissociate in solution equation 2-5 has to be adapted with regard to the system (e.g. salt content). Equation 2-5 allows us to determine the surface excess concentration  $\Gamma_2$  of the surfactant by measuring the surface tension of a solution with varying surfactant concentration.

While aqueous surfactant solutions yield positive surface excess concentrations  $\Gamma$ , aqueous electrolyte solutions, e.g. NaCl solutions, can show an increase in surface tension with increasing concentration in solution. This results in negative surface excess concentrations  $\Gamma$ .<sup>46, 47</sup>

### 2.1.5 Self-assembly of surfactants in aqueous solutions

As already mentioned, next to adsorption to interfaces, surfactants are able to reduce the free energy in aqueous solutions by the formation of aggregates.

Within these structures, the molecules self-assemble in a way that the hydrophobic groups are directed to the interior of the aggregate and with the polar head groups directed towards the surrounding water molecules.

The general characteristics of self-assembly of amphiphilic molecules in water can be summarized as:

1. aggregates form spontaneously
2. aggregation is a start-stop process
3. aggregates have well-defined properties

It is important to note that surfactant self-assembly is a physicochemical process, meaning that the surfactant molecules are associated physically and not chemically. This is very important, since this allows the aggregates to change their size and shape with respect to changes in the system, e.g. concentration, salt content or temperature.<sup>20</sup>

#### 2.1.5.1 Critical micellar concentration and general structure of micelles

Usually, the first aggregation structures being formed with increasing surfactant concentration in aqueous solutions are micelles. They spontaneously form above a certain concentration of surfactant in solution, the so-called critical micellar concentration (cmc).<sup>4, 6, 20, 49, 50</sup>

The formation of micelles (as well as surfactant adsorption) can be understood in terms of the "hydrophobic effect". It describes the interactions between water and a non-polar solute, respectively the hydrophobic group of the surfactant molecule. The hydrophobic effect arises from two contributions.<sup>50-56</sup>

- formation of a cavity in the bulk water to accommodate the hydrophobic group. The associated breakup of strong hydrogen bonds generates a large positive enthalpy (free energy) that is nearly temperature independent.

- structuring (or rearrangement) of the water molecules around the hydrophobic group leading to a negative enthalpy and a positive entropy that partly compensate each other. This part contributes an overall (small) negative free energy and hence increases the solubility of hydrocarbons in water. This contribution is temperature dependent and decreases with increasing temperature. This renders water a "normal" hydrogen-bonding solvent at very high temperatures.

The positive free energy generated by forming the cavity in water is considerably larger than the energy gain by structuring of the water molecules around the hydrophobic group. Thus, surfactant aggregation and hydrophobic interactions between non-polar solutes in water are mainly due to the strong cohesive interactions between water molecules.

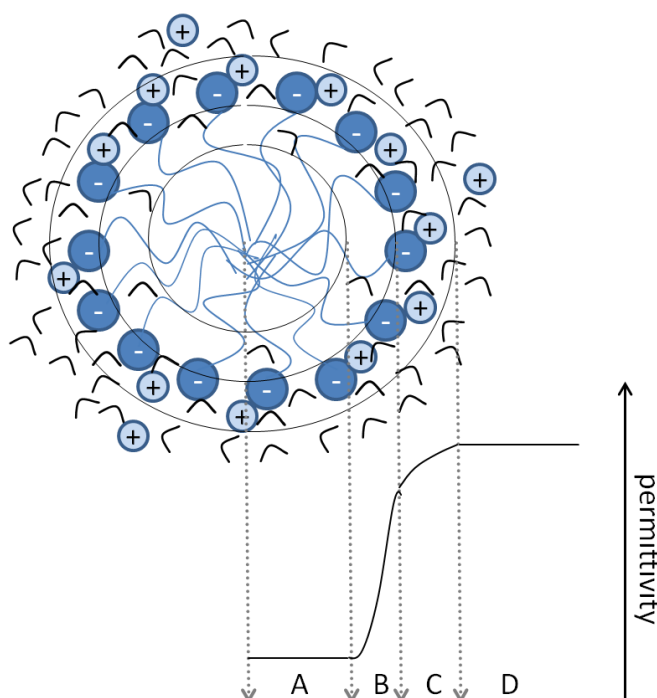


**Figure 2-7:** Simple model of a spherical micelle of an anionic surfactant. The curved lines represent the surfactant's hydrophobic group, the small spheres the counter ion and the big spheres the anionic head groups. The small hooks illustrate water molecules. The extent of the hydrophobic core, the palisade layer and the outer polar layer are also shown. The lower graph represent the course of the permittivity from the interior core to bulk water. The figure is based on reference 57.

A simple model of a spherical ionic micelle is shown in **Figure 2-7**. Different regions, in which a micelle can be divided are also illustrated as well as the course of the permittivity. In the interior hydrophobic core (region A), the hydrophobic groups are in a liquid-like oil state, no water molecules are present and the permittivity is very low ( $\approx 1$ ). Region C is the outer polar layer and made up by the head groups, condensed

counter ions as well as the water molecules "bound" to the head groups. The permittivity increases slowly until the value of pure water is reached ( $\approx 80$ ). The transition region B from pure hydrophobic to pure polar region is called "palisade layer" and comprises the outer micellar core being penetrated by water. Here the permittivity steeply increases because of an increase of the local water volume fraction. Region D corresponds to bulk water with little surfactant molecules and counter ions.<sup>57</sup>

The abrupt change of some physico-chemical properties of a surfactant solution associated with the formation of micelles allows us to determine cmc values. **Figure 2-8** shows the typical course of some physico-chemical properties for an ionic surfactant.<sup>58, 59</sup>

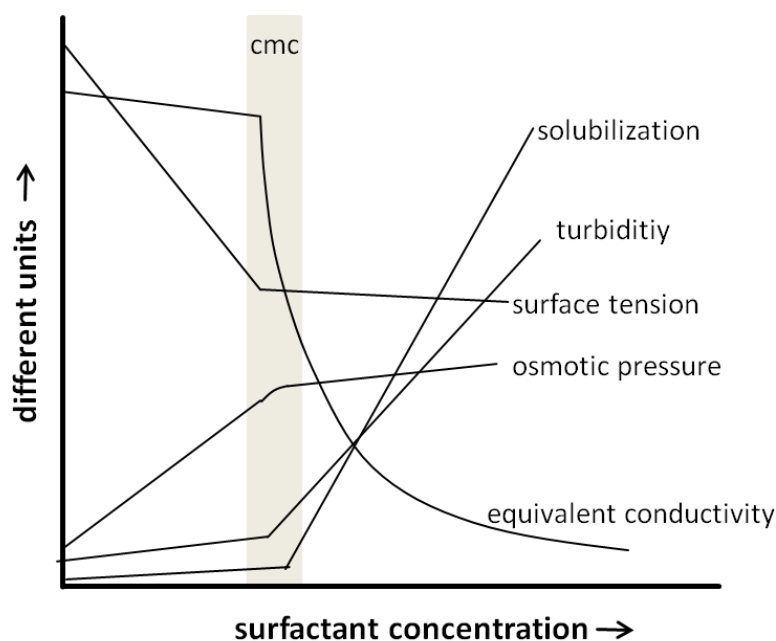


**Figure 2-8:** Schematic variation of different physico-chemical properties of aqueous surfactant solutions with increasing surfactant concentration. The cmc range is illustrated by the colored area. The figure is based on reference 49.

The factors promoting micellization, i.e. hydrophobic interactions ("hydrophobic effect"), and counteracting micellization, i.e. head group repulsions, are strongly dependent on the molecular structure of the surfactant and the system properties (salt content, temperature,...). Therefore, some general trends can be found when comparing surfactant structure and system properties to cmc values:

- For a homologous series of surfactants the cmc decreases with increasing number of carbon atoms in the hydrophobic chain due to an increased "hydrophobic effect". This can be described by Kleven's equation (equation

2-6), where A and B are surfactant specific constants and n is the number of carbon atoms in the alkyl chain.

$$\log(cmc) = A - Bn \quad (2-6)$$

This effect is more pronounced for nonionic surfactants than for ionic ones. As a general rule, the cmc decreases by a factor of 2 for ionics and by a factor of 3 for nonionics by adding one methylene group to the hydrophobic alkyl chain.<sup>6, 58, 60, 61</sup>

- Branching or introduction of a double bond into a surfactant's hydrophobic group with a constant amount of carbon atoms increases the cmc due to a reduced "hydrophobic effect".<sup>6, 49, 60, 61</sup>
- For a given hydrophobic group, non ionic surfactants possess much lower cmc values than ionic ones because of the missing electrostatic repulsions.<sup>58, 60, 61</sup>
- The cmc of ionic surfactants is strongly dependent on counter ion head group interactions as well as the valency of the counter ion. Stronger counter ion head group interactions lead to lower cmc values because of a reduced net charge of the ionic head group.<sup>6, 58, 60, 61</sup> For the "soft" alkyl sulfate group the cmc decreases as follows:  $Li^+ > Na^+ > K^+ > Cs^+ > N(CH_3)_4^+ \approx Ch^+$ .<sup>29, 60, 62, 63</sup> This agrees well with the predicted counter ion head group interactions by Collins' law of matching water affinities (see section 2.2).
- Addition of salt strongly reduces the cmc values of ionic surfactants.<sup>6, 49, 58, 60</sup>
- Cmc values of ionic surfactants show only a small temperature dependence with a minimum around 25 °C. Ethoxylated nonionics however show a strong decrease in cmc with increasing temperature.<sup>58, 61</sup>
- The addition of polar organic co-solutes, like alcohols or amines, can decrease or increase cmc values depending on their chemical structure and solubility behavior in the aqueous solution.

Highly water soluble polar organic compounds, like ethanol, dioxane or acetone, which act as co-solvents and do not or hardly partition into the interior of the micelle, increase the cmc of a surfactant. This can be explained by an increased surfactant solubility due to a weakening of the "hydrophobic effect".

With decreasing water solubility, the polar organic co-solute prefers solubilization inside the micelle. This leads to decreased cmc values, since the micelle is stabilized mainly by decreasing the repulsion of the hydrophilic

head groups of the surfactant. This effect can be nicely observed for medium to long chain alcohols.<sup>6, 60, 61</sup>

### 2.1.5.2 Thermodynamics and kinetics of micelle formation

In literature, micellization is often described by two different thermodynamic models that have gained acceptance as useful (although not necessarily accurate) to understand the energetic basis of the process. These models are the phase separation model and the mass action model. Both models lead to the same useful approximation for the standard free energy of micelle formation (for a non-ionic surfactant) that can be written as:<sup>6, 58, 61</sup>

$$\Delta G_{mic}^0 = RT \ln cmc \quad (2-7)$$

where R is the gas constant and T the temperature. For ionic surfactants, equation 2-7 has to be adapted by introducing the degree of counter ion dissociation.

It must be noted that these models, although having proved very useful, cannot be extended to explain such phenomena as bilayers, cylindrical micelles or vesicles. Particularly, they have not been able to theoretically quantify the part of the molecular geometry in predicting the structures and shape.<sup>6</sup>

In real systems, micelles are not perfectly monodisperse and an aggregation number distribution is present. This can be described by step-wise association models with individual equilibrium constants K for each association step.<sup>50, 58, 61</sup>

Further, a micelle must be regarded as a dynamic species that has a defined, but finite, lifetime. For dilute solutions, kinetic data of micelles can be measured by fast relaxation techniques, like pressure or temperature jump.

Typical micelle lifetimes lay between  $10^{-2}$  –  $10$  s corresponding to a breakdown/formation rate of  $10^{-1}$  –  $10^2$  s<sup>-1</sup>. The timescale for surfactant monomer exchange between different micelles ranges from ms to  $\mu$ s. Both of these processes become much slower as the surfactant's hydrophobic chain length is increased. Because of this fast exchange of monomers between the micelle and the bulk solution, micelles are very dynamic and disordered aggregates exhibiting a continuous movement of molecules inwards and outwards through the interface. For an ionic surfactant, usually having about 70 – 80 % of counter ions loosely "bound" to the micelle surface, the exchange between "bound" and free counter ions proceeds on a time scale of  $10^{-9}$  s.<sup>50, 58</sup>

### 2.1.5.3 Surfactant solubility and Krafft temperature

The solubility of ionic surfactants is dramatically temperature dependent and increases heavily within a narrow temperature range (see **Figure 2-9**). This behavior is called the "Krafft Phenomenon". The temperature, at which the surfactant solubility strongly increases is called "Krafft temperature" ( $T_{Kr}$ ) or "Krafft point".<sup>4, 20, 64</sup>

$T_{Kr}$  is often defined and experimentally determined as the clearing temperature of a 1 wt% aqueous surfactant solution.<sup>65</sup>

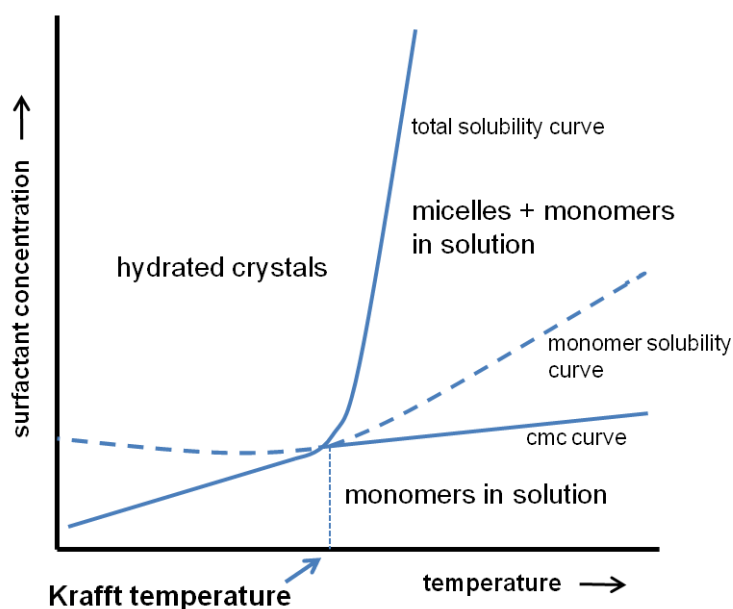


**Figure 2-9:** Temperature-dependence of the cmc, monomer solubility and total solubility of a surfactant. The intersection of the surfactant monomer solubility curve and the cmc curve is referred to the Krafft temperature ( $T_{Kr}$ ). The figure is based on reference 4.

The Krafft temperature is determined by the interplay of two opposing thermodynamic forces. One is the free energy of the micellar solution and the other one the free energy of the surfactants solid crystalline state. The free energy of the micellar solution appears to vary on slightly between different cases, like different chain lengths or counter ions. However, the free energy of the crystalline state can vary heavily due to packing effects.<sup>4</sup>

Usually, in applications a surfactant should be used at or above its cmc and, as a result, above its  $T_{Kr}$ . Too low solubility renders the surfactant ineffective for most applications and non-dissolved surfactant crystals in the solution may even disturb. Unfortunately,  $T_{Kr}$  increases heavily with increasing linear alkyl chain of the surfactant and restricts the use of longer chain surfactants in many low temperature applications. For example, common sodium alkyl sulfates (NaSXX) are only sufficiently water soluble at room temperature up to sodium dodecyl sulfate (NaS12). The longer chain homologues exhibit  $T_{Kr}$  values above room-temperature.<sup>66</sup> The

same is true for simple sodium soaps.<sup>67</sup> Since longer chain surfactants are generally more efficient, it is desirable to reduce  $T_{Kr}$  of longer chain surfactants. As explained above, attempts to reduce  $T_{Kr}$  of a given surfactant should aim at increasing the free energy of the surfactant's solid state. This can be achieved by hindrance of a regular crystal packing of the surfactant. Common strategies to increase the free energy of the solid state and therefore  $T_{Kr}$  are:

- Branching of the alkyl chain or introduction of a double bond in the alkyl chain. In this case, regular crystal packing of the solid surfactant is hampered by reducing symmetry of the hydrophobic chain.<sup>4</sup>
- Changing the counter ion. Here, two situations have to be considered:
  - For relatively small and symmetric ions, a difference in specific head group counter ion interactions can change the free energy of the surfactants solid state. The stronger the counter ion head group interaction, the lower the free energy.<sup>62</sup>
  - Using bulky (and asymmetric) counter ions, again the formation of a regular crystal lattice is prevented.<sup>62</sup>
- Introducing a polar segment, commonly an oxyethylene(EO) group, between the head group and the hydrophobic chain.<sup>4</sup> The increase in the free energy of the surfactant solid state can be explained by the high flexibility of the oxyethylene group that hampers the crystal formation of the surfactant.<sup>68, 69</sup>

It must be mentioned that the listed structural changes of the surfactant (i.e., loss of the straight chain or additional EO groups) can deteriorate its performance in a certain application, even if the total number of C-atoms in the hydrophobic surfactant moiety is increased. Thus, often there has to be made a compromise in surfactant design for a certain application.

In general, the following statements on the Krafft temperature are valid:

- $T_{Kr}$  increases heavily with increasing linear alkyl chain length. The decrease displays an even-odd effect.<sup>4, 44</sup>
- For a given hydrophobic group,  $T_{Kr}$  is strongly dependent on the counter ion and the head group:
  - Divalent counter ions exhibit higher  $T_{Kr}$  values than monovalent ones.<sup>4, 12, 20</sup>

- For alkali alkyl carboxylates,  $T_{Kr}$  increases with decreasing size of the counter ion ( $Li^+ > Na^+ > K^+ > Cs^+$ ), whereas the opposite is true for alkyl sulfates.<sup>4, 70</sup> This is in line with Collins' concept of matching water affinities (see section 2.2), since stronger counter ion - head group interactions lead to higher  $T_{Kr}$ .<sup>62</sup>
- Bulky counter ions, like quaternary ammonium ions (e.g. choline), can considerably reduce  $T_{Kr}$  compared to common alkali ions by preventing a regular crystal packing in the solid state.<sup>62, 70-72</sup> For example, changing the counter from sodium (Na) to choline (Ch) for hexadecyl sulfate (S16) respectively palmitate (C16) reduces  $T_{Kr}$  of these long chain surfactants below room temperature ( $NaS16 \rightarrow ChS16 = 45\text{ °C} \rightarrow 16\text{ °C}$ ;  $NaC16 \rightarrow ChC16 = 60\text{ °C} \rightarrow 12\text{ °C}$ ).<sup>67, 73</sup>
- Introducing a double bond, branching or a polar segment into the alkyl chain results in lower  $T_{Kr}$  values. Again, the formation of a regular crystal lattice is prevented.<sup>4, 44</sup>
- The addition of a third component can have drastic effects on  $T_{Kr}$ :
  - Addition of polar co-solutes, like alcohols, generally decreases  $T_{Kr}$  of a surfactant.<sup>4</sup> This can either be by increasing the surfactant monomer solubility at (nearly) constant cmc values or by decreasing the cmc value at (nearly) constant surfactant monomer solubility. (compare to the effect of polar co-solutes on the cmc in section 2.1.5.1).<sup>74-76</sup> A detailed discussion of this for short and medium chain alcohols is given in reference <sup>74</sup>.
  - The addition of salts can both decrease and increase  $T_{Kr}$  of an ionic surfactant. Here, the situation must be carefully analyzed with regard to the initial surfactant (ionic head group and counter ion) and the added salt.

To understand the effect of added salt on  $T_{Kr}$  of anionic surfactants, one has to analyze the specific interactions of the competing cations with the surfactant head group and/or the whole micelle. Here, it is necessary to distinguish between organic ions possessing a hydrophobic moiety and simple inorganic ions. This will be discussed in detail in Chapter 5.

### 2.1.6 Application in laundry detergency

The main share ( $\approx 50\%$ ) of the global surfactant consumption is made up by the household cleaning sector and laundry detergents contribute by far for the largest portion of this domestic cleaning products market.<sup>21, 30, 77</sup>

According to Smulders<sup>78</sup>, laundry detergency in the broadest sense can be defined as both the removal by water or aqueous surfactant solution of poorly soluble matter and the dissolution of water-soluble impurities from textile surfaces. Nowadays, laundry cleaning products are very complex formulations and can consist of up to 20 individual components, of which each has very specific functions during the washing process. The most important ingredient are surfactants, which are present in all kind of detergents.<sup>39, 79</sup> This fact is due to the surfactant's inherent feature to adsorb at interfaces and modify the interfacial properties, which is a prerequisite for effective cleaning.<sup>80-82</sup>

Laundry detergency is a very complex process that involves interactions between aqueous detergent solutions, soils and fabric surfaces.<sup>82</sup> Three elements are present in every detergency process: (1) the substrate, i.e. the textile that has to be cleaned, (2) the soil, i.e. the material that has to be removed during the detergency process and (3) the aqueous cleaning solution.<sup>80</sup> It is impossible to develop or define a unified mechanism for the cleaning process. This arises from the almost infinite variety of the first two elements. For example, the fabric can be hydrophilic or hydrophobic and vary in their structure, the soil can be liquid or solid, nonpolar or ionic and inert or reactive towards the cleaning solution. Consequently, there exists a number of different mechanisms that are dependent on the nature of substrate and soil.<sup>80</sup> Further, the cleaning process can be divided into the primary step of soil removal from the substrate and a the secondary step of stabilization of the soil in the washing solution and prevention of redeposition on the substrate.<sup>78, 80</sup> In the following, the main mechanisms of liquid and solid/particulate soil removal involving surfactant action are shortly mentioned and explained.

There exist two main models that explain the removal of liquid (oily) soil by detergent solutions, namely the "roll-up" (see **Figure 2-10**, left) and the "emulsification" mechanism (see **Figure 2-10**, right).

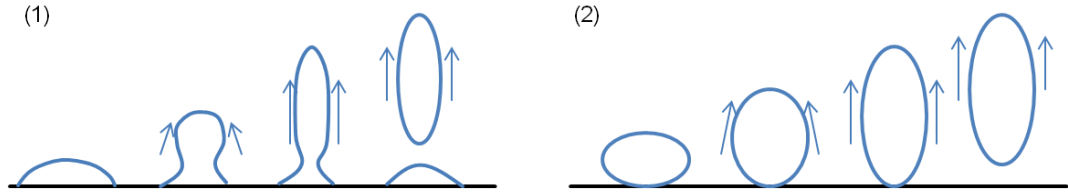


**Figure 2-10:** Schematic illustration of the two main mechanisms of liquid soil removal from flat surfaces. (1): “emulsification” mechanism. (2): “roll-up” mechanism. This figure is based on reference 82.

Let us first consider the roll-up mechanism. Here, the interaction of the textile with the oily soil and the aqueous cleaning solution is most important. The precondition for the roll-up mechanism to become active is that wetting of the substrate by the detergent solution is possible, i.e. the substrate is not completely covered by oily soil. To get insight in this mechanism, Young’s equation has to be considered (equation 2-8), which relates the different interfacial tensions occurring in the washing system to each other:

$$\cos\Theta = \frac{\gamma_{SC} - \gamma_{SO}}{\gamma_{OC}} \quad (2-8)$$

where  $\gamma_{SC}$  is the interfacial tension between the substrate and the cleaning solution,  $\gamma_{SO}$  the interfacial tension between the substrate and the oily soil and  $\gamma_{OC}$  is the interfacial tension between the oily soil and the cleaning solution.  $\Theta$  is the contact angle between the oil and the substrate. To gain complete removal of the oil droplet,  $\Theta$  has to become  $180^\circ$ , which is equal to the condition, that  $\gamma_{SO}$  equals the sum of  $\gamma_{SC}$  and  $\gamma_{OC}$ . Since surfactant adsorption to the oil and the substrate, with the hydrophilic head group towards the cleaning solution, lowers  $\gamma_{SC}$  and  $\gamma_{OC}$ , the contact angle  $\Theta$  increases with increasing surfactant adsorption. The evolution of the contact angle  $\Theta$  as well as of the important interfacial tensions during oil removing by the detergent solution via roll-up is shown in **Figure 2-11**. If the contact angle does not reach  $180^\circ$ , but is bigger than  $90^\circ$ , some hydraulic current or agitation can help to remove the oil droplet.<sup>80, 82</sup>

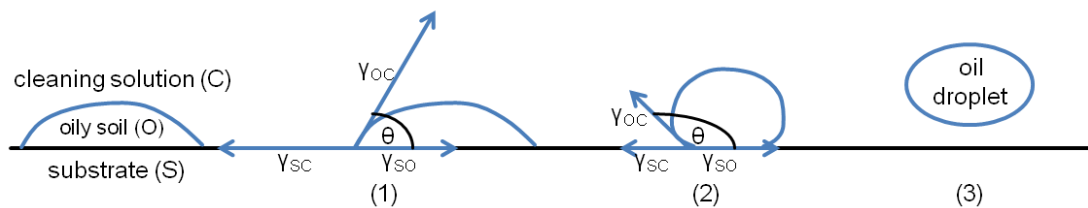


**Figure 2-11:** Different stages during the “roll-up” mechanism. (1): initial situation before surfactant adsorption. (2): situation during surfactant adsorption,  $\gamma_{SC}$  and  $\gamma_{OC}$  decrease. (3): the oil droplet is completely lifted off from the surface.

If the substrate is initially completely covered by oily soil or the contact angle  $\Theta$  after surfactant adsorption is smaller than  $90^\circ$ , which is frequently observed for quite hydrophobic substrates like polyester, the emulsification mechanism becomes important. That kind of liquid soil removal is promoted by low oil-cleaning solution interfacial tensions, which allows easy deformation of the oil film. In general, hydraulic current or agitation are necessary to enable this mechanism.<sup>80, 82</sup> The emulsification mechanism usually takes place at the interface between the oily soil and the cleaning solution. Therefore, it is directly affected by the corresponding oily soil-water-surfactant phase behavior. In many studies, it could be shown that maximum soil removal occurs, if an intermediate (liquid crystal or microemulsion) phase is formed at the oily soil-cleaning solution interface during the washing process. After reaching a certain size, these intermediate phases are broken off and emulsified in the cleaning solution.<sup>82</sup>

Oily soils can also be directly solubilized into surfactant micelles, if the surfactant (mixture) is used above its cmc. As it is the case for emulsification, the solubilization rate can be enhanced, if surfactant-rich liquid crystalline phases are present in the washing solution. Such phases exist, for example, in aqueous solutions of nonionic surfactants above their cloud temperature.<sup>82</sup>

The main function of surfactants in solid (e.g. crystallized organic material) or particulate (inorganic minerals) soil removal is the reduction of the adhesion forces between the soil and the substrate caused by van der Waals attractions. Anionic surfactants reduce adhesion and facilitate soil removal by adsorbing on both the substrate and the solid soil and the accompanied formation of electrical double layers of equal sign (see **Figure 2-12**, left). For nonionic surfactants, which do hardly exhibit an effect on the surface charge during absorption, the development of a disjoining pressure during surfactant adsorption on the soil particle and the substrate is the decisive factor (see **Figure 2-12**, right). Obviously, this effect is also present with ionic surfactants. Although the two mentioned mechanisms reduce the net adhesion between the solid particle and the substrate, almost always mechanical work is required to remove the particle from the substrate. Due the hydrodynamic effects close to the substrate surface, larger particles are easier removed than smaller ones.<sup>78, 80</sup>

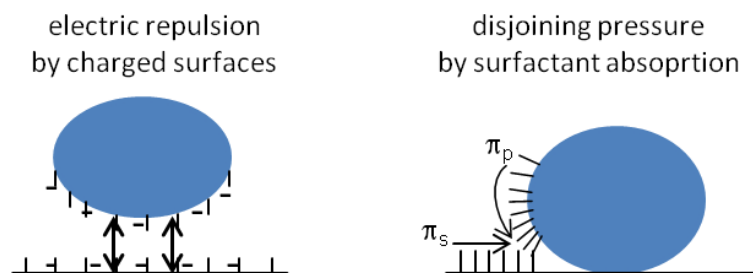


**Figure 2-12:** The two main mechanism for anionic (left) and nonionic surfactants (right) in reducing the adhesion (Van der Waals) forces between a solid particle and a substrate.  $\pi_p$  denotes the splitting pressure of the surfactant layer on the particle and  $\pi_s$  splitting pressure of the surfactant layer on the substrate.

In general, correlations between the chemical structure of a surfactant and its performance in detergency are complicated and hard to make. This arises from the fact that the soils and substrates to be cleaned, the amount of builder within the cleaning solution, the surfactant concentration, the water hardness, the temperature as well as the different mechanisms of soil removal can vary widely between different experiments.<sup>80</sup> Nevertheless, for ionic surfactants, it is usually found that increasing the length of the straight hydrophobic chain leads to a rise in detergency.<sup>29, 79, 80</sup> However, the rise in detergency by increasing the hydrophobic chain of ionic surfactants is strongly limited by the simultaneously reduced water solubility and the susceptibility for precipitation by hard water ions. Thus, optimum detergency is generally achieved by the longest straight-chain surfactants being sufficiently soluble in the cleaning solution under use conditions.<sup>80</sup> Therefore, the above mentioned trend for ionic surfactants with increasing chain length is only observed in millipore water and at (highly) elevated temperatures. This is nicely illustrated for straight chain soaps in an old paper by Preston<sup>83</sup>, who made concentration dependent washing tests at different temperatures with the soap chain length varying from 12 to 18 C-atmos. Another advantage of longer chain surfactants, next to an increase in detergency, is the great reduction of the amount of surfactant being necessary to achieve significant deterative properties compared to shorter chain ones.<sup>29, 83</sup> This is again nicely shown by Preston<sup>83</sup> for alkyl sulfates and soaps.

## **2.2 Specific ion effects and Collins' concept**

Specific ion effects are omnipresent and of great importance in biology, pharmacy and (colloidal) chemistry.<sup>84-86</sup> There are countless publications dealing with specific ion effects, and almost every day, new ones are published.<sup>84</sup> Generally, specific ion effects help to explain the strength of interaction between a certain anion and a certain cation. In ionic surfactant systems, specific ion effects are also of great importance, since they occur between the charged head group and the counter ion. For example, the trend in cmc values for alkali alkyl sulfates (see section 2.1.5.1) as well as the trend in  $T_{Kr}$  values for alkali soaps and alkali alkyl sulfates (see section 2.1.5.3) can be explained by the strength of the individual alkali ion - head group interactions.

More than 100 years ago Hofmeister and co-workers were the first to study ion effects systematically. Their work set a milestone in electrolyte chemistry and was published in a series of seven papers under the German title "Zur Lehre von der Wirkung der Salze".<sup>84, 87</sup> Herein, they methodically investigated the effect of different salts (not ions) on precipitating different proteins, sodium oleate and colloidal ferric oxide beyond the impact of different charges. Based on the results of this extended study, Hofmeister was able to order the salts according to their "water withdrawing capability", which he made responsible for precipitation effect on the different investigated solutes. He concluded: the higher the "water absorbing effect" (nowadays hydration) of a salt, the higher its precipitating effect irrespective of the solute investigated.<sup>84, 87, 88</sup> It must be emphasized that in Hofmeister's papers only an ordering of salts and not of isolated ions is given. Only many years later, the ordering was transferred to isolated ions and is now commonly known as the "Hofmeister series". The typical ordering for cations and anions in the "Hofmeister series" can be found in **Figure 2-13**.<sup>84</sup>

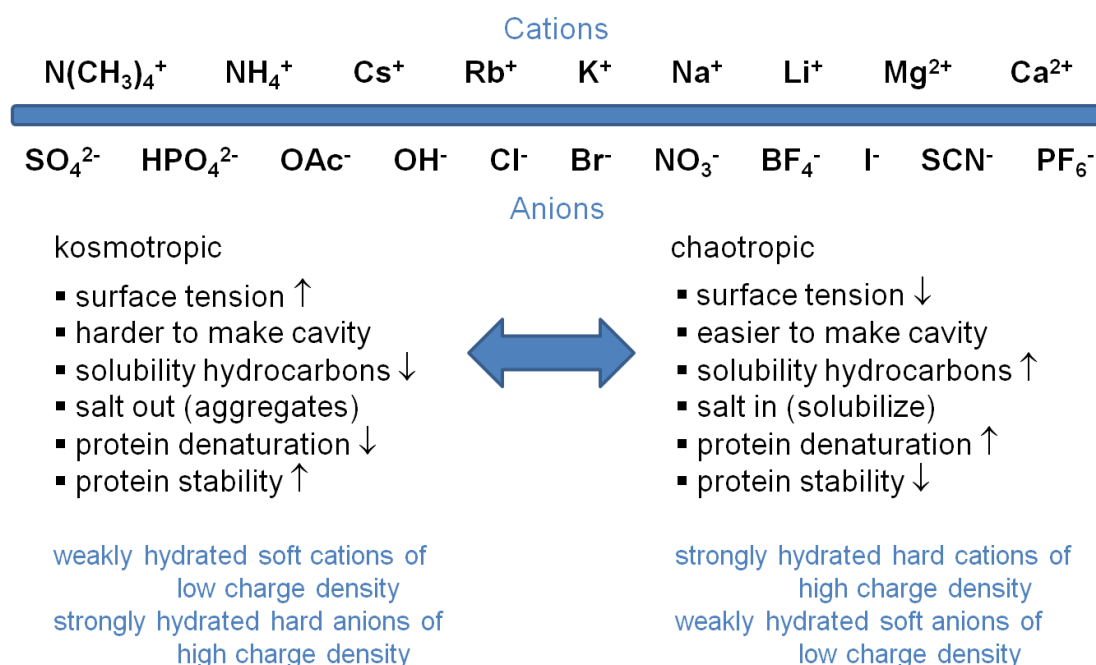


**Figure 2-13:** Typical ordering of anions and cations in the "Hofmeister series". This figure is based on reference 84.

It must be carefully pointed out that this is only a general ordering which is mostly true for biological systems and their general charged groups. If one has a closer look, it appears that the ordering for the cations (soft to hard) is reversed compared to the anions (hard to soft). It will be shown below, that this can be well explained by the different charged groups being present in biological molecules, which differ hardly between common biological compounds. One has to keep in mind that the ordering of this series can change significantly, from bell shaped to reversed, depending on the system's properties respectively ionic groups being present. For example, concerning solubility respectively salting-in and salting-out effects, for many biological systems the above illustrated reversed series for anions and cations is valid. However, this is not the case for simple organic or low polar molecules, like benzene or gases. Here, the effect does not depend on the sign of the charge, small and highly charged ions are mostly salting-out and large and polarisable ions are mostly salting in.<sup>84, 85</sup> Nevertheless, the "Hofmeister series" is frequently used to explain experimental results in biology or chemistry, like protein stability, enzyme activity or bacterial growth.<sup>86, 89, 90</sup>

Originally, it was thought that specific ion effects in water depend a lot on "making" or "breaking" bulk water structure. Ions were classified as "water structure makers" or "water structure breakers" with regard to their effect on the water solubility of a third component (e.g. proteins, macromolecules or other simple inorganic ions). But ongoing research on this topic showed that even polyvalent ions do not alter the

water structure, except in their direct vicinity. These findings show that changes in bulk water structure are not capable of explaining specific ion effects in water.<sup>85, 86, 89</sup>

Thus, new models were (are being) developed that analyze the specific effect of ions more in detail. The main difference to the former water-structuring concept (that does not at all take into the nature of the affected solute) is that direct ion - (charged) solute interactions are made responsible for the observed specific ion effects. The (charged) solute can be a simple inorganic ion, a low molecular uncharged/polar molecule or a complex macromolecule, like proteins. In aqueous solution, specific ion effects are also found for simple inorganic salts.<sup>84-86, 89</sup>

To examine the strength of ion - solute interactions in aqueous solutions, not only the interaction between the different ions (charged groups) has to be considered, but also the interaction between the ions and the surrounding water as well as the interactions between the water molecules themselves. As soon as interfaces are present within the analyzed system, the detailed structure of water itself close these interfaces must be respected. For example, large hydrophobic or polar parts of macromolecules in contact with the aqueous solution can be regarded as an (microscopic) interface. Of course, proper analysis of these interactions requires a very detailed knowledge of the system, i.e. the nature of the ions (charged groups) and the detailed structure of (macro)molecules/interfaces being involved. The most important parameter to evaluate these interactions is the surface charge density of the ions, which is given by the ratio between the charge of the ion and its radius.<sup>85, 86,</sup>

<sup>90</sup> In more complex systems, like macromolecules, more parameters have to be considered.<sup>85</sup> From these considerations, it can be inferred that simple solvent-averaged continuum models for water, utilizing a macroscopic dielectric constant, are not appropriate to describe specific ion effects, because the influence of the water structure is not included. Moreover, they are not capable of accurately describing simple ion specific behaviors like forming contact ion pairs, what is very important to explain specific ion effects.<sup>85, 89</sup>

In 2004, Collins introduced a very simple, but quite powerful model, which considers the points mentioned above. It is called "concept of matching water affinities".<sup>85, 90, 91</sup>

Within this concept, ions are considered as spheres with a point charge in their centers. Furthermore, the ions are ordered according to their interaction with water, compared to pure water - water interactions. Small ions possessing a tightly bound hydration shell are called kosmotropes, whereas large ions possessing a loosely bound hydration shell are named chaotropes. The difference between these two types of ions is defined by the strength of water-water interactions relative to ion - water interactions (see **Figure 2-14** left side). The water molecule is regarded as a

medium-size zwitterion with an anionic portion of ideal size and an cationic portion of ideal size interpolated to the horizontal line in **Figure 2-14**.<sup>85, 90</sup> Furthermore, Collins declares that in aqueous solutions, oppositely charged ions will only form inner sphere ion pairs, if they have a comparable affinity to water.<sup>90, 91</sup> This effect is explained by hydration-dehydration processes.<sup>89</sup> If two kosmotropes meet in solution, the strongly bound hydration shells will break away and the ions will form an inner sphere ion pair, since the interaction between the small ions is stronger than the interaction between the ions and the medium-size water molecules. If two large chaotropes meet in solution, the loosely bound hydration shells will also break down and an inner sphere ion pair will be formed, because the interactions between the medium-size water molecules themselves are stronger than between the large ions and the medium-size water molecules. In the case of one small kosmotrope and one large chaotrope, the interaction between them is not strong enough to cause a breakdown of the small ion's hydration shell. As a result, the formation of an inner sphere ion pair is prohibited.<sup>85, 90</sup> This concept of “like seeks like” is illustrated in **Figure 2-14** at the right side.

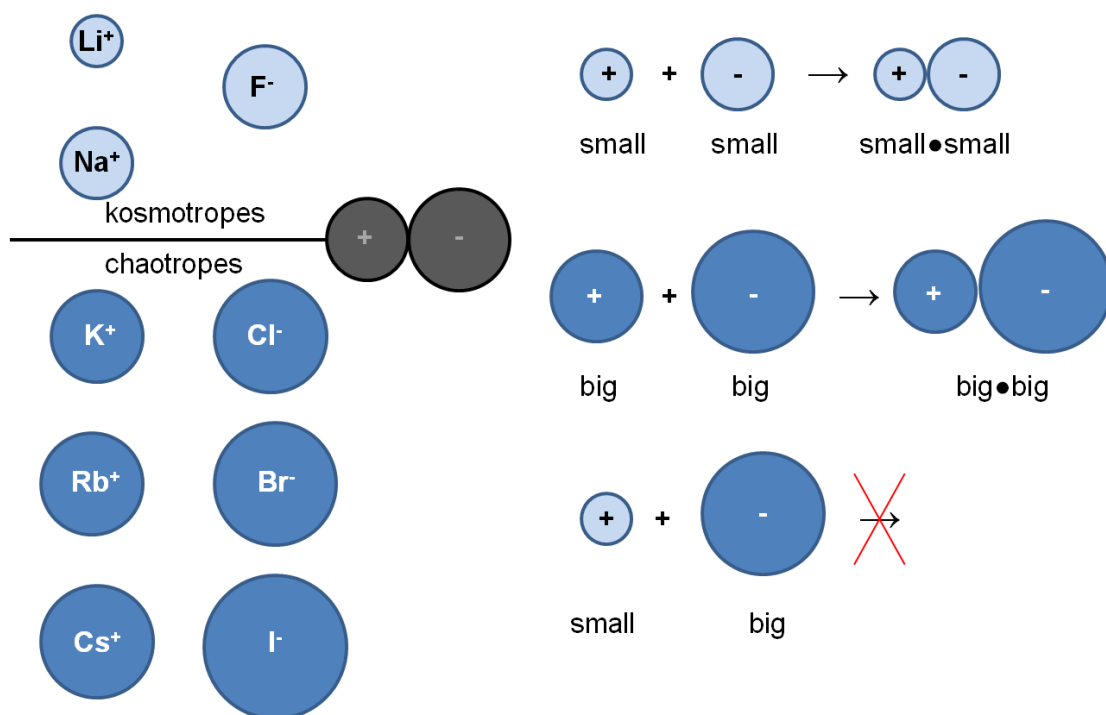


**Figure 2-14:** Left: Division of alkali ions and halide ions into strongly hydrated kosmotropes (above the line) and weakly hydrated chaotropes (below the line). The medium-sized zwitterion in the left illustration represents a water molecule. Ion sizes are drawn true to scale. Right: It is shown that ions have to be similar in size to form inner sphere ion pairs. This figure is based on reference 90.

This concept of “matching water affinities” can both be applied to simple inorganic salt solutions as well as to ions and charged groups on macromolecules occurring in

biology and biochemistry. Despite its simplicity, even for complex colloidal and biological systems, it is a very powerful tool to explain many experimental findings on specific ion effects.<sup>84, 85, 90, 91</sup>

In colloidal chemistry and biological systems, interactions between charged headgroups and ions are most important. Thus, it is very important to have an ordering of typically occurring head groups from chaotropic to kosmotropic according to Collins' concept.<sup>85</sup> Harrison et al. were able to order the cationic headgroups from hard (kosmotropic) to soft (chaotropic) by chromatography experiments.<sup>85, 92</sup> In this work, the trend for the anionic head groups, especially alkyl sulfates and alkyl carboxylates, is by far more important. In this case, in 2007, Vlachy et al. published such a series, which is based on experimental results and molecular dynamics simulations.<sup>85, 88</sup> It is reproduced in **Figure 2-15**. Here, the carboxylate head group is characterized as hard and strongly hydrated (kosmotropic), whereas the sulfate and the sulfonate head group are characterized as soft and weakly hydrated (chaotropic). The phosphate head group is set between the preceding ones. Now, having an ordering from kosmotropic to chaotropic both for simple ions and for the typical head groups at one's disposal, many experimental results on ion specificity in colloidal and biological systems can be explained by applying Collins' concept of "matching water affinities".

First, the reversed ordering of cations and anions in **Figure 2-13** can easily be understood. Biological macromolecules (e.g. proteins) possess mainly hard anionic carboxylate groups and soft cationic ammonium groups. That is why, in general, the interaction of hard cations and soft anions with proteins, which leads to destabilization of the protein, are stronger than the other way round.<sup>85, 91</sup>

The validity of the series shown in **Figure 2-15** has been proved by many experimental observations. For example, counter ion dependence of the cmc for the "soft" alkyl sulfate head group shows the following trend:  $\text{Li}^+ > \text{Na}^+ > \text{K}^+ > \text{Cs}^+ > \text{N}(\text{CH}_3)_4^+$ .<sup>29, 60, 62, 63</sup> This indicates an increasing head group - counter ion interaction from  $\text{Li}^+$  to  $\text{N}(\text{CH}_3)_4^+$ , what agrees well with the predicted counter ion head group interactions by Collins' concept. Further, for alkali alkyl carboxylates,  $T_{\text{Kr}}$  increases with decreasing size of the counter ion ( $\text{Li}^+ > \text{Na}^+ > \text{K}^+ > \text{Cs}^+$ ).<sup>4, 70</sup> Again, this is in line with Collins' concept of matching water affinities, since stronger counter ion - head group interactions lead to higher  $T_{\text{Kr}}$ .<sup>62</sup> For alkyl sulfates, this argumentation is only valid for alkali ions, for which  $T_{\text{Kr}}$  increases with the size of the counter ion.<sup>4, 70</sup> Lower  $T_{\text{Kr}}$  values for choline alkyl sulfates compared to their sodium or potassium homologues are not in line with Collins' concept, which would predict higher  $T_{\text{Kr}}$  values (see **Figure 2-15**). These findings can be explained by the unsymmetrical

and bulky structure of choline, which increases the free energy of the surfactant's solid state and thereby decreases  $T_{Kr}$ . This effect seems to outnumber the stronger counter ion - head group interactions as predicted by Collins' concept.<sup>62</sup> A comparison of the aqueous phase behavior of choline alkyl sulfates (ChS12, ChS16) and choline alkyl carboxylates (ChC12, ChC16) shows a stronger binding of choline to alkyl sulfates than to alkyl carboxylates. This was concluded, since for ChS<sub>n</sub> some cubic phases, mesophases of high curvature, were missing compared to ChC<sub>n</sub>.<sup>62</sup>

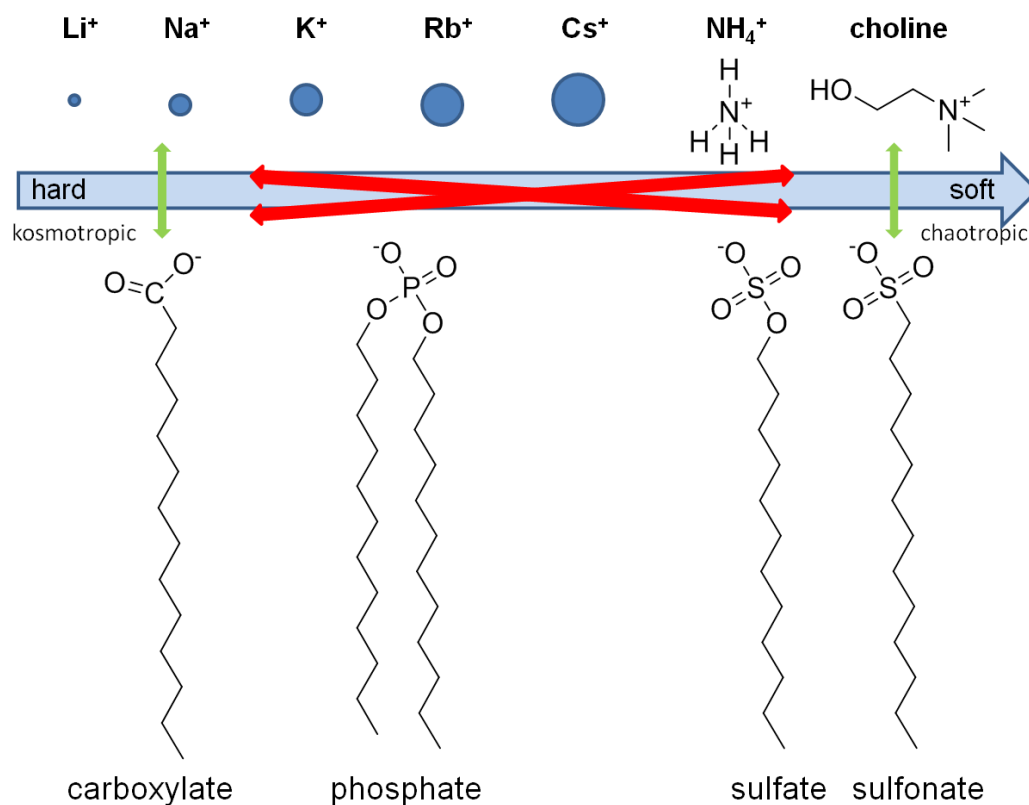


**Figure 2-15:** Ordering of anionic surfactant head groups and some important cations from hard to soft, according to Collins' "law of matching water affinities". The green arrows represent strong ion interactions, the red ones weak interactions. This figure is based on reference 85.

From this short discussion on specific ion effects, it is obvious why, for many systems, the sequence of ions found deviates considerably from the one shown in the "Hofmeister series". As mentioned above, the typical Hofmeister ordering is valid for the majority of biological systems, since always the same charged groups are present in biological molecules. The same way, investigating ion specificity for artificial macromolecules only differing in their overall structure, but always possessing the same charged groups, one would also find a general ion series for most of the artificial macromolecules. The difference between this new series and the "Hofmeister series" would only depend on the difference in the nature of the common biological charged groups and the ones integrated into the artificial

macromolecules. Of course, this is only a very simplified picture that does not take into account molecular structure, which is very important<sup>85, 91</sup>, but it clarifies the general point being addressed: it is impossible to predict a general behavior for a certain ion being valid in every possible system analyzed. It will always be necessary to properly analyze the system's properties, mainly which ions/charged groups can interact, and then some careful predictions can be made by applying some promising models (e.g. Collins' concept). Another important point, frequently ignored, is that one ion alone cannot be investigated. There is always another ion of opposite charge introduced into the aqueous system that can considerably affect the "target ion" - solute interactions depending on its interactions with the "target ion".

## 2.3 Choline - a vital amine

Choline, chemically known as (2-hydroxyethyl)trimethylammonium, is a quaternary ammonium ion of biological origin. Its bulky structure (see **Figure 2-16**) as well as its low-toxic nature and high biodegradability make this molecule a perfect green alternative for similar, but more toxic and less biodegradable ions in surfactants, ionic liquids or deep eutectic solvents.<sup>62, 67, 93-100</sup>

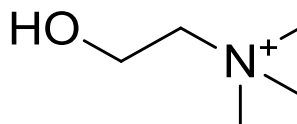


**Figure 2-16:** The structure of the biological ion choline, a vital amine.

Despite its importance and presence in animals and plants, on industrial scale, choline is synthesized from trimethylamine and ethylene oxide (see **Figure 2-17**).<sup>101</sup>

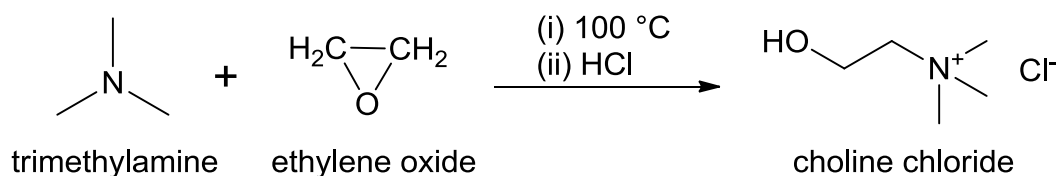


**Figure 2-17:** Reaction scheme of the industrial synthesis of choline from trimethylamine and ethylene oxide. This scheme is taken from reference 101.

In this work, the focus is on choline as a green alternative to common tetraalkylammonium ions as a counter ion for long chain anionic surfactants. More than 25 years ago, Yu et al.<sup>72, 102</sup> showed that using tetrabutylammonium as counter ion of long chain alkyl sulfates considerably decreases  $T_{Kr}$  of these surfactants compared to their sodium equivalents. Similar results were found when using symmetrical tetraalkyl ammonium ions (TAAs) as counter ions for long chain soaps.<sup>71</sup> However, simple TAAs cannot be used as counter ions of surfactants in household products because of their well-known toxicity.<sup>103-107</sup> They can act as phase transfer catalysts or block ion channels. Klein<sup>62, 67</sup> and Rengstl<sup>73</sup> showed that choline used as counter ion for anionic surfactants has similar  $T_{Kr}$  reducing effects like TAAs by being much less toxic. These findings by Klein and Rengstl constitute the basis for the experiments and results presented in the second part of this thesis.

Choline and choline derivatives play a very important role in the second part of the thesis. Therefore, in the following, a short overview on the appearance of choline in food and its several biological functions is given. Moreover, its importance for human health and in brain development is considered.

### 2.3.1 Choline in food and recommended adequate intake

Although humans are able to biosynthesize small amounts of choline, it is important to ingest choline by food to maintain optimal health.<sup>108, 109</sup> In 1998, choline was classified as an essential nutrient for humans by the Institute of Medicine (IOM), and recommendations were issued for the sufficient intake of this amine.<sup>110</sup>

Choline can be found in a variety of food, which can contain choline in its free or in an esterified form (e. g. phosphatidylcholine). Choline is very concentrated in liver, eggs and wheat germ, but also milk can serve as an important choline source. Furthermore, many vegetables and meats include choline, even though not so concentrated. Another possible choline source is dietary supplements. Meanwhile, in every drugstore, there are concentrated products, which contain choline salts or lecithin as choline sources.<sup>108, 109</sup>

The recommended adequate intake for choline, which is based on median intake of nutrient by healthy individuals known not to show deficiency symptoms, lies between 425 mg/d for women and 550 mg/d for lactating women and men. Mainly during pregnancy and lactation, the demand for choline by women is especially high, since a large amount of choline is delivered to the fetus. However, there is an essential variation in dietary choline requirement among humans, which is due to common genetic polymorphisms. Generally spoken, some people are susceptible to choline deficiency and develop deficiency symptoms, while others do not. For example, half of the population has a genetic polymorphism that increases dietary methyl requirements, of which choline is the major source.<sup>108</sup>

Different studies showed that many people do not meet or exceed the recommended values for the consumption of choline. Some are even far below.<sup>108</sup>

### 2.3.2 Biological functions of choline

Choline plays an important role in human metabolism, where it acts as a precursor for many biologically important molecules. The most important biological molecules, for which choline acts as a precursor are listed below and shown in **Figure 2-18**:<sup>108,</sup>

<sup>109</sup>

- Acetylcholine, an important neurotransmitter in the nervous system.
- Phosphatidylcholine and sphingomyelin, which are essential structural components for all biological membranes.
- Betaine, whose methyl groups are used to resynthesize methionine from homocysteine. Methionine is used for the formation of S-adenosylmethionine

(AdoMet), which is the most important methyl group donator in cellular metabolism.

- Platelet-activating factor and Sphingosylphosphorylcholine, two signaling phospholipids.

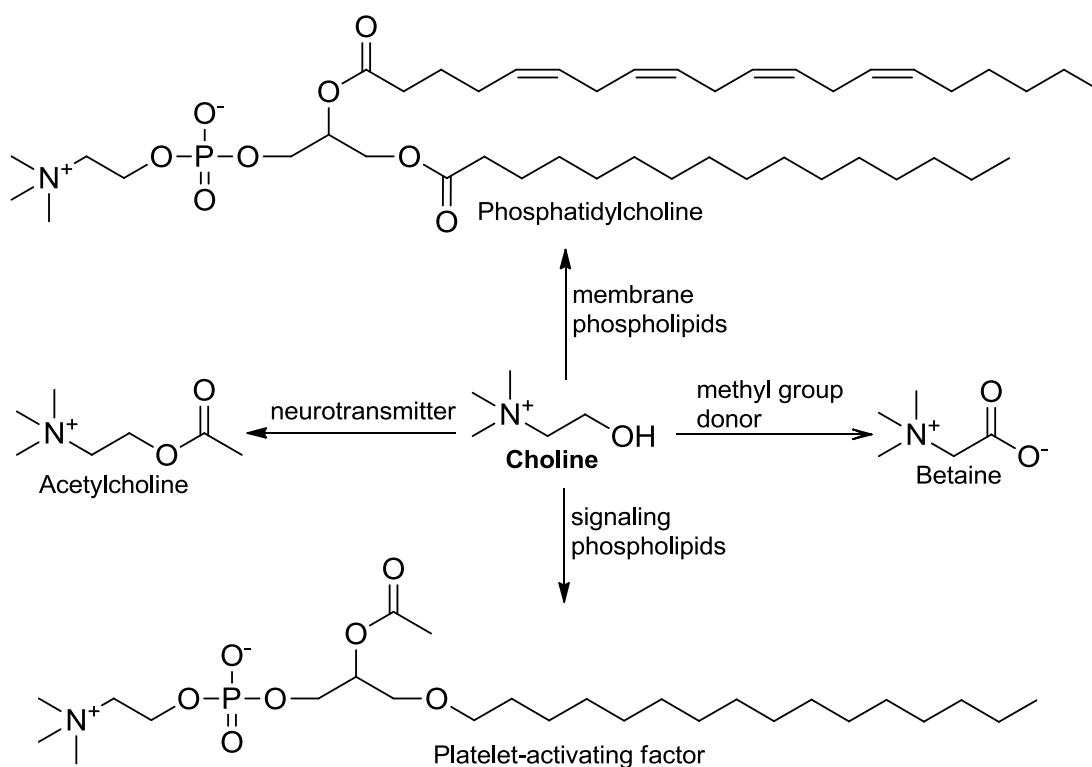


**Figure 2-18:** Structures of the most important molecules, for which choline acts as a precursor in human metabolism. This figure is based on reference 109.

### 2.3.3 Effects of choline on health and brain development

Choline plays a far-reaching role in human metabolism, from neurotransmitter synthesis to cell structure. That is why it is assumed that choline deficiency has an impact on diseases like fatty liver disease, atherosclerosis and possibly neurological disorders. Thus, for optimal health, it is important to consume adequate amounts of choline.<sup>108, 111</sup>

Several studies with humans showed the importance of choline to maintain optimal health. In 2009, Zeisel and da Costa<sup>108</sup> reviewed in detail the most important findings. Some of them are shortly mentioned. In healthy humans, the abdication of choline in diet can lead to fatty liver or muscle damage, which is removed as soon as choline is consumed. Further, if not sufficient choline is available, there will be a reduced capacity to methylate homocysteine to methionine. As a consequence, homocysteine shows increased plasma levels. This is evil, since high homocysteine

plasma levels have been associated with bigger risk for some chronic diseases including cancer, cognitive decline or cardiovascular disease. It was shown that the intake of choline can lower homocysteine plasma levels to a normal height. Other studies suggest that people, who have a choline-rich diet, show lower plasma levels of inflammatory markers. Moreover, it was found that pregnant women with low choline intake had a four times higher risk to bear children with a neural tube defect than women with a high choline intake.

Recent studies with rodents show that choline supplementation during some critical phases of pregnancy can cause positive long-term effects on brain development and memory.<sup>108, 109, 111, 112</sup> For example, parental choline supplementation or depletion during later periods of pregnancy leads to lifelong changes in brain structure and function. Usually, adult rodents show a decline in memory with aging, but rodents, provided extra choline during their time in the uterus, did not do so. Although these results are very promising, it still has to be checked, whether choline supplement during human pregnancy also causes positive, long-term effects on the child's memory and brain function.

In addition, some studies on the effect of short-time choline supplementation on the memory of adult humans have been undertaken. Some of these studies revealed an improvement in memory of the subjects, but there exist also other studies, where no effect of choline intake on memory was found.<sup>111</sup>

With regard to these findings and the importance of choline in human metabolism, it can be inferred that it is advisable to consume sufficient amounts of choline to keep optimal health. A high intake of choline is especially important for pregnant and lactating women, to satisfy their own needs as well as the needs of the offspring.

### 2.3.4 Choline derivatives used in this work

In this thesis, two choline derivatives were also used as counter ions to long chain anionic surfactants and compared to the performance of choline. The structures of the molecules are shown in **Figure 2-19**.

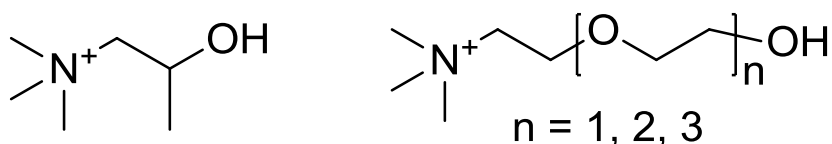


**Figure 2-19:** The molecular structures of beta-methylcholine (left) and ethoxylated choline (right).

The first one was beta-methylcholine (MeCh), which differs to choline only in one methyl group. Beta-methylcholine exhibits some interesting features which render it an interesting counter ion. Like choline, it can be assumed to be much less toxic than common TAAs, since it was identified in some rats and flies as the decarboxylation product of carnitine.<sup>113</sup> It is already commercially available in large scale, since it is an intermediate in Methacholine (acetyl-beta-methylcholine) synthesis.<sup>114</sup> Moreover, the additional methyl group should slightly increase its bulkiness compared to simple choline. For identical anionic surfactants, this should lead to (slightly) lower  $T_{Kr}$  values compared to choline (see section 2.1.5.3). It will be shown that this behavior was actually found.

Secondly, a group of ethoxylated choline derivatives, which differed only in their degree of ethoxylation, was investigated. These molecules are not commercially available and were specially synthesized at BASF. Although the biodegradability and the (eco)toxicology of these structures remains to be investigated, from a structural point of view, these molecules are very interesting as counter ions to long chain surfactants. They combine a very unsymmetrical and bulky structure with the flexibility of an ethoxylated moiety in one molecule. This should render these molecules very promising candidates as counter ions for long chain anionic surfactants to reach very low  $T_{Kr}$  values (see section 2.1.5.3). It will be shown that these molecules are indeed much more effective than simple choline in increasing the solubility of long chain anionic surfactants by counter ion exchange.

## **2.4 Soaps in aqueous systems**

Soaps are the oldest and perhaps most natural surfactants. However, they lost much of their importance since “technical surfactants”, usually based on sulfates or sulfonates, have been developed over the last fifty years.<sup>2, 8</sup> Indeed, soaps are pH- and salt-sensitive<sup>11, 43</sup> and they are irritant<sup>115</sup>, especially to the eyes. In food emulsions, although authorized, they have a bad taste, and long-chain saturated soaps have a high Krafft temperature. However, it should be possible to solve most or perhaps all of these problems with modern formulation approaches.

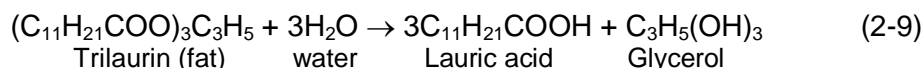
In this section, a general overview on the history of soap and general problems with soaps in common applications is given. The problem of the lacking soap solubility at neutral pH is directly addressed in chapterChapter 3. It will be shown that by adding the edible bio surfactant Rebaudioside A to aqueous sodium oleate solutions, it is possible to obtain highly translucent and stable soap solutions close to neutral pH values.

### **2.4.1 History of soaps**

Soaps are salts consisting of negatively charged fatty acid carboxylates and positively charged counter ions. The fatty acid alkyl chain possesses at least 8 carbon atoms to ensure satisfactory surface activity and the counter ion can both be inorganic, like sodium, potassium or calcium, and organic, like tetraalkylammonium ions. Long chain soaps have 12 or more carbon atoms in their hydrophobic chain.

Soap was the first surface-active agent made by mankind. Excavations revealed that Babylonians already boiled fats with wood ashes to obtain soap-like substances as early as in 2800 BC.<sup>116-118</sup> The Ebers Papyrus (around 1500 BC) provides evidence that the Egyptians used vegetable or animal oil and alkaline salts to synthesize soap-like material for bathing/washing and the treatment of skin diseases.<sup>116</sup> According to writings of Pliny the Elder, the Phoenicians and the Gauls also produced soap from boiling goats' fat with wood ashes. But it is thought that they did not use it to wash themselves, but to clean their clothes or decorate their hair.<sup>118, 119</sup> Although the origin of the word “soap” is not completely sure, it is believed that it comes from Mount Sapo, where, according to a Roman legend, animals were sacrificed. Rainwater containing animal fat and wood ashes from the altar poured down the mountain and formed crude soap in the clay of the Tiber River.<sup>117, 118</sup> In Pompeii, which was destroyed in 79 AD, excavation revealed an entire soap-making factory with finished soap bars that were preserved in the hardened lava. The use of soap as a personal

cleaning agent had become popular during the later centuries of the Roman Empire.<sup>116</sup> In the second century AD, soap was recommended for both washing/bathing and medical purposes by the Greek physician Galen.<sup>116</sup> In Western Europe, after the fall of the Roman Empire, there was a decline in bathing habits and only little soap was produced for cleaning in the European Dark Ages. Many historians assume that the lack of personal cleanness and related unsanitary conditions are significant factors for the outbreak of some great disease plagues.<sup>116</sup> However, soap making was an established craft and survived throughout that time. The countries around the Mediterranean Sea were producing modest amounts of soap by combining animal or vegetable oil, ashes of plants and fragrances.<sup>116, 117, 119</sup> The rise of the soap industry at the beginning of the 19<sup>th</sup> century is ascribed to two French chemists. Le Blanc, who invented a process to obtain cheap soda from salt, and Chevreul, who discovered the chemical nature of fatty acids, glycerol and fat/oil (see equation 2-9).<sup>119</sup> Throughout the 19<sup>th</sup> century, the discovery of many different fatty acids in neutral oil and fats led to a much better understanding of the soap making process. This also led to the establishment of the basic principles of the modern-day process, which involves the saponification of oil or fat by appropriate caustic substances.<sup>117</sup>



While soap was as a luxury product before that time and only affordable by royals and the very rich, the possibility to produce large amounts of cheap soap made it a household item for the personal hygiene of common citizens as well.<sup>120</sup> At the beginning of the 20<sup>th</sup> century, many soap products and “soap specialties” were produced on large scale.<sup>121</sup> For example, the first soap-based heavy-duty detergent was introduced by Henkel in 1907.<sup>8</sup>

Soaps exhibit excellent surfactant properties, are easily prepared from renewable fats or oils<sup>19, 122</sup> and are readily biodegradable under anaerobic and aerobic conditions<sup>31</sup>. However, the use of “natural” long chain soaps in aqueous solutions and formulations suffers from significant drawbacks. These are low tolerance towards electrolytes (water hardness), often low solubility in water at room temperature, i.e. they crystallize from aqueous solutions, and the instability at neutral or acidic pH values.<sup>2, 43</sup> The high pH values of aqueous soap solutions may also be a contributing factor to the higher (skin and eye) irritation potential of soaps in

cleansing products compared to synthetic surfactants, which can be used within the range of human skin pH (4 – 6).<sup>115, 123-126</sup>

In the last century, these shortcomings, the availability of new material feedstock from modern petrochemical industry, progress in chemical processes as well as more specialized application fields led to the development of so-called “synthetic” surfactants.<sup>8, 11</sup> Concerning the drawbacks mentioned above, these surfactant classes exhibit some distinct advantages over classical soaps in many applications. Although, in industrialized countries, soaps have been replaced by synthetic surfactants in many areas of their former applications, they are still widely used in industry. In 2000, soap was still by far the most consumed surfactant in the world and made up the main share of surfactant consumption in the major industrialized areas.<sup>2, 127</sup> Some examples of commercial use of soaps are listed below.

One big area are bodycare products and cosmetics<sup>7, 128</sup>. Alkali soaps are still the main component in many skin-cleansing agents, like toilet soaps.<sup>117, 128, 129</sup> However, due to the high pH values of soap based cleansing products and the resulting irritation potential, the trend goes towards milder formulations based on synthetic surfactants.<sup>128, 130</sup> Further, soaps are used as emulsifiers in cosmetic emulsions, like creams or milks, as solidification agent for sticks or in mascara.<sup>128, 130</sup> In shaving products, like shaving creams, foams or gels, long chain soaps are still the main component, since they cause a swelling of the beard-hair that eases the cutting of the hair by a blade.<sup>128, 131</sup> Soaps find also application in flotation de-inking of paper<sup>132, 133</sup> or in the purification of minerals<sup>134, 135</sup>. In Western countries, soaps are only used as complexing or defoaming agents in laundry detergency products nowadays.<sup>129</sup> Nevertheless, in less developed countries, even now, soap is still the most important surfactant in detergents and cleaners.<sup>7</sup> Soaps of polyvalent ions, often called metal soaps, are used in the plastic industry as lubricants, release agents or stabilizers.<sup>7, 136</sup> In building industry, soaps are added to concrete as waterproofing agents.<sup>136-138</sup>, and in paints they are used as dispersing agents.<sup>136, 139</sup> Moreover, soaps are used as thickeners for organic media, as lubricants and as process aids in pharmaceutical tablet pressing.<sup>136</sup> A much more detailed overview on the application of soaps in industry is given in reference 136.

In the last two decades, surfactant industry has turned its attention to natural raw materials to replace petrochemical products.<sup>19, 25, 140</sup> With regard to their easy and cheap production from renewable material, their excellent biodegradability, their low toxicity and their excellent surfactant properties, soaps represent a promising class of surfactants. These features and their presence in the human body as well as in

animals and plants make soaps the “ultimate green surfactant”. Thus, from an environmental and energetic point of view, specific research in overcoming the drawbacks of soaps in aqueous solutions should be done. In the following part, the drawbacks are explained and promising approaches to overcome these drawbacks are presented. Due to the broad range of possibilities, not all approaches published in literature can be mentioned and only some selected examples are shown. Further, the discussions and the corresponding examples are focused on common saturated soaps with a chain length of 12, 14, 16 and 18 carbon atoms and unsaturated long chain soaps like oleate or omega-3-fatty acids. The striking difference between saturated long chain soaps and unsaturated long chain soaps occurs in the protonated state of the fatty acid: the saturated fatty acids are crystalline at room temperature and the unsaturated ones are in the liquid state (oil). As will be shown in this work, this is what makes the saturated ones so much harder to disperse in aqueous solutions at room temperature, respectively at neutral pH value.

The features of the large amount of synthetic surfactants based on natural oils, fats or fatty acids, which have been synthesized to overcome the problems of “simple” soaps, are not part of this work. Concerning this huge topic, the interested reader is referred to references<sup>19, 25, 127, 140</sup>. The goal of this work is to show that there are possibilities to overcome the well-known problems of soaps and to use them in aqueous formulations. Applications and formulations, which contain soap as a minor ingredient and being far away from simple aqueous soap systems, are not considered either.

## **2.4.2 Water solubility and "Krafft temperature" of soaps**

As soon as it was possible to produce highly pure soaps, it became quickly obvious that their solubility in water is strongly dependent on the constitution of the hydrophobic alkyl chain.<sup>119</sup> In the first half of the 20<sup>th</sup> century, systematic studies on soap/water phase diagrams by McBain and co-workers showed that the water solubility of saturated linear chain sodium soaps decreases with increasing alkyl chain length. Introduction of a double bond into the alkyl chain, however, increases the water solubility of the respective soap. The results show that only for sodium laurate and sodium oleate, a few weight percent (wt%) of soap can be dissolved in water at room temperature. The longer saturated ones exhibited very low water solubility.<sup>141, 142</sup> The same was found by Shedlovsky et al.<sup>143</sup>.

An important feature of surfactants to evaluate their solubility in water is the Krafft temperature ( $T_K$ ). At this temperature, the critical micellar concentration (cmc) curve

intersects the solubility curve of the surfactant monomers in solution, and the total surfactant solubility increases sharply with temperature due to the formation of highly water soluble micelles. For more detailed information see section 2.1.5.3. Inside these micelles, the surfactant chain exhibits a liquid-like physical state and is very flexible. At temperatures above  $T_{Kr}$ , aqueous solutions containing up to several percent of surfactant become clear, are low viscous and no more solid precipitate is present.<sup>4, 20</sup>

It must be noted that for aqueous soap solutions, it would be better to talk about a "clearing temperature" or "solubility temperature" and not the "Krafft temperature". It was shown in literature<sup>142, 144</sup>, at low soap concentrations, lowering the soap concentration results in higher "solubility temperatures". In this work, the same behavior was found for aqueous stearate systems. This is inconsistent with the phase rule for binary systems. It can be explained by the partial protonation of the soap resulting in the corresponding acid, which transforms the aqueous soap solution from a binary to a more complex system.<sup>65, 145</sup> The increase in "solubility temperature" with decreasing soap concentration was explained by a more prominent protonation of the fatty acid in dilute solutions.<sup>142</sup> Thus, from a theoretical point of view, it is somehow wrong to use the expression "Krafft temperature" for the "solubility temperature" of aqueous soap solutions. Nevertheless, in the following, since common practice in literature, the "solubility temperature" of aqueous soap solutions will also be called  $T_{Kr}$ . However, to analyze the effect of different counter ions, it is very important to compare  $T_{Kr}$  values that were measured at the same concentration (commonly 1 wt %).

Usually, it is important that the surfactant is used at or above its cmc and above its  $T_{Kr}$ . In many applications of surfactants, like adsorption to interfaces or surface tension reduction, their effectiveness increases with concentration until it stays nearly constant above the cmc.<sup>146</sup> A further important feature of surfactant solutions, the solubilization of water insoluble material, can only occur above the cmc.<sup>147</sup> In addition, surfactant precipitation is often undesired and disturbs during application. Unfortunately,  $T_{Kr}$  increases with increasing surfactant's alkyl chain length and restricts the use of long chain surfactants in water below a certain temperature.<sup>148</sup>

For a homologous series of surfactants, the cmc decreases with increasing alkyl chain length with evident consequences for application (e.g. surface tension reduction, better detergency or solubilization power).<sup>83, 146, 149</sup> Simply speaking, the efficiency of a surfactant is improving with increasing chain length. On the other hand, the surfactant's  $T_{Kr}$  increase also with increasing chain length. The relations between surfactant's chain length, solubility and performance are nicely illustrated in

an old paper by Preston<sup>83</sup> on detergent action of saturated sodium soaps and sodium alkyl sulfates.

The Krafft temperatures of soaps ranging from sodium laurate up to sodium stearate were determined by Lin et al. who approximated  $T_{Kr}$  as the clearing temperature of an aqueous 1 wt% surfactant solution.<sup>150</sup> The values were 25 °C for laurate (C12), 45 °C for myristate (C14), 59 °C for palmitate (C16) and 71 °C for stearate (C18). This indicates that even NaC12 can hardly be used in aqueous solutions at room temperature.

A promising way to reduce  $T_{Kr}$  of long chain soaps in aqueous solutions is the exchange of the counter-ion. Although it was already known for a long time that potassium soaps exhibit slightly lower  $T_{Kr}$  (around 15 °C<sup>67</sup>) than sodium soaps and the counter-ion can influence the surfactant's solubility,<sup>142</sup> it took until 2004 that a significant progress was made in this context. In that year, Zana showed that the substitution of the counter-ion from sodium to the large and bulky organic tetrabutylammonium (TBA) led to a strong increase in soap solubility in aqueous solutions.<sup>71</sup> The TBA soaps formed micellar solutions at room temperature up to a carbon chain length of 22. The drawback of the use of simple tetraalkylammonium (TAA) ions as a counter-ion for soaps is their known toxicity.<sup>103-107</sup> A non-toxic and green alternative to large organic TAA ions to reduce  $T_{Kr}$  of soaps is choline, a TAA ion of biological origin. Our group could show that the choline (Ch) soaps combined the characteristics of common alkali soaps in the low concentration regime with distinctly lower  $T_{Kr}$  values (ChC12 < 0 °C, ChC14 = 1 °C, ChC16 = 12 °C, ChC18 = 40 °C). Thus, choline soaps with a carbon chain length from 12 to 16, consisting only of material occurring in the human body, represent promising green candidates for the usage of long chain soaps in applications at room temperature.<sup>67, 151</sup> The search for green and more effective counter-ions or additives to further depress  $T_{Kr}$  of long chain soaps is ongoing. In this way, highly water soluble ( $T_{Kr}$  below room temperature) and very efficient long chain soap surfactants can be obtained.

Next to neutralization with strong counter-ion hydroxide bases, other attempts have been made to disperse long chain fatty acids in aqueous solutions at or below room temperature, mainly by making mixtures. It should be noted that  $T_{Kr}$  are often hard to define, since the macroscopic and microscopic state of complex mixtures can be quite different from simple micellar solutions. In the following, only some examples are mentioned.

One way is the usage of weak amine bases, like lysine<sup>152</sup>, ethanolamine<sup>153</sup> or alkylboladiamines<sup>154</sup>. Although the authors show that they can disperse saturated long chain fatty acids up to C18 at room temperature in water, there are two

significant drawbacks. First, the solutions were heated to 60 °C before usage and experiments were not carried out at equilibrium, which is proven by the fact that after storage for one day at room temperature all solutions contained some kinds of fatty acid crystals. The second drawback is the microscopic and macroscopic appearance of the solutions. Common micellar soap solutions (< 5 wt%) are known to be completely clear, transparent and of low viscosity, and the fatty acid alkyl chains are in a liquid-like and very flexible state within the micelles.<sup>20</sup> The metastable solutions of amine-soaps (1 wt%) are turbid (lysine<sup>152</sup> and ethanolamine<sup>153</sup>) or turbid and viscous (alkylboladiamines<sup>154</sup>) at room temperature. On the microscopic scale, the solutions contained vesicles with the soap chains embedded in a gel bilayer phase ( $L_\beta$ ). In  $L_\beta$  phases, the bilayers have rigid and mostly all-trans chains which results in a reduced flexibility of the alkyl chain and mobility of the surfactant.<sup>50</sup> With increasing temperature, a transition from a gel-like bilayer ( $L_\beta$ ) to a liquid-like bilayer ( $L_\alpha$ ) was observed for the lysine (transition temperatures  $T_m$ : C14 = 34 °C, C16 = 51 °C, C18 = 64 °C) and ethanolamine systems. Within these liquid bilayer phase  $L_\alpha$ , the surfactants are in a fluid-like state leading to an increased alkyl chain flexibility and surfactant mobility compared to the  $L_\beta$  phase.<sup>50</sup> The systems with alkylboladiamines transformed to highly viscous solutions composed of wormlike micelles upon heating. To conclude, up to now, amines as counter ions for saturated long chain fatty acids are only able to disperse these long chain amine soaps in a metastable state in water at room temperature. Macroscopically and microscopically, the state significantly differs from the thermodynamic stable micellar solutions obtained with ChC16 or TBAC18 at room temperature.

Another way to disperse long chain fatty acids in water at room temperature is to add a third component to common alkali soaps<sup>155, 156</sup> or to dissolve fatty acids plus a third component in an aqueous buffer solution<sup>157, 158</sup>. In the latter case, at high pH values the cation from the buffer solution plays the role of the counter ion of the fatty acid and soap is formed. An example for adding a third component to common alkali soaps is the system sodium fatty acid (NaC14 – NaC18) plus guanidine hydrochloride (molecular ratio 1:1) in water.<sup>155, 156</sup> At temperatures below the transition temperature  $T_m$  (C14 = 21 °C, C16 = 42 °C, C18 = 57 °C), the aqueous solutions (1 wt%) were turbid and viscous. On the microscopic scale, flat membranes were found with the fatty acids embedded in a gel bilayer phase ( $L_\beta$ ). Interestingly, these systems kept their macroscopic and microscopic structure even after several months at 4 °C. This indicates that the addition of guanidine hydrochloride makes it possible to disperse C14-C18 sodium soaps in water and prevent crystallization at low temperatures. However, again the state of the dispersion is completely different

from that of common micellar solutions. At temperatures above  $T_m$ , the aqueous solutions became viscous and clear. For the C14 system, microscopy revealed the presence of anastomosis-like superstructure, in which the fatty acid chains seem to be as flexible as in micelles.

Two examples for dispersing fatty acid plus additive in an aqueous buffer solution are the palmitic acid(C16)/palmitin system investigated by Douliez et al.<sup>157</sup> and the palmitic acid(C16)/cholesterol system by Lafleur et al.<sup>158, 159</sup>. Let us first consider the palmitic acid/palmitin system. For molecular ratios of palmitic acid to palmitin of 1 and 2 (1 wt%) and pH values of 7 or 9, the mixtures were fully dispersed resulting in viscous and turbid aqueous solutions at room temperature. On the microscopic scale, vesicles were found with the fatty acid chains embedded in a gel bilayer phase ( $L_\beta$ ). With increasing temperature, the bilayer transformed from the gel state ( $L_\beta$ ) into a fluid state ( $L_\alpha$ ). At a pH value of 5, too little palmitic acid was deprotonated to allow full dispersion of the formed membranes and lumps of aggregated membranes were observed in solution. It should be noted that the samples were heated to 60 °C before measurements were carried out and it is not sure whether the systems were in thermodynamic equilibrium at room temperature. For the palmitic acid/cholesterol system (molecular ratio = 1:1;  $\approx$  2 wt%), at a pH value of 5.5 both components were phase separated and in crystalline form below 50 °C. At higher temperatures, a lamellar liquid ordered phase ( $l_o$ ) was formed involving both components. This liquid ordered lamellar phase is well known for phospholipids/cholesterol systems and shares characteristics of the gel bilayer and the liquid bilayer phase.<sup>158</sup> At pH values higher than 8.5, when a significant amount of the palmitic acid is deprotonated, only a lamellar liquid ordered ( $l_o$ ) phase was found in the temperature range from 20 to 70 °C. Unfortunately, the macroscopic phase behavior of these samples (appearance and viscosity) was not described. These two examples also show that the phase behavior of such mixed systems containing fatty acid can be altered by tuning the pH value of the aqueous solution. This feature can be explained by a change in the protonation state of the fatty acid head group (low pH:  $\text{COOH} \leftrightarrow$  high pH:  $\text{COO}^-$ ).<sup>157, 158</sup>

Long chain soaps can also be dispersed in water at room temperature by mixing them with cationic surfactants leading to so-called catanionics. Catanionics represent an own area of research with nearly infinitely possible long chain soap/cationic surfactant compositions and many possible system parameters that can be varied. As a result, many (sometimes unusual) structures are obtained for these systems. Discussion of these systems would go beyond the scope of this work and the interested reader is referred to a recent review article by Fameau and Zemb and

references therein<sup>148</sup>. It should also be noted that the chain-melting transition in catanionic mixtures is typically 30 °C higher than in pure ionic surfactant systems. This means that a huge number of catanionic systems are present in the crystallized state at room temperature.<sup>160</sup>

These examples show that it is possible to disperse saturated long chain fatty acids in water at room temperature by using other substances than strong hydroxide bases. However, assuming that these systems are thermodynamically stable, the macroscopic properties (turbidity and/or viscosity) as well as the microscopic phase behavior/physical state of the fatty acid chain deviates significantly from that of well-known micellar aqueous solutions, which are obtained for simple alkali or TAA soaps above  $T_{Kr}$ . Solubility and mobility as well as the ability of a surfactant to spread at interfaces is strongly affected by its physical state. For many biological processes and technical applications, fast surfactant adsorption and low interfacial tensions are of great importance. It has been shown that the physical state of the vesicle membrane strongly affects the adsorption kinetics of the incorporated surfactants.<sup>161</sup> Only if the membrane was in a liquid like state ( $L_\alpha$ ), adsorption kinetics was fast and a constant minimum value of the surface tension was obtained, independently of temperature. At temperatures below  $T_m$  when the membrane was in a gel like state ( $L_\beta$ ), adsorption kinetics was much slower and the equilibrium surface tension values were considerably higher than above  $T_m$ . This shows that dispersing long chain fatty acids in water at room temperature does not automatically mean improved surface activity and performance in application. A major role plays the microscopic and macroscopic state of the aqueous soap solution as well as the physical state of the fatty acid chain. This can also be deduced from comparing interfacial and foaming properties of different aqueous soap solutions.<sup>148</sup>

### **2.4.3 Salt sensitivity of soaps**

Another drawback of soaps is their very low tolerance against (polyvalent) electrolytes. This can be easily observed with tap water, which contains significant amounts of Ca and Mg ions in many countries ("hard water"). Due to the very low solubility products of Ca and Mg soaps<sup>162, 163</sup>, these alkaline earth metal ions readily precipitate soap molecules from solution and form insoluble "lime-soaps".<sup>121, 164</sup> As a result, soap molecules only act as surfactants when all hard water minerals are removed from solution. In laundry detergency, "lime-soaps" are an issue, since they accumulate on washing machine parts slowing down the machines' efficiency and also incorporate into fabrics leading to yellowish clothes.<sup>78, 164, 165</sup> Another problem

emerges in mixed systems, where the soap possesses a certain counter-ion to obtain a desired  $T_{Kr}$  and other ions are introduced by further ingredients, e.g. builders. In solution, the soap cannot differentiate between the initial counter-ion and other ions introduced by the builder. That means, if choline hexadecanoate is used as surfactant, the addition of ionic sodium builder will increase  $T_{Kr}$  of the hexadecanoate from 12 °C<sup>67</sup> to the value of sodium hexadecanoate (59°C) with increasing ratio of sodium to choline within the system.<sup>62</sup> Thus, to use choline soaps up to C16 in hard water at room temperature, it is necessary to prevent introducing additional sodium ions into the aqueous system. Consequently, ionic builders with choline as counter ion have to be used. Therefore, non-ionic builders would be preferred, if ionic surfactants with low  $T_{Kr}$  are already used. Interestingly, this also works the other way round and  $T_{Kr}$  of sodium soaps can be lowered by the addition of choline or TAA ions to the system.<sup>62, 150</sup> However, for all aqueous long chain soap systems, the removal of all hard water minerals by the builder is an essential requirement to obtain clear and stable solutions.

#### 2.4.4 pH sensitivity and acid-base titration curves of soaps

The third distinct drawback of soap solutions is their high pH value and their sensitivity towards changing the pH value. Above  $T_{Kr}$  and their cmc, aqueous long-chain soap solutions exhibit a pH value higher than 9.<sup>166, 167</sup> Further, these solutions are only clear and macroscopically stable above a certain pH value and become turbid and unstable at lower pH values, where lamellar, crystalline or oil-like phases are formed. This behavior of aqueous soap solutions is well-known and has been intensively studied.<sup>166-172</sup> Sodium oleate, for example, gets turbid and unstable below a pH value of 10, because of the formation of a lamellar phase<sup>173</sup>, potassium laurate below a pH value of 9.3 and potassium myristate at a pH value lower than 10.5, because of the formation of acid-soap crystals.<sup>174</sup> The instability at pH values smaller than 10 prohibits the use of long chain soap solutions in all applications, where a certain pH value must not be exceeded. This can be the case in cosmetics or food, where irritation and compatibility problems can occur. The dependence of the microscopic and macroscopic phase behavior of aqueous soap solutions on the solution pH value is very important for the discussions in Chapter 3. Therefore, in the following, the origin of acid-base titration curves of dilute aqueous long chain soap solutions as well as the related appearance of the solutions will be discussed in detail.

The following discussion is based on studies found in literature and should help to understand the complex system sodium oleate(NaOl) and Rebaudioside A(RebA) in water during titration with hydrochloric acid(HCl) discussed in chapterChapter 3. The general course of titration curves of alkali metal soaps as well as the observed phase behavior is discussed with regard to important parameters like temperature, fatty acid concentration and nature of the hydrophobic carbon chain of the fatty acid used. It is well known that the phase behavior of aqueous fatty acid soap systems is highly dependent on the neutralization state  $\Theta_p$  (percentage of protonated fatty acid molecules) of the fatty acid soap. Therefore, many studies on highly aqueous alkali metal soap systems with varying pH, respectively the ratio of protonated to deprotonated fatty acid have been performed and different techniques were used to determine the formed structures. In dilute aqueous solutions of alkali metal soaps the structures found were micelles, lamellar phases/vesicles, acid-soap crystals, fatty acid crystals or oil-like phases (see **Figure 2-20**).<sup>166-172, 175</sup>

These systematic investigations clearly showed that for different alkali metal soaps the course of the titration curve and the formed aggregates with increasing  $\Theta_p$  depend on the applied temperature and the fatty acid concentration in solution. It was found that the fatty acid must have a chain length of at least eight carbon atoms and a minimum concentration of alkali metal soap (about half the cmc) has to be present in the aqueous system to allow lamellar phases(vesicles) or acid soap crystals to form during titration. Below this concentration, the fatty acid is present as a separate oil phase or as fatty acid crystals, depending on the melting temperature of the fatty acid.<sup>169, 171, 174</sup> The strong temperature dependence of the titration curves can be attributed to a well-known phenomenon of anhydrous fatty acid/fatty acid soap mixtures: the formation of acid soap crystals. These crystals consist of protonated acid and deprotonated acid plus counter-ion (soap) in a fixed stoichiometry. For some fatty acids many anhydrous acid soap crystals with different stoichiometry have been reported.<sup>176</sup> Herein, the aqueous phase behavior of acid soaps, for which the same trend as for simple alkali soaps can be found, is important. The temperature, at which the hydrophobic chains of the acid soap crystals “melt” and form liquid crystalline structures in an aqueous system (defined as “chain melting temperature”  $T_m$ ), decreases with increasing amount of water within the system.<sup>142, 175, 177</sup> Cistola et al.<sup>177</sup> measured  $T_m$  of some saturated and unsaturated potassium acid soap crystals at 80 % water content.  $T_m$  was found to increase for saturated acid soaps with growing number of carbon atoms in the hydrophilic chain (C10: 22°C; C12: 33°C; C14: 43°C; C16: 51°C; C18: 61°C), for oleate, due to the double bond, the lowest value was found (11 °C). At very high

water content, Hargreaves and Deamer<sup>171</sup> found nearly the same transition temperatures from needle-shaped crystals to lamellar structures (vesicles) when titrating potassium soaps with HCl at different temperatures. These  $T_m$  values are in line with the Krafft temperature of the pure soaps, which also rise with increasing chain length and oleate showing the lowest value, too.<sup>67, 142</sup> With regard to the higher Krafft temperatures of sodium soaps compared to potassium soaps<sup>67, 142</sup>,  $T_m$  of sodium acid soaps could possibly deviate a few degrees from those of potassium acid soaps. However, due to the chemical similarity of sodium and potassium the phase behavior and the general course of the titration curves should stay the same. Kaibara et al.<sup>166</sup> showed that the suggested similar behavior (titration curve and phase behavior) of aqueous sodium and potassium soaps during titration with HCl is true for oleate. Moreover, many paper report the formation of vesicles in aqueous NaOI and aqueous NaC10 systems during titration with HCl at 25 °C.<sup>169, 173, 178, 179</sup> This proves that  $T_m$  of NaOI and NaC10 acid-soap crystals is below 25 °C, which is perfectly in line with measured  $T_m$  for the potassium soaps of equal chain length (see above).

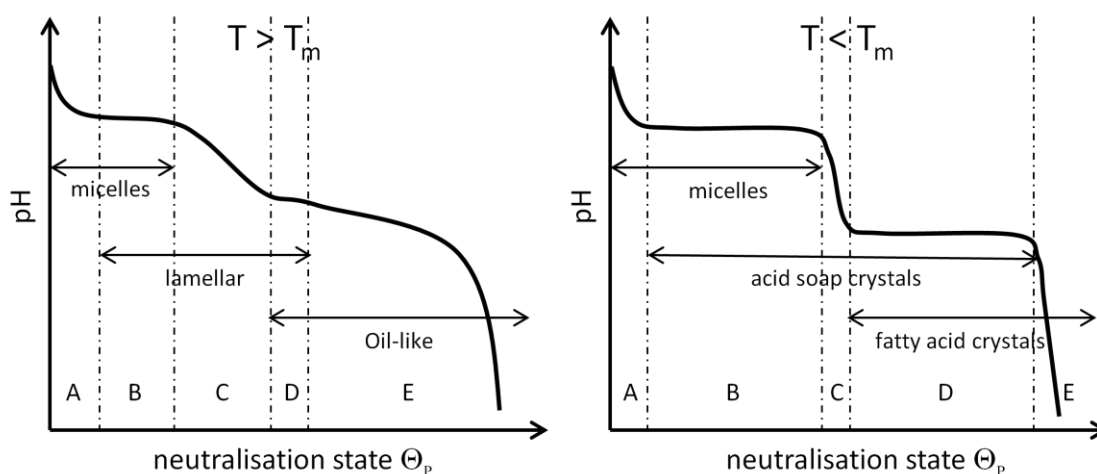


**Figure 2-20:** Typical curves obtained for acidic titration of alkali soaps above the cmc and the formed aggregates within certain zones. The left curve is for temperatures higher than  $T_m$ , the right one for temperatures lower than  $T_m$ . The diagrams are based on data from references 166, 167, 171, 172.

**Figure 2-20** shows the typical course of the titration curve and the formed aggregates at concentrations above the cmc for alkali soaps at temperatures higher (left side) and lower (right side) than  $T_m$ . For concentrations below the cmc, the curves change with respect to the actual concentration applied (not further discussed, see references <sup>167, 172</sup>). On the one hand, these diagrams have been discussed by Cistola and Small<sup>167</sup> by applying the Gibbs' phase rule, on the other hand, these diagrams have been discussed on the molecular level.<sup>171, 172, 174, 180</sup>

The Gibbs' phase rule is given by the equation  $f = c - p + 2$ , with  $f$  = degree of freedom,  $c$  = number of components and  $p$  = number of phases present. For an aqueous alkali soap system titrated with HCl (three components) at constant temperature and pressure the equation is modified to  $f = 3 - p$ . Since an aqueous phase is always present, it can be concluded that as long as the pH value remains constant upon adding HCl, i. e. no degree of freedom is present, two additional phases must be within the system. If the pH value changes, only one additional phase is present.<sup>167</sup>

To analyze the curves on the molecular level, it is assumed that the  $H^+$ -ion concentration near the surface of the fatty acid aggregates formed in solution is considerably lower than the pH value measured in the bulk solution. This is due to electrostatic attractions between  $H^+$ -ions and negatively charged surfaces (e. g. micelles or lamellar phases). Consequently, for negatively charged surfaces, it is convenient to introduce a "surface pH" that is lower than the measured "bulk pH".

This was argued and confirmed by many researchers and is undoubtedly one reason for the strongly increased apparent  $pK_A$  values ( $apK_A$  = the measured  $pK_A$  value of a long chain fatty acid in colloidal systems) of long chain soaps measured by the half-titration-method.<sup>167, 170, 172, 178, 180-183</sup> The  $apK_A$  value of long chain fatty acids is a function of the fatty acid chain length and increases with growing chain length. This is because of stronger interactions between the hydrophobic chains within an aggregate and a subsequent higher packing, respectively negative charge density of the fatty acid aggregates. Double bonds within the hydrophobic chain decrease the  $apK_A$  value due to a lower packing density because of sterical hindrance induced by the double bond(s).<sup>171, 184-187</sup> Another important aspect for the strongly increased  $apK_A$  values is a dielectric discontinuity from the outer water phase to the inner oil phase across the aggregate surface. This leads to intrinsic interfacial  $pK_A$  values (the  $pK_A$  value of a fatty acid incorporated into an interface in the absence of any electrostatic interactions) of fatty acids higher than 4.8.<sup>188-190</sup> Titration curves of long chain fatty acid molecules solubilised in nonionic micelles resulted in suggested intrinsic interfacial  $pK_A$  values of 6.3 to 6.6.<sup>189, 190</sup> Although this is around 1.5  $pK_A$  units higher than for monomeric fatty acids in water, it is still considerably below the  $apK_A$  long chain soaps in micellar solutions.<sup>167, 174, 185</sup> This is clear evidence that electrostatic interactions play an important role. Regarding the discussion of the titration curves of soaps on the molecular level, it is only important to define a decreased surface pH compared to the bulk pH due to electrostatic interactions. That means, the exact value of the intrinsic interfacial  $pK_A$  is not important. Moreover, the intrinsic interfacial  $pK_A$  value is likely to vary by altering the molecular interfacial

composition due to a change in the dielectric environment. For the sake of simplicity, the intrinsic interfacial  $pK_A$  value is regarded as constant throughout the titrations. In other words, it is assumed that the  $H^+$ -ion concentration near the surface ("surface-pH") that is necessary to protonate a carboxylate group being incorporated in a self-aggregated structure remains constant and is independent of the aggregate's surface charge density.

From the explanations stated above, these three statements are derived, on which the molecular discussion of the titration curves is based: 1. The higher the negative surface charge density of the aggregate, the higher the bulk pH at which the surface pH reaches a value sufficient to protonate the carboxylate group. 2. As long as the bulk pH value stays constant during titration with HCl, the surface charge density of the phase in which the carboxylate gets protonated remains constant, too. 3. Since a constant surface charge density within a phase can only be realized if the ratio of protonated to deprotonated fatty acid remains constant, newly formed fatty acid molecules have to be located within another phase.

Accordingly, it is straight forward that the incorporation of other amphiphilic molecules into fatty acid aggregates (mixed aggregate formation) can change the measured  $apK_A$  value by perturbing the molecular packing at the interface. This leads to changes in the surface charge density and/or a shifted intrinsic  $pK_A$  value of the carboxylate group due to another dielectric environment. Note, from this it can also be concluded that a change in the bulk pH value for a given aqueous fatty acid system by addition of an amphiphilic molecule is linked to the formation of mixed aggregates.

The two approaches can be perfectly combined without any contradiction, although, in my opinion, the discussion on the molecular level is more descriptive. To illustrate this, the left curve in **Figure 2-20** is discussed in detail by taking sodium oleate(NaOl) titrated with hydrochloric acid(HCl) as an example:

At the beginning of zone A, a micellar solution is present. Until zone B is reached, the protonated fatty acids are solubilised within the micellar phase and the surface charge density of the micellar phase decreases with increasing amount of HCl. As a consequence, the bulk pH value has to decrease so that the  $H^+$ -ion concentration near the micelles remains high enough to protonate the carboxylate groups. The phase rule predicts two phases. Within zone A the solution is perfectly clear as water.<sup>167, 173, 178, 191</sup>

In zone B, the pH value remains constant and the phase rule predicts three phases. Now the micellar phase is saturated with protonated fatty acid and the newly formed fatty acid molecules have to be placed in a new phase. At water concentrations

higher than 95 wt%, this is a lamellar phase containing vesicles and bilayers which consist of protonated and deprotonated fatty acids.<sup>167, 171, 184</sup> Due to the constant pH value in zone B, the composition of the micellar phase stays constant with increasing amount of HCl. The amount of micelles decreases at the expense of the lamellar phase. The formation lamellar bilayers and vesicles leads to turbid and translucent solutions. The turbidity increases with the amount of HCl added.<sup>167, 173, 178, 191</sup> The pH value at which formation of a lamellar phase starts is highly dependent on the fatty acid and increases with growing alkyl chain length of the soap.<sup>171, 180, 184</sup> This phenomenon is caused by an increase in surface charge density of the soap micelles with growing alkyl chain length. This is attributed to a higher packing density due to stronger hydrophobic interactions between the alkyl chains.<sup>171, 180, 184, 185, 187</sup>

With respect to the falling pH value, only two phases can be present in zone C, an aqueous phase and a lamellar phase.<sup>167, 171, 184</sup> Again, the turbidity increases with increasing amount of HCl added.<sup>178, 191</sup> The change in pH also shows that the surface charge density of the phase getting protonated decreases. This is, since the newly formed fatty acid molecules are incorporated into the existing lamellar phase which consequently alters its composition. This also points out that the formation of the lamellar phase is not restricted to a fixed soap to fatty acid concentration, like it is the case for crystalline acid-soaps.<sup>167</sup> The ratio from soap to fatty acid within the lamellar phase can vary from the beginning till the end of zone C.

At the beginning of zone D, the solution is milky white and starts to separate macroscopically.<sup>173, 178</sup> The constant pH value suggests the formation of a third phase, in which newly protonated fatty acid molecules are incorporated. In this short area of the diagram a lamellar phase and an oil-like phase coexist.<sup>167, 178</sup>

As soon as area E is reached and the pH value starts to fall and only an oil-like phase and an aqueous phase are present. The solution also phase separates quickly.<sup>167, 173, 178</sup> The ratio of protonated to deprotonated fatty acid in this oil-like phase is constantly increased until 100 % neutralization of the soap. Again, the related decrease of the oil-like phase's charge density causes the fall of the pH value. The formation of an oil-like phase and no fatty acid crystals is caused by the small difference in the chain melting temperature for acid soap crystals and for pure fatty acid crystals.<sup>167, 171, 175</sup> A certain amount of deprotonated soap molecules has to be present in the oil phase throughout zone E. Therefore, it is quite likely that some kinds of inverted hexagonal, inverted cubic or inverted micellar oil-like phases are present which also contain a certain amount of water. This has already been proposed and shown by Edwards et al.<sup>170</sup> who constructed a schematic phase diagram of the ternary system water/NaOl/oleic acid and made some cryo-TEM

pictures of aqueous NaOI solutions at different pH values. Janke et al.<sup>192</sup> modeled aqueous NaOI solutions at high water content with different ratios of NaOI to oleic acid and their results suit very well to experimental observations. By increasing the share of oleic acid, they found micelles, vesicles and inverted oil structures.

The overall aggregation behavior of aqueous NaOI with increasing neutralization can easily be explained qualitatively by applying the concept of packing constraints and analyzing the packing parameter  $p$ . It is defined as  $V / l * a$ , where  $V$  is the volume of the alkyl chain,  $l$  is the maximum chain length and  $a$  is the effective head group area. This concept links the molecular shape of a surfactant to its preferred aggregation state in dilute solutions. For small values of  $p$  ( $< 0.5$ ) aggregates with a high positive curvature, spherical ( $p < 0.33$ ) and cylindrical micelles ( $0.33 < p < 0.5$ ) are present. At medium  $p$  values ( $0.5 - 1$ ), a lamellar phase (vesicles or bilayers) is preferred. As soon as  $p$  reaches higher values than one, inverted structures with a negative curvature are formed.<sup>6, 20, 193</sup> This is perfectly in line with the observed aggregate structure with increasing amount of HCl added. The protonation of the carboxylate group leads to a decrease in the effective head group area  $a$ , since less electrostatic repulsion is present and hydrogen bonds can be formed between the protonated and deprotonated fatty acid species. As a consequence, the value of  $p$  rises with increasing amount of protonated fatty acid within the aggregates, respectively amount of HCl added, and the structures transform from micelles over lamellar structures to inverted structures.

The same discussion is applicable for the titration curve on the right side in **Figure 2-20**, except that no fluid lamellar and oil-like phases are formed. In this case, acid-soap crystals and fatty acid crystals form, since the curve is valid below the chain melting temperature  $T_m$  of the acid soap crystals and the pure fatty acid.

This very detailed discussion of acid-base titration curves of long chain soaps, respectively their related phase behavior with varying pH values, constitutes an ideal basis to discuss the influence of Rebaudioside A on aqueous sodium oleate and sodium dodecanoate solutions in the following section.

## 2.5 Literature

1. Holmberg, K.; Shah, D. O.; Schwuger, M. J., *Handbook of applied surface and colloid chemistry*. Wiley: Chichester [etc.], 2002.
2. Myers, D., An Overview of Surfactant Science and Technology. In *Surfactant Science and Technology*, John Wiley & Sons, Inc.: 2005; pp 1-28.
3. Holmberg, K.; Jönsson, B.; Kronberg, B.; Lindman, B., Introduction to Surfactants. In *Surfactants and Polymers in Aqueous Solution*, John Wiley & Sons, Ltd: 2003; pp 1-37.
4. Lindman, B., Physico-Chemical Properties of Surfactants. In *Handbook of Applied Surface and Colloid Chemistry (Volume 1)*, Holmberg, K., Ed. Wiley: 2002; pp 421-443.
5. Myers, D., Fluid Surfaces and Interfaces. In *Surfactant Science and Technology*, John Wiley & Sons, Inc.: 2005; pp 80-106.
6. Myers, D., Surfactants in Solution: Monolayers and Micelles. In *Surfactant Science and Technology*, John Wiley & Sons, Inc.: 2005; pp 107-159.
7. Schmalstieg, A.; Wasow, G. W., Anionic surfactants. In *Handbook of Applied Surface and Colloid Chemistry (Volume 1)*, Holmberg, K., Ed. Wiley: 2002; pp 271-292.
8. Smulders, E.; Rähse, W.; von Rybinski, W.; Steber, J.; Sung, E.; Wiebel, F., Historical Review. In *Laundry Detergents*, Wiley-VCH Verlag GmbH & Co. KGaA: 2003; pp 1-6.
9. Brackmann, B.; Hager, C.-D., The Statistical World of Raw Materials, Fatty Alcohols and Surfactants. In *CESIO 6th World Surfactant Congress*, Berlin, 2004.
10. Levinson, M., Surfactant Production. In *Handbook of Detergents, Part F*, Zoller, U.; Sosis, P., Eds. CRC Press: 2008; pp 1-37.
11. Myers, D., The Organic Chemistry of Surfactants. In *Surfactant Science and Technology*, John Wiley & Sons, Inc.: 2005; pp 29-79.
12. Fell, B., Raw Materials and Intermediate Products for Anionic Surfactant Synthesis. In *Anionic Surfactants: Organic Chemistry*, Stache, H., Ed. Marcel Dekker: 1996; pp 1-38.
13. Burns, N., Surfactants Global Markets and Trends. In *3rd Petrochemical Conclave*, Delhi, 2014.
14. *Focus on Surfactants* **2016**, 2016 (12), 3.
15. Kagaya, M., Efficient Anionic Surfactant Which Can Change Soil into Co-Surfactant, Leading to More with Less In *CESIO 10th World Surfactant Congress*, Istanbul, 2015.
16. CESIO, CESIO Statistics 2013. 2014.

17. Houston, J., Surfactant Sustainability outlook to 2025. In *CESIO 10th World Surfactant Congress*, Istanbul, 2015.
18. Yu, Y.; Zhao, J.; Bayly, A. E., *Chin J Chem Eng* **2008**, 16 (4), 517-527.
19. Johansson, I.; Svensson, M., *Curr Opin Colloid Interface Sci* **2001**, 6 (2), 178-188.
20. Evans, D. F.; Wennerström, H., Solutes and Solvents, Self-Assembly of Amphiphiles. In *The Colloidal Domain: Where Physics, Chemistry, Biology, and Technology Meet*, Wiley: 1999; pp 1-44.
21. Karsa, D. R.; Houston, J., What are Surfactants? In *Chemistry and Technology of Surfactants*, Farn, R. J., Ed. Blackwell Publishing Ltd: 2007; pp 1-23.
22. Patel, M., *J Ind Ecol* **2003**, 7 (3-4), 47-62.
23. Mudge et al., S., How Would Changing the Feedstock Alter the Rate or Risk of my Fatty Alcohol-based Surfactants. In *CESIO 10th World Surfactant Congress*, Istanbul, 2015.
24. Svensson, M., Surfactants Based on Natural Fatty Acids. In *Surfactants from Renewable Resources*, Kjellin, M.; Johansson, I., Eds. John Wiley & Sons, Ltd: 2010; pp 1-19.
25. Foley, P.; Kermanshahi pour, A.; Beach, E. S.; Zimmerman, J. B., *Chem Soc Rev* **2012**, 41 (4), 1499-1518.
26. Smulders, E.; Rähse, W.; von Rybinski, W.; Steber, J.; Sung, E.; Wiebel, F., Toxicology. In *Laundry Detergents*, Wiley-VCH Verlag GmbH & Co. KGaA: 2003; pp 203-208.
27. Bartnik, F.; Künstler, K., Biological Effects, Toxicology and Human Safety. In *Surfactants in Consumer Products*, Falbe, J., Ed. Springer Berlin Heidelberg: 1987; pp 475-503.
28. Helenius, A.; Simons, K., *Biochim Biophys Acta, Rev Biomembr* **1975**, 415 (1), 29-79.
29. Domingo, X., Alcohol and Alcohol Ether Sulfates. In *Anionic Surfactants: Organic Chemistry*, Stache, H., Ed. Marcel Dekker: 1996; pp 223-312.
30. Huber, L.; Nitschke, L., Environmental Aspects of Surfactants. In *Handbook of Applied Surface and Colloid Chemistry (Volume 1)*, Holmberg, K., Ed. Wiley: 2002; pp 509-536.
31. Scott, M. J.; Jones, M. N., *Biochim Biophys Acta - Biomembranes* **2000**, 1508 (1-2), 235-251.
32. Slater, P. J.; Farn, R. J.; Clark, P. E.; Bernstein, M., Relevant European Legislation. In *Chemistry and Technology of Surfactants*, Farn, R. J., Ed. Blackwell Publishing Ltd: 2007; pp 236-268.
33. Smulders, E.; Rähse, W.; von Rybinski, W.; Steber, J.; Sung, E.; Wiebel, F., Ecology. In *Laundry Detergents*, Wiley-VCH Verlag GmbH & Co. KGaA: 2003; pp 165-203.

34. Benrraou, M.; Bales, B. L.; Zana, R., *J Phys Chem B* **2003**, 107 (48), 13432-13440.
35. Correa, N. M.; Silber, J. J.; Riter, R. E.; Levinger, N. E., *Chemical Reviews* **2012**, 112 (8), 4569-4602.
36. Gerike, P., Environmental Impact. In *Surfactants in Consumer Products*, Falbe, J., Ed. Springer Berlin Heidelberg: 1987; pp 450-474.
37. Ratledge, C., *Biochemistry of Microbial Degradation*. Kluwer: 1994.
38. Swisher, R. D., *Surfactant Biodegradation, Second Edition*. Taylor & Francis: 1986.
39. Scheibel, J. J., *J Surfact Deterg* **2004**, 7 (4), 319-328.
40. Issa, J.; Hattori, Y.; Driedger, A., Relevant Legislation – Australia, Japan and USA. In *Chemistry and Technology of Surfactants*, Blackwell Publishing Ltd: 2007; pp 269-299.
41. Evonik-Industries, Evonik commercializes biosurfactants. *Press Release* June 2016, 2016.
42. Kaumanns, O., Sporolipids - A new class of Surfactants. In *SEPAWA Nordic*, Malmo, 2015.
43. Rosen, M. J., Characteristic Features of Surfactants. In *Surfactants and Interfacial Phenomena*, John Wiley & Sons, Inc.: 2004; pp 1-33.
44. Rosen, M. J., Reduction of Surface and Interfacial Tension by Surfactants. In *Surfactants and Interfacial Phenomena*, John Wiley & Sons, Inc.: 2004; pp 208-242.
45. Holmberg, K.; Jönsson, B.; Kronberg, B.; Lindman, B., Surface Tension and Adsorption at the Air–Water Interface. In *Surfactants and Polymers in Aqueous Solution*, John Wiley & Sons, Ltd: 2003; pp 337-355.
46. Rosen, M. J., Adsorption of Surface-Active Agents at Interfaces: The Electrical Double Layer. In *Surfactants and Interfacial Phenomena*, John Wiley & Sons, Inc.: 2004; pp 34-104.
47. Evans, D. F.; Wennerström, H., Surface Chemistry and Monolayers. In *The Colloidal Domain: Where Physics, Chemistry, Biology, and Technology Meet*, Wiley: 1999; pp 45-98.
48. Dörfler, H. D., Grenzflächenthermodynamik. In *Grenzflächen und kolloid-disperse Systeme: Physik und Chemie*, Springer: 2002; pp 19-38.
49. Gecol, H., The Basic Theory. In *Chemistry and Technology of Surfactants*, Blackwell Publishing Ltd: 2007; pp 24-45.
50. Hassan, S.; Rowe, W.; Tiddy, G. J. T., Surfactant Liquid Crystals. In *Handbook of Applied Surface and Colloid Chemistry (Volume 1)*, Holmberg, K., Ed. Wiley: 2002; pp 465-508.

51. Evans, D. F.; Wennerström, H., Forces in Colloidal Systems. In *The Colloidal Domain: Where Physics, Chemistry, Biology, and Technology Meet*, Wiley: 1999; pp 217-294.
52. Mancera, R. L.; Kronberg, B.; Costas, M.; Silveston, R., *Biophys Chem* **1998**, 70 (1), 57-63.
53. Kronberg, B.; Castas, M.; Silvestonti, R., *J Dispersion Sci Technol* **1994**, 15 (3), 333-351.
54. Costas, M.; Kronberg, B.; Silveston, R., *J Chem Soc, Faraday Trans* **1994**, 90 (11), 1513-1522.
55. Evans, D. F., *Langmuir* **1988**, 4 (1), 3-12.
56. Shinoda, K., *J Phys Chem* **1977**, 81 (13), 1300-1302.
57. Zemb, T.; Testard, F., Solubilization. In *Handbook of Applied Surface and Colloid Chemistry (Volume 2)*, Holmberg, K., Ed. Wiley: 2002; pp 159-188.
58. Evans, D. F.; Wennerström, H., Structure and Properties of Micelles. In *The Colloidal Domain: Where Physics, Chemistry, Biology, and Technology Meet*, Wiley: 1999; pp 153-216.
59. Mukerjee, P.; Mysels, K. J., *Critical micelle concentrations of aqueous surfactant systems*. U.S. National Bureau of Standards; for sale by the Supt. of Docs., U.S. Govt. Print. Off.: 1971.
60. Rosen, M. J., Micelle Formation by Surfactants. In *Surfactants and Interfacial Phenomena*, John Wiley & Sons, Inc.: 2004; pp 105-177.
61. Holmberg, K.; Jönsson, B.; Kronberg, B.; Lindman, B., Surfactant Micellization. In *Surfactants and Polymers in Aqueous Solution*, John Wiley & Sons, Ltd: 2003; pp 39-66.
62. Klein, R.; Kellermeier, M.; Touraud, D.; Müller, E.; Kunz, W., *J Colloid Interface Sci* **2013**, 392 (0), 274-280.
63. Mukerjee, P.; Mysels, K.; Kapauan, P., *J Phys Chem* **1967**, 71 (13), 4166-4175.
64. Dörfler, H.-D., Mizellkolloide. In *Grenzflächen und kolloid-disperse Systeme*, Springer: 2002; pp 373-404.
65. Laughlin, R. G., The Characteristic Features of Surfactant Phase Behavior In *The Aqueous Phase Behaviour of Surfactants*, Academic Press: 1994; pp 102-154.
66. Weil, J. K.; Stirton, A. J.; Nuñez-Ponzoa, M. V., *J Am Oil Chem Soc* **1966**, 43 (11), 603-606.
67. Klein, R.; Touraud, D.; Kunz, W., *Green Chem* **2008**, 10 (4), 433-435.
68. Klein, R.; Zech, O.; Maurer, E.; Kellermeier, M.; Kunz, W., *J Phys Chem B* **2011**, 115 (29), 8961-8969.

69. Zech, O.; Hunger, J.; Sangoro, J. R.; Iacob, C.; Kremer, F.; Kunz, W.; Buchner, R., *Phys Chem Chem Phys* **2010**, 12 (42), 14341-14350.
70. Klein, R.; Kellermeier, M.; Drechsler, M.; Touraud, D.; Kunz, W., *Colloids Surf A Physicochem Eng Asp* **2009**, 338 (1–3), 129-134.
71. Zana, R., *Langmuir* **2004**, 20 (14), 5666-5668.
72. Yu, Z. J.; Zhang, X.; Xu, G.; Zhao, G., *J Phys Chem* **1990**, 94 (9), 3675-3681.
73. Rengstl, D., Dissertation. Universität Regensburg: 2013.
74. Wolfrum, S., Master Thesis. Universität Regensburg: 2013.
75. Kaneshina, S.; Kamaya, H.; Ueda, I., *J Colloid Interface Sci* **1981**, 83 (2), 589-598.
76. Nakayama, H.; Shinoda, K.; Hutchinson, E., *J Phys Chem* **1966**, 70 (11), 3502-3504.
77. Smallwood, P., Global Cleaning Trends and their Effect on Surfactant Choice. In *CESIO 10th World Surfactant Congress*, Istanbul, 2015.
78. Smulders, E.; Rähse, W.; von Rybinski, W.; Steber, J.; Sung, E.; Wiebel, F., Physical Chemistry of the Washing Process. In *Laundry Detergents*, Wiley-VCH Verlag GmbH & Co. KGaA: 2003; pp 7-38.
79. Smulders, E.; Rähse, W.; von Rybinski, W.; Steber, J.; Sung, E.; Wiebel, F., Detergent Ingredients. In *Laundry Detergents*, Wiley-VCH Verlag GmbH & Co. KGaA: 2003; pp 38-98.
80. Rosen, M. J., Detergency and Its Modification by Surfactants. In *Surfactants and Interfacial Phenomena*, John Wiley & Sons, Inc.: 2004; pp 353-378.
81. von Rybinski, W., Surface Chemistry in Detergency. In *Handbook of Applied Surface and Colloid Chemistry (Volume 1)*, Holmberg, K., Ed. Wiley: 2002; pp 53-72.
82. Miller, C. A.; Raney, K. H., *Colloids Surf A Physicochem Eng Asp* **1993**, 74 (2–3), 169-215.
83. Preston, W. C., *J Phys Colloid Chem* **1948**, 52 (1), 84-97.
84. Kunz, W.; Neueder, R., An Attempt of a General Overview. In *Specific Ion Effects*, WORLD SCIENTIFIC: 2009; pp 3-54.
85. Kunz, W., *Curr Opin Colloid Interface Sci* **2010**, 15 (1–2), 34-39.
86. Zhang, Y.; Cremer, P. S., *Current Opinion in Chemical Biology* **2006**, 10 (6), 658-663.
87. Kunz, W.; Henle, J.; Ninham, B. W., *Curr Opin Colloid Interface Sci* **2004**, 9 (1–2), 19-37.
88. Vlachy, N.; Jagoda-Cwiklik, B.; Vácha, R.; Touraud, D.; Jungwirth, P.; Kunz, W., *Adv Colloid Interface Sci* **2009**, 146 (1–2), 42-47.

89. Collins, K. D.; Neilson, G. W.; Enderby, J. E., *Biophys Chem* **2007**, 128 (2–3), 95-104.
90. Collins, K. D., *Methods* **2004**, 34 (3), 300-311.
91. Collins, K. D., *Biophys Chem* **2006**, 119 (3), 271-281.
92. Harrison, C. R.; Sader, J. A.; Lucy, C. A., *Journal of Chromatography A* **2006**, 1113 (1–2), 123-129.
93. Radošević, K.; Cvjetko Bubalo, M.; Gaurina Srček, V.; Grgas, D.; Landeka Dragičević, T.; Radojčić Redovniković, I., *Ecotoxicology and Environmental Safety* **2015**, 112, 46-53.
94. Zhang, Q.; De Oliveira Vigier, K.; Royer, S.; Jerome, F., *Chem Soc Rev* **2012**, 41 (21), 7108-7146.
95. Restolho, J.; Mata, J. L.; Saramago, B., *Fluid Phase Equilib* **2012**, 322–323 (0), 142-147.
96. Liu, Q.-P.; Hou, X.-D.; Li, N.; Zong, M.-H., *Green Chem* **2012**, 14 (2), 304-307.
97. Petkovic, M.; Seddon, K. R.; Rebelo, L. P. N.; Silva Pereira, C., *Chem Soc Rev* **2011**, 40 (3), 1383-1403.
98. Pernak, J.; Syguda, A.; Mirska, I.; Pernak, A.; Nawrot, J.; Pradzynska, A.; Griffin, S. T.; Rogers, R. D., *Chemistry* **2007**, 13 (24), 6817-27.
99. Fukaya, Y.; Iizuka, Y.; Sekikawa, K.; Ohno, H., *Green Chem* **2007**, 9 (11), 1155-1157.
100. Abbott, A. P.; Boothby, D.; Capper, G.; Davies, D. L.; Rasheed, R. K., *J Am Chem Soc* **2004**, 126 (29), 9142-9147.
101. Wittcoff, H. A.; Reuben, B. G.; Plotkin, J. S., Chemicals from Methane. In *Industrial Organic Chemicals*, John Wiley & Sons, Inc.: 2012; pp 407-462.
102. Yu, Z. J.; Xu, G., *J Phys Chem* **1989**, 93 (21), 7441-7445.
103. Hrobárik, T.; Vrbka, L.; Jungwirth, P., *Biophys Chem* **2006**, 124 (3), 238-242.
104. Kutluay, E.; Roux, B.; Heginbotham, L., *Biophys J* **2005**, 88 (2), 1018-1029.
105. Luzhkov, V. B.; Åqvist, J., *FEBS Lett* **2001**, 495 (3), 191-196.
106. O'Leary, M. E.; Kallen, R. G.; Horn, R., *J Gen Physiol* **1994**, 104 (3), 523-539.
107. Moberg, R.; Boekman, F.; Bohman, O.; Siegbahn, H. O. G., *J Am Chem Soc* **1991**, 113 (10), 3663-3667.
108. Zeisel, S. H.; da Costa, K. A., *Nutr Rev* **2009**, 67 (11), 615-23.
109. Blusztajn, J. K., *Science* **1998**, 281 (5378), 794-795.

110. *Dietary Reference Intakes for Thiamin, Riboflavin, Niacin, Vitamin B6, Folate, Vitamin B12, Pantothenic Acid, Biotin, and Choline*. The National Academies Press: 1998.
111. Zeisel, S. H., *Annu Rev Nutr* **2006**, 26, 229-50.
112. Zeisel, S. H.; Niculescu, M. D., *Nutr Rev* **2006**, 64 (4), 197-203.
113. Khairallah, E. A.; Wolf, G., *J Biol Chem* **1967**, 242 (1), 32-39.
114. Vardanyan, R. S.; Hruby, V. J., Cholinomimetics. In *Synthesis of Essential Drugs*, Elsevier: Amsterdam, 2006; pp 179-193.
115. Landeck, L.; Baden, L.; John, S.-M., Detergents. In *Kanerva's Occupational Dermatology*, Rustemeyer, T.; Elsner, P.; John, S.-M.; Maibach, H., Eds. Springer Berlin Heidelberg: 2012; pp 847-857.
116. Toedt, J.; Koza, D.; Van Cleef-Toedt, K., *Chemical composition of everyday products*. Greenwood Publishing Group: 2005.
117. Willcox, M., Soap. In *Poucher's Perfumes, Cosmetics and Soaps*, Butler, H., Ed. Springer Netherlands: 2000; pp 453-465.
118. Routh, H. B.; Bhowmik, K. R.; Parish, L. C.; Witkowski, J. A., *Clin Dermatol* **1996**, 14 (1), 3-6.
119. Preston, W. C., *J Chem Educ* **1925**, 2 (11), 1035-1044.
120. Wolf, R.; Wolf, D.; Tüzün, B.; Tüzün, Y., *Clin Dermatol* **2001**, 19 (4), 393-397.
121. Preston, W. C., *J Chem Educ* **1925**, 2 (12), 1130-1139.
122. Stache, H., *Anionic Surfactants: Organic Chemistry*. Marcel Dekker: 1996.
123. Ali, S. M.; Yosipovitch, G., *Acta Derm Venereol* **2013**, 93 (3), 261-269.
124. Ananthapadmanabhan, K. P.; Lips, A.; Vincent, C.; Meyer, F.; Caso, S.; Johnson, A.; Subramanyan, K.; Vethamuthu, M.; Rattinger, G.; Moore, D. J., *Int J Cosmet Sci* **2003**, 25 (3), 103-112.
125. Baranda, L.; González-Amaro, R.; Torres-Alvarez, B.; Alvarez, C.; Ramírez, V., *Int J Dermatol* **2002**, 41 (8), 494-499.
126. Murahata, R. I.; Aronson, M. P., *J Soc Cosmet Chem* **1994**, 45 (5), 239-246.
127. Hill, K., *Pure Appl Chem* **2007**, 79 (11), 1999-2011.
128. Fiedler, H. P.; Umbach, W., Cosmetics and Toiletries. In *Surfactants in consumer products: Theory, Technology and Application*, Falbe, J., Ed. Springer Science & Business Media: 1987; pp 350-387.
129. Ho Han Tai, L., *Formulating Detergents and Personal Care Products*. AOCS Press: 2000.
130. Abamba, G., Skin preparations. In *Poucher's Perfumes, Cosmetics and Soaps*, Butler, H., Ed. Springer Netherlands: Dordrecht, 2000; pp 393-452.

131. Paniccia, P., Men's toiletries. In *Poucher's Perfumes, Cosmetics and Soaps*, Butler, H., Ed. Springer Netherlands: Dordrecht, 2000; pp 345-375.
132. Theander, K.; Pugh, R. J., *Colloids Surf A Physicochem Eng Asp* **2004**, 240 (1–3), 111-130.
133. Borchardt, J. K., *Curr Opin Colloid Interface Sci* **1997**, 2 (4), 402-408.
134. Quast, K. B., *Miner Eng* **2000**, 13 (13), 1361-1376.
135. Pascoe, R. D.; Doherty, E., *Int J Miner Process* **1997**, 51 (1), 269-282.
136. Nora, A.; Szczepanek, A.; Koenen, G., Metallic Soaps. In *Ullmann's Encyclopedia of Industrial Chemistry*, Wiley-VCH Verlag GmbH & Co. KGaA: 2000.
137. Falchi, L.; Zendri, E.; Müller, U.; Fontana, P., *Cem Concr Compos* **2015**, 59, 107-118.
138. Lanzón, M.; García-Ruiz, P. A., *Constr Build Mater* **2009**, 23 (10), 3287-3291.
139. Izzo, F. C.; van den Berg, K. J.; van Keulen, H.; Ferriani, B.; Zendri, E., Modern Oil Paints – Formulations, Organic Additives and Degradation: Some Case Studies. In *Issues in Contemporary Oil Paint*, van den Berg, J. K.; Burnstock, A.; de Keijzer, M.; Krueger, J.; Learner, T.; Tagle, A.; Heydenreich, G., Eds. Springer International Publishing: Cham, 2014; pp 75-104.
140. Kjellin, M.; Johansson, I., *Surfactants from renewable resources*. John Wiley & Sons: 2010.
141. McBain, J.; Lee, W., *Oil & Soap* **1943**, 20 (2), 17-25.
142. McBain, J.; Sierichs, W., *J Am Oil Chem Soc* **1948**, 25 (6), 221-225.
143. Shedlovsky, L.; Miles, G. D.; Scott, G. V., *J Phys Colloid Chem* **1947**, 51 (2), 391-407.
144. Klein, R., Dissertation. Universität Regensburg: 2011.
145. Laughlin, R. G., Phase Diagrams and the Phase Rule. In *The Aqueous Phase Behaviour of Surfactants*, Academic Press: 1994; pp 67-101.
146. Rosen, M. J., *Surfactants and Interfacial Phenomena*. John Wiley & Sons, Inc.: 2004.
147. Rosen, M. J., Solubilization by Solutions of Surfactants: Micellar Catalysis. In *Surfactants and Interfacial Phenomena*, John Wiley & Sons, Inc.: 2004; pp 178-207.
148. Fameau, A.-L.; Zemb, T., *Adv Colloid Interface Sci* **2014**, 207, 43-64.
149. Dörfler, H. D., *Grenzflächen und kolloid-disperse Systeme: Physik und Chemie*. Springer: 2002.
150. Lin, B.; McCormick, A. V.; Davis, H. T.; Strey, R., *J Colloid Interface Sci* **2005**, 291 (2), 543-549.

151. Klein, R.; Muller, E.; Kraus, B.; Brunner, G.; Estrine, B.; Touraud, D.; Heilmann, J.; Kellermeier, M.; Kunz, W., *RSC Adv* **2013**, 3 (45), 23347-23354.
152. Novales, B.; Riaublanc, A.; Navailles, L.; Houinsou Houssou, B. r. n.; Gaillard, C. d.; Nallet, F. d. r.; Douliez, J.-P., *Langmuir* **2010**, 26 (8), 5329-5334.
153. Novales, B.; Navailles, L.; Axelos, M.; Nallet, F.; Douliez, J.-P., *Langmuir* **2007**, 24 (1), 62-68.
154. Douliez, J.-P.; Navailles, L.; Nallet, F., *Langmuir* **2006**, 22 (2), 622-627.
155. Fameau, A.-L.; Houinsou-Houssou, B.; Ventureira, J. L.; Navailles, L.; Nallet, F.; Novales, B.; Douliez, J.-P., *Langmuir* **2011**, 27 (8), 4505-4513.
156. Douliez, J.-P.; Houinsou-Houssou, B.; Fameau, A.-L.; Novales, B.; Gaillard, C., *J Colloid Interface Sci* **2010**, 341 (2), 386-389.
157. Douliez, J.-P., *Langmuir* **2004**, 20 (5), 1543-1550.
158. Ouimet, J.; Croft, S.; Paré, C.; Katsaras, J.; Lafleur, M., *Langmuir* **2003**, 19 (4), 1089-1097.
159. Paré, C.; Lafleur, M., *Langmuir* **2001**, 17 (18), 5587-5594.
160. Zemb, T.; Dubois, M., *Aust J Chem* **2003**, 56 (10), 971-979.
161. Lee, S.; Kim, D. H.; Needham, D., *Langmuir* **2001**, 17 (18), 5544-5550.
162. Irani, R. R., *J Chem Eng Data* **1962**, 7 (4), 580-581.
163. Irani, R. R.; Callis, C. F., *J Phys Chem* **1960**, 64 (11), 1741-1743.
164. Singer, J. J., *J Chem Educ* **1972**, 49 (5), 330.
165. Borghetty, H. C.; Bergman, C. A., *J Am Oil Chem Soc* **1950**, 27 (3), 88-90.
166. Kaibara, K.; Ogawa, T.; Kawasaki, H.; Suzuki, M.; Maeda, H., *Colloid Polym Sci* **2003**, 281 (3), 220-228.
167. Cistola, D. P.; Hamilton, J. A.; Jackson, D.; Small, D. M., *Biochemistry* **1988**, 27 (6), 1881-1888.
168. Hirai, A.; Kawasaki, H.; Tanaka, S.; Nemoto, N.; Suzuki, M.; Maeda, H., *Colloid Polym Sci* **2006**, 284 (5), 520-528.
169. Apel, C. L.; Deamer, D. W.; Mautner, M. N., *Biochim Biophys Acta - Biomembranes* **2002**, 1559 (1), 1-9.
170. Edwards, K.; Silvander, M.; Karlsson, G., *Langmuir* **1995**, 11 (7), 2429-2434.
171. Hargreaves, W. R.; Deamer, D. W., *Biochemistry* **1978**, 17 (18), 3759-3768.
172. Rosano, H. L.; Breindel, K.; Schulman, J. H.; Eydt, A. J., *J Colloid Interface Sci* **1966**, 22 (1), 58-67.

173. Fukuda, H.; Goto, A.; Yoshioka, H.; Goto, R.; Morigaki, K.; Walde, P., *Langmuir* **2001**, 17 (14), 4223-4231.
174. Feinstein, M. E.; Rosano, H. L., *J Phys Chem* **1969**, 73 (3), 601-607.
175. Small, D. M., *Physical chemistry of lipids*. Plenum Press: 1986.
176. Lynch, M. L., *Curr Opin Colloid Interface Sci* **1997**, 2 (5), 495-500.
177. Cistola, D. P.; Atkinson, D.; Hamilton, J. A.; Small, D. M., *Biochemistry* **1986**, 25 (10), 2804-2812.
178. Walde, P.; Namani, T.; Morigaki, K.; Hauser, H., Formation and properties of fatty acid vesicles (liposomes). In *Liposome technology*, Gregoriadis, G., Ed. CRC Press: 2006; Vol. 1, pp 1-19.
179. Morigaki, K.; Walde, P.; Misran, M.; Robinson, B. H., *Colloids Surf A Physicochem Eng Asp* **2003**, 213 (1), 37-44.
180. Rosano, H. L.; Christodoulou, A. P.; Feinstein, M. E., *J Colloid Interface Sci* **1969**, 29 (2), 335-344.
181. Haines, T. H., *Proc Natl Acad Sci U S A* **1983**, 80 (1), 160-164.
182. Gebicki, J. M.; Hicks, M., *Chem Phys Lipids* **1976**, 16 (2), 142-160.
183. Davies, J.; Rideal, E., *Interfacial Phenomena*. Academic Press, NY: 1963.
184. Morigaki, K.; Walde, P., *Curr Opin Colloid Interface Sci* **2007**, 12 (2), 75-80.
185. Kanicky, J. R.; Shah, D. O., *Langmuir* **2003**, 19 (6), 2034-2038.
186. Kanicky, J. R.; Shah, D. O., *J Colloid Interface Sci* **2002**, 256 (1), 201-207.
187. Kanicky, J. R.; Poniatowski, A. F.; Mehta, N. R.; Shah, D. O., *Langmuir* **1999**, 16 (1), 172-177.
188. Söderman, O.; Jönsson, B.; Olofsson, G., *J Phys Chem B* **2006**, 110 (7), 3288-3293.
189. Whiddon, C. R.; Bunton, C. A.; Söderman, O., *J Phys Chem B* **2002**, 107 (4), 1001-1005.
190. da Silva, F. L. B.; Bogren, D.; Söderman, O.; Åkesson, T.; Jönsson, B., *J Phys Chem B* **2002**, 106 (13), 3515-3522.
191. Kaibara, K.; Iwata, E.; Eguchi, Y.; Suzuki, M.; Maeda, H., *Colloid Polym Sci* **1997**, 275 (8), 777-783.
192. Janke, J. J.; Bennett, W. F. D.; Tieleman, D. P., *Langmuir* **2014**, 30 (35), 10661-10667.
193. Israelachvili, J. N.; Mitchell, D. J.; Ninham, B. W., *Journal of the Chemical Society, Faraday Transactions 2: Molecular and Chemical Physics* **1976**, 72 (0), 1525-1568.



## **Chapter 3 Highly translucent and stable solutions of NaOl and RebA at neutral pH and room temperature**

### **3.1 Abstract**

It is well known that with the food emulsifier sodium oleate (NaOl), clear and stable aqueous solutions can only be obtained at pH values higher than 10. A decrease in the pH value leads to turbid and unstable solutions.<sup>1, 2</sup> This effect is not compatible with the formulation of aqueous stable and drinkable formulations with neutral or even acidic pH values. However, the pH value/phase behavior of aqueous soap solutions can be altered by the addition of other surfactants. Such a surfactant can be Rebaudioside A (RebA), a steviol glycoside from the plant *Stevia rebaudiana* which is used as a natural food sweetener. In a recent paper, Marcus et al.<sup>3</sup> showed the influence of RebA on the  $pK_a$  value of sodium oleate in a beverage microemulsion and on its clearing temperature.

In this work, the effect of the edible bio-surfactant RebA on the macroscopic and microscopic phase behavior of simple aqueous sodium oleate solutions at varying pH values is reported. The macroscopic phase behavior is investigated by visual observation and turbidity measurements. The microscopic phase behavior is analyzed by acid-base titration curves, phase-contrast and electron microscopy.

It turned out that even at neutral pH, aqueous NaOl/RebA solutions can be completely clear and stable for more than 50 days at room temperature. This is for the first time that a long chain soap could be really solubilised in water at neutral pH at room temperature. At last, these findings were applied to prepare stable, highly translucent and drinkable aqueous solutions of omega-3-fatty acids at a pH value of 7.5.

At the end of this chapter, an outlook and some strategies are given, how the well-known problems of soaps in application can possibly be overcome in a green way.

### **3.2 Introduction**

Sodium oleate (NaOl) and oleic acid (OA) are natural food ingredients approved for direct addition to food by the US Food and Drug Administration as well as by the

European committee.<sup>4-6</sup> NaOI is used as emulsifier in food and finds application in food packaging and in cosmetics.<sup>7</sup> Its protonated form, oleic acid (OA), is an essential molecule in biology and a lipid part of many membrane structures in the mammal body.<sup>8, 9</sup> Furthermore, it is the main fatty acid within the triglycerides of olive, sunflower and hazelnut oil and regularly consumed via daily food.<sup>10, 11</sup>

In dilute aqueous solutions, NaOI is well known to self-assemble into micellar aggregates which can vary in structure when the concentration is increased.<sup>12, 13</sup> These solutions remain clear and stable only at pH values higher than 10, a consequence of the high apparent  $pK_A$  value ( $apK_A$  = the measured  $pK_A$  value of a long chain fatty acid in colloidal systems) for long chain fatty acids in solution due to aggregate formation.<sup>2, 13-21</sup> A decrease in pH leads to an increased ratio of OA to oleate affecting the aggregated species being formed. The aqueous NaOI/OA system has been investigated with different techniques at room temperature and the following structures were found with decreasing pH: micelles, lamellar phases (bilayers) and oil-like phases, with the latter leading to turbid and macroscopically unstable solutions.<sup>2, 13, 18, 19, 22</sup> In the present study, in a 1wt% aqueous solution of NaOI, a lamellar phase was formed at a pH value around 10. Decreasing the pH value resulted in highly turbid translucent solutions showing macroscopic phase separation after 1 day. At a pH value slightly higher than 8, oil droplets were observed and the solutions were milky white with a fast tendency to phase separate macroscopically. These observations are in line with the findings of several other authors.<sup>2, 18, 19, 22</sup>

Although the pH value in many beverages is acidic (2.0-4.0), the World Health Organization WHO, the Safe Drinking Water Act and the European Community list a guide number for the pH value of drinking water of 6.5-8.5.<sup>23</sup> However, the unpleasant look (high turbidity and macroscopically phase separation) of aqueous NaOI solutions at pH values lower than 8.5 and its soapy taste are strong barriers for consumable aqueous solutions on the basis of NaOI/OA. To overcome these two disadvantages, Rebaudioside A can be used.

Rebaudioside A (RebA) is a natural, non-caloric high efficiency sweetener which is extracted from the plant *Stevia rebaudiana* and known in high purity under the name Rebiana.<sup>24-26</sup> Next to RebA, other steviol glycosides, like stevioside (see **Figure 3-1** right), can be extracted from *Stevia rebaudiana*. These steviol glycosides exhibit similar chemical structures. All of them consist of the diterpenoid aglycone steviol, but vary in the amount and kind of sugars connected to the steviol backbone. RebA and stevioside only possess glucose units connected to steviol with RebA having four of them and stevioside only having three (see **Figure 3-1**).<sup>25, 27, 28</sup> All steviol

glycosides are known to have high sweetening capacities. In literature it is found that RebA and stevioside have a sweetness potency which is at least 200 times higher than sucrose.<sup>25-29</sup> Although Stevia sweeteners have been used for decades in Japan, China, Korea and South America to sweeten various foods, it was not before 2008/2009 that U.S. FDA approved highly pure steviol glycosides extracted from stevia leaves as GRAS (generally recognized as safe) for the use in food. In Europe, the European Committee allowed the usage of pure steviol glycosides as a food additive finally in November 2011.<sup>28-30</sup> Steviol Glycosides have not only been shown to be non-toxic, non-mutagenic and non-carcinogenic for humans, there are also many studies which point out the therapeutic value and the health effect of steviol glycosides.<sup>26-28, 30, 31</sup> Of course, this opened a lot of new markets for food sweetened with steviol glycosides and now many food containing steviol glycosides can be found in the super market. In the last years, the main ingredient of steviol glycosides based high potency sweeteners changed from stevioside to RebA due to its superior taste characteristics compared to stevioside.<sup>28, 29</sup>

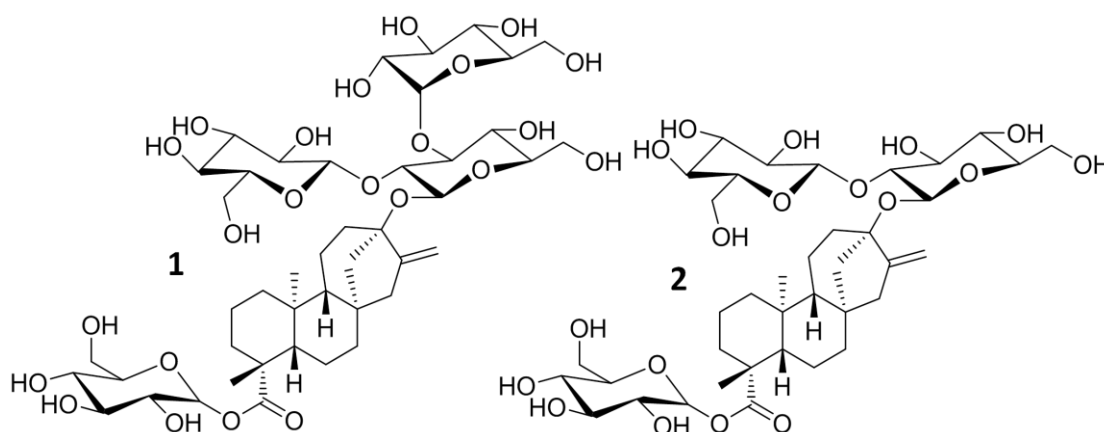


**Figure 3-1:** Comparison of the chemical structures of rebaudioside A (1) and stevioside (2).

In a recent paper<sup>3</sup>, it was shown that RebA lowers significantly the apKa value of sodium oleate in a beverage microemulsion and is further able to lower its clearing temperature. Due to its effects on the microemulsion, RebA was considered as a weak surfactant or at least as a co-surfactant. This is in line with what was found for structurally similar steviol glycosides. In a series of papers, Wan et al.<sup>32-34</sup> demonstrated the surface activity of stevioside and called it a bio-surfactant. They displayed its ability to form micelles, determined its critical micellar concentration (cmc) and showed that it can stabilize emulsions and foams by adsorbing at the interface. In 2012, Uchiyama et al.<sup>35</sup> reported a cmc for alpha-glucosyl stevia (stevioside plus additional glucose units<sup>36</sup>) and the formation of nanocomposites/mixed micelles between alpha-glucosyl stevia and sodium lauryl

sulfate. Although in literature only one patent<sup>37</sup> could be found reporting aggregates in aqueous RebA solutions determined by dynamic light scattering, RebA is likely to behave like the chemically similar stevioside or alpha-glucosyl stevia.

Moreover, it is well known that mixing of fatty acid soaps/fatty acids with other surfactants or alcohols in aqueous solution can lead to the formation of mixed aggregates, which alter their properties compared to those of the pure fatty acid soap solutions. These features could be for example the  $pK_A$  of the fatty acid within the mixed system, respectively a change in the pH value at a given neutralization state of the fatty acid or a change in the observed phase behavior with regard to system composition and/or prevailing pH value.<sup>13, 14, 16, 17, 38-50</sup>

In an attempt to stabilize a soap at consumable pH values, investigations on the macroscopic and microscopic phase behavior of aqueous NaOI solutions at different pH values containing a certain amount of the natural, high-efficient sweetener Rebaudioside A were carried out.

In the present work, first the water solubility of RebA was investigated and its surfactant-like behavior of RebA was verified by determining its cmc with the help of surface tension and DLS measurements. Then, the influence of different amounts of RebA on the dilute aqueous NaOI system was investigated at different pH values, by adding a given amount of HCl. The macroscopic and microscopic phase behavior of the prepared solutions was examined by visual observation and turbidity measurements, respectively acid-base titration curves, phase contrast and electron microscopy. At the end, the findings were applied to make aqueous solutions of omega-3-fatty acid salts at neutral pH.

### 3.3 Results and discussion

First, results obtained for the pure surfactant solutions will be shown and afterwards the mixed systems will be discussed. It starts with the cmc of the used Rebaudioside A and its dissolution behavior in water. For this purpose, the stability of aqueous solutions with different amounts of RebA are presented. Then, the macroscopic and microscopic aqueous phase behavior of pure NaOI solutions at different neutralization states  $\Theta_p$  is discussed. In the second part, the macroscopic and microscopic aqueous phase behavior of mixed NaOI + RebA systems are discussed for different neutralization states  $\Theta_p$  and compared to the single component solutions. Finally, it is shown how the conclusions from these results can be applied to conceive aqueous solutions of choline omega-3-fatty acid salts at drinkable pH values.

### 3.3.1 Aqueous solubility and cmc of RebA

Although the thermodynamic equilibrium solubility for RebA in water is 0.8 wt% at 25 °C, highly supersaturated aqueous solutions ( $\approx 30$  wt%) can be prepared. Depending on the conditions how RebA is crystallized from alcohol/water mixtures during purification, an amorphous form, a solvate form, an anhydrous form or a hydrate form is obtained. These polymorphs show a significantly different dissolution behavior in water. The first three forms readily provide supersaturated aqueous solutions. However, these solutions are not stable and RebA quickly crystallizes in its hydrate form until the concentration of RebA in solution is 0.8 wt%.<sup>24, 25</sup>

To get insight in the solubility behavior of the RebA used in this study and its stability in water, six aqueous solutions with 0.2, 0.4, 0.6, 0.8, 1.0 and 4.0 wt% RebA were prepared and observed during aging at room-temperature. Photos of these solutions after different time of aging are shown in **Figure 3-2**.

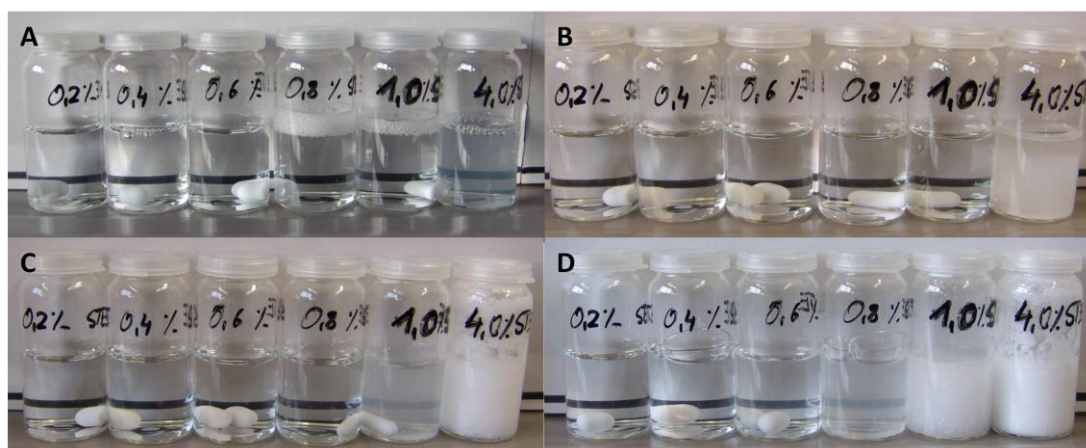


**Figure 3-2:** Aqueous solutions of RebA after different times of aging at room temperature. Photo A was taken 0.5 h after preparation, B after 1 d, C after 14 d and D after 75 d. The concentration increases from left to right (0.2, 0.4, 0.6, 0.8, 1.0 and 4.0 wt%).

The solution containing 4 wt% of RebA was visibly turbid directly after preparation and with time more and more solid particles and precipitate is observed making the solutions nontransparent white. Although the solutions with 0.8 and 1 wt% RebA appear clear immediately after preparation, on closer examination some schlieren are observed during slewing. With time the solutions also contained some big solid particles and some precipitate which made the solutions look turbid and white. This effect was more pronounced for the higher concentrated solution. The solution containing 0.6 wt% also was not stable. With time more and more solid particles appeared which made the solution slightly turbid. After 75 days of aging at room temperature, only solutions with 0.2 and 0.4 wt% RebA contained no white

precipitate in solution, suggesting an aqueous equilibrium solubility of the used RebA between 0.4 and 0.6 wt%.

The markedly lower value compared to the value reported in literature could be caused by the small amount of impurities (< 5 wt%), respectively less soluble steviol glycosides or the fact that the aqueous solubility of RebA reported in literature was determined with solutions that had not yet reached thermodynamic equilibrium. Degradation of RebA in pure aqueous solutions can be ruled out, since RebA was found to be very stable in aqueous solutions at ambient temperature in a pH range from 3-8 with a half-life of about ten years at pH 8. It has to be mentioned that no data for higher pH values were reported in this reference.<sup>25</sup> However, during two hours no difference in the stability of aqueous stevioside solutions was found within the pH range between 2 and 10 at 60 and 80 °C.<sup>51</sup> Regarding the chemical similarity of Reb A and stevioside (both exhibit the identical ester bond, see **Figure 3-1**), it can be expected that RebA is sufficiently stable in aqueous solutions at ambient temperatures up to a pH value of at least 10. Note that this is an important fact for the mixed NaOl/RebA/water systems prepared further on.

To prove the surfactant-like behavior of RebA, concentration dependent surface tension,  $\sigma$ , measurements were performed at 25°C to determine its cmc. In literature, only two surface tension values for different concentrations of RebA in water could be found which clearly show the surface activity of RebA, as well as a patent that reports the formation of aggregated species in aqueous solutions of RebA by light scattering.<sup>28, 37</sup> 1 wt% RebA was chosen as a starting concentration for the measurements. For this concentration, after preparation the solutions appeared macroscopically clear and contained only very little solid material which could affect the measurement. Measurements were started as fast as possible to prevent further crystallization of RebA from the 1 wt% solution (see discussion above and **Figure 3-2**). As can be seen in **Figure 3-3**, the obtained curves show a change in the gradient within a narrow concentration range indicating the presence of a cmc and match perfectly at lower concentration. Slight deviations at higher concentrations could be due to the fact that the initial concentration of the RebA solutions was above the equilibrium solubility of RebA and different amounts of small crystal particles affecting the measurement had already formed in solution. The cmc of RebA in water was found to be  $4570 \pm 210$  mg/l ( $0.475 \pm 0.02$  wt%) or  $4.73 \pm 0.22$  mmol/l. This is in line with the findings of Wan et al.<sup>33</sup>, who measured a cmc of 4200 mg/l for stevioside. The same is true for the reported surface tension values in

reference 38, which are 64.21 mN/m for a 0.01 wt% solution of RebA and 49.37 for a 0.5 wt% solution of RebA at 22 °C.

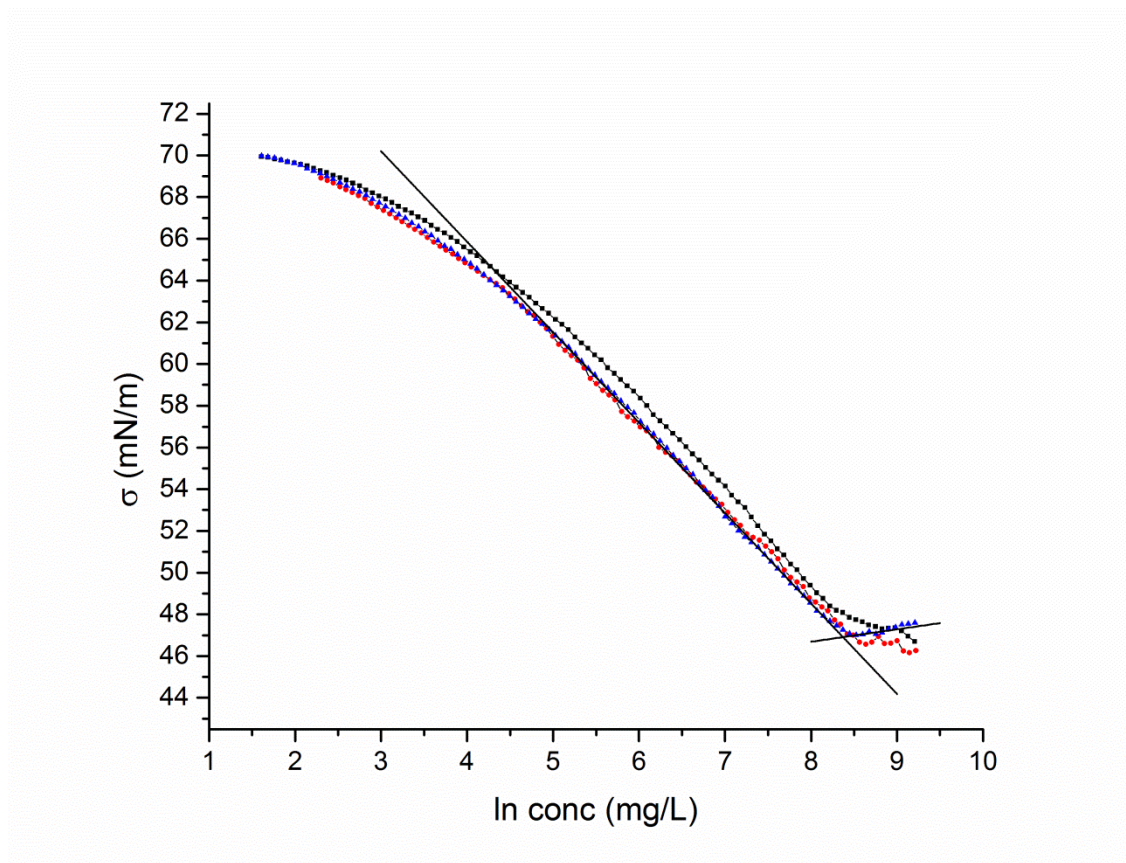


**Figure 3-3:** Plot of the surface tension  $\sigma$  versus the  $\ln$  of RebA concentration. The cmc for each curve is defined by the intersection of the two linear parts of the curve as it is illustrated.

Concentration dependent DLS measurements of aqueous RebA solutions support the surface tension data and also indicate the evolution of structures in solution with increasing concentration of RebA (see **Figure 3-4**). DLS data suggests a cmc of RebA around 0.6 wt% which is close to the value determined by surface tension measurements. At 0.1 wt% and 0.2 wt%, considerably below the cmc determined by surface tension measurements (0.475 wt%), no correlation is found. From 0.4 to 0.6 wt%, slightly below and above the cmc, a correlation function indicating structures gradually evolves. At 0.8 wt%, considerably above the cmc, a nice correlation function suggesting the formation of structures (micelles) is found.

*As a result, it can be concluded that RebA can be regarded as a true bio-surfactant.*

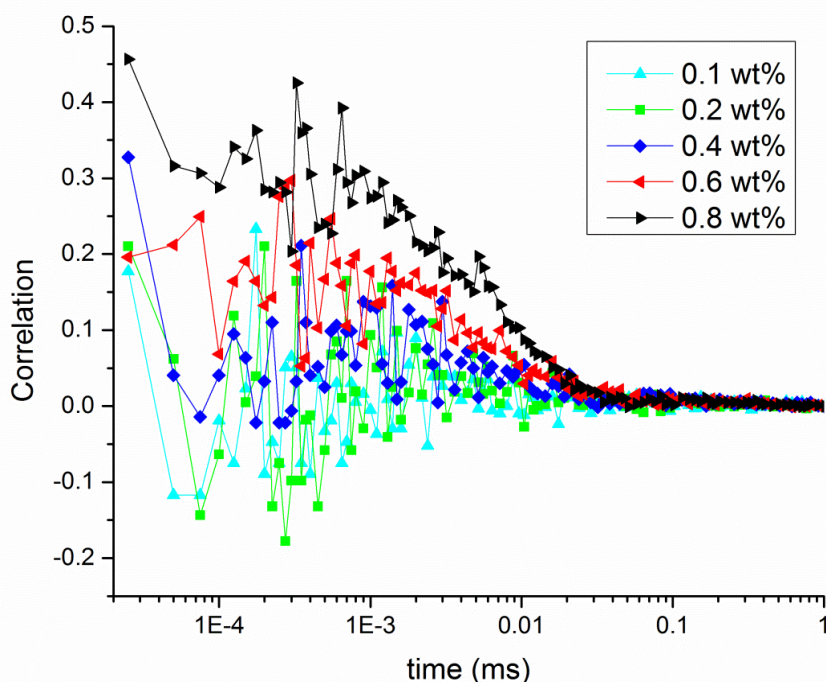


**Figure 3-4:** Evolution of the correlation functions from DLS measurements of aqueous RebA solutions at different concentrations.  $\blacktriangleright$  = 0.8wt%.  $\blacktriangleleft$  = 0.6 wt%,  $\blacklozenge$  = 0.4 wt%,  $\blacksquare$  = 0.2 wt%,  $\blacktriangle$  = 0.1 wt%.

### 3.3.2 Phase behavior of aqueous NaOl solutions at different neutralization states

It is well known that the phase behavior of aqueous long chain soap systems is highly dependent on the neutralization state  $\Theta_P$  (percentage of protonated fatty acid molecules) of the soap. Therefore, many studies have been performed on aqueous alkali metal soap systems with varying pH, respectively varying the ratio of protonated to deprotonated fatty acid, and many different techniques were used to determine the formed structures. In dilute aqueous solutions of alkali metal soaps the structures found were micelles, bilayers, acid-soap crystals, fatty acid crystals or inverted oil-like phases (see **Figure 3-5**).<sup>1, 13, 19, 20, 46, 52-55</sup>

For different alkali metal soaps, these systematic investigations clearly showed that the titration curves and the formed aggregates with increasing  $\Theta_P$  depend on the applied temperature and on the soap concentration. The strong temperature dependence of the titration curves can be attributed to the formation of acid soap crystals.<sup>56</sup> In diluted aqueous solutions, acid soap crystals exhibit a chain melting temperature  $T_m$ , above which the hydrophobic chains of the acid soap crystals “melt” and liquid crystalline structures (bilayers) are formed.<sup>19, 20, 57</sup>  $T_m$  for alkali oleate is

below room-temperature (25 °C), whereas for saturated alkali soaps with 12 and more carbon atoms,  $T_m$  is above 25 °C.<sup>20, 22, 57</sup> Consequently, at 25 °C, the phase behavior and the titration curve shown on the left side in **Figure 3-5** are found for alkali oleate soaps, whereas for dodecanoate and longer saturated alkyl chains the right one is valid. On the one hand, these diagrams have been interpreted by Cistola et al.<sup>19</sup> by applying Gibbs' phase rule, on the other hand, these diagrams have been discussed on the molecular level.<sup>20, 21, 55, 58</sup> The particular course of the acid-base titration curves and their origin is discussed very detailed in section 2.4.4.

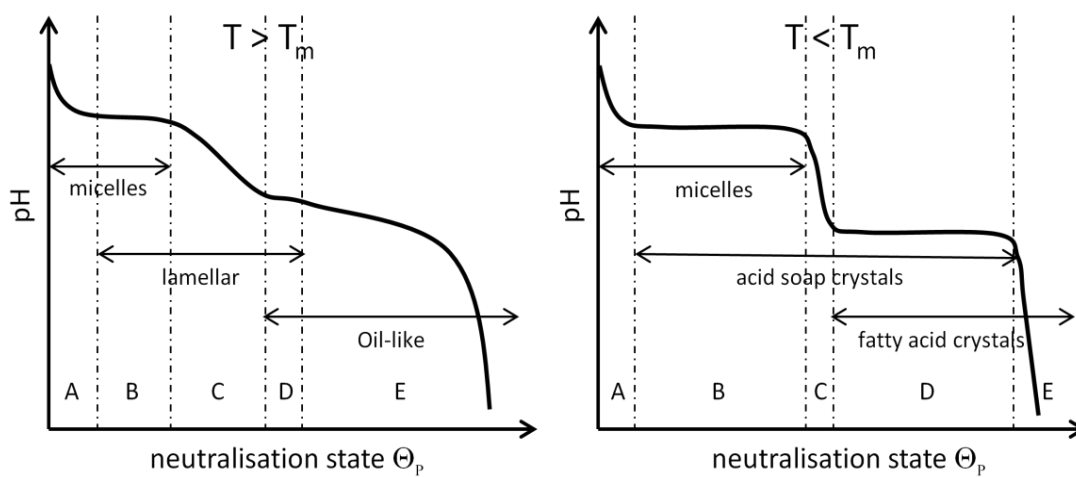


**Figure 3-5:** Typical curves obtained for acidic titration of alkali soaps above the cmc and the formed aggregates within certain zones. The left curve is for temperatures higher than  $T_m$ , the right one for temperatures lower than  $T_m$ . The diagrams are based on data from references 1, 19, 20, 55.

The measured titration curve for the pure aqueous 1 wt% NaOI solution with 0.2 M HCl is shown in **Figure 3-6**. For this study, the ranges of  $\Theta_p$  for different phases could be obtained by comparing the measured titration curve to titration curves presented in literature as schematically shown in **Figure 3-5** by the zones A - E and discussed in detail in section 2.4.4. The results are listed in **Table 3-1**. The determined ranges of  $\Theta_p$  for the different phases are in agreement with literature data.<sup>1, 19, 59</sup> The  $\text{ap}K_A$  value for NaOI at this concentration was 8.25 and also matches values reported in literature.<sup>1, 19</sup> The value of  $\Theta_p$ , above which an oil-like phase started to appear is called  $\Theta_{oil}$  and was 0.52 for an aqueous 1 wt% solution of NaOI.

To verify the phase behavior of the 1 wt% NaOI solution which is listed in **Table 3-1** and derived from the titration curve, samples with different values of  $\Theta_p$  were analyzed by phase-contrast microscopy (see section 3.3.4.2). The observed structures agree very well with the predicted phases in **Table 3-1**.

Range of $\Theta_p$	Range of pH	Phases in solution
0.00 - 0.05	10.5 - 10	aqueous/micellar
0.05 - 0.25	$\approx 10$	aqueous/micellar/lamellar
0.25 - 0.50	10 - 8.25	aqueous/lamellar
0.50 - 0.55	$\approx 8.2$	aqueous/lamellar/oil-like
> 0.55	< 8.1	aqueous/oil-like

**Table 3-1:** Range of  $\Theta_p$  and pH for which different phases are present in an aqueous 1 wt% solution of NaOl. The values are rounded.

The overall aggregation behavior of aqueous NaOl with increasing neutralization can easily be explained qualitatively by applying the concept of packing constraints and analyzing the packing parameter  $p$ . It is defined as  $V / l * a$ , where  $V$  is the volume of the alkyl chain,  $l$  is the maximum chain length and  $a$  is the effective headgroup area. This concept links the molecular shape of a surfactant to its preferred aggregation state in dilute solutions. For small values of  $p$  ( $< 0.5$ ) aggregates with a high positive curvature, spherical ( $p < 0.33$ ) and cylindrical micelles ( $0.33 < p < 0.5$ ) are present. At medium  $p$  values ( $0.5-1$ ), a lamellar phase (vesicles or bilayers) is preferred. As soon as  $p$  reaches higher values than one, inverted structures with a negative curvature are formed.<sup>60-62</sup> This is perfectly in line with the observed aggregate structure with increasing amount of HCl added. The protonation of the carboxylate group leads to a decrease in the effective headgroup area  $a$ , since less electrostatic repulsion is present and hydrogen bonds can be formed between the protonated and deprotonated fatty acid species. As a consequence,  $p$  increases with increasing amount of protonated fatty acid within the aggregates, respectively amount of HCl added, and the structures transform from micelles over lamellar structures to inverted structures.

Macroscopic phase behavior was investigated by visual observations and turbidity measurements. The turbidity remained more or less constant from preparation up to 30 days of aging (then no more measurements were carried out). The turbidity curve after 21 days of aging is shown in **Figure 3-9**. The values measured for different values of  $\Theta_p$  agree very well the data of Kaibara et al.<sup>18</sup>, who performed the same experiments, but plotted the turbidity against the prevailing pH value.

The macroscopic observations made in this study for an aqueous 1 wt% solution of NaOl at different values of  $\Theta_p$  also agree well with what was already reported in literature.<sup>1, 2, 18, 22</sup> The solution with  $\Theta_p = 0.0$  was as clear as water. For  $\Theta_p$  values between 0.1 and 0.5 (pH = 10-8.25) the turbidity of the samples increased constantly (see **Figure 3-9**) and the solutions became whitish translucent. All these solutions phase separated within a few days and a white spongy deposit with some bigger flocks was visible at the surface of a turbid aqueous phase. As soon as  $\Theta_p$  was larger than 0.5 (pH < 8.25), the turbidity sharply increased and remained nearly constant

irrespective of  $\Theta_P$ . This was due to the formation of an oil-like phase. Now the solutions were non-transparent and white with a higher tendency to phase separate than the ones without an oil-like phase. Photo A in **Figure 3-8** shows the appearance of aqueous 1 wt% NaOI solutions at different neutralization states after 21 days of aging.

*To conclude, an aqueous 1 wt% solution of NaOI is only macroscopically stable and clear at pH values higher than 10. At lower pH values, which are recommended for beverages (pH = 6.5-8.5)<sup>23</sup> and where skin-compatibility in cosmetics is increased<sup>63, 64</sup>, the solutions phase separate and are hardly or not translucent at all. As already mentioned, these macroscopic features make it impossible to use the aqueous NaOI/OA system as a basis for cosmetics or drinkable food formulations.*

### **3.3.3 Influence of RebA on aqueous NaOI solutions at different neutralization states**

As mentioned before, many properties of mixed systems of soaps with co-surfactants or other additives (e. g. cmc, phase behavior, adsorption behavior, solubility behavior) can deviate significantly from those of the pure soap solution, because of synergism and the formation of mixed aggregates.<sup>48, 65, 66</sup>

Shankland<sup>49</sup> investigated the influence of bile salts on the titration curves of aqueous solutions of NaOI and found considerable differences compared to the pure aqueous NaOI system. Further, the macroscopic appearance at certain neutralization state  $\Theta_P$  of the oleate changed, too. Vlachy et al.<sup>43</sup> showed that mixing long chain soap with alkyloligoethyleneoxide carboxylate shifts the pH region in which lamellar structures are observed to lower values. The same effect can be achieved by mixing the ionic surfactant sodium dodecylbenzenesulfonate with sodium decanoate.<sup>50</sup> On the other hand, alcohols are known to expand the pH range in which lamellar structures are observed to higher values.<sup>20, 41, 46</sup> The influence of the cationic surfactant didecyldimethylammonium bromide on the phase behavior of dilute NaOI solutions during titration with HCl was investigated by Suga et al.<sup>38</sup> They observed a change in the titration curve, and the formation of certain phases was shifted to other pH values compared to the pure NaOI solution. A synergism in surfactant mixtures of NaOI and nonionic alkylethoxylates was reported by Theander and Pugh<sup>44</sup>. Ouimet et al.<sup>67</sup> showed that it is possible to prevent palmitic acid from crystallization at room temperature due to mixed aggregate formation with cholesterol. Further, Borne et

al.<sup>45, 68</sup> showed that the addition of monoolein to aqueous NaOI solutions considerably changes the observed (micro)structures.

Although no systematic studies involving RebA, except a recent publication from our group<sup>3</sup>, could be found, there exist some data for other steviol glycosides in mixed systems. Synergistic interactions between alpha-glucosyl stevia and ionic surfactants were found by Uchiyama et al.<sup>35</sup>. They reported an enhanced dissolution of flurbiprofen in the mixed system compared to the single surfactant systems as a consequence of the formation of a nanocomposite complex between the two surfactants. In a series of papers, Wan et al. reported synergistic interfacial effects between stevioside and soy proteins.<sup>32-34</sup>

Consequently, adding the bio-surfactant RebA to the aqueous NaOI system at different neutralization states could have two advantages. On the one hand, forming mixed aggregates between NaOI and RebA could change the microscopic and the macroscopic phase behavior as well as the  $\text{apK}_\text{A}$  of NaOI in solution. This could possibly lead to stable solutions at consumable pH values. Further, the high sweetening effect of RebA could attenuate the soapy taste of the oleate soap, which is another problem concerning the application of NaOI in food.

The  $\text{apK}_\text{A}$  value of long chain soaps in solution, defined as the pH value at  $\Theta_\text{p} = 0.5$ , is markedly shifted to higher values compared to short chain fatty acids.<sup>15</sup> This is explained in detail in section 2.4.4 and only briefly summarized in the following. The main reason for this fact is the aggregate formation by long chain soaps. These aggregates exhibit a certain negative surface charge density which leads to higher  $\text{H}^+$ -ion concentrations near the surface of the aggregate compared to the  $\text{H}^+$ -ion concentration in the bulk phase.<sup>13, 19, 21, 22, 55, 69-71</sup> In other words, the proton concentration near the negatively charged aggregate surface ("surface-pH") experienced by the carboxylate group is higher (lower) than the measured one in the bulk phase ("bulk-pH"). The higher the negative surface charge density of an aggregate, the bigger is the difference between the "surface-pH" and the "bulk-pH" being measured. In further discussions, it is assumed that the  $\text{H}^+$ -ion concentration near the surface ("surface-pH") that is necessary to protonate a carboxylate group being incorporated in a self-aggregated structure stays constant and is independent of the aggregate's surface charge density. For protonation to occur, it can be assumed that the "surface-pH" experienced by the carboxylate groups has to be around 5 just as for monomeric fatty acids or slightly higher due to a dielectric discontinuity across the aggregate surface.<sup>17</sup> Then, a decrease in the surface charge density of the aggregate requires an increase in the  $\text{H}^+$ -ion concentration in the bulk

solution to achieve the  $H^+$ -ion concentration near the surface that is necessary to protonate the carboxylate group. Accordingly, it is reasonable to expect that the incorporation of other/non-ionic amphiphilic molecules into soap aggregates (mixed aggregate formation) can change the measured  $apK_A$  value by perturbing the molecular packing at the interface, which leads to a change in the surface charge density.

The titration curves of aqueous 1 wt% NaOI solutions with different amounts of RebA (0.2-2.0 wt%) are shown in **Figure 3-6**. The downward shift of the titration curves with increasing amount of RebA can be explained by a decrease in surface charge density of the soap aggregates caused by the incorporation of uncharged RebA molecules into the interfacial film. Thus, the  $H^+$ -ion concentration in the bulk phase has to be higher at a certain  $\Theta_P$  value so that the  $H^+$ -ion concentration at the surface is sufficient to protonate the carboxylate group. Moreover, the shape of the curve changes gradually until the typical titration curve of a weak monoprotic acid is obtained. A similar downward shift of NaOI titration curves as well as a change in the course of the curves to that of a weak monoprotic acid was also reported by Shankland in the case of bile salts.<sup>49</sup>

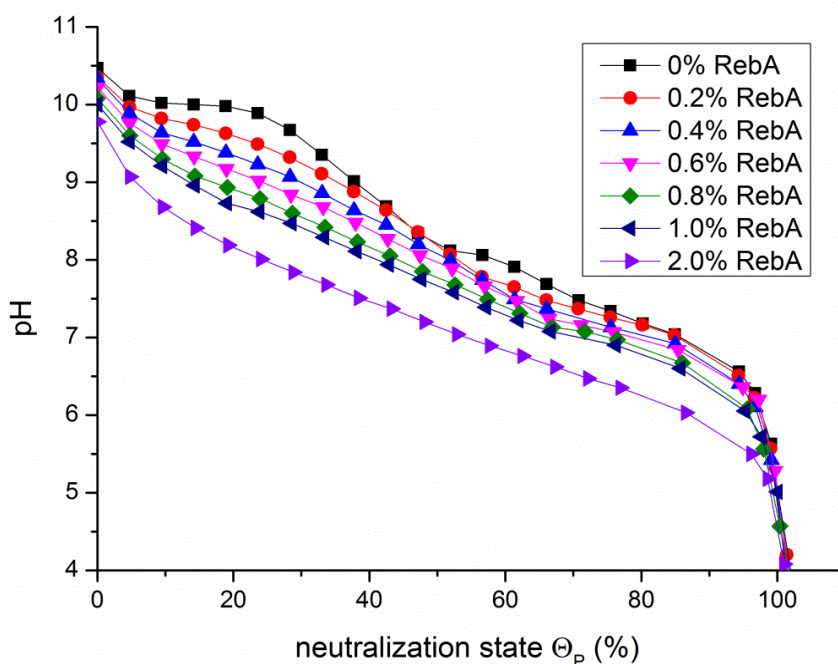


**Figure 3-6:** Titration curves of 1 wt% NaOI solutions with different amounts of RebA at 25 °C. The solutions were titrated with 0.2 M HCl and the pH was measured after 7 d of aging at room temperature. The added amount of RebA in wt% is: ■ = 0, ● = 0.2, ▲ = 0.4, ▼ = 0.6, ◆ = 0.8, ◀ = 1.0, ▶ = 2.0.

The  $\text{apK}_\text{A}$  values of NaOI decrease almost linearly from 8.25 without RebA to 7.15 with 2 wt% RebA (see **Figure 3-7**). This is in line with what was found in a beverage microemulsion containing NaOI.<sup>3</sup>

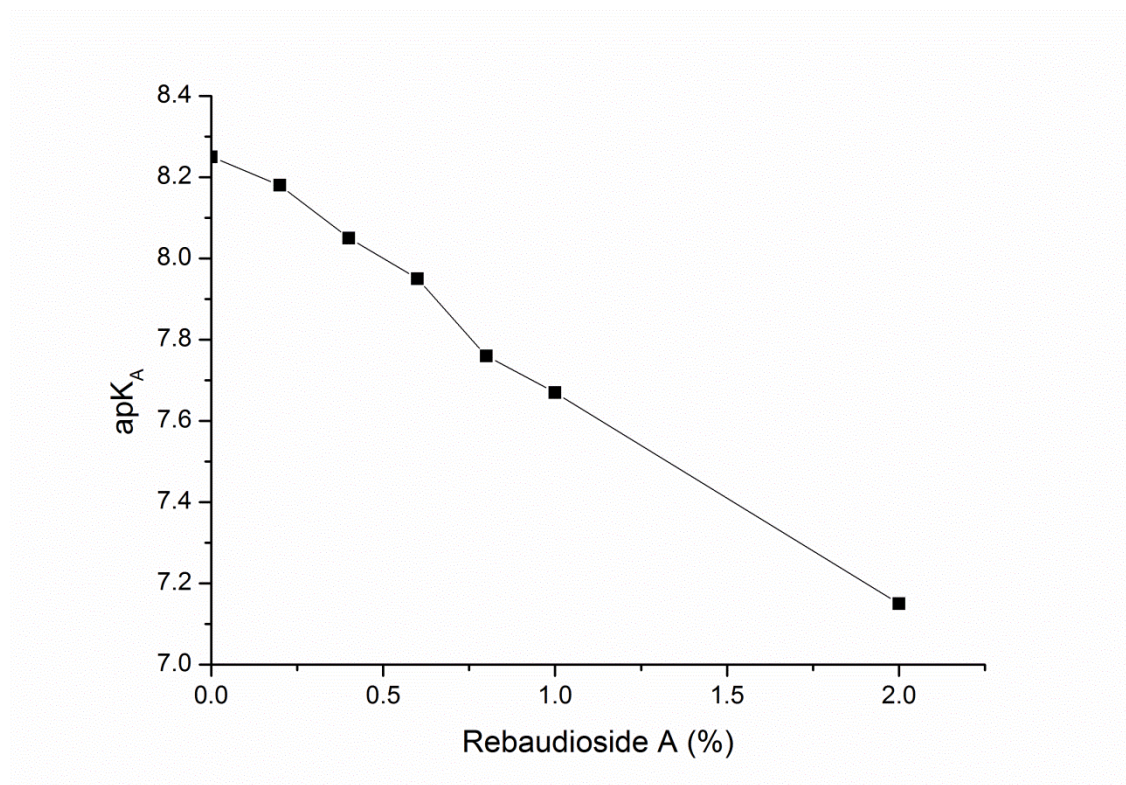


**Figure 3-7:** Plot of the determined  $\text{apK}_\text{A}$  values of an aqueous 1 wt% NaOI solution versus the concentration of RebA present in solution.

### 3.3.4 Phase behavior of mixtures containing NaOI and RebA at different neutralization states

Before discussing the phase behavior of the NaOI solutions with different amounts of RebA, an important note has to be made.

As will be shown in 3.3.4.5, these are complex and dynamic systems which change their macroscopic appearance as well as their phase behavior with time. It is difficult to be sure of thermodynamic equilibrium. For this reason, a certain time of aging has to be chosen to compare the stability and the phase behavior of the systems. It was, somewhat arbitrarily, decided to compare the systems after 21 days of aging.

Two series of mixtures were prepared, one with a constant amount of NaOI and varying amounts of RebA and another one with a constant NaOI to RebA ratio and varying overall concentrations of both. Detailed information about the systems can

be found in **Table 3-2**(section 3.3.4.3). The initial ratio of the systems is defined as the mass ratio of NaOI to RebA before the addition of HCl.

First, the macroscopic phase behavior of the solutions, which was investigated by visual observations and turbidity measurements, will be discussed. Then, the microscopic phase behavior, which was investigated by phase contrast microscopy and freeze fracture electron microscopy, will be considered.

Afterwards, outstanding features of these mixed systems will be highlighted and a tentative phase diagram for the aqueous 1 wt% NaOI system with different amounts of RebA will be presented. Moreover, a possible mode of action of RebA within the mixed NaOI/RebA/water system is suggested.

At the end, the time dependent phase behavior of the 1 wt% NaOI/0.8 wt% RebA system will be discussed.

### **3.3.4.1 Macroscopic phase behavior**

In what follows, the macroscopic phase behavior of the solutions containing 1 wt% NaOI and different amounts of RebA (0.2-2.0 wt%) will be discussed in detail. Further, the macroscopic phase behavior of the other systems listed in **Table 3-2** (section 3.3.4.3) will be briefly mentioned.

To illustrate the effect of RebA on the macroscopic phase behavior after three weeks, the macroscopic phase behavior of aqueous 1 wt% NaOI solutions with different amounts of RebA (0-2.0 wt%) is shown in **Figure 3-8**. Samples with the same number located in different pictures refer to the same neutralization states  $\Theta_p$ , but different initial ratios of NaOI to RebA.

Moreover, the absorbance of each series (0-2.0 wt % RebA) at 350nm was measured after 21 days. The data is shown in **Figure 3-9**.

All samples were shaken before taking the photo or measuring the turbidity to homogenize samples which had already phase separated.

*From both the pictures and the turbidity measurements, it is obvious that the addition of RebA to aqueous NaOI solutions considerably changes the macroscopic phase behavior compared to the pure NaOI solution.*



**Figure 3-8:** Photos of aqueous 1 wt% NaOI solutions with different amount of RebA after 21 days of aging. All samples have been shaken before taking the photo. The amounts of RebA are in wt%: A = 0.0, B = 0.2, C = 0.4, D = 0.6, E = 0.8, F = 1.0, D = 2.0. The neutralization state  $\Theta_P$  is given on the bottom of the figure and increases from left to right. Samples on a vertical line possess the same  $\Theta_P$  (deviation < 0.01) and can be directly compared.

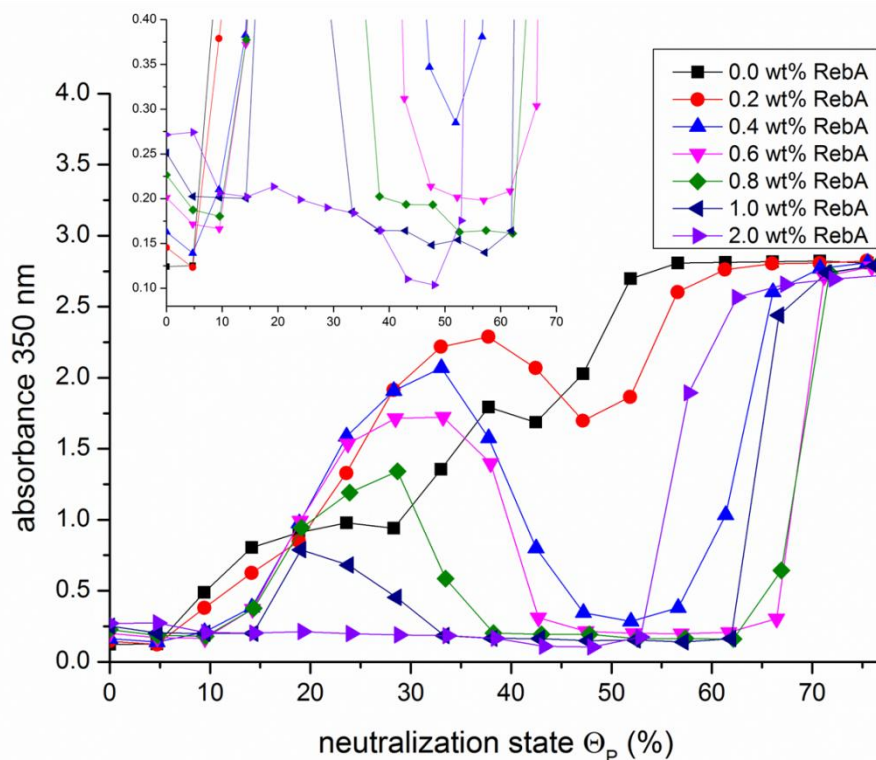


**Figure 3-9:** Absorbance of aqueous 1 wt% NaOI solutions at 350 nm with varying amounts of RebA at different neutralization states  $\Theta_P$  after 21 days of aging. The legend and the units also apply to the small inset, which is a magnification at low absorbance. Note that all solutions were shaken before measuring to obtain homogenous solutions if phase separation already took place. The added amount of RebA in wt% is:  $\blacksquare$  = 0,  $\bullet$  = 0.2,  $\blacktriangle$  = 0.4,  $\blacktriangledown$  = 0.6,  $\blacklozenge$  = 0.8,  $\blacktriangleleft$  = 1.0,  $\blacktriangleright$  = 2.0.

For small  $\Theta_P$  values, the solutions appeared clear with some solid precipitate that turned into schlieren after slewing. For 0.8 wt% RebA and  $\Theta_P = 0$ , phase contrast microscopy showed small dendroid crystals in solution (data not shown). This effect was more pronounced as the amount of RebA increased. However, most of the NaOI/OA and RebA being present in solutions were likely to form some small aggregates like mixed micelles which were too small to be resolved with a light microscope. The amount of precipitate decreased with increasing  $\Theta_P$  values for each concentration of RebA. These two observations are illustrated in the inset of **Figure 3-9**. The turbidity of the samples at  $\Theta_P = 0$  rises with increasing amount of RebA and an increase in  $\Theta_P$  leads to a small decline in turbidity until it rises sharply.

The value of  $\Theta_P$ , at which the turbidity increased sharply and the solutions became visibly turbid, increased with the amount of RebA in solution. Close to the first maximum in absorbance, which can also be observed on photos B-F in **Figure 3-8**, the solutions had a high tendency to phase separate into a bluish translucent solution phase with a white spongy phase floating on its surface ( $\Theta_P \approx 0.1$ -0.45, depending on the amount of RebA). The higher the turbidity, the more pronounced

the phase separation was. According to phase contrast microscopy, the spongy phase mainly consisted of aggregated spherical multilamellar vesicular structures as shown in picture E in **Figure 3-11** and section 3.3.4.2. The phase separation effect was more pronounced for the solutions with RebA concentrations between 0.2-1.0 wt% compared to the pure NaOI system. Only at higher RebA concentrations, the turbidity decreased markedly again and also the  $\Theta_p$  range over which the systems were turbid. In parallel, the turbidity maximum was shifted to lower values of  $\Theta_p$ . In the systems containing 2 wt% RebA, the solution phase remained completely clear up to high neutralization states around  $\Theta_p = 0.6$ . However, these solutions always contained some solids and were not stable (see below). Probably, these solids were formed by RebA, since the concentration was far above its solubility limit in water.

Interestingly, highly translucent and macroscopically stable solutions were obtained for solutions containing 0.4-1.0 wt% RebA for neutralization states  $\Theta_p$  between 0.4 and 0.6. **Table 3-2** (section 3.3.4.3) summarizes for each initial ratio of NaOI to RebA the range of  $\Theta_p$  over which stable and highly translucent solutions were obtained ( $\Delta\Theta_p$  stable), the corresponding range of pH values of these solutions ( $\Delta\text{pH}$  stable) and the lowest neutralization state  $\Theta_p$  when an oil-like phase was present ( $\Theta_{oil}$ ). **Figure 3-8** and **Figure 3-9** clearly show that the addition of RebA leads to a minimum in turbidity around 50 % neutralization, whereas the pure NaOI solutions exhibit a monotonous increase in turbidity. For the solutions with 0.2 wt% RebA, the effect was already observed, but the turbidity was only slightly lowered. However, with an amount of 0.4 wt% RebA and more, this effect became very significant. Also the  $\Delta\Theta_p$  stable range widened with rising amount of RebA (0.4-1 wt%). Precise visual observation revealed that an increased amount of RebA led to clearer solutions, respectively the solutions exhibited a less bluish translucent character. This can also be seen in the small inset in **Figure 3-9**, where the minimum absorbance is shifted to lower values with increasing amounts of RebA. This can be explained by the formation of smaller structures which scatter visible light more weakly. Although  $\Theta_{oil}$  remained constant from 0.6 to 1.0 wt% RebA,  $\Delta\text{pH}$  stable spread to lower values, since an increased amount of RebA led to a downward shift of the titration curve of NaOI (see **Figure 3-6** and section 3.3.3). It has to be mentioned that the transition from the unstable to the stable region was sometimes hard to define and some solution appeared clear and show a low turbidity in **Figure 3-9**, although they exhibited very little separated phase at the surface. These solutions were treated as unstable.

At  $\Theta_P$  values smaller  $\Theta_{oil}$ , for the system with 1 wt% NaOI and 2 wt% RebA no macroscopic spongy phase was observed and no lamellar phase dark structures could be identified by phase contrast microscopy. Only crystals and very small “black dots” being too small to be clearly identified were present in solution. However, these clear aqueous solutions were not stable and always contained some white precipitate consisting of small white particles and some big flocculent particles. The amount of precipitate decreased with increasing value of  $\Theta_P$ . The absence of a white spongy phase and the decline in precipitate is illustrated by a constant fall of the turbidity curve until an oil-like phase is formed (see **Figure 3-9**).

For pH values lower than those corresponding to this stable and translucent region, the turbidity rose sharply and the solutions became non-transparent and white. Phase contrast microscopy confirmed that this was due to the formation of an oil-like phase.  $\Theta_{oil}$  increased from 0 to 0.6 wt% RebA, remained constant up to 1 wt% and decreased again for the system with 2 wt% RebA (see **Table 3-2**, section 3.3.4.3). The fact that  $\Theta_{oil}$  markedly decreased as soon as the initial ratio of NaOI to RebA was lowered from 1 to 0.5 proved that RebA did not act as a simple solubilising agent for the OA formed during titration. If this were the case, an increasing amount of RebA would solubilize more OA and consequently would shift  $\Theta_{oil}$  to higher values, which was not observed. Things are definitely subtler in this complex system as will be pointed out below. These findings are different from the ones reported by Shankland<sup>49</sup> who investigated the influence of different concentrations of bile salt (sodium cholate) on the phase behavior of NaOI during titration. He found that  $\Theta_{oil}$  increases when increasing the initial ratio of sodium cholate to NaOI until the systems remain clear up to 100 % of neutralization of NaOI even at pH values smaller than 7. This was explained by the high solubilisation power of sodium cholate micelles for OA and the formation of mixed micelles. In other words, the oleic acid oil is simply solubilised by sodium cholate micelles as other similar oils or long chain alcohols would be, too. Actually, the same effect should be attained with other surfactants that exhibit a high solubilisation power.

Other solutions with an initial ratio NaOI to RebA of 1.25 but a different overall concentration of NaOI plus RebA showed the same general microscopic and macroscopic phase behavior as the system with 1 wt% NaOI and 0.8 wt% RebA. The important parameters concerning stability of these solutions are also given in **Table 3-2** (section 3.3.4.3). The results of the absorbance measurements are shown in **Figure 3-10**. An increase in the overall concentration caused an upward shift of

the turbidity curves. This behavior was expected, because more substance being able to form aggregates was present in solution. It was very significant for the system with 2.5 wt% NaOI. Nevertheless, stable solutions within the 2.5 wt% NaOI system were still highly translucent, but possessed also a yellowish shimmer. This yellowish shimmer was also observed for crude solutions of 2.5 wt% NaOI at  $\Theta_p = 0$ . The extent of phase separation and the turbidity for values of  $\Theta_p$  between 0.1 and 0.4 increased for the systems up to 1 wt% NaOI and decreased again in the system with 2.5 wt% NaOI. The maximum of turbidity was independent of the overall concentration. Although the increase in turbidity for the system with 2.5 wt% NaOI was not very pronounced, visual observation clearly showed a white spongy phase at the surface of the solutions. After slewing, these unstable solutions were markedly more turbid and whitish than the stable and highly translucent solutions of this system. The same behavior was observed for the system 0.25 wt% NaOI/0.2 wt% RebA.

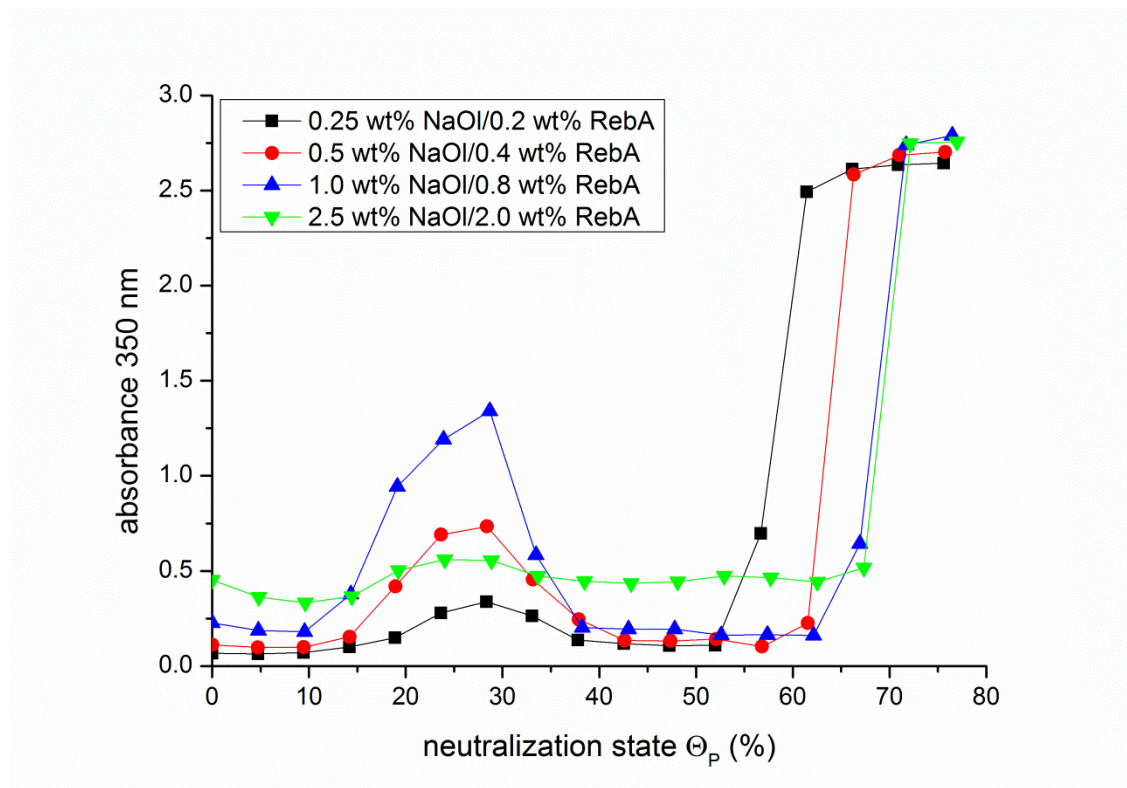


**Figure 3-10:** Absorbance of aqueous NaOI/RebA solutions with an initial ratio NaOI to RebA of 1.25 at 350 nm and at different neutralization states  $\Theta_p$  after 21 days of aging. The initial concentrations of NaOI were 2.5 (▼), 1 (▲), 0.5(●) and 0.25 (■) wt%. Note that all solutions were slewed before measuring to obtain homogenous solutions if phase separation took place.

Finally, a further system with the initial ratio NaOI to RebA of 0.5 was investigated (0.5 wt% NaOI/1 wt% RebA). The same general microscopic and macroscopic phase

behavior as for the system 1 wt% NaOI/2 wt% RebA was found. Again, at  $\Theta_P$  values smaller than  $\Theta_{oil}$  no lamellar phase could be identified, but always some white precipitate and flocculent particles were present.  $\Theta_{oil}$  was even lower than in the NaOI solutions without RebA. However, it remains to be checked, whether solutions with an initial NaOI to RebA ratio of 0.5 still contain tiny lamellar structures at  $\Theta_P$  values smaller than  $\Theta_{oil}$  or some kind of mixed micelles.

### **3.3.4.2 Microscopic phase behavior**

To investigate the influence of RebA on aqueous NaOI solutions on the microscopic scale, phase contrast microscopy and freeze fracture electron microscopy were carried out for selected samples. The RebA influence will be discussed for the tests series with initial amounts of 1 wt% NaOI and 0.8 wt% RebA. For the other series with an initial ratio NaOI/RebA between 1 and 2.5 the results from phase contrast microscopy were similar, merely  $\Theta_P$  values for certain structures/phases slightly changed (see **Table 3-2**, section 3.3.4.3).

**Figure 3-11** shows phase contrast microscope pictures at certain neutralization states  $\Theta_P$  (0.28, 0.48, 0.56) of aqueous 1 wt% NaOI solutions without (A-D) and with 0.8 wt% RebA (E-H).

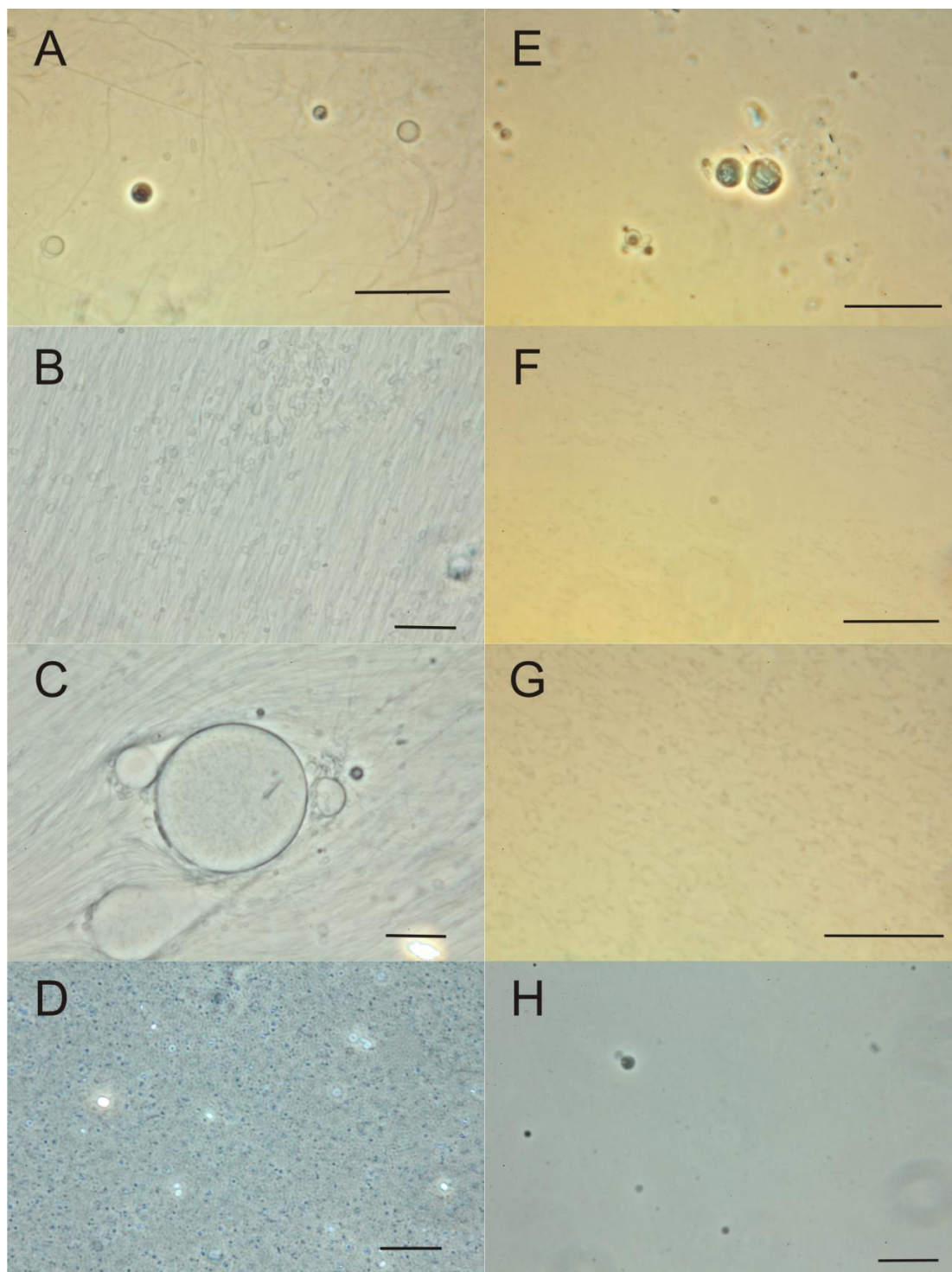


**Figure 3-11:** Phase-contrast microscopy of aqueous 1 wt% NaOI solutions without (A – D) and with 0.8wt% RebA (E – H) at different values of  $\Theta_P$  and several days after preparation. The scale bar always represents 20  $\mu\text{m}$ . (A)  $\Theta_P = 0.28$ : Uni- and multilamellar vesicular structures, elongated lamellar structures as well as threadlike structures could be seen; (B) and (C)  $\Theta_P = 0.47$ : The same structures as in picture A were present. However, the amount of lamellar structures was much higher. Long threadlike structures covered almost the whole photos. (D)  $\Theta_P = 0.56$ : Shiny oil-like-droplets were present in solution. The other spherical structures were also meant to be oil-like, but they were not focused. E)  $\Theta_P = 0.28$ : big multilamellar vesicular structures being partly aggregated were the main structure; (F)  $\Theta_P = 0.48$ : small “black dots” and small threadlike structures were observed. In the middle one bigger lamellar structure is visible (G) and (H) both  $\Theta_P = 0.57$ : in picture G the same structures as in picture F can be seen. Picture H shows that also some bigger phase dark multilamellar structures could be found.

As expected from literature and **Table 3-1**, solutions without RebA at  $\Theta_P = 0.28$  and  $\Theta_P = 0.47$  showed a mixture of different lamellar structures (see **Figure 3-11**, A, B and C). Next to spherical multi- and unilamellar vesicular structures that were heterogeneous in size and partly aggregated, elongated lamellar structures and very long and flexible threadlike structures could be identified. Both solutions showed the same variety in lamellar structures, but the solution with a higher value of  $\Theta_P$  contained much more of them. All of these structures appeared phase dark or had only a low contrast, indicating a lamellar phase. The rise in big structures also explains the increase in turbidity with increasing  $\Theta_P$ . At  $\Theta_P = 0.56$  (D), bright droplets indicating the presence of an oil-like phase were observed.

Markedly different results were obtained for solutions with additional 0.8 wt% RebA. At  $\Theta_P = 0.28$ , where the maximum turbidity in the unstable region is found (see **Figure 3-9** and sample 7 in picture E in **Figure 3-8**). Mainly phase dark multilamellar as well as aggregated multilamellar vesicular structures were found (see **Figure 3-11**, E). Threadlike or unilamellar structures, which could be found in pure NaOI solutions, were hardly observed. The separated spongy phase also consisted mainly of aggregated spherical multilamellar structures (photos not shown).

Pictures of solutions with 0.8 wt% RebA at  $\Theta_P = 0.48$  and 0.57 also showed a great difference compared to the pure NaOI system (compare **Figure 3-11**, B, C, D and F, G, H). For both neutralization states, the observations were similar. Very much small “black dots”, which were too small to be clearly identified, as well as some small threadlike and unilamellar vesicular structures could be observed (see **Figure 3-11**, F, G). Rarely, some bigger phase dark multilamellar structures could be identified, too (see **Figure 3-11**, H).

To summarize the observation made by phase contrast microscopy for these solutions: upon addition of RebA, apparently the same lamellar structures as in the pure NaOI system were present at  $\Theta_P = 0.48$ , but much smaller in size. Probably, the small “black dots” were small uni- or multilamellar vesicular structures being too small to be sufficiently resolved by the phase contrast microscope. For  $\Theta_P = 0.57$ , the difference to the pure NaOI system was more significant, since droplets having an oil-like interior were observed for the pure NaOI system. The observations made by phase contrast are completely in line with the macroscopic appearance of the solutions (see **Figure 3-8** and **Figure 3-9**). The crude NaOI solutions were highly turbid or nontransparent and white due to the presence of many big lamellar structures or oil-like droplets, whereas the solutions with 0.8 wt% RebA were much more translucent because of smaller structures within the solutions. No obvious

change in the size or shape of the structures could be observed during 30 days of aging.

Further, freeze etching electron microscopy was used to get deeper insight to the structural changes taking place. The investigated samples contained 1 wt% NaOI at  $\Theta_P = 0.47/0.48$  without and with 0.8 wt% RebA, since both samples showed no oil-like phase in phase contrast microscopy, but differed heavily in their macroscopic appearance (see **Figure 3-8**, compare solution number 11 in A and E). Moreover, due to the equal amount of NaOI and OA within each system, the effect of RebA on the microstructure could be observed immediately.

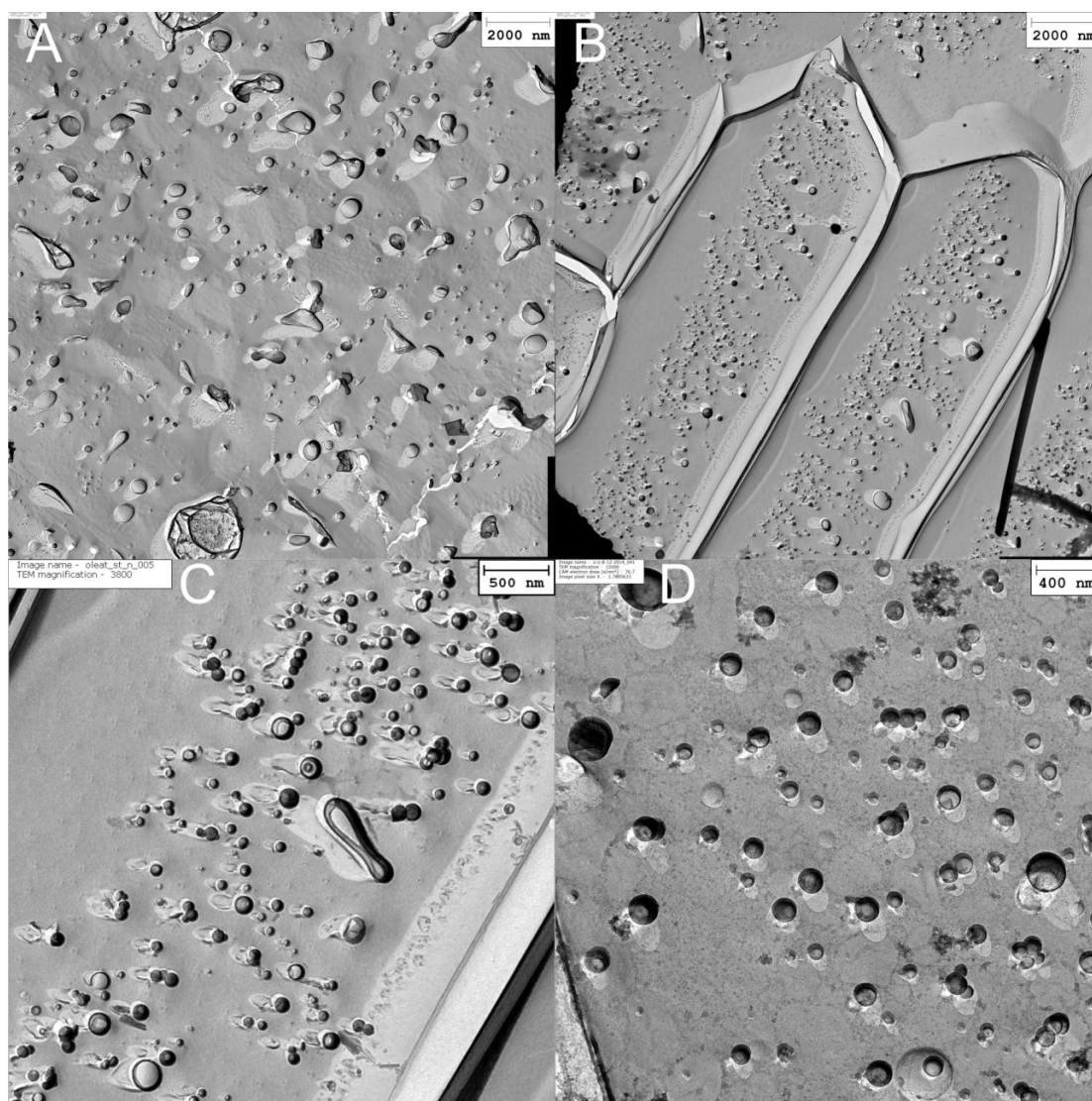


**Figure 3-12:** FE-TEM pictures of 1 wt% NaOI solutions without and with 0.8 wt% RebA at identical  $\Theta_P$  values (0.47/0.48). Replica for pictures A, B and C were prepared directly after preparation of the samples. Replica for picture D were prepared 6 weeks after preparation of the sample. (A) pure NaOI solution directly after preparation; (B) and (C): 1 wt% NaOI + 0.8 wt% RebA directly after preparation; the streaks are artefacts from freeze etching; (D): 1 wt% NaOI + 0.8 RebA six weeks after preparation.

The pure NaOI solution exhibited a very heterogeneous size distribution of spherical and elongated lamellar structures with diameters from a few nm up to some  $\mu\text{m}$ . Picture A in **Figure 3-12** illustrates the broad size distribution and shows also big multilamellar structures. However, no big threadlike structures could be found, in contrast to the structures seen in phase contrast microscopy.

The 1 wt% NaOI solution with 0.8 wt% RebA also contained mainly spherical and some elongated structures having a similar look and shape like these observed without RebA, but the average size was much smaller. Nearly all structures were smaller than 500 nm and only rarely bigger structures could be observed (see **Figure 3-12**, B, C). As can be seen in picture D in **Figure 3-12**, the size and the shape of the structures did not change significantly during six weeks of aging.

These findings agree well with those made by phase contrast microscopy, which also indicated much smaller structures within the 1 wt% NaOI system with additional 0.8 wt% RebA.

The spherical structures within the solutions with RebA were very small and from the electron microscopy pictures it is hard to say whether these structures are unilamellar, multilamellar or even have a dense interior. Comparing the TEM pictures for the NaOI solution without and with RebA reveals that structures of equal size look very similar for both systems. Therefore, in discussions, it is assumed that these small and mostly spherical aggregates formed in the mixed NaOI/OA/RebA system also have a lamellar structure. To undoubtedly prove this assumption, cryo-TEM pictures or neutron scattering experiments should be made.

The formation of a lamellar phase as well as the formation of an oil-like phase at a certain value of  $\Theta_p$  no matter whether RebA is present in solution or not (at least for systems with an initial ratio of NaOI to RebA  $\geq 1$ ) suggests that the actual ratio of OA to Oleate in solution defines the rough phase behavior in the mixed NaOI/RebA systems. RebA only seems to change  $\Theta_{oil}$  and the microscopic structure of the lamellar phase what can also be seen by a change in turbidity and macroscopic appearance.

### **3.3.4.3 Important parameters of stable systems and tentative phase diagram**

Based on the results presented in sections 3.3.4.1 and 3.3.4.2, the range of  $\Theta_p$  over which stable and highly translucent solutions were obtained ( $\Delta\Theta_p$  stable), the corresponding range of pH values of these solutions ( $\Delta\text{pH}$  stable) and the lowest

neutralization state  $\Theta_P$  when an oil-like phase was present ( $\Theta_{oil}$ ), was determined for each system that has been investigated. The values are summarized in **Table 3-2**.

Initial system (ratio)	$\Delta\Theta_P$ stable	$\Theta_{oil}$	$\Delta pH$ stable
0.25 wt% NaOI (-)	0 - 0.05	0.52	not measured
1.0 wt% NaOI (-)	0 - 0.05	0.52	10.5 - 10.1
1.0 wt% NaOI / 0.2 wt% RebA (5.0)	-	0.57	-
1.0 wt% NaOI / 0.4 wt% RebA (2.5)	0.47 - 0.57	0.62	8.20 - 7.74
1.0 wt% NaOI / 0.6 wt% RebA (1.67)	0.47 - 0.62	0.67	8.06 - 7.47
1.0 wt% NaOI / 0.8 wt% RebA (1.25)	0.43 - 0.62	0.67	8.05 - 7.31
1.0 wt% NaOI / 1.0 wt% RebA (1.0)	0.38 - 0.62	0.67	8.11 - 7.22
1.0 wt% NaOI / 2.0 wt% RebA (0.5)	-	0.57	-
0.25 wt% NaOI / 0.2 wt% RebA (1.25)	0.43 - 0.52	0.57	8.38 - 8.05
0.5 wt% NaOI / 0.4 wt% RebA (1.25)	0.43 - 0.57	0.62	8.23 - 7.70
2.5 wt% NaOI / 2.0 wt% RebA (1.25)	0.43 - 0.62	0.67	7.78 - 7.05
0.5 wt% NaOI / 1.0 wt% RebA (0.5)	-	0.48	-

**Table 3-2:** Characteristics of aqueous NaOI/RebA mixtures investigated in this study.  $\Delta\Theta_P$  stable/ $\Delta pH$  stable stands for the range of  $\Theta_P$ /pH, over which stable and highly translucent solutions were obtained,  $\Theta_{oil}$  for the neutralization state, from which an oil phase was present in solution. The values were measured after 21 days of aging.

As already discussed in detail in section 3.3.4.1, for solutions with 1 wt% NaOI,  $\Delta\Theta_P$  stable and  $\Theta_{oil}$  increase with decreasing initial NaOI/RebA ratio (2.5-1) and  $\Delta pH$  stable is slightly shifted to lower values. At a constant initial ratio NaOI/RebA = 1.25,  $\Delta\Theta_P$  stable,  $\Delta pH$  stable and  $\Theta_{oil}$  weakly varied with the overall concentration.  $\Delta\Theta_P$  stable widened and  $\Theta_{oil}$  increased with increasing overall concentration. This suggests that a higher overall concentration in solution stabilizes lamellar structures and prevents the formation of a separate oil-like phase at higher values of  $\Theta_P$ . To rule out that the effect is caused by the phase behavior of pure NaOI solutions, a test series with only 0.25 wt% NaOI was prepared and again the same value of  $\Theta_{oil}$  was determined as for the 1 wt% NaOI system. The downward shift of  $\Delta pH$  stable at equal values of  $\Delta\Theta_P$  stable with increasing overall concentration (compare systems 1 wt% NaOI / 0.8 wt% RebA and 2.5 wt% NaOI / 2 wt% RebA) is very probably due to a higher ionic strength in solution at equal values of  $\Theta_P$ . An enhanced ionic strength leads to a stronger screening of electrostatic interactions and therefore the titration curves are shifted to lower pH values.<sup>17</sup> This effect is nicely illustrated in reference 1. Further, **Table 3-2** shows that macroscopically stable and highly translucent solutions with 1 and 2 wt% RebA can only be obtained for initial NaOI/RebA ratios higher than 0.5. This indicates that a certain initial amount of NaOI has to be present to stabilize RebA in aqueous solution considerably above its solubility limit (0.4-0.6 wt%). This fact could be explained by the formation of mixed RebA/oleate/OA aggregates, respectively the incorporation of RebA in the aggregate-water interface. This is meant to increase the solubility of RebA within the aqueous system. As a

result, a minimum amount of oleate/OA aggregates, respectively a minimum interfacial area is necessary to accommodate and stabilize a certain amount of RebA.

*This shows that within this complex system a kind of mutual solubility enhancement, respectively macroscopic stability enhancement is active between NaOl/OA and RebA. On the one hand, it was not possible to obtain stable and translucent aqueous solutions of pure NaOl around half neutralization. Further, aqueous solutions of pure RebA were not stable either at concentrations higher than 0.6 wt % after 21 days of aging. Interestingly, by mixing appropriate amounts of the pure substances, it is possible to overcome these problems and to obtain highly translucent and macroscopically stable solutions.*

*To summarize **Table 3-2**: crude aqueous NaOl solutions were only stable at very low values of  $\Theta_P$  and at pH values higher than 10. By contrast, for initial ratios of NaOl to RebA between 1.0 and 2.5, stable and highly translucent solutions could be obtained at values of  $\Theta_P$  around 0.5 and initial concentrations of NaOl ranging from 0.25 to 2.5 wt%. Probably, this is also possible for higher initial concentrations of NaOl. The pH value of these stable solutions was always between 7 and 8.4, which is perfectly within the pH range recommended for drinking water and around the pH of human blood (pH = 7.3).<sup>23</sup>*

*To the best of my knowledge, this is the first time that such concentrations of a long chain soap are really solubilised, i.e. the aqueous solution is low viscous, clear and stable, at neutral pH values and at room temperature. Further, the long chain soap is the main component in the mixed system and oleic acid does not act as an oil phase being simply solubilised in a given foreign matrix formed by other amphiphiles ([nano]emulsions, big micelles, phospholipid bilayers,...)(see below). Here, the long chain soap is mandatory for the formation of the stable microstructures and governs the phase behavior. Further, the solutions are very easily prepared and the additive is a very green and natural bio-surfactant that can efficiently cover the soapy taste of the long chain soap, too.*

In literature, there are many examples of aqueous systems, in which fatty acids are dispersed at neutral or acidic pH values. However, all of these systems do not fulfill at least one of the above mentioned criteria to denote the long chain fatty acid as “really solubilised”: either the fatty acid is not the main component and/or does not

act as a surfactant or the physical state of the solution is not water-like. In the following, only a few representative examples are mentioned.

Unsaturated long chain fatty acids, like oleic acid or omega-3-fatty acids (e.g. docosahexaenoic and eicosapentaenoic acid), are liquid at room-temperature and can be solubilised by other surfactants like any other oil. Oleic acid<sup>72</sup> and docosahexaenoic acid<sup>73</sup> were used to prepare thermodynamic stable microemulsions for usage in clinical studies at neutral or even acidic pH values. However, the fatty acids are used as the oil phase and a large amount of non-ionic surfactant is necessary in each system. In food-grade emulsions or nanoemulsions for the delivery of omega-3-fatty acids, these fatty acids are also used as simple oils and suspended by other surfactants at neutral or acidic pH values of the solution.<sup>74, 75</sup> Moreover, these systems are not always translucent and the fatty acids are often used in their glyceride form (fish oil).<sup>76, 77</sup>

Mixing phosphatidylethanolamine with long chain fatty acids in aqueous solution at neutral or slightly acidic pH leads to dispersion of the fatty acid in the form of mixed membranes (liposomes).<sup>78, 79</sup> These systems attracted interest as possible drug carriers because of their potential of liposome aggregation, destabilization or fusion upon changing the pH value. But within these systems, the molar ratio of phosphatidylethanolamine to fatty acid was always 7 to 3 and the fatty acid has to be regarded as a minor component that is incorporated into a membrane mainly composed of phospholipids. Edwards et al.<sup>13</sup> showed that aqueous solutions of phosphatidylcholine (PC) plus oleic acid are only macroscopically stable at pH values of 7.4 or 6, if the amount of oleic acid does not exceed a certain ratio. Further, PC forms vesicular structures on their own at these pH values, and the fatty acid can be regarded as solubilised in the given PC structures. At last, it must be mentioned that in none of the papers, the macroscopic appearance as well as the stability of the aqueous solutions were described.

There are aqueous systems, in which the fatty acid represents the main component and is dispersed at neutral or acidic pH values, but whose macroscopic appearance is far away from being water-like. For the above mentioned long chain alkali soap plus guanidine hydrochloride systems, it was possible to disperse myristic acid within vesicular structures in solution up to a pH value of 7.2.<sup>80</sup> However, these systems were non-translucent white and no information about the macroscopic stability of the solutions was given. Another example is the palmitic acid/palmitin system described by Douliez.<sup>81</sup> For molecular ratios of palmitic acid to palmitin of 1 or 2, it was possible to fully disperse palmitic acid at a solution pH of 7 by the formation of a mixed lamellar phase (vesicles). Again, the resulting aqueous solutions were turbid and

highly viscous. Nevertheless, these systems can find application, if a water-like macroscopic state and long time stability of the solutions are not necessary. For example, it was shown that vesicular fatty acid solutions form more stable foams and emulsions than comparable micellar fatty acid solutions.<sup>82</sup>

Of course, there are also countless complex aqueous cosmetic or food products at neutral or acidic pH values, in which numerous substances are included and fatty acid constitutes only a minor component that does not markedly affect the macroscopic state of the formulation.

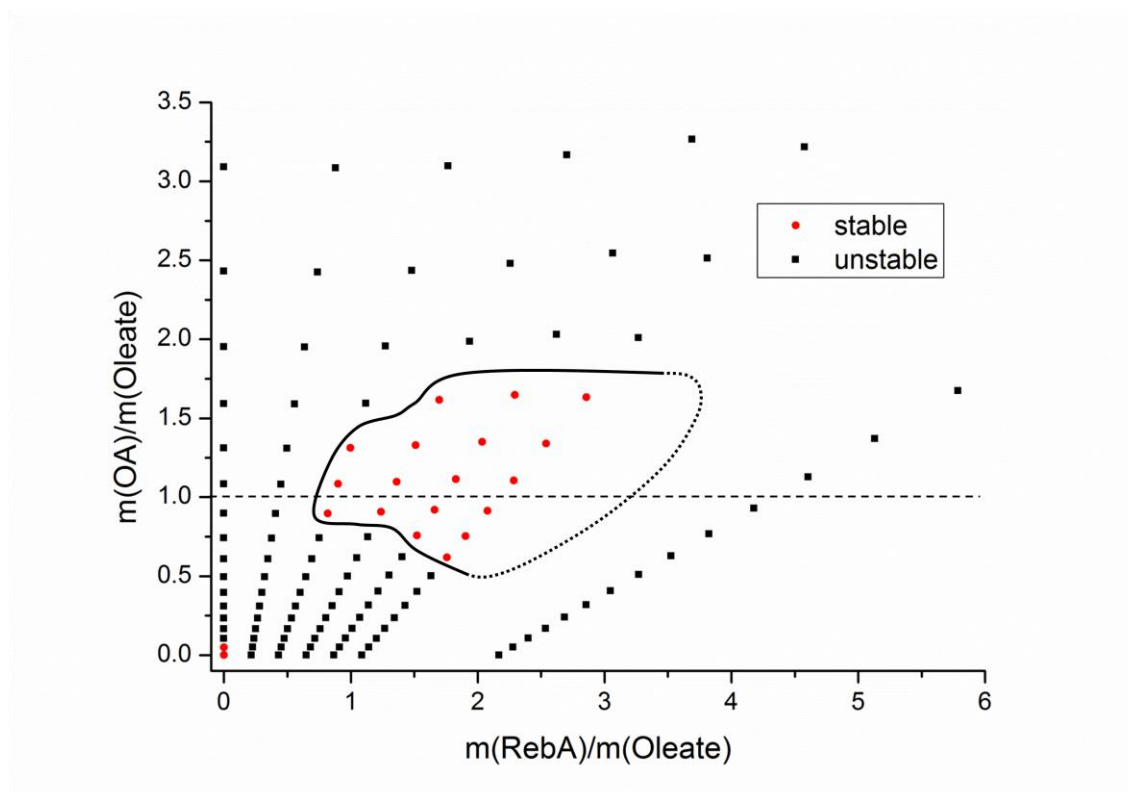


**Figure 3-13:** Composition of samples in the mixed NaOl/RebA systems. The mass ratio of OA to oleate is plotted against the mass ratio of RebA to oleate for each system with 1 wt% NaOl and 0-2 wt% RebA. The masses of oleate, OA and RebA within each sample were calculated. Each inclined line represents one NaOl/RebA system with a certain initial ratio of NaOl to RebA. The initial ratio decreases from left to right. The figure is valid for samples after 21 days of aging.  $m(\text{OA})/m(\text{Oleate}) = 0.5$  corresponds to a neutralization state  $\Theta_p$  of 0.33 and  $m(\text{OA})/m(\text{Oleate}) = 2$  to  $\Theta_p$  of 0.67. The marked area shows the compositions of stable solutions, where the dotted part is estimated. The dashed horizontal line marks  $m(\text{OA})/m(\text{Oleate}) = 1$ . ■ denotes unstable samples and ● stable ones.

**Figure 3-13** illustrates a tentative phase diagram of the systems containing 1 wt% NaOl/0-2 wt% RebA and points out the area of stable and highly translucent samples.

**Figure 3-13** also reveals the complexity of the systems. The restricted area of stable solutions illustrates that oleate, OA and RebA must be present within a certain ratio.

Neither a certain ratio of RebA to oleate nor a certain ratio of OA to oleate is sufficient to obtain macroscopically stable and highly translucent solutions.

The area of stable solutions at certain mass ratios of RebA to oleate is situated around a horizontal line where  $m(\text{OA})/m(\text{Oleate})$  is equal to one. This suggests that nearly an equal amount of OA to oleate is necessary to obtain stable solutions, whereas the amount of RebA within the system defines the extent of the stable region, i. e.  $\Delta\Theta_P$  stable. The effectiveness of RebA in stabilizing the samples increases up to a certain ratio of RebA to oleate in solution and  $\Delta\Theta_P$  stable widens. However, at too high ratios of RebA to oleate no stable solutions are obtained.

#### 3.3.4.4 Possible mode of action of RebA within the mixed systems

Phase contrast microscopy of 1 wt% NaOI solutions without and with 0.8 wt% RebA revealed a great influence of RebA on the size and shape of the observed structures at various neutralization states  $\Theta_P$  (see **Figure 3-11** and section 3.3.4.2). However, for both systems only lamellar structures were observed for  $\Theta_P$  values between 0.1 and  $\Theta_{oil}$ . The addition of RebA led to much smaller lamellar structures compared to the pure NaOI solutions within the  $\Theta_P$  range of highly translucent and stable solutions. RebA was even able to stabilize lamellar structures at  $\Theta_P$  values bigger than  $\Theta_{oil}$  of the pure NaOI solution. The same observations were made for the systems containing 0.25 wt% NaOI without and with 0.2 wt% RebA (see **Table 3-2**).

Electron microscopy images showed the same result for 1 wt% NaOI solutions without and with 0.8 wt% RebA at a  $\Theta_P$  value of 0.48 (see **Figure 3-12** and section 3.3.4.2). In the solutions with RebA, mainly spherical structures were observed, the structures being much smaller than the ones in the pure NaOI solutions.

These observations and the absence of a lamellar phase in the mixed systems at small values of  $\Theta_P$  suggests that, like for the pure aqueous NaOI system, a certain ratio of OA to oleate within the system is the important factor, which initiates the formation of a lamellar phase and determines the general phase behavior in the mixed systems. RebA only seems to change  $\Theta_{oil}$  and the microscopic appearance of the lamellar phase. This is also reflected by a change in turbidity and macroscopic appearance. A possible mode of action of RebA can be derived from the molecular interactions that stabilize fatty acid bilayers/lamellar structures.

The formation of bilayers (lamellar aggregates/vesicles) in long-chain soap systems is caused by a complex interplay of hydrophobic interactions between the carbon

chains and hydrophilic interactions between the headgroups, counter-ions and the surrounding solvent.

Recently, Xu et al.<sup>83</sup> systematically investigated the formation of bilayers in fatty acid systems with different techniques and showed that the formation of bilayers (lamellar aggregates) involves three weak interactions: hydrophobic interactions between the carbon chains, electrostatic interactions among the carboxylate head groups and between the carboxylate head groups and the counter-ions, and the formation of hydrogen bonds between the protonated and deprotonated carboxylate head groups. Apel et al.<sup>46</sup> also pointed out the importance of hydrogen bonds for the formation of bilayers in fatty acid systems and in mixed fatty acid/alcohol systems. Dejanovic et al.<sup>84</sup> investigated the surface property of NaOI/OA vesicles by electron spin resonance spectroscopy and reported the formation of a hydrogen bond network at the surface of the NaOI/OA aggregates. Other authors also suggested hydrogen bonds between fatty acid head groups or between fatty acid headgroups and alcohol molecules to be an important criterion for the formation of stable bilayers.<sup>20, 22, 70</sup>

Hydrogen bonds are important for the formation of lamellar structures (bilayers) within a certain range of  $\Theta_P$  in aqueous soap systems. Throughout the whole molecule, RebA possesses many hydroxyl groups, which are able to form hydrogen bonds (see **Figure 3-1**). With regard to these two facts, the following mode of action for RebA within the NaOI/OA system can be proposed: the addition of RebA to aqueous NaOI solutions at  $\Theta_P = 0$  leads to the formation of mixed aggregates due to the amphiphilic structures of the two compounds. An increase in  $\Theta_P$  and the related formation of OA initiates the formation of lamellar structures no matter, whether RebA is present in solution or not (at least for systems with an initial ratio of NaOI to RebA  $\geq 1$ ). The difference in size and shape of the lamellar aggregates as well as in the macroscopic appearance of samples without and with RebA is likely to be due to the incorporation of RebA into the lamellar NaOI/OA structures. Possibly, RebA expands on the surface or in the interface of the lamellar structures forming hydrogen bonds between its hydroxyl groups and the oleate/OA head groups. Owing to its big size and the presence of hydroxyl groups throughout the whole molecule, RebA could form a hydrogen bond network and strengthen the lateral forces within the lamellar aggregates leading to a more rigid and stable interface. Moreover, the surface charge density of the lamellar structures should be decreased by incorporating RebA. Maybe, these two effects lead to a change in size and shape of the lamellar aggregates. The proposed formation of a stable hydrogen bond network can also explain the stabilization of lamellar structures at higher neutralization states

$\Theta_P$ , i.e. an increase in  $\Theta_{oil}$  compared to the pure NaOl systems, for systems with an initial NaOl to RebA ratio between 1 and 2.5 after 21 days of aging.

However, the ratio of oleate to OA is also very important for the different lamellar microstructures being formed. This can be seen by the strong difference in shape and size of the lamellar structures at  $\Theta_P$  values around 0.3 and at  $\Theta_P$  values around 0.5 for the system 1 wt% NaOl/0.8 wt% RebA (see **Figure 3-11** and section 3.3.4.2).

### **3.3.4.5 Time dependent phase behavior of the system 1 wt% NaOl/0.8 wt% RebA**

In the following, the microscopic and macroscopic evolution of the system 1 wt% NaOl/0.8 wt% RebA is presented, starting from the time directly after preparation up to 100 days of aging. Visual observation revealed that the other systems with 1 wt% NaOl and an initial ratio of NaOl to RebA between 1 and 2.5 behaved similarly.

Measurements of the pure 1 wt% NaOl system showed that the turbidity remained more or less constant from preparation until 30 days of aging for each value of  $\Theta_P$  (data not shown).

This is not the case for the solutions containing additional 0.8 wt% RebA. The change in turbidity for these solutions with time is shown in **Figure 3-14**. The data match perfectly with visual observations. Immediately after preparation, the samples with  $\Theta_P$  values ranging from 0.14 to 0.62 were only slightly bluish, homogeneous and stable and looked very similar. All solutions with smaller  $\Theta_P$  values contained some small particles causing a slight increase in turbidity (see section 3.3.4.1). Samples with a larger value of  $\Theta_P$  were non-translucent and white and possessed a huge turbidity that did not change markedly with time.

The kinetic stabilization effect of RebA was less pronounced for the samples with  $\Theta_P$  values between 0.14 and 0.38. Within four days, these solutions became more and more bluish and turbid until a white spongy phase floating on top of the solution could be observed. The appearance was equal to that found after 21 days, which is described in section 3.3.4.1. Samples with  $\Theta_P$  values ranging from 0.43 to 0.53 hardly changed with time. The slight but constant increase in turbidity after 15 days indicates a slow growth of the structures being present in solution. Even after 100 days these solutions were highly translucent and showed no obvious sign of phase separation.

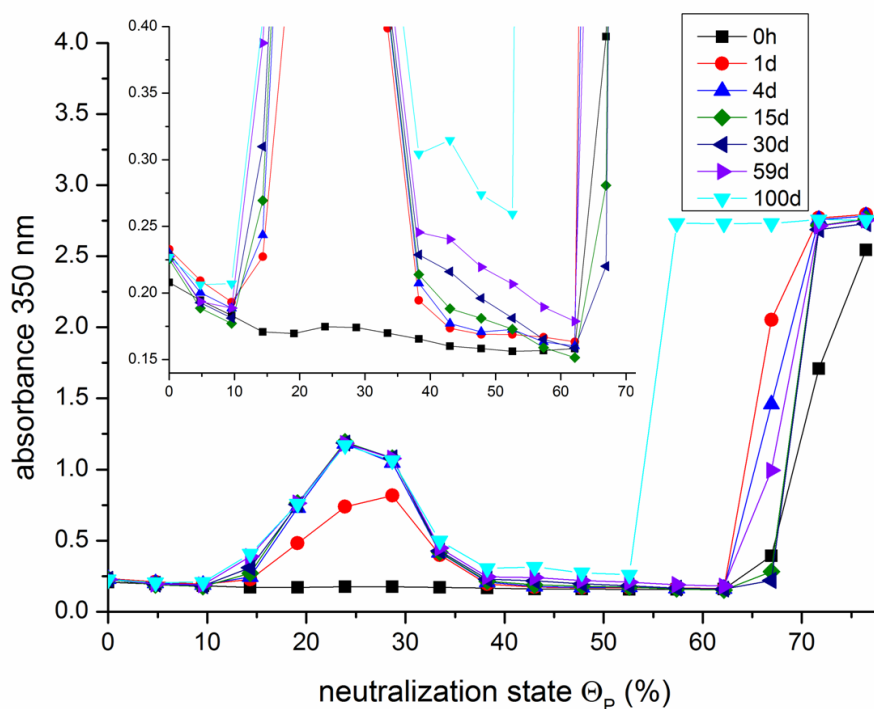


**Figure 3-14:** Absorbance of aqueous solutions with 1 wt% NaOI and 0.8 wt% RebA at 350 nm at different neutralization states  $\Theta_p$  after different time of aging ( $\blacksquare$  = 0 d,  $\bullet$  = 1 d,  $\blacktriangle$  = 4 d,  $\blacklozenge$  = 15 d,  $\blacktriangleleft$  = 30 d,  $\blacktriangleright$  = 59 d,  $\blacktriangledown$  = 100 d). The legend and the units also apply to the small inset, which is a magnification at low absorbance. Note that all solutions were slewed before measuring to obtain homogenous solutions if phase separation took place.

The samples with a neutralization state of 0.57 and 0.62 did not change their appearance within the first 30 days. The next 30 days, a slight increase in turbidity took place, but the samples were still highly translucent and showed no sign of phase separation. After that, the samples became slowly more whitish with some deposit being present on the surface. The process took a few days, and at the end the samples phase separated and were turbid and white after slewing with an appearance similar to solutions with larger  $\Theta_p$  values. This is in line with the strong increase in turbidity for these two solutions after 60 days. Phase contrast microscopy showed oil-like droplets within these non-transparent solutions. This was also observed for the systems with 1 wt% NaOI and 0.6 or 1.0 wt% RebA. In all cases, the sample with a  $\Theta_p$  value of 0.62 became unstable few days earlier than the sample with a value of 0.57.

The results show that RebA can kinetically stabilize highly translucent and macroscopically stable systems within a certain range of  $\Theta_p$ . However, the stabilization effect is strongly dependent on the ratio of OA to oleate. The kinetically most stable region was found to be at nearly equal amounts of oleate and OA in solution where the most hydrogen bonds can be formed between oleate and OA.<sup>85</sup>

This supports the assumption that RebA operates by modifying the oleate/OA hydrogen bond network at the aggregate/water interface.

The instability and formation of an oil-like phase after a certain time of aging in the samples with  $\Theta_P$  values higher than  $\Theta_{oil}$  of the pure NaOI solutions indicates that the thermodynamic phase behavior of the mixed systems is governed by the phase behavior of the pure aqueous NaOI system.

### 3.3.5 Influence of RebA on aqueous sodium dodecanoate solutions at different neutralization states

As discussed in section 2.4.4 and shown in **Figure 2-20**, the phase behavior and the shape of the titration curve of aqueous long chain soap systems is highly dependent on temperature. Below the chain melting temperature  $T_m$  of the hydrophobic carbon chains, acid soap salt crystals and fatty acid crystals are present, whereas above  $T_m$  lamellar liquid crystalline phases and oil-like phases are present.<sup>19, 20, 57</sup> While for NaOI,  $T_m$  of the acid soap salt crystals as well as the  $T_m$  of oleic acid are below room temperature, for sodium dodecanoate (NaC12),  $T_m$  of the acid soap crystals is slightly higher than 30 °C, and  $T_m$  of dodecanoic acid is 44 °C.

Consequently, NaC12 is the appropriate case to investigate, whether RebA has also an effect on the aqueous phase behavior of long chain soaps during titration below  $T_m$  of the hydrophobic carbon chain, or whether this effect is only observed at temperatures above  $T_m$ , as it is the case for the aqueous NaOI system.

Test series with 1 wt% NaC12 without and with 1.16 wt% RebA were prepared. This ensured an initial molecular ratio of NaC12 to RebA, which was between the initial molecular ratios of NaOI to RebA in the systems 1 wt% NaOI/0.8 wt%, respectively 1 wt% NaOI/1 wt% RebA. These systems yielded the broadest range of  $\Theta_P$ , over which stable and highly translucent NaOI solutions were formed.

First, pH and turbidity measurements were carried out at 25 °C after seven days of aging. Since no effect of RebA was observed on turbidity, the samples were heated above  $T_m$  of the acid soap crystals and the pure acid (45 °C) for two hours and turbidity measurements were repeated at this elevated temperature.

**Figure 3-15** illustrates the change in the titration curve of an aqueous 1 wt% solution of NaC12 by adding 1.16 wt% of RebA. The  $pK_A$  of an aqueous 1 w% NaC12 solution with 1.16 wt% RebA is approximately 1 unit lower than without RebA, indicating mixed aggregate formation between C12 and RebA (see section 3.3.3).

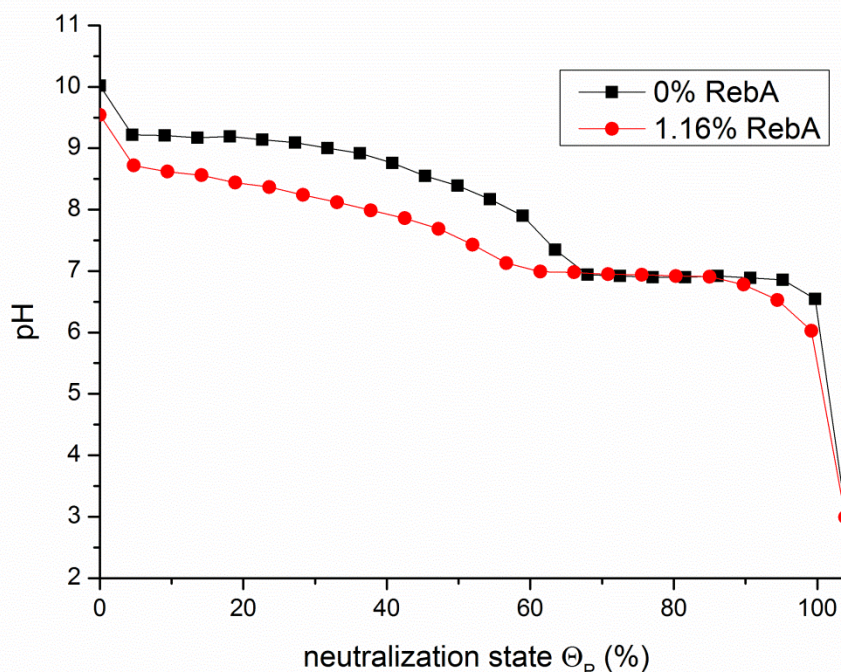


**Figure 3-15:** Titration curves of 1 wt% NaC12 solutions without (■) and with 1.16 wt% of RebA (●) at 25 °C. The solutions were titrated with 0.2 M HCl and the pH was measured seven days after preparation.

The shape of the titration curve as well as the phase behavior at different values of  $\Theta_P$  for KC12 has been discussed in detail.<sup>19, 21, 55, 58</sup> The pH values at the two plateaus of the titration curve of the pure NaC12 system as well as its shape agree very well with the one for KC12 reported by Rosano and Feinstein<sup>58</sup>. Along the first plateau (pH  $\approx$  9.2), micelles with a high negative charge density are present and converted into acid soap crystals. As soon as the pH value decreases, the monomeric concentration of C12 in solution is below the cmc and smaller (pre-micellar) aggregates with a lower negative surface charge density or C12 monomers are transformed to acid soap crystals up to a  $\Theta_P$  value of 0.67. There, only acid soap is present.<sup>58</sup> Consequently, at the end of the first plateau ( $\Theta_P \approx 0.3$ ), the concentration of C12 which is not already incorporated into acid soap crystals should correspond to the cmc of NaC12. With a C12 concentration of around 23 mM, this was nearly fulfilled (cmc (NaC12) = 24.4 mM<sup>86</sup>). The only difference by changing the counter ion from potassium to sodium is the shift of the beginning of the second plateau, i. e. the value of  $\Theta_P$  at which all micelles and C12 monomers are converted to acid soap crystals, from 0.5 to approximately 0.67. This suggests that NaC12 forms acid soap crystals composed of two fatty acids and one soap molecule, whereas KC12 forms 1:1 acid soap crystals.<sup>19, 55</sup> Other than in the NaOI system, RebA shifts the titration curve of NaC12 to lower values only up to  $\Theta_P$  values smaller

than 0.67. This can be well explained with regard to the phase behavior of the crude NaC12 solution during neutralization. As long as micelles or C12 monomers are present in solution, the addition of RebA leads to mixed aggregates with a reduced surface charge density compared to the pure C12 micelles/aggregates. This leads to lower pH values at a certain value of  $\Theta_P$ . As soon as only crystalline acid soap is present in solution ( $\Theta_P > 0.67$ ), the pH values are equal for solutions without and with RebA, indicating that RebA cannot be incorporated into NaC12 acid soap crystals.

**Figure 3-16** shows the absorbance of 1 wt% NaC12 solutions without and with 1.16 wt% RebA at 25 and 45 °C. At 25 °C, RebA had no effect on the macroscopic phase behavior of aqueous 1 wt% NaC12 solutions at different values of  $\Theta_P$ . The only exception was at  $\Theta_P = 0$ , where the crude NaC12 solution was clear and the solution containing RebA showed little white precipitate. As for the oleate system, this is likely to be due to some kind of co-precipitation. Above  $\Theta_P$  values of 0.05, big crystals were visible with both the naked eye and in the light microscope. This led to macroscopically unstable solutions which were highly turbid after slewing (see **Figure 3-16**). The decline in the turbidity curve for NaC12 plus 1.16 wt% RebA at 25 °C between 0.6 and 0.9 is due to the presence of large crystals that quickly sedimented, and not to an increase in stability or translucence. To conclude: RebA cannot prevent the formation of crystals below  $T_m$  of NaC12 acid soap/lauric acid and has no effect on the macroscopic stability and appearance of aqueous NaC12 solutions at different values of  $\Theta_P$  at 25 °C.

To check whether RebA is able to influence the macroscopic appearance above  $T_m$ , as it is the case in the NaOl system, the samples were stirred for two hours at 45 °C and the turbidity of the samples was measured again. As expected, no more crystals were visible in all of the samples. The turbidity curves in **Figure 3-16** and the photos shown in **Figure 3-17** clearly show that RebA has a significant influence on the macroscopic appearance of the samples above  $T_m$ . NaC12 solutions without RebA were highly turbid and non-translucent for  $\Theta_P$  values larger than 0.15. The presence of RebA led to highly transparent solutions up to  $\Theta_P$  values of 0.4, and even up to a value of 0.8 the samples remained translucent. The big difference in appearance of the 1 wt% NaC12 solutions without and with RebA is also clearly illustrated in **Figure 3-17**. The photos were taken after stirring the samples for 2 h at 45 °C. Cooling to room temperature led to the formation of crystals again.

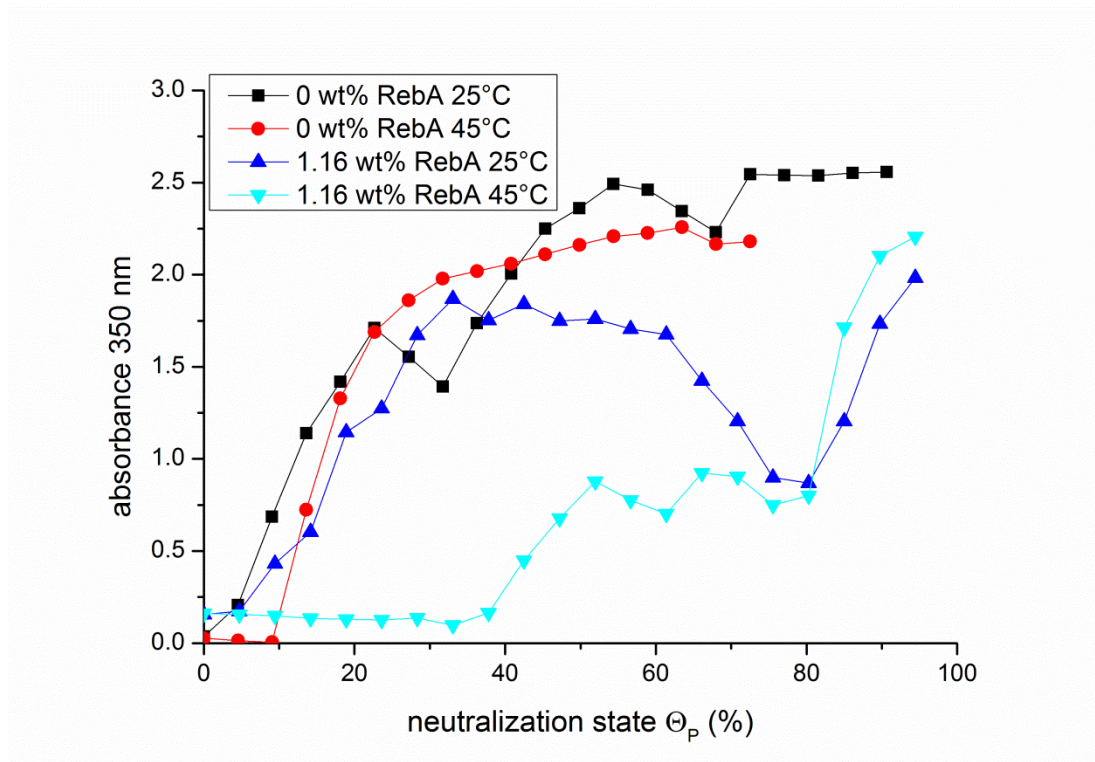


**Figure 3-16:** Absorbance of aqueous 1 wt% NaC12 solutions at 350 nm without (■ at 25 °C, ● at 45 °C) and with 1.16 wt% RebA (▲ at 25 °C, ▼ at 45 °C) at different neutralization states  $\Theta_p$  after seven days of aging. The measurements were performed at 25 °C and 45 °C. Note that all solutions were slewed before measuring to obtain homogenous solutions if phase separation took place.

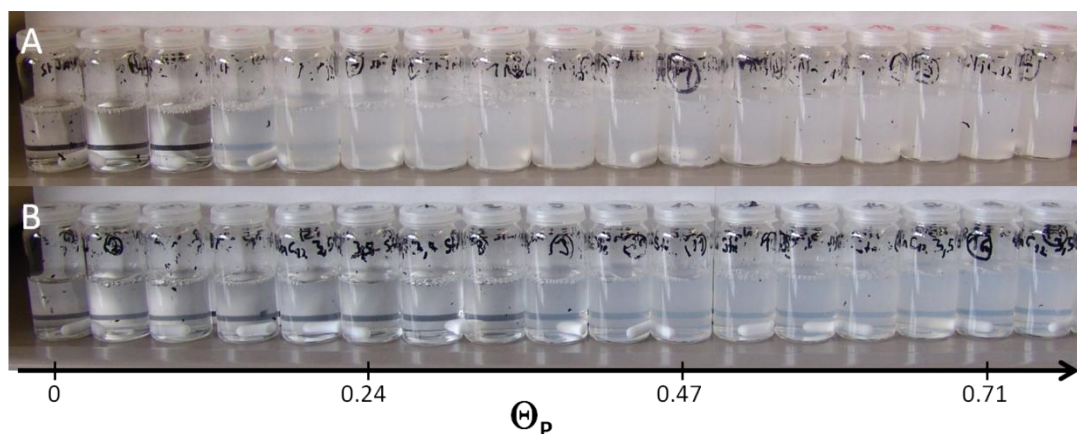


**Figure 3-17:** Photos of aqueous 1 wt% NaC12 solutions without (A) and with (B) 1.16 wt% RebA after stirring for 2h at 45 °C. The neutralization state  $\Theta_p$  is given on the bottom of the figure and increases from left to right. Samples on a vertical line possess the same  $\Theta_p$  (deviation < 0.01) and can be directly compared.

The results clearly show that RebA can only affect the macroscopic appearance of long chain soaps at certain values of  $\Theta_p$ , if the experiments are carried out above the chain melting temperature  $T_m$  of the hydrophobic carbon chain of the acid soap/fatty acid crystals.

### 3.3.6 Stable and highly translucent solutions of $\omega$ -3-fatty acids

Omega-3-fatty acids ( $\omega$ -3-FAs) are natural polyunsaturated long chain fatty acids, out of which docosahexaenoic acid (DHA) and eicosapentaenoic acid (EPA) have the greatest interest, since they are well known to have distinct beneficial effects on human health.<sup>87</sup> These effects can be found for cardiovascular, inflammatory and neurological diseases, for example. Furthermore, DHA is meant to play an important role in brain development and development of cognitive functions during gestation and after birth. Many studies and reviews have been published covering these topics.<sup>87-95</sup> Because of these beneficial effects on human health, many important organizations recommend daily intakes for DHA and EPA. For example, the 2010 Dietary Guideline for Americans recommends an intake of 250 mg EPA and DHA per day, the European Food Safety Agency 250-500 mg of EPA and DHA per day and the World Health Organization 200 to 500 mg of EPA and DHA.<sup>74</sup> Aside from some species of algae, the only naturally sources being rich in DHA and EPA are fish and other seafood.<sup>87</sup> Since in many countries people do not consume recommended amounts of EPA and DHA via daily diet, many dietary supplements containing  $\omega$ -3-FAs are available in the super market.<sup>89, 90, 93</sup> These are often capsules that contain fish oil concentrates ("fish-oil capsules") with a high amount of DHA and EPA in its ethyl ester or triglycerol form.<sup>90, 93, 96, 97</sup> Another approach to increase the intake of  $\omega$ -3-FAs is to enrich conventional food with a certain amount of  $\omega$ -3-FAs.<sup>87, 97</sup> A general problem of  $\omega$ -3-FAs restricting their usage is the low oxidative stability because of a high degree of unsaturation.<sup>97</sup>

According to the findings presented above, RebA should have an effect on the appearance of aqueous  $\omega$ -3-FA salt solutions during titration. These highly unsaturated fatty acids are all liquid at room temperature with a  $T_M$  far below 0 °C and no crystals should be formed during titration with HCl.<sup>98</sup> This assumption is proven by the formation of bilayers (vesicles) in aqueous sodium docosahexaenoate solution at room temperature during titration with HCl.<sup>99</sup>

Since no pure  $\omega$ -3-FAs could be obtained, fish oil concentrate provided by BASF (OMEVITAL 3322 EE, allowed for usage in food) containing  $\omega$ -3-FAs in their ethyl ester form was used for the experiments.

For two reasons choline was preferred as counter ion to sodium. First, choline as counter ion reduces the Krafft-temperature of long chain carboxylates compared to sodium due to its bulky structure.<sup>86</sup> This should enhance the water solubility of the prepared fatty acid salts. Secondly, choline is classified as an essential nutrient for humans by the Institute of Medicine (IOM), acts as a precursor for biologically

important molecules in the human metabolism and many studies have shown the necessity of choline intake to maintain health as well as its importance during pregnancy and in brain development.<sup>100-102</sup> Dietary supplements containing choline salts or lecithin as choline sources are commercially available, too. For more detailed information see section 2.3.

Simple titration experiments of the 2 wt% choline fatty acid stock solution ( $\approx 1.2$  wt% choline  $\omega$ -3-FAs) containing different amounts of RebA showed the same results as for the NaOI systems. The  $\text{apK}_\text{A}$  value of the fatty acid mixture decreased with increasing concentration of RebA and the titration curve was shifted downwards (data not shown).

The effect of RebA on the macroscopic appearance of the aqueous choline  $\omega$ -3-FAs solution at a pH value of 7.5 was significant. **Figure 3-18** shows the macroscopic appearance of the different samples after 3 h of aging. Solution 1 contained no RebA, from solution 2 to 7 the concentration increased constantly. In contrast to the sample without RebA, which was non translucent and white, all other samples were translucent. As it was observed for the NaOI systems, the visual turbidity decreased with increasing amount of RebA, and above a certain concentration of RebA highly translucent solutions were obtained. The solutions were macroscopically stable for at least two days. The lower stability of the solutions compared to the NaOI systems could be due to the low oxidative stability of the polyunsaturated fatty acids or the presence of other ingredients, like long chain saturated fatty acids, that originate from the fish oil. Solution 7, for example, contained around 0.9 wt %  $\omega$ -3-FAs (1.5 wt% fatty acids in total), 0.5 wt% choline and 1 wt% RebA.

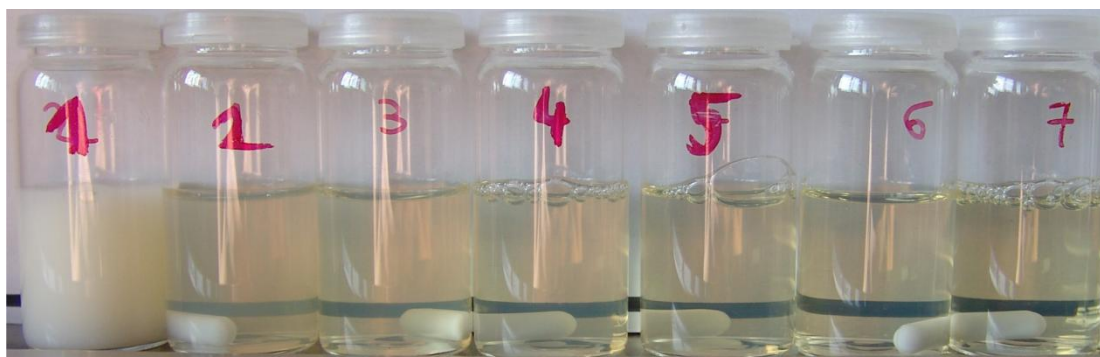


**Figure 3-18:** Photo of aqueous 2 wt% choline fatty acid carboxylate solutions (1.2 wt% choline  $\omega$ -3-FAs) with different amounts of RebA and a pH value of 7.5 after 3 h hours of aging. Sample 1 contained no RebA, from sample 2 - 7 the concentration of RebA increased.

Although the investigated aqueous  $\omega$ -3-FA system contained other fatty acids and a small amount of fatty acid ethyl esters, it could be shown that RebA has a significant effect on the macroscopic appearance of aqueous  $\omega$ -3-FA solutions at a pH value of 7.5, and that highly translucent solutions could be obtained.

Compared to the water insoluble ethyl ester or triglycerol forms of  $\omega$ -3-FAs, choline  $\omega$ -3-FA salts were found to be water soluble at room temperature and RebA can help producing stable and highly translucent aqueous solutions at consumable pH values. Moreover, due to its high sweetening ability, RebA could also cover the soapy taste of the long chain fatty acid.

Maybe, this system could be the basis for the development of a water soluble fizzy tablet being merchandised as a dietary supplement which comprises the positive effects on human health both of  $\omega$ -3-FAs and of choline.

### **3.4 Conclusion and "green" strategies to overcome problems with soaps in application**

This work shows that the natural steviol glycoside Rebaudioside A has a significant influence on the macroscopic and microscopic phase behavior as well as the stability and optical appearance of aqueous sodium oleate solutions at different neutralization states,  $\Theta_P$ . It was possible to prepare stable and highly translucent NaOl solutions at consumable pH values (7-8.5) at room temperature. Long time stability tests showed that these systems were stable for at least 60 days at room temperature. These findings open new fields to use aqueous NaOl systems in food preparation, since RebA does not only improve the stability and appearance of NaOl solutions at nearly neutral pH values, but can also overcome the soapy taste of the oleate due to its high sweetening capacity. It should be mentioned that skin as well as eye irritancy problems caused by soaps are mainly caused by the high natural pH values of their aqueous solutions. So this issue is implicitly fixed by moderate to neutral pH values. Thus, these findings can also be of interest for aqueous soap based cosmetic formulations.

Moreover, RebA had an influence on the measured titration curves and led to a decrease in the  $\text{ap}K_A$  value of NaOl. It is proposed that the incorporation of RebA into the NaOl/OA structures and the formation of a hydrogen bond network between the oleate/OA head groups and the hydroxyl groups of RebA at the surface of the mixed aggregate could be responsible for to the observed difference in phase behavior and macroscopic appearance.

Temperature dependent tests with aqueous sodium dodecanoate solutions showed that RebA can only influence the macroscopic appearance of aqueous long chain soap systems at different neutralization states, if the temperature exceeds the chain melting temperature  $T_m$  of the acid soap and the fatty acid crystals.

Finally, these findings were applied to a mixture of choline fatty acid salts containing high amounts of omega-3-fatty acids. In this way, stable and highly translucent solutions could be prepared at a pH value of 7.5. Possibly, choline  $\omega$ -3-FAs plus RebA could be the starting composition of a water-soluble dietary supplement which combines the positive effects on human health of both  $\omega$ -3-FAs and of choline.

At last, possible "green" approaches in developing aqueous systems based on long chain soaps being stable at room temperature will be presented. To allow safe application in food or cosmetics, the formulation should also be stable at a pH value close to neutral. It has to be mentioned that for me, two further important criteria are the true solution appearance, i.e. low viscosity and high transparency, and the use of green substances, i.e. biogenic, low-toxic and biodegradable. Moreover, the long chain soap is meant to be the main ingredient of the systems and simple solubilisation by microstructures mainly composed of synthetic amphiphilic compound is not considered. In what follows, important results being based on the discussions in section 2.4 and findings presented in this chapter are shortly summarized as well as some possible "green" ways to overcome existing problems, are mentioned (see also **Figure 3-19**).

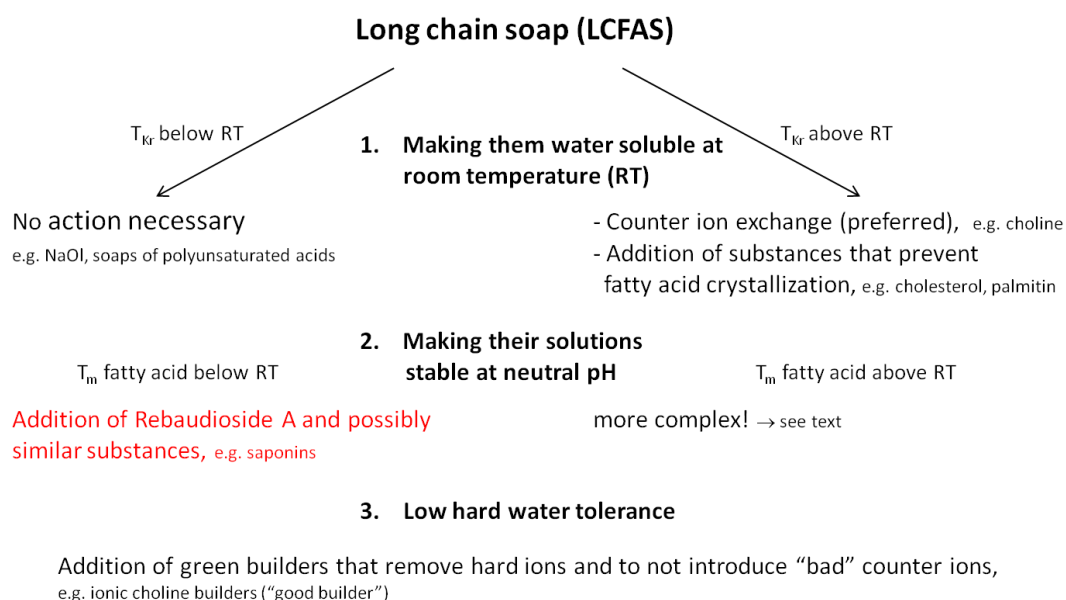


**Figure 3-19:** The problems in usage of long chain soaps as basis of aqueous formulations for application in food or cosmetics and possible green ways to overcome them. The red part is the contribution of the work presented in this chapter.

First, it is important that the long chain soap is highly soluble and therefore its Krafft temperature ( $T_{Kr}$ ) has to be below room temperature. If this is not the case, like for sodium myristate or sodium palmitate, the preferred way to decrease  $T_{Kr}$  below room

temperature is using a "good counter ion". It should be green and has to be very bulky to prevent the crystallization of the long chain soap. Choline is a good candidate that fulfills these requirements. Due to their acidic character, bulky amines are inappropriate, since the formed solutions are only metastable at room temperature. Another way would be the addition of other natural substances like cholesterol or palmitin. The advantage of using a "good counter ion" over the addition of further substances is the formation of clear and low viscous micellar solutions. The addition of other compounds described in literature, however, always led to the formation of mixed lamellar structures and turbid and/or viscous solutions.

The second problem of long chain soaps is their instability at neutral or acidic pH values. In this work, an easy way to overcome the problems in stability and macroscopic appearance of long chain soap solutions is shown, as long as the chain melting temperature  $T_m$  of the acid soap/fatty acid is below room temperature. The addition of RebA to aqueous NaOI or choline omega-3-FA allowed the formation of stable and highly translucent solutions at neutral pH values at room temperature. Possibly, molecules with a similar molecular structure, e.g. saponins, could show a similar behavior and should be investigated.

For saturated long chain fatty acids, this was not possible and some kind of fatty acid crystals formed with decreasing pH value. Here, the situation becomes more complex. If a bulky counter ion prevents the precipitation of long chain soap at high pH values, it is not sure that it also prevents the crystallization of acid soap crystals or crystals of protonated fatty acid with  $T_m$  above room temperature at neutral pH value. And even if the system does not crystallize at pH values close to neutral at room temperature and a kind of lamellar phase with "fluid" hydrocarbon tails is formed, the macroscopic phase behavior has to be considered, too. It is quite likely that the solutions become turbid and unstable, similar to a pure NaOI solution. Then, a possible way to overcome this problem could be the addition of a second component acting like RebA in the aqueous NaOI system. Unfortunately, first attempts in combining choline as "good counter ion" and RebA as additive for dodecanoate, i.e. choline dodecanoate plus RebA, were not promising. At around 25 % percent neutralization of dodecanoate crystals were formed and the aqueous solutions became unstable at room temperature. However, more experiments with other counter ions and with other similar additives like RebA should be considered.

In the buffered mixed system palmitic acid/palmitin, vesicles were also formed at a pH value of 7.<sup>81</sup> However, as already mentioned in section 2.4.2, the solutions were turbid and highly viscous. Perhaps adding a third component, like RebA, could lead

to less viscous and translucent solutions. But then, the fraction of fatty acid in the mixture is likely to become very low. This will probably be the problem for every system of long chain soap, in which an additive prevents crystallization of fatty acid crystals at room temperature.

To our knowledge, up to now, no aqueous, translucent and low viscous system based on saturated long chain soaps has been formulated that is stable at neutral or acidic pH at room temperature. It is obvious that the situation is much more complex for these systems of saturated long chain soaps with  $T_m$  above room temperature than for unsaturated soaps with  $T_m$  below room temperature. This can mainly be attributed to the fact that a “good counter ion” and/or an additive have to prevent the crystallization of any fatty acid crystals and have to interact with the long chain soap in a way so that small and stable microstructures are formed. Although, these systems are very complex, it seems worth trying different counter ion/additive couples to solve the current problems.

If hard tap water is used for the soap solution, it does not matter whether  $T_m$  of the fatty acid is below or above room temperature.  $T_{Kr}$  of calcium or magnesium long chain soaps is always above room temperature and the corresponding crystals will precipitate from the solution. The only way to prevent this and ensure the formation of clear and stable solutions in tap water is removing all these hard water minerals by builders. As already mentioned in section 2.4.3, when “good counter ions” (choline) are used, the builder may not introduce “bad counter ions” (sodium) that will increase  $T_{Kr}$  of the long chain soap. This means that sodium builders should not be used in the case of aqueous choline palmitate solutions at room temperature, since  $T_{Kr}$  of sodium palmitate is above room temperature. For example, choline builder should be used instead, which we call a “good builder”. From an environmental point of view, amino acid-N,N-diacetic acids and citrate should be used instead of common builders like sodium tripolyphosphate (STPP), nitrilotriacetic acid (NTA) or ethylenediamine tetraacetic acid (EDTA).<sup>103</sup> Of course, the used substance has to be approved for the desired application, e.g. in food or cosmetics.

All in all, if properly formulated, there is a real future for soaps, and, they can be used in many types of formulations that, up to now, are based on synthetic surfactants.

This work could be a contribution to make chemicals greener (no sulphatation, no ethylene oxide groups) and modern high performance formulations accessible to developing countries, since soaps are easy to make. Further, making long chain

soaps water soluble at room temperature opens new fields of application of triglycerides derived from European plants, which are mostly composed of C18 chains.

## 3.5 Experimental

### 3.5.1 Chemicals

Sodium salts of Oleate (NaOI > 82 %) and laurate (NaC12 > 99 %) were purchased by Sigma Aldrich and used as supplied. HCl (0.2 M) was prepared by dilution of 1 M HCl solution from Merck TitriPUR and choline hydroxide (45 wt% in water) was provided by TAMINCO. Rebaudioside A (Truvia Stevia FCC RA 95, RebA > 95 %) was kindly provided by Cargill.

### 3.5.2 Sample preparation

Pure NaOI and mixed NaOI/RebA test samples were prepared at different neutralization rates  $\Theta_P$  as follows: an aqueous stock solution with the initial amounts of RebA and NaOI was prepared by weighing RebA, NaOI and water. The solution was stirred for 30-45 min. Then, 10 g of the stock solution were transferred into vials and a defined amount of aqueous 0.2 M HCl solution was added stepwise to each vial during stirring. After the addition of HCl, the solutions were stirred for further 15 minutes. Samples with sodium dodecanoate (NaC12) were prepared in the same way. The samples were kept at room temperature (20-25 °C) and observed visually during aging. Additionally, after three weeks the turbidity of the samples was measured for each system. For time-dependent turbidity measurements of the binary 1 wt% NaOI water mixture and the ternary 1 wt% NaOI/0.8 wt% RebA system in water, additional test series were prepared.

Samples for electron microscopy and phase contrast microscopy were prepared without stock solution, but otherwise in the same way as explained above.

Note that the concentrations indicated further on are the initial concentrations of NaOI and RebA in each sample before adding HCl. The addition of HCl generates a defined amount of Oleic Acid (OA) and causes a certain dilution effect.

Moreover, the used substances (NaOI and RebA) are natural products and not completely pure. So, it is likely that some impurities and other substances (other steviol glycosides and fatty acids) have been present within the systems.

The choline omega-3-fatty acid ( $\omega$ -3-FA) stock solution and samples containing RebA were prepared with OMEVITAL 3322 EE. This is a fish oil concentrate allowed for usage in food and provided by BASF. It contains  $\omega$ -3-FAs in their ethyl ester form. The total amount of  $\omega$ -3-FAs is 560mg/g, with 300 mg/g eicosapentaenoic acid (EPA) and 190 mg/g docosahexaenoic acid (DHA). The other part is mainly a mixture of fatty acid ethyl esters of other fatty acids being present in fish oil. OMEVITAL 3322 EE and choline hydroxide (aqueous 45 wt%, TAMINCO) were stirred in a water/ethanol (0.15/0.85) mixture under nitrogen atmosphere over night at 60°C. The amount of choline hydroxide was chosen such that around 95 % of the fatty acid ethyl esters were cleaved and transformed to choline fatty acid salts. Completeness of the reaction was checked by acid-base titration. Because of the low oxidative stability, the following steps were carried out as fast as possible. The ethanol was removed via rotary evaporation and a yellow jelly like residue was obtained. It consisted of choline fatty acid salts, little uncleaved fatty acid ethyl esters and a bit of water was. The residue was diluted with water to get a solution with 2 wt% choline fatty acids ( $\approx$  1.2 wt% choline  $\omega$ -3-FAs,  $\approx$  0.8 wt% other choline fatty acids present in fish oil) and a small amount of remaining fatty acid ethyl esters ( $<$  0.2 wt%). Then, 10g of the stock solution was transferred into vials and a certain amount of RebA was dissolved in each sample during stirring. The pH value of each sample was adjusted to 7.5 ( $\pm$  0.1) with 1M HCl. The samples were kept at room temperature.

### **3.5.3 Cmc measurements**

The cmc values were determined by concentration dependent surface tension measurements, which were performed at 25 °C with a Krüss tensiometer (model K100 MK2) using a platinum-iridium ring. The recording of the surface tension as a function of the surfactant concentration was done automatically. Dilution of the surfactant solution during the measuring was carried out with degassed millipore water. The data correction was performed according to the procedure proposed by Harkins and Jordan.<sup>104</sup>

### **3.5.4 Turbidity measurements**

Turbidity, respectively absorbance measurements were carried out with a Perkin Elmer Lambda 18 Spectrometer at 350 nm and room temperature. Each sample was shaken before measuring to homogenize solutions that had already phase separated and to gain meaningful data.

### 3.5.5 pH measurements

Titration curves were obtained by measuring the pH value as a function of added HCl for each sample of a certain test series after 7 days of aging at room-temperature. The  $\text{pK}_\text{A}$  value of the fatty acid was determined as the pH value at half neutralization of the soap. The pH measurements were carried out with a PC5000L, pHenomenal from VWR.

### 3.5.6 Phase contrast microscopy

Selected samples were examined with an Olympus BX 60 phase contrast microscope at room temperature after different times of aging. Photos were taken with a Canon 60D digital camera. It is well known that unilamellar vesicles, multilamellar vesicles and oil droplets can be distinguished by phase-contrast microscopy. Differences in the refractive index of lipid and water result in different appearances for oil droplets (phase-bright droplets), multilamellar structures/vesicles (phase-dark spheres) and unilamellar structures/vesicles (low phase-contrast spheres).<sup>20, 52</sup>

### 3.5.7 Freeze fracture transmission electron microscopy

Some samples of pure NaOl and NaOl plus RebA systems were further investigated with electron microscopy after different times of aging.

The freeze etch replica were prepared as follows: 2  $\mu\text{l}$  aliquots of the suspensions of the samples were applied onto gold carriers for freeze-etching, plunge-frozen in liquid nitrogen, and transferred at  $T < -160^\circ\text{C}$  into a high-vacuum freeze-etching device (CFE 50; Cressington, Watford, UK). After raising the sample temperature to  $-97^\circ\text{C}$ , samples were fractured with a cold ( $T < -180^\circ\text{C}$ ) knife and then freeze-etched for 4 min at  $T = -97^\circ\text{C}$ . The samples were immediately shadowed with 1 nm Platinum (by electron-beam evaporation; angle  $45^\circ$ ) and then backed with about 10 nm Carbon (again, e-beam evaporation; angle  $90^\circ$ ). The replicas were cleaned at room temperature for 14 hours on sulfuric acid (70%) and washed with distilled water three times for 30 min each. Replicas were taken up on Cu grids (600 mesh, hexagonal) and the samples then analyzed in a transmission electron microscope using 120 keV electrons (CM12, FEI Co, Eindhoven, The Netherlands). Images were recorded digitally using a CCD camera (0124, TVIPS, Gauting, Germany).

### 3.5.8 Dynamic light scattering

Before measuring, all samples were filtered with a 200 nm PTFE membrane filter to remove dust. The measurements were carried out with a CGS-3 goniometer system from ALV which was equipped with a vertical polarized HeNe laser and an ALV-7004/FAST Multiple Tau digital correlator. All measurements were done at 25 °C and at an angle of 90°.

## 3.6 Literature

1. Kaibara, K.; Ogawa, T.; Kawasaki, H.; Suzuki, M.; Maeda, H., *Colloid Polym Sci* **2003**, 281 (3), 220-228.
2. Fukuda, H.; Goto, A.; Yoshioka, H.; Goto, R.; Morigaki, K.; Walde, P., *Langmuir* **2001**, 17 (14), 4223-4231.
3. Marcus, J.; Wolfrum, S.; Touraud, D.; Kunz, W., *J Colloid Interface Sci* **2015**, 460, 105-112.
4. Commission, E., *Official Journal of the European Union L* **2011**, 295 (4).
5. FDA, U., 21CFR172.860.
6. FDA, U., 21CFR172.863.
7. Ash, M.; Ash, I., *Handbook of Green Chemicals*. Synapse Information Resources: 2004.
8. Heude, B.; Ducimetière, P.; Berr, C., *Am J Clin Nutr* **2003**, 77 (4), 803-808.
9. Neuringer, M.; Anderson, G. J.; Connor, W. E., *Annu Rev Nutr* **1988**, 8 (1), 517-541.
10. Benitez-Sánchez, P.; León-Camacho, M.; Aparicio, R., *Eur Food Res Technol* **2003**, 218 (1), 13-19.
11. Izquierdo, N.; Aguirrezábal, L.; Andrade, F.; Pereyra, V., *Field Crops Res* **2002**, 77 (2-3), 115-126.
12. Hildebrand, A.; Garidel, P.; Neubert, R.; Blume, A., *Langmuir* **2003**, 20 (2), 320-328.
13. Edwards, K.; Silvander, M.; Karlsson, G., *Langmuir* **1995**, 11 (7), 2429-2434.
14. Söderman, O.; Jönsson, B.; Olofsson, G., *J Phys Chem B* **2006**, 110 (7), 3288-3293.
15. Kanicky, J. R.; Shah, D. O., *Langmuir* **2003**, 19 (6), 2034-2038.
16. Whiddon, C. R.; Bunton, C. A.; Söderman, O., *J Phys Chem B* **2002**, 107 (4), 1001-1005.

17. da Silva, F. L. B.; Bogren, D.; Söderman, O.; Åkesson, T.; Jönsson, B., *J Phys Chem B* **2002**, 106 (13), 3515-3522.
18. Kaibara, K.; Iwata, E.; Eguchi, Y.; Suzuki, M.; Maeda, H., *Colloid Polym Sci* **1997**, 275 (8), 777-783.
19. Cistola, D. P.; Hamilton, J. A.; Jackson, D.; Small, D. M., *Biochemistry* **1988**, 27 (6), 1881-1888.
20. Hargreaves, W. R.; Deamer, D. W., *Biochemistry* **1978**, 17 (18), 3759-3768.
21. Rosano, H. L.; Christodoulou, A. P.; Feinstein, M. E., *J Colloid Interface Sci* **1969**, 29 (2), 335-344.
22. Walde, P.; Namani, T.; Morigaki, K.; Hauser, H., Formation and properties of fatty acid vesicles (liposomes). In *Liposome technology*, Gregoriadis, G., Ed. CRC Press: 2006; Vol. 1, pp 1-19.
23. DeZuane, J., *Handbook of drinking water quality*. John Wiley & Sons: 1997.
24. Prakash, I.; Dubois, G. E.; King, G. A.; Upreti, M. Rebaudioside A composition and method for purifying rebaudioside A. US Patent No. 8,791,253, 2014.
25. Prakash, I.; DuBois, G. E.; Clos, J. F.; Wilkens, K. L.; Fosdick, L. E., *Food Chem Toxicol* **2008**, 46 (7, Supplement), 75-82.
26. Carakostas, M. C.; Curry, L. L.; Boileau, A. C.; Brusick, D. J., *Food Chem Toxicol* **2008**, 46 (7, Supplement), 1-10.
27. Rolly, M., *Innovare Journal of Food Sciences* **2014**, 2 (1), 7-13.
28. Carakostas, M.; Prakash, I.; Kinghorn, A. D.; Wu, C. D.; Soejarto, D. D., Steviol glycosides. In *Alternative Sweeteners*, O'Brian-Nabors, L., Ed. 2011; pp 159-180.
29. Christaki, E.; Bonos, E.; Giannenas, I.; Karatzia, M. A.; Florou-Paneri, P., *Journal of Food & Nutrition Research* **2013**, 52 (4), 195-202.
30. Gupta, E.; Purwar, S.; Sundaram, S.; Rai, G., *J Med Plant Res* **2013**, 7, 3343-3353.
31. Lemus-Mondaca, R.; Vega-Gálvez, A.; Zura-Bravo, L.; Ah-Hen, K., *Food Chem* **2012**, 132 (3), 1121-1132.
32. Wan, Z.-L.; Wang, L.-Y.; Wang, J.-M.; Zhou, Q.; Yuan, Y.; Yang, X.-Q., *Food Hydrocoll* **2014**, 39 (0), 127-135.
33. Wan, Z.-L.; Wang, L.-Y.; Wang, J.; Yuan, Y.; Yang, X.-Q., *J Agric Food Chem* **2014**, 62 (28), 6834-6843.
34. Wan, Z.-L.; Wang, J.-M.; Wang, L.-Y.; Yang, X.-Q.; Yuan, Y., *J Agric Food Chem* **2013**, 61 (18), 4433-4440.

35. Uchiyama, H.; Tozuka, Y.; Nishikawa, M.; Takeuchi, H., *Int J Pharm* **2012**, 428 (1–2), 183-186.
36. Uchiyama, H.; Tozuka, Y.; Imono, M.; Takeuchi, H., *Eur J Pharm Biopharm* **2010**, 76 (2), 238-244.
37. Shi, J.; Wang, H.; Deng, M. Stevia sweetener with a surfactant. US Patent Application No. 13/362,673, 2012.
38. Suga, K.; Yokoi, T.; Kondo, D.; Hayashi, K.; Morita, S.; Okamoto, Y.; Shimanouchi, T.; Umakoshi, H., *Langmuir* **2014**, 30 (43), 12721-12728.
39. Fameau, A.-L.; Zemb, T., *Adv Colloid Interface Sci* **2014**, 207, 43-64.
40. Fameau, A.-L.; Arnould, A.; Saint-Jalmes, A., *Curr Opin Colloid Interface Sci* **2014**, 19 (5), 471-479.
41. Rendón, A.; Carton, David G.; Sot, J.; García-Pacios, M.; Montes, R.; Valle, M.; Arrondo, J.-Luis R.; Goñi, Felix M.; Ruiz-Mirazo, K., *Biophys J* **2012**, 102 (2), 278-286.
42. Morrow, B. H.; Wang, Y.; Wallace, J. A.; Koenig, P. H.; Shen, J. K., *J Phys Chem B* **2011**, 115 (50), 14980-14990.
43. Vlachy, N.; Merle, C.; Touraud, D.; Schmidt, J.; Talmon, Y.; Heilmann, J.; Kunz, W., *Langmuir* **2008**, 24 (18), 9983-9988.
44. Theander, K.; Pugh, R. J., *J Colloid Interface Sci* **2003**, 267 (1), 9-17.
45. Borné, J.; Nylander, T.; Khan, A., *J Colloid Interface Sci* **2003**, 257 (2), 310-320.
46. Apel, C. L.; Deamer, D. W.; Mautner, M. N., *Biochim Biophys Acta - Biomembranes* **2002**, 1559 (1), 1-9.
47. Kronberg, B., *Curr Opin Colloid Interface Sci* **1997**, 2 (5), 456-463.
48. Scamehorn, J. F., An Overview of Phenomena Involving Surfactant Mixtures. In *Phenomena in Mixed Surfactant Systems*, Scamehorn, J. F., Ed. American Chemical Society: 1986; Vol. 311, pp 1-27.
49. Shankland, W., *J Colloid Interface Sci* **1970**, 34 (1), 9-25.
50. Namani, T.; Walde, P., *Langmuir* **2005**, 21 (14), 6210-6219.
51. Kroyer, G. T., *Lebensm Wiss Technol* **1999**, 32 (8), 509-512.
52. Hirai, A.; Kawasaki, H.; Tanaka, S.; Nemoto, N.; Suzuki, M.; Maeda, H., *Colloid Polym Sci* **2006**, 284 (5), 520-528.
53. Janke, J. J.; Bennett, W. F. D.; Tieleman, D. P., *Langmuir* **2014**, 30 (35), 10661-10667.
54. Small, D. M., *Physical chemistry of lipids*. Plenum Press: 1986.

55. Rosano, H. L.; Breindel, K.; Schulman, J. H.; Eyd, A. J., *J Colloid Interface Sci* **1966**, 22 (1), 58-67.
56. Lynch, M. L., *Curr Opin Colloid Interface Sci* **1997**, 2 (5), 495-500.
57. Cistola, D. P.; Atkinson, D.; Hamilton, J. A.; Small, D. M., *Biochemistry* **1986**, 25 (10), 2804-2812.
58. Feinstein, M. E.; Rosano, H. L., *J Phys Chem* **1969**, 73 (3), 601-607.
59. Morigaki, K.; Walde, P., *Curr Opin Colloid Interface Sci* **2007**, 12 (2), 75-80.
60. Myers, D., Surfactants in Solution: Monolayers and Micelles. In *Surfactant Science and Technology*, John Wiley & Sons, Inc.: 2005; pp 107-159.
61. Evans, D. F.; Wennerström, H., Solutes and Solvents, Self-Assembly of Amphiphiles. In *The Colloidal Domain: Where Physics, Chemistry, Biology, and Technology Meet*, Wiley: 1999; pp 1-44.
62. Israelachvili, J. N.; Mitchell, D. J.; Ninham, B. W., *Journal of the Chemical Society, Faraday Transactions 2: Molecular and Chemical Physics* **1976**, 72 (0), 1525-1568.
63. Ananthapadmanabhan, K. P.; Lips, A.; Vincent, C.; Meyer, F.; Caso, S.; Johnson, A.; Subramanyan, K.; Vethamuthu, M.; Rattinger, G.; Moore, D. J., *Int J Cosmet Sci* **2003**, 25 (3), 103-112.
64. Baranda, L.; González-Amaro, R.; Torres-Alvarez, B.; Alvarez, C.; Ramírez, V., *Int J Dermatol* **2002**, 41 (8), 494-499.
65. Ogino, K.; Abe, M., *Mixed surfactant systems*. CRC Press: 1992.
66. Holland, P. M.; Rubingh, D. N., *Mixed surfactant systems*. American Chemical Society Washington, DC: 1992; Vol. 1.
67. Ouimet, J.; Croft, S.; Paré, C.; Katsaras, J.; Lafleur, M., *Langmuir* **2003**, 19 (4), 1089-1097.
68. Borné, J.; Nylander, T.; Khan, A., *Langmuir* **2001**, 17 (25), 7742-7751.
69. Haines, T. H., *Proc Natl Acad Sci U S A* **1983**, 80 (1), 160-164.
70. Gebicki, J. M.; Hicks, M., *Chem Phys Lipids* **1976**, 16 (2), 142-160.
71. Davies, J.; Rideal, E., *Interfacial Phenomena*. Academic Press, NY: 1963.
72. Hoppel, M.; Ettl, H.; Holper, E.; Valenta, C., *Int J Pharm* **2014**, 475 (1-2), 156-162.
73. Lee, J.-J.; Park, J.-H.; Lee, J.-Y.; Jeong, J. Y.; Lee, S. Y.; Yoon, I.-S.; Kang, W.-S.; Kim, D.-D.; Cho, H.-J., *Colloids Surf B Biointerfaces* **2016**, 140, 239-245.
74. Walker, R.; Decker, E. A.; McClements, D. J., *Food Func* **2015**, 6 (1), 41-54.
75. Huber, G. M.; Vasantha Rupasinghe, H. P.; Shahidi, F., *Food Chem* **2009**, 117 (2), 290-295.

76. Lidich, N.; Aserin, A.; Garti, N., *J Colloid Interface Sci* **2016**, *463*, 83-92.
77. Gulotta, A.; Saberi, A. H.; Nicoli, M. C.; McClements, D. J., *J Agric Food Chem* **2014**, *62* (7), 1720-1725.
78. Hazemoto, N.; Harada, M.; Komatsubara, N.; Haga, M.; Kato, Y., *Chem. Pharm. Bull.* **1990**, *38* (3), 748-751.
79. Duzgunes, N.; Straubinger, R. M.; Baldwin, P. A.; Friend, D. S.; Papahadjopoulos, D., *Biochemistry* **1985**, *24* (13), 3091-3098.
80. Douliez, J.-P.; Houssou, B. H.; Fameau, A. L.; Navailles, L.; Nallet, F.; Grélard, A.; Dufourc, E. J.; Gaillard, C., *Langmuir* **2016**, *32* (2), 401-410.
81. Douliez, J.-P., *Langmuir* **2004**, *20* (5), 1543-1550.
82. Novales, B.; Navailles, L.; Axelos, M.; Nallet, F.; Douliez, J.-P., *Langmuir* **2007**, *24* (1), 62-68.
83. Xu, W.; Song, A.; Dong, S.; Chen, J.; Hao, J., *Langmuir* **2013**, *29* (40), 12380-12388.
84. Dejanović, B.; Noethig-Laslo, V.; Šentjerc, M.; Walde, P., *Chem Phys Lipids* **2011**, *164* (1), 83-88.
85. Morrow, B. H.; Koenig, P. H.; Shen, J. K., *Langmuir* **2013**, *29* (48), 14823-14830.
86. Klein, R.; Touraud, D.; Kunz, W., *Green Chem* **2008**, *10* (4), 433-435.
87. Calder, P. C.; Deckelbaum, R. J., *Curr Opin Clin Nutr Metab Care* **2008**, *11* (2), 91-93.
88. Lorente-Cebrián, S.; Costa, A. V.; Navas-Carretero, S.; Zabala, M.; Laiglesia, L.; Martínez, J. A.; Moreno-Aliaga, M., *J Physiol Biochem* **2015**, *71* (2), 341-349.
89. Kuratko, C.; Nolan, C.; Salem, N., Jr., *Nutrafoods* **2014**, *13* (2), 49-60.
90. Calder, P. C., *Eur J Lipid Sci Technol* **2014**, *116* (10), 1280-1300.
91. Brenna, J. T.; Carlson, S. E., *J Hum Evol* **2014**, *77* (0), 99-106.
92. Elmadfa, I.; Kornsteiner, M., *Ann Nutr Metab* **2009**, *55* (1-3), 56-75.
93. Calder, P. C., *Schweiz Z Ernährungsmed* **2008**, *5*, 23-28.
94. Calder, P. C., *Mol Nutr Food Res* **2008**, *52* (8), 885-97.
95. Calder, P. C. *Omega-3 Fatty Acids: The good Oil?*; Institute Danone: Brussel, 2008.
96. Ackman, R. G., Fish Oils. In *Bailey's Industrial Oil and Fat Products*, John Wiley & Sons, Inc.: 2005.

97. Finley John, W.; Shahidi, F., The Chemistry, Processing, and Health Benefits of Highly Unsaturated Fatty Acids: An Overview. In *Omega-3 Fatty Acids*, Shahidi, F.; Finley John, W., Eds. American Chemical Society: 2001; Vol. 788, pp 2-11.
98. Bell, M. V.; Henderson, R. J.; Sargent, J. R., *Comp Biochem Physiol B* **1986**, 83 (4), 711-719.
99. Namani, T.; Ishikawa, T.; Morigaki, K.; Walde, P., *Colloids Surf B Biointerfaces* **2007**, 54 (1), 118-123.
100. Zeisel, S. H.; da Costa, K. A., *Nutr Rev* **2009**, 67 (11), 615-23.
101. Zeisel, S. H., *Annu Rev Nutr* **2006**, 26, 229-50.
102. Blusztajn, J. K., *Science* **1998**, 281 (5378), 794-795.
103. Yu, Y.; Zhao, J.; Bayly, A. E., *Chin J Chem Eng* **2008**, 16 (4), 517-527.
104. Harkins, W. D.; Jordan, H. F., *J Am Chem Soc* **1930**, 52 (5), 1751-1772.

## **Chapter 4 Choline and beta-methylcholine as counter ion for long chain alkyl sulfates**

### **4.1 Abstract**

Compared to classical sodium soaps, sodium alkyl sulfates show some significant advantages being important in many formulations. They are less salt sensitive and the highly acidic sulfate head group leads to aqueous solutions around neutral pH value.<sup>1</sup> However, long chain sodium alkyl sulfates still exhibit a high Krafft temperature  $T_{Kr}$ . It was shown that choosing choline as counter ion for dodecyl sulfate and hexadecyl sulfate significantly decreases  $T_{Kr}$  of these surfactants while simultaneously keeping them low toxic and ready biodegradable.<sup>1, 2</sup>

In the present study, choline and beta-methylcholine dodecyl sulfate, hexadecyl sulfate and octadecyl sulfate were prepared by ion exchange. Their  $T_{Kr}$  values, cmc values as well as other physico-chemical parameters were determined by solubility, surface tension and conductivity measurements and compared to the ones of their sodium homologues.

It was found that both choline and beta-methyl choline alkyl sulfates exhibit much lower  $T_{Kr}$  and slightly lower cmc values than their sodium homologues with beta-methylcholine being a bit more effective than choline. Finally, it will be shown that choline and beta-methylcholine octadecyl sulfate possess a temperature and concentration dependent solubility behavior that is completely different from the one of sodium octadecyl sulfate and incompatible with the commonly found Krafft phenomena for surfactant solutions.

### **4.2 Introduction**

Sodium dodecyl sulfate (NaS12) is a common low cost alkyl sulfate surfactant that is often used as a reference substance in many physicochemical and chemical determinations. This is because NaS12 can be obtained with a purity close to 100 %, shows outstanding surfactant properties and is well water soluble at 25 °C.<sup>3, 4</sup> Compared to classical soap surfactants, alkyl sulfates possess two distinct advantages: their aqueous solutions exhibit a pH value close to neutral and they are

less sensitive to water hardness or alkali ions.<sup>1, 3</sup> Moreover, alkyl sulfates are also readily biodegradable in aerobic and anaerobic conditions, low toxic and can be fully synthesized from renewable raw materials.<sup>3-5</sup> That explains why NaS12 is widely used in personal care products (e.g. toothpastes, shampoos or synthetic soaps) or in detergents and manual dishwash formulations.<sup>4, 6</sup>

Although longer chain homologues of NaS12 show an increased interfacial activity and detergency power as well as lower cmc values, their use in aqueous applications is restricted by their poor solubility in water at room temperature.<sup>3, 4, 7</sup> An important feature to evaluate the solubility of surfactants in water is the Krafft temperature ( $T_{Kr}$ ). At this temperature, the solubility curve of the surfactant monomers in solution intersects the critical micellar concentration (cmc) curve, and the total surfactant solubility rises strongly with temperature caused by the formation of micelles.<sup>8</sup> In general, it is necessary that the surfactant is used above its  $T_{Kr}$  and at or above its cmc. In agreement with the common convention, the Krafft temperatures ( $T_{Kr}$ ) are usually taken as the clearing temperature of a 1 wt% aqueous surfactant solution.<sup>9</sup> The 1 % Krafft temperature ( $T_{Kr}$ ) of sodium dodecyl sulfate (NaS12) was found to be 16 °C, the ones sodium tetradecyl sulfate (NaS14), sodium hexadecyl sulfate (NaS16) and sodium octadecyl sulfate (NaS18) were found to be above room temperature, namely 30 °C, 45 °C and 56 °C.<sup>10</sup>

About 25 years ago, Yu et al.<sup>11, 12</sup> showed that using tetrabutylammonium as counter ion of tetradecyl sulfate (TBAS14) and octadecyl sulfate (TBAS18) decreases  $T_{Kr}$  of these surfactants below room temperature. Similar results were found when using symmetrical tetraalkylammonium ions (TAAs) as counter ions for long chain soaps.<sup>13</sup> However, despite the general ability of TAAs to reduce  $T_{Kr}$  of longer-chain and more surface active surfactants, they cannot be used in household products because of their well-known toxicity.<sup>14-18</sup> Our group could show that same  $T_{Kr}$  reducing effect can be achieved by using choline, a quaternary ammonium ion of biological origin. Choline is classified as an essential nutrient for humans and acts as a precursor for many important molecules in the human metabolism.<sup>1, 19, 20</sup>  $T_{Kr}$  of choline alkyl sulfates and choline soaps were found to be below room temperature up to a surfactant chain length of 16 Carbon atoms.<sup>2, 19</sup> Further, these surfactants show a low cytotoxicity similar to their corresponding sodium equivalents and are readily biodegradable.<sup>1, 21</sup>

According to Collins' concept of "matching water affinities"<sup>22, 23</sup> and the corresponding classification of surfactant head groups<sup>24</sup>, for alkyl sulfates counter ion-head group interactions are meant to increase with increasing size of the cation ( $Li^+ < Na^+ < K^+ < Rb^+ < Cs^+ < TAA^+$ ). This has been confirmed by a combined SANS

and SAXS study for alkali dodecyl sulfates.<sup>25</sup> Usually, stronger counter ion-head group interactions result in higher  $T_{Kr}$  and lower cmc values because of a lower effective charge at the surfactant head group caused by the reduced counter ion-head group dissociation.<sup>1</sup> The cmc values for dodecyl sulfate show exactly the predicted behavior and decrease with increasing size of the counter ion in the way  $Na^+ > K^+ > Cs^+ > TMA^+ > TEA^+ > TPrA^+ > TBA^+$ .<sup>26, 27</sup> Concerning  $T_{Kr}$ , the predicted increase with growing counter ion size is only valid for alkali alkyl sulfates.<sup>1, 28</sup> As already mentioned, TAA alkyl sulfates possess considerably lower  $T_{Kr}$  values than their corresponding sodium or potassium alkyl sulfates. This is contradictory to the above stated prediction based on Collins' concept of "matching water affinities". However, these findings can be explained by the bulkiness of the TAAs compared to simple alkali ions making the solid crystalline state energetically less favorable and thus promoting surfactant solubility in water.<sup>1, 19, 29</sup>

In this part of the work, choline (Ch) and beta-methylcholine (MeCh) dodecyl sulfate (S12), hexadecyl sulfate (S16) and octadecyl sulfate (S18) were synthesized. The molecular structures of these molecules are shown in **Figure 4-1**. It must be noted that ChS12 and ChS16 were already characterized by Klein et al.<sup>1</sup> and Rengstl<sup>2</sup>. However, to allow better comparison of the counter ion dependence of the surfactants' physico-chemical properties, which can be affected by impurities or experimental procedure, it was necessary to prepare Ch and MeCh surfactants from the same sodium alkyl sulfate starting material and to analyze them identically. Different physico-chemical properties were determined by temperature dependent turbidity measurements and concentration dependent surface tension, respectively conductivity measurements. MeCh is very interesting as counter ion because of three reasons: like Ch, it should be less toxic than simple TAAs, since it was identified in some flies and in rats as the decarboxylation product of carnitine.<sup>30</sup> Further, it is already commercially available, since it is an intermediate in the synthesis of the drug Methacholine (acetyl-beta-methylcholine).<sup>31</sup> And finally, it was possible to investigate the influence of an additional methyl group in the counter ion on the physico-chemical properties of the resulting surfactant with regard to bulkiness and hydrophobicity of the counter ion.

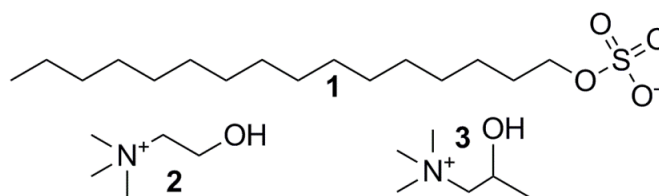


**Figure 4-1:** The molecular structures of an alkyl sulfate (1), choline (2) and beta-methylcholine (3).

The results will be compared to common sodium alkyl sulfates and discussed with the help of Collins` concept of "matching water affinities"<sup>23</sup>, the bulkiness of the counter ions and mixed micellization between alkyl sulfates and organic counter ions.

At the end of this chapter, unusual differences in appearance between NaS18 and ChS18, respectively MeChS18 observed in temperature and concentration dependent solubility measurements will be addressed.

## 4.3 Results and discussion

First,  $T_{Kr}$ , cmc and the micelle ionization degree  $\alpha$  will be discussed in detail followed by other physico-chemical parameters derived from concentration dependent surface tension measurements, which will be surface excess concentration  $\Gamma$ , area per molecule at the surface  $A$ , efficiency of surface tension reduction  $pC_{20}$  and effectiveness in surface tension reduction  $\gamma_{cmc}$ .

The last part points out the differences in temperature and concentration dependent solubility behavior between NaS18 and ChS18/MeChS18.

### 4.3.1 Krafft temperature

The solubility of surfactants is dramatically temperature dependent and increases heavily in a narrow temperature range. This is called the "Krafft phenomenon".<sup>8, 9</sup> In agreement with the common convention, the Krafft temperatures ( $T_{Kr}$ ) were taken as the clearing temperature of a 1 wt% aqueous surfactant solution.<sup>9</sup>

$T_{Kr}$  is determined by the interplay of two opposing thermodynamic forces. These are the free energy of the micellar surfactant solution and the free energy of the solid crystalline state of the surfactant. The free energy of the micellar solution seems only to vary little for different surfactant chain lengths or counter ions. However, the solid crystalline state can vary drastically.<sup>29</sup> Strong head group-counter ion interactions as well as the possibility of an effective packing of the surfactant in a crystal lattice lead to low free energies of the solid crystalline state. As a result,  $T_{Kr}$  is shifted to higher temperatures.<sup>19</sup> Common strategies to increase the free energy of the solid state and therefore  $T_{Kr}$  are: branching of the alkyl chain, introduction of a double bond in the alkyl chain, introduction of a polar segment between alkyl chain and the headgroup as well as changing the counter ion.<sup>29</sup>

The effect of changing the counter ion from sodium (Na) to choline (Ch) or beta-methylcholine (MeCh) for alkyl sulfates is shown in **Figure 4-2**. The measured

values for NaS16 (44 °C) and NaS18 (58 °C) agree very well with the ones reported in literature.<sup>4</sup> It is obvious that both Ch and MeCh have a strong  $T_{Kr}$  reducing effect, which is markedly below room temperature up to S16 (ChS16 = 13 °C; MeChS16 = 7 °C). The measured  $T_{Kr}$  value for ChS16 is slightly lower than the one reported by Rengstl<sup>2</sup>. Compared to Na alkyl sulfates, for which  $T_{Kr}$  increases linearly with the surfactant hydrophobic chain length, a much steeper increase is found from S16 to S18 than from S12 to S16 for Ch and MeCh alkyl sulfates (ChS18 = 49 °C; MeChS18 = 44 °C).  $T_{Kr}$  values for ChS12 and MeChS12 are identical (2 °C). Possibly, these values are even lower, but 2 °C is the lowest temperature that can be measured by the turbidity apparatus. It represents the temperature, at which the samples melt and can become transparent.

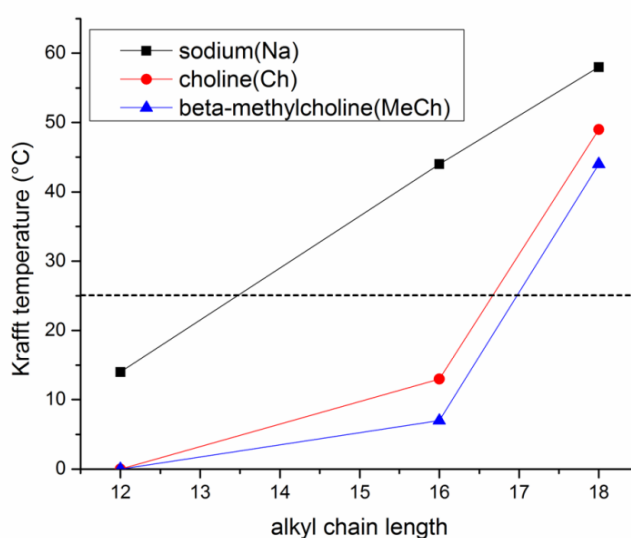


**Figure 4-2:** Comparison of the Krafft temperatures of sodium(■), choline(●) and beta-methylcholine(▲) alkyl sulfates with a Carbon atom chain length of 12, 16 and 18. The value for NaS12 is taken from reference 1. The dashed horizontal line represents room temperature (25 °C).

Lower  $T_{Kr}$  values of Ch and MeCh alkyl sulfates compared to their Na homologues can be attributed to the unsymmetrical and bulky structure of the organic Ch and MeCh ions, which hinders the formation of a regular crystalline packing and thereby decrease  $T_{Kr}$ . Weakly higher  $T_{Kr}$  values when using Ch as counter ion to alkyl sulfates instead of the slightly more bulky MeCh support this explanation. The same behavior was found for simple symmetrical TAAs.<sup>11, 26, 32</sup>

### 4.3.2 Critical micellar concentration (cmc)

The critical micellar concentration of Ch and MeCh alkyl sulfates were obtained by two different methods, concentration dependent conductivity and concentration

dependent surface tension measurements. In general, low cmc values are desired, since a decrease in the cmc value usually reflects an increase in surface activity of the surfactant and lower amounts of surfactant are necessary to achieve the desired effect. Moreover, low cmc values are also wanted, if solubilization of water-insoluble molecules by surfactants is addressed.

The cmc values of ChSXX and MeChSXX obtained by surface tension<sup>a</sup> and conductivity<sup>b</sup> measurements as well as the micelle ionization degree  $\alpha$  calculated from conductivity measurements are listed in **Table 4-1**. For comparison reasons, values for NaSXX found in literature are also listed.

Surfactant	CMC <sup>a</sup> [mM]	CMC <sup>b</sup> [mM]	$\alpha$
<b>ChS12</b>	4.67 ± 0.03 (25°C)	5.99 ± 0.06 (25°C) <sup>1</sup>	0.25 (25°C) <sup>1</sup>
<b>ChS16</b>	0.323 ± 0.002 (25°C) / 0.40 ± 0.03 (40°C) <sup>2</sup>	0.334 ± 0.021 (25°C) / 0.44 ± 0.01 (40°C) <sup>2</sup>	0.25 ± 0.01 (25°C) 0.24 (40°C) <sup>2</sup>
<b>ChS18</b>	0.092 ± 0.000 (25°C) / 0.098 ± 0.001 (40°C)	0.126 ± 0.001 (50°C)	0.29 ± 0.01 (50°C)
<b>MeChS12</b>	3.84 ± 0.09 (25°C)	4.91 ± 0.01 (25°C)	0.24 ± 0.00 (25°C)
<b>MeChS16</b>	0.289 ± 0.003 (25°C)	0.299 ± 0.001 (25°C)	0.25 ± 0.00 (25°C)
<b>MeChS18</b>	0.089 ± 0.004 (40°C)	0.105 ± 0.003 (50°C)	0.31 ± 0.01 (50°C)
<b>NaS12</b>	6.77 ± 0.10 (25°C)	8.65 (40°C) <sup>33</sup>	0.23 (25°C) <sup>26</sup>
<b>NaS16</b>	0.6 (45°C) <sup>34</sup>	0.58 (40°C) <sup>33</sup>	0.21 (40°C) <sup>33</sup>
<b>NaS18</b>	0.17 (60°C) <sup>35</sup>	0.17 (50°C) <sup>36</sup>	0.33 (40°C) <sup>33</sup>

**Table 4-1:** Critical micellar concentration and micelle ionization degree  $\alpha$  of choline and beta-methylcholine alkyl sulfates at different temperatures in comparison to respective sodium alkyl sulfates. The values were obtained by surface tension<sup>a</sup> and conductivity<sup>b</sup> measurements or taken from literature.

The cmc values of ChSXX and MeChSXX determined by surface tension measurements are always slightly lower than the ones obtained from conductivity measurements. The fact that different methods yield weakly different cmc values for identical systems is well-known in literature and thus an expected result.<sup>37</sup> Further, the cmc values of ChSXX and MeChSXX slightly increase by increasing the temperature from 25 °C to 40 or 50°C. This is also known from literature, where a minimum in the cmc of ionic surfactants is often observed around room temperature.<sup>29, 38</sup> The fact that it was possible to measure the cmc of ChS18 at 25 °C well below the 1 wt% Krafft-temperature will be discussed in detail in section 4.3.4.

For identical alkyl sulfate chain length, independently from the determination method, the cmc is always found to decrease in the order: Na<sup>+</sup> > Ch<sup>+</sup> > MeCh<sup>+</sup>. The measured values for ChS12 and ChS16 at 25 °C are in good agreement with the ones determined by Klein et al.<sup>1</sup> and Rengstl<sup>2</sup>. Changing the counter ion from Ch to MeCh, i.e. introducing an additional methyl group and increasing the hydrophobic/chaotropic nature, reduces the cmc values by about 18 % for S12, about 10 % for S16 and about 15 % for S18 (see **Table 4-1**). Comparing the

obtained cmc values for ChS12 and MeChS12 to the ones reported in literature for TMAS12 ( $\approx 5.5$  mM by conductivity<sup>26</sup>) suggests that the additional hydroxy group has no significant influence on the cmc value.

The logarithm of the cmc is known to vary linearly with the surfactant's chain length and decreases with increasing number of Carbon atoms  $n$  (see section 2.1.5.1).

$$\log(\text{cmc}) = A - Bn \quad (4-1)$$

Taking into account the cmc values (in mol/l) for ChSXX and MeChSXX derived from surface tension measurements at 25 °C (for MeChS18, with regard to the temperature dependence of the cmc value of ChS18, 95 % of the cmc value at 40 °C were used for linerization), the following equations were obtained:

$$\text{Choline:} \quad \log(\text{cmc}) = 1.09 - 0.29n \quad (4-2)$$

$$\text{Beta-methylcholine:} \quad \log(\text{cmc}) = 0.90 - 0.28n \quad (4-3)$$

Literature values for NaSXX at 25 °C are 0.3 for B and 1.51 for A. Nearly identical B values for Na<sup>+</sup>, Ch<sup>+</sup> and MeCh<sup>+</sup> illustrate the common observation that the cmc decreases by a factor of 2 with each additional methylene group in the hydrocarbon chain. The decrease in the A values in the order Na<sup>+</sup> > Ch<sup>+</sup> > MeCh<sup>+</sup> demonstrates the decrease in the cmc value for a given surfactant chain length in the same order. Studies from literature show the same trend as found in this study. The cmc decreases with increasing size/chaotropic nature of the counter ion the following way: Li<sup>+</sup> > Na<sup>+</sup> > K<sup>+</sup> > Cs<sup>+</sup> > TMA<sup>+</sup> > TEA<sup>+</sup> > TPrA<sup>+</sup> > TBA<sup>+</sup>.<sup>26, 27</sup> This is perfectly in line with Collins' concept of "matching water affinities".<sup>23, 24</sup> For the chaotropic alkyl sulfate head group, it predicts stronger counter ion-head group interactions, and therefore lower cmc values, with increasing chaotropic nature of the counter ion.

However, values of the micelle ionization degree  $\alpha$  suggest that counter ion binding of Na<sup>+</sup> and Ch<sup>+</sup> or MeCh<sup>+</sup> is quite similar. The obtained values for ChS12 and MeChS12 are a bit higher than the ones determined by Benrraou et al.<sup>26</sup>, who found  $\alpha$  values about 0.2 for TAAS12 varying from TMA<sup>+</sup> until TBA<sup>+</sup>. For ChSXX and MeChSXX,  $\alpha$  values are identical within the experimental error independently from the surfactant's chain length. While  $\alpha$  values remain constant for S12 and S16, a marked increase is found from S16 to S18. The same behavior is found for Na<sup>+</sup> (see **Table 2-1**). Compared to their sodium homologues,  $\alpha$  values for Ch/MeChS12 and

Ch/MeChS16 are slightly higher, whereas for S18 the situation is reversed. This is clearly in contrast to the change in the cmc values.

Whether TAAs bound more strongly to alkyl sulfate micelles than simple Na ions, as predicted by Collins' concept and indicated by the measured cmc values, has been the subject of some discussions.<sup>1</sup> Data on the micelle ionization degree  $\alpha$  of TAA alkyl sulfates from SANS measurements<sup>39, 40</sup>, conductivity measurements<sup>1, 26</sup> and molecular dynamic studies<sup>41</sup> suggest that the counter ion binding of sodium and TAAs to alkyl sulfate micelles is quite similar. The results from this study support these findings. According to these results, it is reasonable to explain the lower cmc values of TAAs alkyl sulfates compared to alkali alkyl sulfates mainly by mixed micellization instead of Collins' concept.<sup>12, 26, 41-43</sup> In 2016, Wei et al.<sup>44</sup> also showed mixed micellization for ChS12 applying molecular dynamics simulations. The cmc-reducing effect of TAAs by mixed micellization can be explained as follows: due to the presence of hydrophobic moieties in TAAs, not only specific ion interactions but also hydrophobic interactions have to be considered. Therefore, TAAs exhibit a tendency to interact with the water exposed hydrophobic areas of the micelle as well as to penetrate into the hydrophobic interior of the alkyl sulfate micelle. Of course, stronger head group-counter ion interactions, as predicted by Collins concept, can support this process. Consequently, TAAs tend to separate the ionic head groups and simultaneously reduce the repulsive electrostatic interactions between them. This effect favors the formation of micelles, as can be seen for example by the addition of alcohols or non-ionic surfactants to ionic ones.<sup>45-47</sup> As expected, the bigger the hydrophobic moiety of the TAA, the lower the cmc<sup>26, 27</sup> due to a higher tendency of the alkyl chains to penetrate into the micelle. This hypothesis of mixed micellization is supported by the fact that cmc values also markedly decrease for dodecanoate surfactants when going from TMA to TBA.<sup>48</sup> Collins' concept would predict weaker interactions between the kosmotropic carboxylat head group and the chaotropic TAAs with increasing hydrophobicity and therefore higher cmc values. Further, TBA as counter ion for myristate, palmitate and stearate yields lower cmc values than for identical sodium soaps.<sup>37, 49</sup> This is also contradictory to Collins' concept.

#### **4.3.3 Other physico-chemical properties derived from cmc measurements ( $\Gamma$ , $A$ , $pC_{20}$ , $\gamma_{cmc}$ )**

Further, the surface excess concentration  $\Gamma$ , the area per molecule at the surface  $A$  as well as the efficiency and the effectiveness of surface tension reduction were

derived from surface tension data and are listed in **Table 4-2**. The efficiency in surface tension reduction is calculated with the surfactant concentration necessary to decrease the surface tension of water  $\gamma_0$  by 20 mN/m and given as the  $pC_{20}$  value, the effectiveness is reflected by the surface tension value at the cmc  $\gamma_{cmc}$ . Values for NaS16 found in literature are listed for comparison reasons. It should be mentioned that the change in surface tension with time before taking the  $\gamma$  value at a certain concentration always was  $< 0.05 \text{ mNm}^{-1}\text{min}^{-1}$ . Thus, the calculated parameters should all be very close to thermodynamic equilibrium values.

Surfactant	$\Gamma \cdot 10^6 [\text{mol/m}^2]$	$A [\text{\AA}^2]$	$pC_{20}$	$\gamma_{cmc} [\text{mN/m}]$
<b>ChS12</b>	$2.79 \pm 0.01 (25^\circ\text{C})$	$59.52 \pm 0.23 (25^\circ\text{C})$	$2.68 (25^\circ\text{C})$	$40.85 (25^\circ\text{C})$
<b>ChS16</b>	$3.02 \pm 0.03 (25^\circ\text{C})$	$55.03 \pm 0.57 (25^\circ\text{C})$	$3.82 (25^\circ\text{C})$	$40.83 (25^\circ\text{C})$
<b>ChS18</b>	$2.49 \pm 0.05 (25^\circ\text{C})$	$66.63 \pm 1.23 (25^\circ\text{C})$	$4.36 (25^\circ\text{C})$	$42.89 (25^\circ\text{C})$
	$3.08 \pm 0.03 (40^\circ\text{C})$	$53.89 \pm 0.57 (40^\circ\text{C})$	$4.36 (40^\circ\text{C})$	$39.60 (40^\circ\text{C})$
<b>MeChS12</b>	$2.64 \pm 0.07 (25^\circ\text{C})$	$63.00 \pm 1.64 (25^\circ\text{C})$	$2.83 (25^\circ\text{C})$	$39.65 (25^\circ\text{C})$
<b>MeChS16</b>	$2.87 \pm 0.03 (25^\circ\text{C})$	$57.90 \pm 0.67 (25^\circ\text{C})$	$3.90 (25^\circ\text{C})$	$40.40 (25^\circ\text{C})$
<b>MeChS18</b>	$2.98 \pm 0.07 (40^\circ\text{C})$	$55.77 \pm 1.38 (40^\circ\text{C})$	$4.45 (40^\circ\text{C})$	$38.20 (40^\circ\text{C})$
<b>NaS12</b>	$3.54 \pm 0.09 (25^\circ\text{C})$	$46.94 \pm 1.21 (25^\circ\text{C})$	$2.50 (25^\circ\text{C})$	$37.64 (25^\circ\text{C})$
<b>NaS16</b>	$3.3 (60^\circ\text{C})^{50}$	$50.3 (60^\circ\text{C})^{50}$	$3.70 (25^\circ\text{C})^{50}$	$37 (60^\circ\text{C})^{50}$

**Table 4-2:** Surface excess concentration  $\Gamma$ , area per molecule at the surface  $A$ , efficiency of surface tension reduction  $pC_{20}$  and effectiveness in surface tension reduction  $\gamma_{cmc}$  of choline and beta-methylcholine alkyl sulfates at different temperatures in comparison to respective sodium alkyl sulfates. The values were obtained from surface tension measurements or taken from literature.

The area per molecule at the surface  $A$  and the surface excess concentration are inversely proportional. So discussing the  $A$  values is sufficient.

$A$  values of ChSXX are always a bit lower ( $\approx 3 \text{ \AA}^2$ ) than the values obtained for MeChSXX. Probably, this is due to the additional methyl group in MeCh. The effectiveness in surface tension reduction was more or less equal with MeCh alkyl sulfates exhibiting slightly smaller  $\gamma_{cmc}$  values ( $\approx 1 \text{ mN/m}$ ). The  $\gamma_{cmc}$  values obtained for ChS12 and ChS16 match perfectly the values reported by Rengstl<sup>2</sup>. Increasing the alkyl sulfate chain length from 12 to 16, for both Ch and MeCh the value of  $A$  slightly decreases. Minor effects on  $A$  when increasing the saturated surfactant chain from 10 to 16 carbon atoms are known from literature.<sup>51</sup> An interesting result can be seen when comparing the  $A$  values of ChS18 at 25 and 40 °C. The  $A$  value at 25 °C is considerably larger ( $\approx 13 \text{ \AA}^2$ ) than the one at 40 °C. In parallel,  $\gamma_{cmc}$  is increased by 3 mN/m. The same results were obtained for S18 with ethoxylated choline as counter ion (see section 6.3.1.2). In contrast, Rengstl<sup>2</sup> obtained nearly identical  $A$  and  $\gamma_{cmc}$  values at 25 and 40 °C for ChS16. Thus, the strong temperature dependence of  $A$  can be attributed to the nature of the S18 chain. The increase in  $A$  when increasing the number of Carbon atoms from 16 to 18 in the straight surfactant

chain is known in literature. It was explained by coiling of the C18-hydrophobic chain that consequently causes larger  $A$  values.<sup>51</sup> Possibly, for ChS18 these coiling effects disappear by increasing the temperature from 25 to 40 °C leading to  $A$  values that would be expected with respect to the results of ChS12 and ChS16. The  $A$  and  $\gamma_{cmc}$  values obtained for NaS12 are markedly lower ( $\approx 14 \text{ \AA}^2$  and 3 mN/m) than the ones of ChS12 or MeChS12. This can be explained by the smaller Na ion compared to the two bulky organic ions allowing a closer packing of the surfactant molecules at the surface. Values from literature for NaS16, although measured at 60 °C, show the same trend when compared to ChS16 and MeChS16.<sup>50</sup> Mitra et al.<sup>43</sup> measured considerably higher  $A$  values for TPrAS12 ( $120 \text{ \AA}^2$ ) and TBAS12 ( $93 \text{ \AA}^2$ ) as well as considerably lower  $\gamma_{cmc}$  values (31.9 mN/m respectively 32.5 mN/m). These results show that the counter ions have a strong influence on the surface tension reduction, since for identical surfactants larger  $A$  values, i.e. less tight packing at the interface, should lead to higher  $\gamma_{cmc}$  values.

The larger the  $pC_{20}$  value, the more efficiently the surfactant reduces the surface tension of the aqueous solutions, i.e. the more surface active the surfactant is. Usually, the efficiency in surface tension reduction rises with increasing hydrophobic character of the surfactant chain and can be directly related to the standard free energy of transfer of the surfactant chain from bulk to the surface. For a given surfactant, this yields a linear relationship between efficiency, i.e.  $pC_{20}$ , and the number of Carbon atoms in the straight surfactant chain (compare to cmc).<sup>51, 52</sup> The  $pC_{20}$  values of the investigated ChSXX and MeChSXX are completely in line with these general findings. For both ChSXX and MeChSXX,  $pC_{20}$  values increase with increasing surfactant chain length from S12 to S18. Further, plotting  $pC_{20}$  values against the surfactant chain length leads to perfect straight lines for both ChSXX and MeChSXX. Identical  $pC_{20}$  for ChS18 at 25 and 40°C suggest that the efficiency in surface tension reduction is hardly temperature-dependent. For a given alkyl sulfate chain length, the efficiency in surface tension reduction ( $pC_{20}$  value) decreases in the order  $\text{MeCh}^+ > \text{Ch}^+ > \text{Na}^+$ . This reflects the decline in cmc values from MeChSXX to NaSXX and the accompanied shift of the concentration dependent surface tension curves to lower surfactant concentrations.

#### 4.3.4 Differences in phase behavior between NaS18 and ChS18/MeChS18

$T_{Kr}$  values presented in section 4.3.1 correspond to the temperature, at which the 1 wt% aqueous surfactant solution became as clear as water. The typical temperature

dependent solubility behavior of surfactants in water shows a strong increase in surfactant solubility as soon as micelles are formed (see section 2.1.5.3, **Figure 2-9**). Therefore, for concentrations above the surfactant's cmc, values of  $T_{Kr}$  determined by solubility experiments should only rise slightly within a broad concentration range. For simple alkali and alkaline earth alkyl sulfates in aqueous solutions, this was proven by measuring temperature-dependent solubility curves.<sup>28, 53, 54</sup> In such systems, the amount of surfactant exceeding the solubility limit precipitates as hydrated crystals.<sup>55, 56</sup>

During the work with NaS18, ChS18 and MeChS18, it became obvious that only NaS18 behaves as it would be expected from the statements above. Although, for all of the surfactants a 1 wt% aqueous solution was nontransparent turbid at room temperature, significant differences in the macroscopic and microscopic appearance were observed. Further, the change in macroscopic appearance during heating, i.e. the curves obtained by turbidity measurements, was completely different for NaS18 compared to ChS18/MeChS18. In the following, these differences will be shown and a possible explanation for the observed behavior will be given.

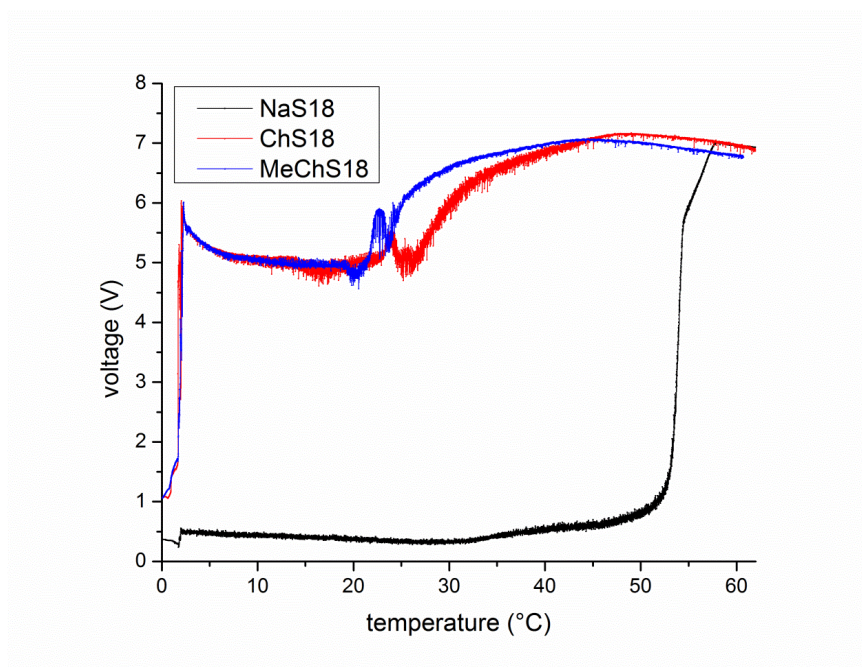


**Figure 4-3:** Comparison of the turbidity curves of NaS18, ChS18 and MeChS18 measured by a home-built apparatus. The transmittance of the samples, measured as the voltage  $V$ , is plotted against the temperature.

The curves obtained from turbidity measurements are shown in **Figure 4-3**. All samples were frozen at  $-20\text{ }^{\circ}\text{C}$  before starting a measurement. The temperature was increased with about  $1.5\text{ }^{\circ}\text{C/h}$  and the transmittance was measured. The maximum

of the curves which is found around 7, was taken as the 1 wt %  $T_{Kr}$  presented in **Figure 4-2**.

**Figure 4-3** illustrates the differences in the turbidity curves between NaS18 and ChS18/MeChS18. The transmittance of the NaS18 sample is very low up to a few degrees before the maximum is reached and the rise is very steep and within a few degrees. This behavior is expected from solubility measurements of alkali and alkaline earth alkyl sulfates.<sup>4, 28, 53, 54</sup> Close to the temperature, at which the steep increase sets in, the monomer surfactant solubility should be equal to the surfactant's cmc. As expected, turbidity curves measured for NaS16 showed exactly the same course.

However, the curves obtained for ChS18 and MeChS18 are completely different. They exhibit considerable transmittance after melting of the samples ( $\approx 2\text{ }^{\circ}\text{C}$ ), which remains constant until it rises over a broad temperature range ( $\approx 25\text{ }^{\circ}\text{C}$ ). After a quite steep increase within the first degrees, the curve levels off and rises slightly until the maximum is reached. Compared to ChS18, the curve for MeChS18 is shifted about  $5\text{ }^{\circ}\text{C}$  to lower temperatures resulting in lower a 1 wt%  $T_{Kr}$  (see **Figure 4-2**). The same course is found for the turbidity curve of ChS16 only exhibiting  $T_{Kr}$  well below room temperature. Probably, this behavior is not observed for MeChS16, since  $T_{Kr}$  ( $6\text{ }^{\circ}\text{C}$ ) is just too close to the melting temperature of the sample. This long and slow decrease in transmittance for an aqueous 1 wt% surfactant solution is in contrast to the common temperature dependent solubility behavior of surfactants as reflected by the curve measured for NaS18.

Observations made during heating experiments in a water bath ( $\approx 5\text{ }^{\circ}\text{C}/\text{min}$ ) are in perfect agreement with the measured turbidity curves. After melting of the samples, the 1wt% NaS18 solution was turbid, white with big solid particles and exhibited a normal viscosity. Samples of 1 wt% ChS18 and MeChS18, however, were turbid without visible particles and showed an increased viscosity. During slewing, the samples were inhomogeneous and showed some streaks. As indicated by the curves in **Figure 4-3**, the NaS18 sample kept its appearance over a broad temperature range and quickly cleared within a few degrees. The ChS18 and MeChS18 samples kept their appearance up to 27, respectively 23  $^{\circ}\text{C}$ . Then, they got more and more translucent with increasing temperature. 10-15  $^{\circ}\text{C}$  before the samples were as clear as water, they already appeared homogeneously bluish and translucent.

The appearance of 1 wt% NaS18 and ChS18 aqueous solutions after stirring over night at  $25\text{ }^{\circ}\text{C}$  are shown in **Figure 4-4**. Picture A illustrates the turbid-white appearance of the 1 wt% NaS18 as well as solid particles at the surface. The ChS18

sample shows no such particles and appears more turbid-gray than white. Photo B was taken between crossed polarizers and clearly shows some birefringent areas for the ChS18 solution, while the NaS18 solution appears homogeneously turbid again with particles at the surface. It was not possible to analyze the birefringent samples with a polarizing optical microscopy. This is a known phenomena, since the intensity of birefringence is dependent of sample thickness. For low-concentrated solutions with weakly birefringent liquid crystals, birefringence may be clearly visible in samples with about 1 cm thickness, but not in samples being a few microns thick as it is the case in the microscope.<sup>57</sup> In contrast, for NaS18 samples, well defined and birefringent crystals were observed. After several days of aging, a phase separation took place in both samples. In the NaS18 sample, lots of solid particles were present at the bottom and the surface of the sample. The ChS18 sample, however, separated into a clear aqueous upper phase and a lower sponge-like and birefringent phase (see **Figure 4-4**, picture C).

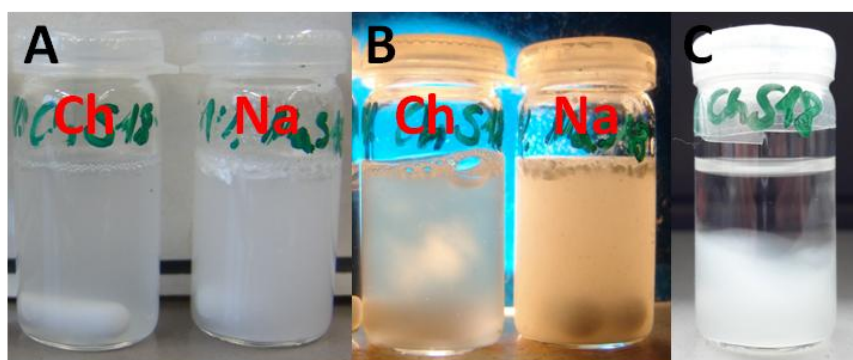


**Figure 4-4:** Photos of 1 wt% aqueous solution of NaS18 and ChS18 after stirring for 1d at 25 °C. Photo B was taken between crossed polarizers. Photo C shows the phase separation of a 1 wt% ChS18 solution after several days of aging at room temperature.

Further, concentration dependent solubility tests with NaS18, ChS18 and MeChS18 were performed (0.02/0.1/0.2/1 wt%) at 25 °C. Note that 0.02 wt % surfactant corresponds to at least 4 times the measured cmc values. As expected from Krafft theory, the NaS18 samples always contained some solid particles whose amount increased with increasing surfactant concentration. The results changed dramatically for ChS18 and MeChS18. For both surfactants, the 0.02 wt% solution was as clear as water. Thus, it was possible to measure the cmc at a temperature far below the 1 wt%  $T_{Kr}$ . Identical concentration dependent surface tension curves for ChS18 at 25 and 40 °C, only differing in  $\gamma_{cmc}$ , also indicate the presence of a micellar solution at 25 °C (see **Figure 4-6**). It must be pointed out that the ChS18 used for surface tension measurements at 25 °C was not heated above this temperature and ChS18 was dissolved during stirring at around 20 °C. At 0.1 and 0.2 wt%, the solutions were

slightly turbid/bluish and showed some streaks, which was more pronounced at higher concentrations. The appearance of the 1 wt% sample is already described above. This uncommon solubility behavior for surfactant concentrations well above the cmc is illustrated for MeChS18 in **Figure 4-5**.



**Figure 4-5:** Appearance of aqueous MeChS18 solutions with different concentrations after stirring for 2 d at 25 °C. MeChS18 concentrations: 1 = 0.02 wt%, 2 = 0.1 wt%, 3 = 0.2 wt%, 4 = 1 wt%.

All these observations mentioned above clearly depict the difference between NaS18 and ChS18 respectively MeChS18 in aqueous solutions. For the latter ones, the commonly observed Krafft phenomena, a transition from hydrated crystals to micelles around the cmc connected to a steep increase in surfactant solubility, is not found. Turbidity curves and heating experiments carried out with these surfactants show a slow and gradual increase in translucence over a broad temperature range. While at 0.02 wt% surfactant, which is well above the cmc, a clear solution is obtained at room temperature, at 1 wt% surfactant, the solution is turbid, birefringent and shows an increased viscosity. Further, no particles or crystals can be observed in solution and phase separation into a clear aqueous upper phase and a turbid and sponge-like lower phase takes place room temperature.

An explanation for these results could be the formation of a liquid crystalline phase in aqueous ChS18 and MeChS18 solutions, which seems to be triggered by an increase in surfactant concentration. Possibly, strong head group-counter ion interactions as well as a kind of co-surfactant behavior of the ethanol moiety of Ch or MeCh are responsible for that. Alcohols used as co-surfactants are well-known to trigger the formation of various liquid crystalline phases at low surfactant concentration in aqueous solutions.<sup>58</sup> Thus, the 1 wt%  $T_{Kr}$  of ChS18 and MeChS18 (according to turbidity curves also of ChS16) can be described as the temperature, at which the liquid crystalline has completely vanished and only micelles are present leading to solutions with a water-like appearance. Assuming that the S18 alkyl chains are in a fluid-like state within these liquid crystals, the transition from hydrated

crystals to micellar aggregates, i.e.  $T_{Kr}$  by definition, has to be below room temperature. Otherwise, it would not have been possible to dissolve 0.02 wt% ChS18 or MeChS18 well above their cmc at room temperature.

This could also explain the strong increase in  $T_{Kr}$  from S16 to S18 for Ch and MeCh, while Na shows an linear increase compared to  $T_{Kr}$  of the shorter chain surfactants (see **Figure 4-2**).

These are just assumptions based on the presented observations. To prove this, temperature, concentration and time dependent scattering as well as electron microscopy experiments have to be done.

## 4.4 Conclusion

It could be shown that, compared to classical Na alkyl sulfates, changing the counter ion to MeCh has the same  $T_{Kr}$ -reducing effects as it is the case for Ch. MeCh turned out to be a bit more effective, which can be attributed to its slightly more bulky structure. The predicted rise in counter ion-head group interactions by Collins' concept is outperformed by an increase in free energy of the surfactant's solid crystalline state due to the bulky structure of the counter ion. An unusual temperature and concentration dependent solubility behavior being contradictory to the Krafft theory was found for ChS18 and MeChS18. While the 1 wt% Krafft temperature was found to be about 25 °C above room temperature, clear and micellar aqueous solutions were obtained for a surfactant concentration of 0.02 wt% at room temperature. These findings can be reasonably explained by the formation of a liquid crystalline phase in aqueous ChS18 and MeChS18 solutions with increasing surfactant concentration. However, this interesting and very unusual solubility behavior deserves closer investigation.

Further, Ch and MeCh alkyl sulfates exhibit lower cmc values compared to their common Na homologues, which is a beneficial effect, since lower cmc values usually indicate higher surface activity. This is reflected by an increased efficiency in surface tension reduction  $pC_{20}$  ( $MeCh^+ > Ch^+ > Na^+$ ) with decreasing cmc value. The effectiveness in surface tension reduction  $\gamma_{cmc}$  slightly decreases for ChSXX and MeChSXX compared to their respective sodium homologues, whereas the area per molecule at the surface  $A$  was found to be considerably larger due to the larger size of the organic ions.

To sum up, by using MeCh and Ch as counter ion to alkyl sulfates, it is possible to prepare clear micellar solutions at room temperature up to a surfactant chain length of 18 Carbon atoms. For Na alkyl sulfates, this is only possible up to a surfactant

chain length of 12. This renders these two biological molecules promising candidates as counter ions for long chain alkyl sulfates in aqueous systems designed for low temperature application.

## 4.5 Experimental

### 4.5.1 Chemicals

Sodium dodecyl sulfate (NaS12, AppliChem, > 99.8 %), sodium hexadecyl sulfate (NaS16, Alfa Aesar, > 99 %, LOT: 10167796), sodium octadecyl sulfate (NaS18, Alfa Aesar, > 98 %, LOT: 10176541), choline chloride (ChCl, Sigma, > 98 %), beta-methylcholine chloride (MeChCl, TCI, > 98 %) were used as received. Choline hydroxide solution (ChOH,  $\approx$  46.5 wt% in water) and beta-methylcholine hydroxide solution (MeChOH,  $\approx$  38.5 wt% in water) were provided by TAMINCO.

### 4.5.2 Surfactant synthesis

ChS12 and MeChS12 were prepared by ion exchange according to a procedure described elsewhere.<sup>1</sup> A strong acidic ion exchanger (Merck, Type I) was first rinsed with 1 M HCl (Merck) and afterwards with millipore water until the effluent had a pH around 7. The ion exchange resin was loaded with an 1 M aqueous ChCl/MeChCl solution (the amount of the organic cation was 8 times the maximum exchange capacity). Then, to ensure complete loading, 100 mL of 5 wt% ChOH/MeChOH solution were used. Afterwards, a 0.1 M NaS12 solution slowly passed the column at ambient temperature. The amount of used surfactant was around 1/4 of the maximum exchange capacity. The preparation of the hexadecylsulfate and octadecylsulfate surfactants was done identically except that the sodium surfactants were used in a concentration of 0.025 M and the column was heated above  $T_{Kr}$  of the respective surfactant ( $\approx$  55 °C for NaS16 and  $\approx$  65 °C for NaS18). After the water was removed by freeze drying, the solid surfactant was further dried at  $10^{-2}$  bar in an desiccator for 1-2 weeks. All surfactants were obtained as white powders.

Purity of the surfactants was checked by  $^1\text{H}$  NMR and  $^{13}\text{C}$  NMR in  $\text{CDCl}_3$  and electron spray mass spectroscopy (ES-MS). Mass spectroscopy was carried out with a ThermoQuest Finnigan TSQ 7000 instrument or an Agilent Q-TOF 6540 UHD instrument. NMR spectra were recorded on a Bruker Advance 300 spectrometer at 300 MHz and tetramethylsilane as internal standard.

- ChS12:**
- <sup>1</sup>H-NMR** (300 MHz, CDCl<sub>3</sub>, 25 °C, TMS): δ = 0.87 (t, 3H; CH<sub>2</sub>CH<sub>3</sub>), 1.25 (m, 18H; CH<sub>2</sub>CH<sub>2</sub>CH<sub>3</sub>), 1.64 (quin, 2H; CH<sub>2</sub>CH<sub>2</sub>SO<sub>4</sub><sup>-</sup>), 3.30 (s, 9H; N(CH<sub>3</sub>)<sub>3</sub>), 3.64 (t, 2H; N(CH<sub>3</sub>)<sub>3</sub>CH<sub>2</sub>), 3.98 (t, 2H; CH<sub>2</sub>SO<sub>4</sub><sup>-</sup>), 4.07 (m, 2H; CH<sub>2</sub>OH)
- <sup>13</sup>C-NMR** (300 MHz, CDCl<sub>3</sub>, 25 °C, TMS): δ = 14.15 (CH<sub>2</sub>CH<sub>3</sub>), 22.71 (CH<sub>2</sub>CH<sub>3</sub>), 25.84 (CH<sub>2</sub>CH<sub>2</sub>CH<sub>3</sub>), 29.39-29.71 (CH<sub>2</sub>CH<sub>2</sub>), 31.94 (CH<sub>2</sub>CH<sub>2</sub>SO<sub>4</sub><sup>-</sup>), 54.43 (N(CH<sub>3</sub>)<sub>3</sub>), 56.41 (CH<sub>2</sub>OH), 67.87 (CH<sub>2</sub>SO<sub>4</sub><sup>-</sup>), 68.44 (N(CH<sub>3</sub>)<sub>3</sub>CH<sub>2</sub>)
- ES-MS (Agilent):** m/z (+p): 104.11 [M<sup>+</sup>], 148.13, 192.16; (p-): 265.15 [M<sup>-</sup>], 531.30 [(2M<sup>-</sup> + H<sup>+</sup>)<sup>-</sup>]
- MeChS12:**
- <sup>1</sup>H-NMR** (300 MHz, CDCl<sub>3</sub>, 25 °C, TMS): δ = 0.87 (t, 3H; CH<sub>2</sub>CH<sub>3</sub>), 1.28 (m, 21H; CH<sub>2</sub>CH<sub>2</sub>CH<sub>3</sub>; CHCH<sub>3</sub>OH), 1.65 (quin, 2H; CH<sub>2</sub>CH<sub>2</sub>SO<sub>4</sub><sup>-</sup>), 3.33 (s, 9H; N(CH<sub>3</sub>)<sub>3</sub>), 3.46 (m, 2H; N(CH<sub>3</sub>)<sub>3</sub>CH<sub>2</sub>), 4.00 (t, 2H; CH<sub>2</sub>SO<sub>4</sub><sup>-</sup>), 4.43 (m, 1H; CHCH<sub>3</sub>OH)
- <sup>13</sup>C-NMR** (300 MHz, CDCl<sub>3</sub>, 25 °C, TMS): δ = 14.16 (CH<sub>2</sub>CH<sub>3</sub>), 22.04 (CHCH<sub>3</sub>OH), 22.71 (CH<sub>2</sub>CH<sub>3</sub>), 25.83 (CH<sub>2</sub>CH<sub>2</sub>CH<sub>3</sub>), 29.39-29.70 (CH<sub>2</sub>CH<sub>2</sub>), 31.94 (CH<sub>2</sub>CH<sub>2</sub>SO<sub>4</sub><sup>-</sup>), 54.58 (N(CH<sub>3</sub>)<sub>3</sub>), 62.46 (CHCH<sub>3</sub>OH), 68.50 (CH<sub>2</sub>SO<sub>4</sub><sup>-</sup>), 71.50 (N(CH<sub>3</sub>)<sub>3</sub>CH<sub>2</sub>)
- ES-MS (Agilent):** m/z (+p): 118.12 [M<sup>+</sup>]; (p-): 265.15 [M<sup>-</sup>], 531.30 [(2M<sup>-</sup> + H<sup>+</sup>)<sup>-</sup>]
- ChS16:**
- <sup>1</sup>H-NMR** (300 MHz, CDCl<sub>3</sub>, 25 °C, TMS): δ = 0.87 (t, 3H; CH<sub>2</sub>CH<sub>3</sub>), 1.25 (m, 26H; CH<sub>2</sub>CH<sub>2</sub>CH<sub>3</sub>), 1.65 (quin, 2H; CH<sub>2</sub>CH<sub>2</sub>SO<sub>4</sub><sup>-</sup>), 3.31 (s, 9H; N(CH<sub>3</sub>)<sub>3</sub>), 3.64 (t, 2H; N(CH<sub>3</sub>)<sub>3</sub>CH<sub>2</sub>), 4.00 (t, 2H; CH<sub>2</sub>SO<sub>4</sub><sup>-</sup>), 4.08 (m, 2H; CH<sub>2</sub>OH)
- <sup>13</sup>C-NMR** (300 MHz, CDCl<sub>3</sub>, 25 °C, TMS): δ = 14.16 (CH<sub>2</sub>CH<sub>3</sub>), 22.72 (CH<sub>2</sub>CH<sub>3</sub>), 25.83 (CH<sub>2</sub>CH<sub>2</sub>CH<sub>3</sub>), 29.40-29.75 (CH<sub>2</sub>CH<sub>2</sub>), 31.95 (CH<sub>2</sub>CH<sub>2</sub>SO<sub>4</sub><sup>-</sup>), 54.47 (N(CH<sub>3</sub>)<sub>3</sub>), 56.44 (CH<sub>2</sub>OH), 67.91 (CH<sub>2</sub>SO<sub>4</sub><sup>-</sup>), 68.59 (N(CH<sub>3</sub>)<sub>3</sub>CH<sub>2</sub>)
- ES-MS (Agilent):** m/z (+p): 104.11 [M<sup>+</sup>], 148.13, 192.16; (p-): 321.21 [M<sup>-</sup>], 643.43 [(2M<sup>-</sup> + H<sup>+</sup>)<sup>-</sup>]

<i>MeChS16:</i>	<p><b><sup>1</sup>H-NMR</b> (300 MHz, CDCl<sub>3</sub>, 25 °C, TMS): δ = 0.87 (t, 3H; CH<sub>2</sub>CH<sub>3</sub>), 1.26 (m, 29H; CH<sub>2</sub>CH<sub>2</sub>CH<sub>3</sub>; CHCH<sub>3</sub>OH), 1.64 (quin, 2H; CH<sub>2</sub>CH<sub>2</sub>SO<sub>4</sub><sup>-</sup>), 3.33 (s, 9H; N(CH<sub>3</sub>)<sub>3</sub>), 3.46 (m, 2H; N(CH<sub>3</sub>)<sub>3</sub>CH<sub>2</sub>), 3.98 (t, 2H; CH<sub>2</sub>SO<sub>4</sub><sup>-</sup>), 4.42 (m, 1H; CHCH<sub>3</sub>OH)</p> <p><b><sup>13</sup>C-NMR</b> (300 MHz, CDCl<sub>3</sub>, 25 °C, TMS): δ = 14.16 (CH<sub>2</sub>CH<sub>3</sub>), 22.04 (CHCH<sub>3</sub>OH), 22.71 (CH<sub>2</sub>CH<sub>3</sub>), 25.85 (CH<sub>2</sub>CH<sub>2</sub>CH<sub>3</sub>), 29.39-29.74 (CH<sub>2</sub>CH<sub>2</sub>), 31.94 (CH<sub>2</sub>CH<sub>2</sub>SO<sub>4</sub><sup>-</sup>), 54.57 (N(CH<sub>3</sub>)<sub>3</sub>), 62.46 (CHCH<sub>3</sub>OH), 68.35 (CH<sub>2</sub>SO<sub>4</sub><sup>-</sup>), 71.51 (N(CH<sub>3</sub>)<sub>3</sub>CH<sub>2</sub>)</p> <p><b>ES-MS (Agilent):</b> m/z (+p): 118.12 [M<sup>+</sup>], 176.16; (p-): 321.21 [M<sup>-</sup>], 643.43 [(2M<sup>-</sup> + H<sup>+</sup>)]<sup>-</sup></p>
<i>ChS18:</i>	<p><b><sup>1</sup>H-NMR</b> (300 MHz, CDCl<sub>3</sub>, 25 °C, TMS): δ = 0.87 (t, 3H; CH<sub>2</sub>CH<sub>3</sub>), 1.25 (m, 30H; CH<sub>2</sub>CH<sub>2</sub>CH<sub>3</sub>), 1.64 (quin, 2H; CH<sub>2</sub>CH<sub>2</sub>SO<sub>4</sub><sup>-</sup>), 3.31 (s, 9H; N(CH<sub>3</sub>)<sub>3</sub>), 3.65 (t, 2H; N(CH<sub>3</sub>)<sub>3</sub>CH<sub>2</sub>), 3.99 (t, 2H; CH<sub>2</sub>SO<sub>4</sub><sup>-</sup>), 4.08 (m, 2H; CH<sub>2</sub>OH)</p> <p><b><sup>13</sup>C-NMR</b> (300 MHz, CDCl<sub>3</sub>, 25 °C, TMS): δ C= 14.16 (CH<sub>2</sub>CH<sub>3</sub>), 22.72 (CH<sub>2</sub>CH<sub>3</sub>), 25.84 (CH<sub>2</sub>CH<sub>2</sub>CH<sub>3</sub>), 29.41-29.75 (CH<sub>2</sub>CH<sub>2</sub>), 31.95 (CH<sub>2</sub>CH<sub>2</sub>SO<sub>4</sub><sup>-</sup>), 54.48 (N(CH<sub>3</sub>)<sub>3</sub>), 56.44 (CH<sub>2</sub>OH), 67.91 (CH<sub>2</sub>SO<sub>4</sub><sup>-</sup>), 68.56 (N(CH<sub>3</sub>)<sub>3</sub>CH<sub>2</sub>)</p> <p><b>ES-MS (Agilent):</b> m/z (+p): 104.11 [M<sup>+</sup>], 148.13, 192.16; (p-): 349.24 [M<sup>-</sup>], 699.49 [(2M<sup>-</sup> + H<sup>+</sup>)]<sup>-</sup></p>
<i>MeChS18:</i>	<p><b><sup>1</sup>H-NMR</b> (300 MHz, CDCl<sub>3</sub>, 25 °C, TMS): δ = 0.87 (t, 3H; CH<sub>2</sub>CH<sub>3</sub>), 1.26 (m, 33H; CH<sub>2</sub>CH<sub>2</sub>CH<sub>3</sub>; CHCH<sub>3</sub>OH), 1.64 (quin, 2H; CH<sub>2</sub>CH<sub>2</sub>SO<sub>4</sub><sup>-</sup>), 3.32 (s, 9H; N(CH<sub>3</sub>)<sub>3</sub>), 3.46 (m, 2H; N(CH<sub>3</sub>)<sub>3</sub>CH<sub>2</sub>), 3.99 (t, 2H; CH<sub>2</sub>SO<sub>4</sub><sup>-</sup>), 4.43 (m, 1H; CHCH<sub>3</sub>OH)</p> <p><b><sup>13</sup>C-NMR</b> (300 MHz, CDCl<sub>3</sub>, 25 °C, TMS): δ = 14.16 (CH<sub>2</sub>CH<sub>3</sub>), 22.04 (CHCH<sub>3</sub>OH), 22.72 (CH<sub>2</sub>CH<sub>3</sub>), 25.85 (CH<sub>2</sub>CH<sub>2</sub>CH<sub>3</sub>), 29.40-29.75 (CH<sub>2</sub>CH<sub>2</sub>), 31.95 (CH<sub>2</sub>CH<sub>2</sub>SO<sub>4</sub><sup>-</sup>), 54.55 (N(CH<sub>3</sub>)<sub>3</sub>), 62.46 (CHCH<sub>3</sub>OH), 68.38 (CH<sub>2</sub>SO<sub>4</sub><sup>-</sup>), 71.51 (N(CH<sub>3</sub>)<sub>3</sub>CH<sub>2</sub>)</p> <p><b>ES-MS (ThermoQuest):</b> m/z (+p): 117.9 [M<sup>+</sup>], 175.8, 585.4 [(2M<sup>+</sup> + M<sup>-</sup>)]<sup>+</sup>; (p-): 349.1 [M<sup>-</sup>], 816.6 [(2M<sup>-</sup> + M<sup>+</sup>)]<sup>-</sup></p>

### 4.5.3 Determination of $T_{Kr}$

$T_{Kr}$  values were obtained by turbidity measurements with an automated home built apparatus being equipped with a computer controlled thermostat, a light emitting diode (LED) and a light dependent resistor (LDR). Turbidity was detected by recording the transmission of light through the samples while constantly increasing the temperature. The heating rate was 1.5 °C/h. All samples were frozen at -20 °C before measuring.  $T_{Kr}$  was taken as the temperature where the transmission reached its maximum value.

Moreover, some heating experiments in a water bath were carried out. Again the samples were frozen at -20 °C and afterwards analyzed with a heating rate of around 1°C/5 min. The samples were visually observed during the measurement and  $T_{Kr}$  was taken as the temperature, from which on the surfactant solution was as clear as water.

### 4.5.4 Surface tension measurements

Surface tension measurements ( $\sigma$ ) were performed on a Krüss tensiometer (model K100 MK2) using a platinum-iridium ring. The tensiometer was equipped with a double dosing system (Metrohm Liquino 711) and the recording of the surface tension was done automatically as a function of the surfactant concentration. The temperature was monitored and kept constant ( $25 \pm 0.5$  °C and  $42 \pm 0.5$  °C). The data correction happened after the procedure developed by Harkins and Jordan.<sup>59</sup>

The measured concentration dependent surface tension curves are shown in **Figure 4-6** for ChSXX and in **Figure 4-7** for MeChS18. The cmc is determined by the intersection of the two linear parts of the curve as shown for ChS12 in **Figure 4-6**. The surface tension is plotted against the  $\ln$  of the concentration, which made it possible to determine the surface excess concentration  $\Gamma$  by using the Gibbs adsorption equation for a dilute solution of a complete dissociated surfactant without additional salt.<sup>51</sup>

$$-d\gamma = RT \left[ \Gamma_{S^-} d(\ln c_{S^-}) + \Gamma_{C^+} d(\ln c_{C^+}) \right] \quad (4-4)$$

In equation 4-4,  $S^-$  denotes the alkyl sulfate SXX and  $C^+$  the used counter ion  $Ch^+$ ,  $MeCh^+$  or  $Na^+$ . Electroneutrality at the surface requires  $\Gamma_{S^-} = \Gamma_{C^+} = \Gamma$  and  $c_{S^-} = c_{C^+} = c$  and equation 4-4 turns into equation 5-4, which allows the calculation of the surface

excess concentration  $\Gamma$  by taking the slope of the curve at concentrations lower than the cmc.<sup>51</sup>

$$\Gamma = -\frac{d\gamma}{2RTd \ln c} \quad (5-4)$$

The area at the surface per molecule  $A$  in  $\text{\AA}^2$  is calculated from  $\Gamma$  given in  $\text{mol}/\text{cm}^2$  by the following equation where  $N$  is Avogadro's number:<sup>51</sup>

$$A = \frac{10^{16}}{\Gamma N} \quad (6-4)$$

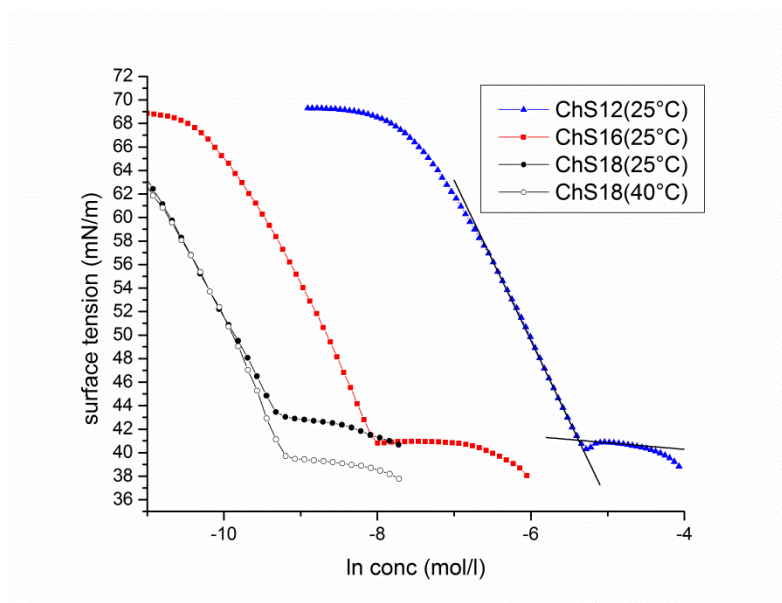


**Figure 4-6:** Surface tension versus  $\ln(c)$  plots for choline alkyl sulfates (ChSXX).  $\blacktriangle$  = ChS12 at 25 °C,  $\blacksquare$  = ChS16 at 25 °C,  $\bullet$  = ChS18 at 25 °C,  $\circ$  = ChS18 at 40 °C. For ChS12, the two linear parts of the curve necessary to determine the cmc are fitted and the cmc is given by their intersection.

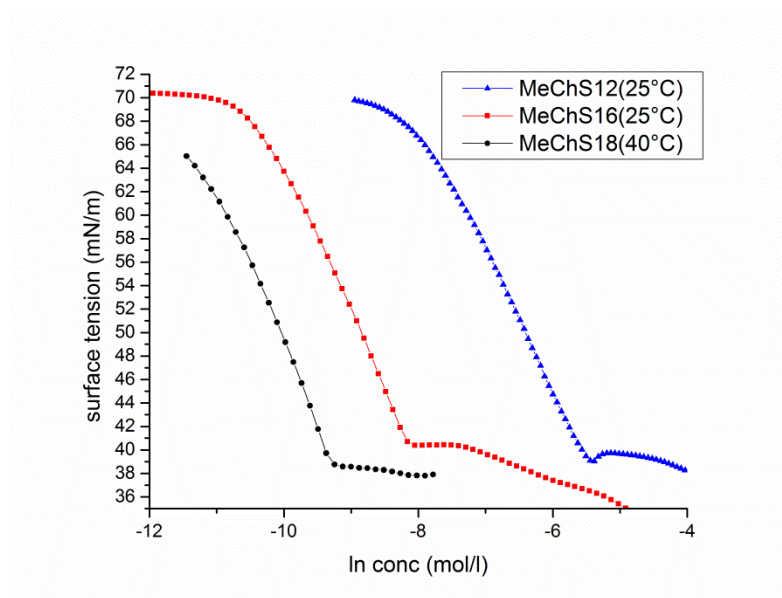


**Figure 4-7:** Surface tension versus  $\ln(c)$  plots for beta-methylcholine alkyl sulfates (MeChSXX).  $\blacktriangle$  = MeChS12 at 25 °C,  $\blacksquare$  = MeChS16 at 25 °C,  $\bullet$  = MeChS18 at 40 °C.

#### 4.5.5 Conductivity measurements

Specific conductivity ( $\kappa$ ) was measured with a WTW Conductivity-Meter LBR at  $25 \pm 0.1$  °C for S12 and S16 and at  $50 \pm 0.1$  °C for S18 surfactants. Solutions of different concentrations were prepared by dilution of surfactant stock solutions. The cell constant was determined by measuring a 0.01 M potassium chloride solution at 25 °C, since the cell constant can be regarded as constant from 25 to 50 °C.<sup>60</sup> Plotting the specific conductivity  $\kappa$  against the concentration yields the cmc as the breakpoint of the slope (see **Figure 4-8**). The micelle ionization degree  $\alpha$  at the cmc can be calculated by equation 7-4 derived by Evans, after converting it into equation 8-4.<sup>33</sup>

$$0 = \left[ N^{\frac{2}{3}} (1000 \cdot S_1 - \Lambda_{C^+}) \right] \alpha^2 + \lambda_{C^+} \alpha - 1000 \cdot S_2 \quad (7-4)$$

$$\alpha_{1/2} = \frac{-\Lambda_{C^+} \pm \sqrt{\Lambda_{C^+}^2 + 4 \cdot N^{\frac{2}{3}} (1000 \cdot S_1 - \Lambda_{C^+}) 1000 \cdot S_2}}{2 \cdot N^{\frac{2}{3}} (1000 \cdot S_1 - \Lambda_{C^+})} \quad (8-4)$$

In equation 8-4,  $S_1$  and  $S_2$  represent the slopes of the linear fits of the specific conductivity versus surfactant concentration plot before and after the cmc,  $\Lambda_{C^+}$  is the molar conductivity of the counter ion and  $N$  the surfactant aggregation number. In

literature, only the value for  $\Lambda_{\text{Ch}^+}$  at 25 °C, which is 42 S·cm<sup>2</sup>, can be found. From this value,  $\Lambda_{\text{Ch}^+}$  at 50 °C could be obtained with the help of the Walden Product, which relates the product of the molar conductivity  $\Lambda$  and the solvent viscosity  $\eta$  at different temperatures according to equation 9-4. Applied for one solvent, this rule provides very useful values. The viscosity of water at 25 °C and 50 °C is well known. In this way,  $\Lambda_{\text{Ch}^+}$  at 50 °C was determined 68.35 S·cm<sup>2</sup>. For MeCh<sup>+</sup>, also the molar conductivity values of Ch<sup>+</sup> were taken to calculate  $\alpha$ .

$$\Lambda_1(25^\circ\text{C}) \cdot \eta_1(25^\circ\text{C}) = \Lambda_2(50^\circ\text{C}) \cdot \eta_2(50^\circ\text{C}) \quad (9-4)$$

Assuming spherical micelles with fully extended hydrocarbon chains, the surfactant aggregation number  $N$  was calculated by expressions introduced by Tanford.<sup>61</sup> Calculations were done with one Carbon atom less than present in the alkyl chain, since the first methylene group(s) may not belong to the hydrophobic core of the micelle.<sup>61, 62</sup> However, the value for  $\alpha$  is not very sensitive to the value of  $N$ .

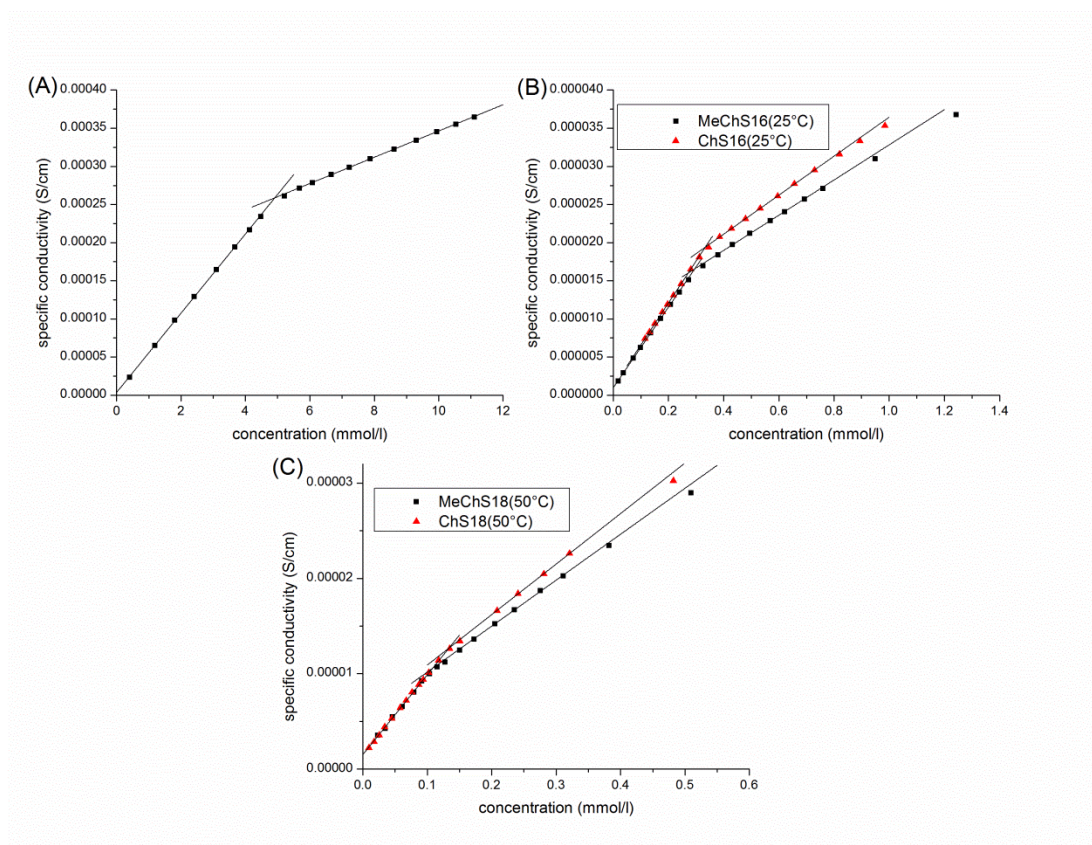


**Figure 4-8:** Plotting the specific conductivity  $\kappa$  in S/cm against the surfactant concentration in mmol/l for ChS12 at 25 °C (A), ChS16 (▲) and MeChS16 (■) at 25 °C (B) as well as ChS18 (▲) and MeChS18 (■) at 50 °C (C).

Surfactant	1000*S <sub>1</sub> [Scm <sup>2</sup> /mol]	1000S <sub>2</sub> [Scm <sup>2</sup> /mol]
MeChS12 (25°C)	51.8 ± 0.1	17.1 ± 0.1
MeChS16 (25°C)	52.2 ± 0.4	22.9 ± 0.1
MeChS18 (50°C)	82.5 ± 1.0	50.5 ± 0.3
ChS16 (25°C)	54.4 ± 0.7	25.4 ± 0.3
ChS18 (50°C)	86.2 ± 1.1	53.5 ± 1.0

**Table 4-3:** Slope S<sub>1</sub> and S<sub>2</sub> obtained from fitting of the linear parts in the specific conductivity  $\kappa$  versus concentration  $c$  plots for choline and beta-methylcholine alkyl sulfates.

## 4.6 Literature

1. Klein, R.; Kellermeier, M.; Touraud, D.; Müller, E.; Kunz, W., *J Colloid Interface Sci* **2013**, 392 (0), 274-280.
2. Rengstl, D., Dissertation. Universität Regensburg: 2013.
3. Schmalstieg, A.; Wasow, G. W., Anionic surfactants. In *Handbook of Applied Surface and Colloid Chemistry (Volume 1)*, Holmberg, K., Ed. Wiley: 2002; pp 271-292.
4. Domingo, X., Alcohol and Alcohol Ether Sulfates. In *Anionic Surfactants: Organic Chemistry*, Stache, H., Ed. Marcel Dekker: 1996; Vol. 56, pp 223-312.
5. Scott, M. J.; Jones, M. N., *Biochim Biophys Acta - Biomembranes* **2000**, 1508 (1-2), 235-251.
6. Hibbs, J., Anionic Surfactants. In *Chemistry and Technology of Surfactants*, Farn, R. J., Ed. Blackwell Publishing Ltd: 2006; pp 91-132.
7. Preston, W. C., *J Phys Colloid Chem* **1948**, 52 (1), 84-97.
8. Evans, D. F.; Wennerström, H., *The Colloidal Domain: Where Physics, Chemistry, Biology, and Technology Meet*. Wiley: 1999.
9. Laughlin, R. G., *The Aqueous Phase Behaviour of Surfactants*. Academic Press: 1994; p 107-108.
10. Weil, J. K.; Stirton, A. J.; Nuñez-Ponzoa, M. V., *J Am Oil Chem Soc* **1966**, 43 (11), 603-606.
11. Yu, Z. J.; Zhang, X.; Xu, G.; Zhao, G., *J Phys Chem* **1990**, 94 (9), 3675-3681.
12. Yu, Z. J.; Xu, G., *J Phys Chem* **1989**, 93 (21), 7441-7445.
13. Zana, R., *Langmuir* **2004**, 20 (14), 5666-5668.
14. Hrobárik, T.; Vrbka, L.; Jungwirth, P., *Biophys Chem* **2006**, 124 (3), 238-242.
15. Kutluay, E.; Roux, B.; Heginbotham, L., *Biophys J* **2005**, 88 (2), 1018-1029.
16. Luzhkov, V. B.; Åqvist, J., *FEBS Lett* **2001**, 495 (3), 191-196.
17. O'Leary, M. E.; Kallen, R. G.; Horn, R., *J Gen Physiol* **1994**, 104 (3), 523-539.

18. Moberg, R.; Boekman, F.; Bohman, O.; Siegbahn, H. O. G., *J Am Chem Soc* **1991**, *113* (10), 3663-3667.
19. Klein, R.; Touraud, D.; Kunz, W., *Green Chem* **2008**, *10* (4), 433-435.
20. Blusztajn, J. K., *Science* **1998**, *281* (5378), 794-795.
21. Klein, R.; Muller, E.; Kraus, B.; Brunner, G.; Estrine, B.; Touraud, D.; Heilmann, J.; Kellermeier, M.; Kunz, W., *RSC Adv* **2013**, *3* (45), 23347-23354.
22. Collins, K. D.; Neilson, G. W.; Enderby, J. E., *Biophys Chem* **2007**, *128* (2-3), 95-104.
23. Collins, K. D., *Methods* **2004**, *34* (3), 300-311.
24. Vlachy, N.; Jagoda-Cwiklik, B.; Vácha, R.; Touraud, D.; Jungwirth, P.; Kunz, W., *Adv Colloid Interface Sci* **2009**, *146* (1-2), 42-47.
25. Joshi, J. V.; Aswal, V. K.; Goyal, P. S., *J Phys Condens Matter* **2007**, *19* (19), 196219.
26. Benrraou, M.; Bales, B. L.; Zana, R., *J Phys Chem B* **2003**, *107* (48), 13432-13440.
27. Mukerjee, P.; Mysels, K.; Kapauan, P., *J Phys Chem* **1967**, *71* (13), 4166-4175.
28. Schwuger, M. J., *Kolloid-Z.u.Z.Polymere* **1969**, *233* (1-2), 979-985.
29. Lindman, B., Physico-Chemical Properties of Surfactants. In *Handbook of Applied Surface and Colloid Chemistry (Volume 1)*, Holmberg, K., Ed. Wiley: 2002; pp 421-443.
30. Khairallah, E. A.; Wolf, G., *J Biol Chem* **1967**, *242* (1), 32-39.
31. Vardanyan, R. S.; Hruby, V. J., Cholinomimetics. In *Synthesis of Essential Drugs*, Elsevier: Amsterdam, 2006; pp 179-193.
32. Zana, R.; Benrraou, M.; Bales, B. L., *J Phys Chem B* **2004**, *108* (47), 18195-18203.
33. Evans, H. C., *J Chem Soc* **1956**, (0), 579-586.
34. Schick, M., *J Phys Chem* **1964**, *68* (12), 3585-3592.
35. Powney, J.; Addison, C. C., *T Faraday Soc* **1937**, *33* (0), 1243-1260.
36. Lange, H., *Kolloid-Z.u.Z.Polymere* **1953**, *131* (2), 96-103.
37. Mukerjee, P.; Mysels, K. J., *Critical micelle concentrations of aqueous surfactant systems*. U.S. National Bureau of Standards; for sale by the Supt. of Docs., U.S. Govt. Print. Off.: 1971.
38. Kronberg, B.; Castas, M.; Silvestonti, R., *J Dispersion Sci Technol* **1994**, *15* (3), 333-351.

39. Brown, P.; Butts, C.; Dyer, R.; Eastoe, J.; Grillo, I.; Guittard, F.; Rogers, S.; Heenan, R., *Langmuir* **2011**, 27 (8), 4563-4571.
40. Berr, S. S.; Coleman, M. J.; Jones, R. R. M.; Johnson, J. S., *J Phys Chem* **1986**, 90 (24), 6492-6499.
41. Liu, G.; Zhang, H.; Liu, G.; Yuan, S.; Liu, C., *Phys Chem Chem Phys* **2016**, 18 (2), 878-885.
42. Lin, J. H.; Chen, W. S.; Hou, S. S., *J Phys Chem B* **2013**, 117 (40), 12076-12085.
43. Mitra, D.; Chakraborty, I.; Bhattacharya, S. C.; Moulik, S. P., *Langmuir* **2007**, 23 (6), 3049-3061.
44. Wei, Y.; Wang, H.; Liu, G.; Wang, Z.; Yuan, S., *RSC Adv* **2016**, 6 (87), 84090-84097.
45. Scamehorn, J. F., An Overview of Phenomena Involving Surfactant Mixtures. In *Phenomena in Mixed Surfactant Systems*, Scamehorn, J. F., Ed. American Chemical Society: 1986; Vol. 311, pp 1-27.
46. Zana, R.; Yiv, S.; Strazielle, C.; Lianos, P., *J Colloid Interface Sci* **1981**, 80 (1), 208-223.
47. Shirahama, K.; Kashiwabara, T., *J Colloid Interface Sci* **1971**, 36 (1), 65-70.
48. Jansson, M.; Jönsson, A.; Li, P.; Stilbs, P., *Colloids Surf* **1991**, 59, 387-397.
49. Fameau, A.-L.; Ventureira, J.; Novales, B.; Douliez, J.-P., *Colloids Surf A Physicochem Eng Asp* **2012**, 403, 87-95.
50. Rosen, M. J., Reduction of Surface and Interfacial Tension by Surfactants. In *Surfactants and Interfacial Phenomena*, John Wiley & Sons, Inc.: 2004; pp 208-242.
51. Rosen, M. J., Adsorption of Surface-Active Agents at Interfaces: The Electrical Double Layer. In *Surfactants and Interfacial Phenomena*, John Wiley & Sons, Inc.: 2004; pp 34-104.
52. Myers, D., Fluid Surfaces and Interfaces. In *Surfactant Science and Technology*, John Wiley & Sons, Inc.: 2005; pp 80-106.
53. Hat, M.; Shinoda, K. z., *B Chem Soc JPN* **1973**, 46 (12), 3889-3890.
54. Nakayama, H.; Shinoda, K.; Hutchinson, E., *J Phys Chem* **1966**, 70 (11), 3502-3504.
55. Evans, D. F.; Wennerström, H., Solutes and Solvents, Self-Assembly of Amphiphiles. In *The Colloidal Domain: Where Physics, Chemistry, Biology, and Technology Meet*, Wiley: 1999; pp 1-44.
56. Laughlin, R. G., The Characteristic Features of Surfactant Phase Behavior In *The Aqueous Phase Behaviour of Surfactants*, Academic Press: 1994; pp 102-154.

57. Laughlin, R. G., The Structures and Properties of Surfactant Phases. In *The Aqueous Phase Behaviour of Surfactants*, Academic Press: 1994; pp 181-237.
58. Hoffmann, H.; Ulbricht, W., *Chemie in unserer Zeit* **1995**, 29 (2), 76-86.
59. Harkins, W. D.; Jordan, H. F., *J Am Chem Soc* **1930**, 52 (5), 1751-1772.
60. Barthel, J.; Feuerlein, F.; Neueder, R.; Wachter, R., *J Solution Chem* **1980**, 9 (3), 209-219.
61. Tanford, C., *J Phys Chem* **1972**, 76 (21), 3020-3024.
62. Zemb, T.; Testard, F., Solubilization. In *Handbook of Applied Surface and Colloid Chemistry (Volume 2)*, Holmberg, K., Ed. Wiley: 2002; pp 159-188.

## **Chapter 5 Choline and beta-methylcholine salts to reduce $T_{Kr}$ of long chain sodium alkyl sulfates - the "2 in 1"-builder-concept**

### **5.1 Abstract**

In the previous chapter, the counter ion dependence of  $T_{Kr}$  was utilized and it was shown that changing the counter ion of long chain alkyl sulfates from Na to Ch or MeCh heavily increases the solubility of these surfactants. However, for both alkyl sulfates and soaps, it was also shown in literature that the addition of cations different from the original counter ion of the anionic surfactant can considerably change  $T_{Kr}$  of the aqueous surfactant solution.<sup>1-3</sup> Especially symmetrical TAAs as well as choline were found to decrease  $T_{Kr}$  of both sodium alkyl sulfates and sodium soaps.

In this chapter, the effect of different Ch, MeCh and Na salts on  $T_{Kr}$  of Na and Ch alkyl sulfates was investigated at different surfactant concentrations in millipore as well as in hard water.

It was found that both Ch and MeCh salts can depress  $T_{Kr}$  of NaS16 below room temperature in millipore water as soon as the molecular ratio of Ch/MeCh to Na in solution is  $\geq 2$ . For NaS18,  $T_{Kr}$  can only be reduced below room temperature by Ch and MeCh salts, if a certain amount of the nonionic alcohol ethoxylate surfactant Lutensol AO7 is present.

Finally, it will be shown that this concept can also be applied in hard water by a reasonable choice of the anionic component of the Ch or MeCh salt. The anionic compound has to be a chelating agent that strongly binds hard water ions by the formation of water soluble complexes and thereby softens the water. Due to the fact that such compounds are used in detergents as builders, the newly introduced concept will be termed "2 in 1"-builder-concept.

## 5.2 Introduction

It is well-known that changing the counter ion of an anionic surfactant can considerably change its Krafft temperature.<sup>1, 4</sup> This effect is discussed in detail in the previous chapter and was utilized to reduce  $T_{Kr}$  of long chain Na alkyl sulfates by changing the counter ion to Ch or MeCh.

Another possibility to influence  $T_{Kr}$  of anionic surfactants is the addition of salt to the aqueous surfactant solution. The addition of additional cations different from the original counter ion of the anionic surfactant can both increase or decrease  $T_{Kr}$  of the initial surfactant.

A famous example for increasing  $T_{Kr}$  of the initial surfactant is observed when trying to dissolve NaS12 or NaC12, actually water-soluble at room temperature, in hard water containing calcium or magnesium ions. The increase in  $T_{Kr}$  for NaS12 and NaC12 in hard water can be attributed to strong interactions between the divalent alkaline earth metals and the surfactant anion that results in bivalent cation-anionic surfactant precipitate. Thus, the large  $T_{Kr}$  values of for alkyl sulfates<sup>5, 6</sup> or soaps<sup>7-9</sup> with bivalent counter ions are responsible for the "hard water problem" in detergency and other applications.

In 1990, Yu et al.<sup>3</sup> showed that the addition of TBA to Na alkyl sulfates (S10-S18) considerably reduces  $T_{Kr}$  of the initial sodium surfactants. 15 years later, Strey et al.<sup>2</sup> reported the same results when adding symmetrical TAAs to long chain Na soaps. The effect increased with increasing size of the TAA. Both authors explain the effect by a counter ion exchange in solution from sodium to TAA, i.e. from high  $T_{Kr}$  sodium surfactant to low  $T_{Kr}$  TAA surfactant. The reasons for lower  $T_{Kr}$  values of TAA surfactants compared to sodium surfactants are discussed in detail in the previous chapter. Recently, Klein et al.<sup>1</sup> systematically investigated the influence of alkali metal chlorides and ChCl on  $T_{Kr}$  of alkali and Ch dodecyl sulfates, respectively dodecanoates. Regarding the influence on  $T_{Kr}$ , for the alkali ions ( $Li^+$ ,  $Na^+$  and  $K^+$ ), an reversed ordering was found when changing the surfactant's head group from sulfate to carboxylate. This reversed series, also known for  $T_{Kr}$  of pure alkali alkyl sulfates and alkali soaps, could be well explained by specific ion effects using Collins' concept of matching water affinities. As it is the case for  $T_{Kr}$  of the pure surfactants, the addition of ChCl reduces  $T_{Kr}$  of both alkali dodecyl sulfate and alkali dodecanoate. These findings are explained by possible attractions between the hydrophobic moieties of the surfactant and the organic Ch ion.

The results of the systematic investigations by Klein et al.<sup>1</sup> prove the reasonable assumption that for such mixed system consisting of ionic surfactant plus additional

salt,  $T_{Kr}$  is only dependent of the actual composition and molecular ratios of the different ions to each other. In other words, it does not matter whether a specific ion is introduced by the ionic surfactant or added salt, since in the dissolved state the surfactant cannot distinguish between these two possibilities. This fact should always be kept in mind.

In this part of the work, the effect of Ch, MeCh and Na salts on  $T_{Kr}$  of NaS16, NaS18 and ChS18 was investigated by turbidity measurements as well as heating and longtime stirring experiments. To reduce  $T_{Kr}$  of the system NaS18 plus additional salt below room temperature, a certain amount of nonionic alcohol ethoxylate surfactant was used. Finally, it will be shown that the results obtained in millipore water can also be achieved in hard water by choosing a hard water ion chelating agent, in this case ethylenediaminetetraacetate (EDTA) and citrate, as anion of the added salt. This will be introduced as the "2 in 1-builder-concept". All experiments were also carried out with the respective Na salts to prove that the desired effects are really caused by a clever combination of the ions in the added salt.

## **5.3 Results and discussion**

First, the effect of additional Ch, MeCh and Na ions on NaS16, NaS18 and ChS18 will be presented at different surfactant concentrations in millipore water. For NaS18 systems, also experiments with the nonionic surfactant Lutensol AO7 are described. Afterwards, it will be shown how these effects can also be obtained in hard water by reasonable choice of the added salt and the "2 in 1"-builder-concept will be introduced.

The work presented in this chapter was part of a industry cooperation with TAMINCO, a subsidiary of the Eastman Chemical Company. The main goal was to realize clear and stable aqueous solutions of long chain alkyl sulfates at room temperature for detergency applications. Therefore, many experiments presented in this chapter were carried out with a surfactant concentration of 0.1 wt% or close to this value, since this is the common concentration of surfactants in the washing liquor in a washing machine.

If not specially mentioned, the calculated ratios given in this section are all molar. Prior to turbidity measurements, the samples were frozen at -20 °C. Samples investigated by heating ( $\approx 1$  °C/5 min) or stirring experiments were cooled for several days at 4 °C until some precipitate had formed or the solutions were visibly turbid or bluish. In general, samples with additional Ch or MeCh ions were less turbid than

similar samples containing only Na ions. However, all samples described in this chapter got at least well visibly bluish during cooling and could be properly analyzed.

### 5.3.1 Experiments in millipore water

#### 5.3.1.1 Influence of Ch salt on $T_{Kr}$ of ChS18 and Na salt on $T_{Kr}$ of NaS16 and NaS18

The influence of additional Na ions on  $T_{Kr}$  of NaS16 and NaS18, respectively the effect of additional Ch ions on  $T_{Kr}$  of ChS18 was investigated by heating experiments. The cations were added as the citrate salt ( $\text{Na}_3\text{Cit}$  and  $\text{Ch}_3\text{Cit}$ ) and the surfactant concentration in the aqueous solution was 1 wt%.

The results clearly showed that the addition of cations being already present as counter ion of the alkyl sulfate has nearly no effect on  $T_{Kr}$  ( $\pm 1$  °C) up to a molar ratio of counter ion to alkyl sulfate of 5. The determined  $T_{Kr}$  values were 51 °C for ChS18, 61 °C for NaS18 and 47 °C for NaS16. The values are a bit (2-3 °C) higher than the ones obtained from measurements with the turbidity apparatus. This is a kinetic effect, which is caused by the higher heating rate and will quite often be found in this chapter. Moreover, it can be deduced that the addition of citrate has also no influence on  $T_{Kr}$  within the investigated concentration range.

#### 5.3.1.2 Influence of Na salt on $T_{Kr}$ of ChS18

The effect of Na ions on  $T_{Kr}$  of an aqueous 1 wt% solution of ChS18 was investigated by heating experiments. A defined amount of  $\text{Na}_3\text{Cit}$  was added with a molar ratio of Na to Ch ranging from 0 to 4.

**Figure 5-1** illustrates that  $T_{Kr}$  of ChS18 gradually increases with increasing ratio of Na to Ch within the samples. For a ratio of Na to Ch of 4,  $T_{Kr}$  of pure NaS18 is nearly reached. Klein et al.<sup>1</sup> have already shown that the same is true for the addition of sodium ions to aqueous solutions of ChS12.

It can be expected that the effect of Na ions on  $T_{Kr}$  of ChS16, MeChS16 and MeChS18 is identical.

Therefore, to benefit from the  $T_{Kr}$  lowering effect of Ch and MeCh compared to Na, it is important that no Na ions or other ions that could increase  $T_{Kr}$  of ChSXX or MeChSXX are brought into the aqueous system.

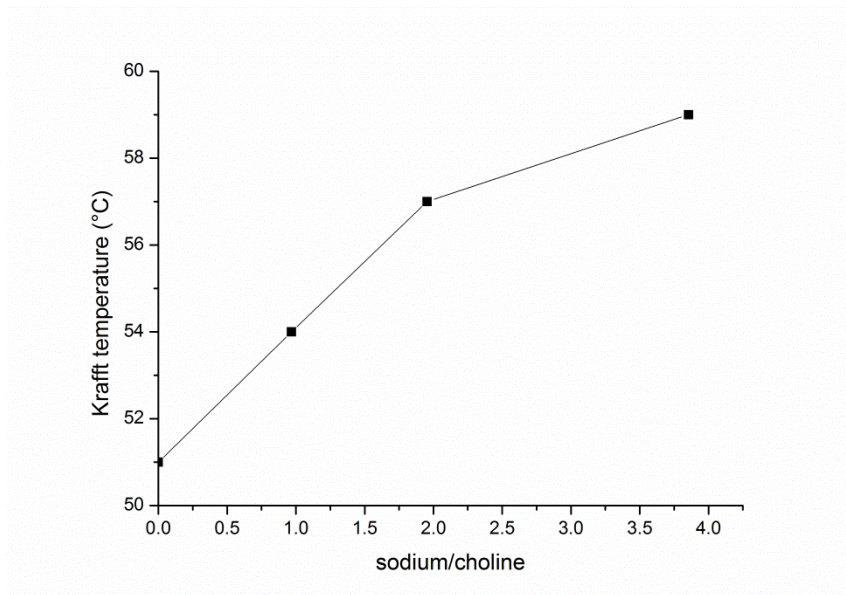


**Figure 5-1:** Influence of additional Na ions on  $T_{Kr}$  of aqueous 1 wt% solutions of ChS18.

### 5.3.1.3 Influence of Ch, MeCh salts on $T_{Kr}$ of NaS16 and NaS18

The effect of Ch and MeCh ions on  $T_{Kr}$  of aqueous NaS16/NaS18 solutions was tested by turbidity measurements and heating experiments. For the turbidity measurements, the amount of surfactant was 1 wt% and the ratio of Ch/MeCh to Na was adjusted by adding the chloride salt. For heating experiments, NaS16/NaS18 concentration was 0.1 wt% (0.2 wt% in the case of NaS18 +  $\text{Ch}_3\text{Cit}$ ) and  $\text{Ch}_3\text{Cit}$  or MeChCl was added.

The results for the NaS16 systems are shown in **Figure 5-2**. It depicts that both Ch and MeCh significantly reduce  $T_{Kr}$  of NaS16. The effect is most pronounced up to a Ch/MeCh to Na ratio of 2, continues up to a value of 4 and levels off at higher ratios. This same course of such curves was already found by Klein et al.<sup>1</sup> and Strey et al.<sup>2</sup> when adding salt to alkyl sulfates and soaps. Turbidity measurements with 1 wt% surfactant show that MeCh is slightly more efficient and effective than Ch. For Ch, it is possible to decrease  $T_{Kr}$  to 25 °C and for MeCh to 20 °C. This is in line with the lower  $T_{Kr}$  value of pure MeChS16 (7 °C) compared to ChS16 (13 °C). However, the minimum values obtained for high ratios are always around 15 °C higher than  $T_{Kr}$  of pure ChS16/MeChS16. Less precise heating measurements with 0.1 wt% surfactant yielded nearly identical curves for Ch and MeCh.

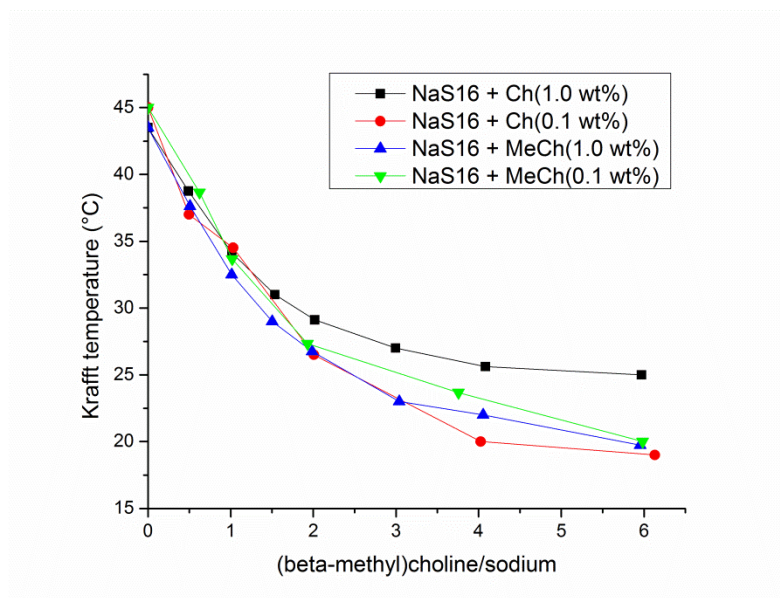


**Figure 5-2:** Influence of Ch and MeCh on  $T_{Kr}$  of aqueous NaS16 solutions. The curves were obtained by turbidity measurements (1 wt%) and heating experiments (0.1 wt%). ■ = 1 wt% NaS16 + ChCl, ● = 0.1 wt% NaS16 + Ch<sub>3</sub>Cit, ▲ = 1 wt% NaS16 + MeChCl, ▼ = 0.1 wt% NaS16 + ChCl.

The same behavior was found for the NaS18 systems (see **Figure 5-3**). Compared to NaS16, the only difference is that the minimum value of  $T_{Kr}$  is already reached at a Ch/MeCh to Na ratio of 2. Again, MeCh is a bit more efficient and effective than Ch. The minimum value of  $T_{Kr}$  obtained for the 1 wt% surfactant solutions is 50 °C for Ch and 47 °C for MeCh. These values are slightly higher than the values for pure ChS18 (49 °C) and MeChS18 (44 °C). It must be noted, that with increasing ratio of Ch/MeCh to Na, the turbidity curves showed more and more the course of the pure ChS18/MeChS18 with a slow decrease in turbidity at values close to  $T_{Kr}$ .

The identical  $T_{Kr}$  value (54 °C) for 1 wt% ChS18 + Na ions at a Ch to Na ratio of 1 (see **Figure 5-1**) and 1 wt% NaS18 + Ch ions at the same ratio just illustrates that only the actual composition of the aqueous system determines  $T_{Kr}$  and it does not matter how the ions were introduced into the system.

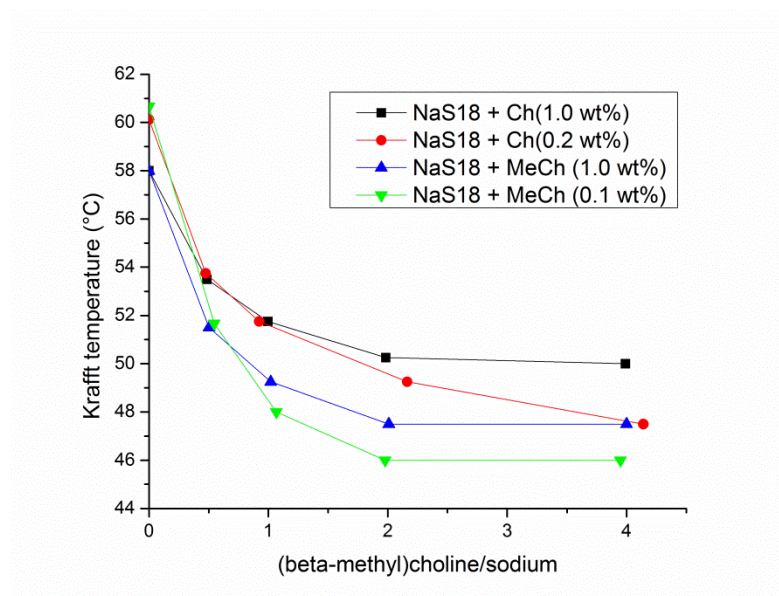


**Figure 5-3:** Influence of Ch and MeCh on  $T_{Kr}$  of aqueous NaS18 solutions. The curves were obtained by turbidity measurements (1 wt%) and heating experiments (0.1 wt%). ■ = 1 wt% NaS18 + ChCl, ● = 0.2 wt% NaS18 + Ch<sub>3</sub>Cit, ▲ = 1 wt% NaS18 + MeChCl, ▼ = 0.1 wt% NaS18 + ChCl.

Further, systems 0.1 wt% NaS16 plus Ch<sub>3</sub>Cit with an increased ratio of Na to S16 were investigated by heating experiments. The ratio of Na to S16 was adjusted to 3, 5 and 10 with NaCl and the ratio of Ch to Na was varied from 0 to 6 for each system. The results are illustrated in **Figure 5-4** and clearly show that values of  $T_{Kr}$  are nearly independent of the ratio Na to S16, only the actual ratio of Ch to Na seems to define  $T_{Kr}$  of these systems within the investigated range.

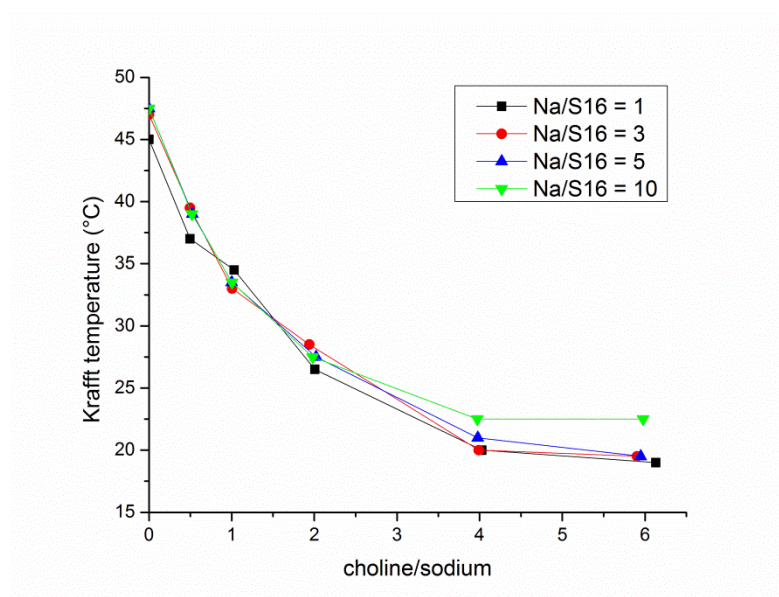


**Figure 5-4:** Influence of Ch on  $T_{Kr}$  of aqueous 0.1 wt% NaS16 solutions at different Na to S16 ratios. The curves were obtained by heating experiments. The ratio sodium to S16 is: ■ = 1, ● = 3, ▲ = 5, ▼ = 10.

Next to turbidity measurements and heating experiments, longtime stirring experiments were carried out to investigate the appearance of the mixed NaS16 plus salt solutions at room temperature. The surfactant concentration was 0.1 wt% and the solutions were stirred over night at 25 °C.

The appearance of solutions with 0.1 wt% NaS16 plus different amounts of Ch is shown in **Figure 5-5** for the series with an Na to S16 ratio of 10. The other systems with an ratio of Na To S16 of 1,3 and 5 looked identically. Up to a ratio of Ch to Na of 1, the samples were nontransparent and white. For ratios of 2 and higher, the samples became as clear as water. **Figure 5-6** shows the system 0.1 wt% NaS16 plus MeCh at a Na to MeCh ratio of 1. The behavior is the same as for the Ch systems except that the solution with a MeCh to S16 ratio of 1 is somewhat less turbid. The fact that the samples with a Ch/MeCh to Na ratio of 2 become as clear as water, indicates that the  $T_{Kr}$  values determined by heating experiments are a bit too high. The determined  $T_{Kr}$  values were about 27.5 °C. Certainly, this is a kinetic dissolution effect caused by the high heating rates (1 °C/5 min). However, the kinetic effect should not be very distinct, since the solutions with a Ch/MeCh to Na ratio of 1, for which  $T_{Kr}$  values of about 33.5 °C were determined, are still markedly turbid.



**Figure 5-5:** Photo of the series 0.1 wt% NaS16 plus Ch with additional Na after stirring for 1 d at 25 °C. The ratio of Na to S16 is 10 and the ratio of Ch to Na is: 13 = 0.0, 14 = 0.52, 15 = 1.0, 16 = 1.98, 17 = 3.97, 18 = 5.98.

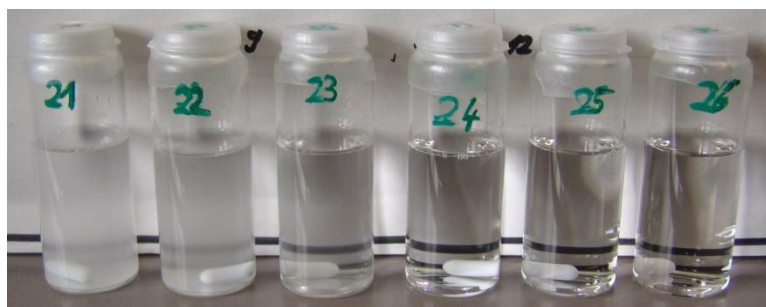


**Figure 5-6:** Photo of 0.1 wt% NaS16 plus different amounts of MeCh chloride after stirring for 1 d at 25 °C. The ratio of MeCh to Na is: 21 = 0.0, 22 = 0.62, 23 = 1.02, 24 = 1.93, 25 = 3.76, 26 = 5.91.

Based on the results presented above and the tests in hard water described in section 5.3.2, the effect of equal molar amounts of  $\text{Ch}_4\text{EDTA}$  and  $\text{Na}_4\text{EDTA}$  on the appearance of an 0.05 wt% NaS16 solutions at 25 °C was investigated. The amount of salt was chosen that the ratio of additional cation to NaS16 was 3, since this ratio of Ch to Na should yield clear solutions at 25 °C (see **Figure 5-4** and **Figure 5-5**). The solutions were stirred over night at 25 °C and the photo is shown in **Figure 5-7**. While the 0.05 wt% NaS16 solutions without salt and with  $\text{Na}_4\text{EDTA}$  is highly turbid and white, the sample with  $\text{Ch}_4\text{EDTA}$  is as clear as water.



**Figure 5-7:** Comparison of different samples containing 0.05 wt% NaS16 without and with  $\text{Na}_4\text{EDTA}$  or  $\text{Ch}_4\text{EDTA}$  after stirring for 1 d at 25 °C. Sample 20 = 0.05 wt% NaS16, sample 21 = NaS16 +  $\text{Ch}_4\text{EDTA}$  ( $\text{Ch}/\text{NaS16} = 3$ ) and sample 23 = NaS16 +  $\text{Na}_4\text{EDTA}$  ( $\text{Na}/\text{S16} = 4$ ).

These results show that the addition of Ch or MeCh to aqueous NaS16/NaS18 solutions considerably lowers  $T_{Kr}$ . For 1 wt% NaS16 and a molecular ratio of Ch/MeCh to sodium of 2,  $T_{Kr}$  is reduced below 30 °C. At the same ratio and a concentration of 0.1 wt% NaS16, Ch and MeCh are able to decrease  $T_{Kr}$  even below 25 °C. It was also shown that this effect is only dependent on the ratio of Ch to Na in solution and independent of the Na to S16 ratio. No such effect is found for adding additional Na ions to NaSXX solutions. For solutions with 0.1 and 1 wt% NaS18, it was not possible to reduce  $T_{Kr}$  below room temperature by adding Ch or MeCh salts. A way to reduce  $T_{Kr}$  of these mixed systems below room temperature will be presented in the following section.

The  $T_{Kr}$ -reducing effect of TAAs on Na alkyl sulfates, respectively Na soaps, was explained by Yu et al.<sup>3</sup>, respectively Strey et al.<sup>2</sup>, by counter ion exchange of the anionic surfactant in solution from Na to TAA. Possibly, this counter ion exchange is driven by mixed micellization between TAA ions and anionic surfactant micelles due to hydrophobic interactions between the organic ions and hydrophobic parts of the micelle (see section 4.3.2). Studies on the mixed systems NaS12 plus TAAs ( $\text{TMA}^+$

to TBA<sup>+</sup>) showed that these organic ions have a strong tendency to interact with the NaS12 micelle by simultaneously replacing Na ions from the micelle surface.<sup>10, 11</sup> Collins' concept also predicts stronger interactions for TAAs with the alkyl sulfate head group than for Na<sup>12, 13</sup>, which would support mixed micellization and the replacement of Na ions by TAAs on the micelle surface. NMR experiments show that this effect is very pronounced for TAA to NaS12 ratios smaller than 1. At higher TAA to Na ratios the effect gets weaker until it levels off indicating saturation of the micelle by TAAs. Further, the effect was more distinct the larger the TAA ion.<sup>10</sup> Assuming that the replacement of Na ions by TAAs at the surfactant head groups is responsible for the decrease in  $T_{Kr}$ , these findings would explain the similar course of the obtained  $T_{Kr}$  curves in this study as well as the slightly stronger effect observed for MeCh compared to Ch. In a very simplified way, one could say that the organic ions form a kind of (hydrophobic) shell that protects the alkyl sulfate surfactants from interactions and the consequent precipitation with the Na ions. Further, from the above mentioned NMR experiments, it can be deduced that a kind of competition for binding to the alkyl sulfate micelles, which is very distinct around equimolarity, exists between Na and TAAs. Therefore, it is reasonable that the addition of Na ions to ChSXX increases  $T_{Kr}$  (see **Figure 5-1** and reference 1). Systematic effects on  $T_{Kr}$  observed by the addition of alkali ions to alkali alkyl sulfates or alkali soaps, as shown by Klein et al.<sup>1</sup>, suggests that specific ion effects play an important role, too. This can be seen by considerable differences in the direction and the extent of the effect on  $T_{Kr}$  depending on the initial surfactant (alkali cation + anion) and the added alkali cation. For example, the addition of Na to KS12 reduces  $T_{Kr}$  by 4 °C at a Na to K ratio of 1, however the addition of K to NaS12 increases  $T_{Kr}$  by 20 °C at the same ratio.<sup>1</sup> This suggests a much stronger binding of K to alkyl sulfate micelles than sodium, which is in line with Collins' concept of matching water affinities<sup>12, 13</sup> and was proven for S12 micelles by a combined SANS and SAXS study<sup>14</sup>.

Of course, these are only assumptions and the situation in these mixed systems is certainly much more complex. Independently from any possible explanations for the observed effects, the only statement that can be made for sure is the following: the addition of Ch/MeCh or other TAAs to NaSXX must reduce the free energy of the micellar state in the mixed system compared to the pure NaSXX system. This must be true, since the formation of NaSXX crystals, exhibiting the same free energy as in the pure NaSXX system, is still possible within the mixed systems. Further, comparing the results of this study and the ones of Klein et al.<sup>1</sup>, it seems that a general behavior for alkyl sulfate and soap systems with monovalent cations can be deduced. If  $T_{Kr}$  of the initial surfactant is higher than  $T_{Kr}$  of the "new" surfactant

consisting of the cation of the added salt plus initial surfactant anion, the addition of salt will decrease  $T_{Kr}$  of the mixed system. The same is true the other way round. The extent of this effect, however, is dependent of the initial surfactant (cation + anion) and the added cation. Further, the salt effect is more pronounced at low salt concentrations and levels off at higher ones.

#### **5.3.1.4 Effect of nonionic alcohol ethoxylate on $T_{Kr}$ of ChS18 and NaS18**

As already mentioned, the goal of this work was to prepare solutions of long chain alkyl sulfates exhibiting a  $T_{Kr}$  value below room temperature for detergent applications. Since it was not possible to depress  $T_{Kr}$  of NaS18 below room temperature by adding Ch or MeCh (see **Figure 5-3**), the nonionic alcohol ethoxylate surfactant Lutensol AO7 (LutAO7 = C13-15EO7) was used to depress  $T_{Kr}$  of the S18 surfactants. This strategy was chosen, since common detergent formulations contain a mixture of anionic and nonionic surfactants.

First, 1 wt % ChS18 and NaS18 solutions with different mass ratios of LutAO7 to surfactant (steps of 0.2) were prepared and stirred for 2 d at 25 °C. It must be noted that all samples containing NaS18 plus LutAO7 were only analyzed by longtime stirring experiments, since heating experiments gave much too high  $T_{Kr}$  values due to very distinct kinetic dissolution effects.

LutAO7 was able to reduce  $T_{Kr}$  of both surfactant solutions below room temperature. However, the LutAO7 to surfactant mass ratio necessary to obtain clear solutions at room temperature was much lower for ChS18 (1.4) than for NaS18 (2.8). The difference in appearance between a 1 wt% NaS18 solutions and a 1 wt% ChS18 with a LutAO7 to surfactant mass ratio of 1.4 after stirring for 2 d at 25 °C is shown in **Figure 5-8**. The ChS18 sample is clear, while the NaS18 is nontransparent white. Possibly, this big difference results from the different "states" of the pure surfactant solutions at room temperature (see section 4.3.4). While for NaS18, LutAO7 must dissolve surfactant crystals, for ChS18 it has only to destruct a liquid crystalline phase with fluid surfactant chains.



**Figure 5-8:** Photo of 1 wt% NaS18 (left) and ChS18 (right) plus additional LutAO7. The mass ratio of LutAO7 to surfactant was always around 1.4.

Further, samples with 0.05 wt% NaS18 without salt, with Na<sub>4</sub>EDTA and with Ch<sub>4</sub>EDTA were prepared. The added amount of Ch or Na introduced by the salt was 3 times the initial amount of Na originating from NaS18. According to the results presented in **Figure 5-3**, this ratio of Ch to Na should be sufficient to decrease  $T_{Kr}$  of aqueous 0.05 wt% NaS18 solutions close to the value of pure 0.05 wt % ChS18. To each sample, different amounts of LutAO7 were added. The mass ratio of LutAO7 to NaS18 ranged from 0 to 2.0 in steps of 0.2 for the samples containing NaS18 plus Ch<sub>4</sub>EDTA, and from 0 to 2.8 in steps of 0.4 for the samples with NaS18 plus Na<sub>4</sub>EDTA. The samples were stirred for 2 days at 25 °C.

Again, the LutAO7 to NaS18 ratio necessary to obtain clear solutions was found to be much smaller for the samples with Ch<sub>4</sub>EDTA (1.4) than for the samples with Na<sub>4</sub>EDTA (2.4). **Figure 5-9** illustrates the great difference in appearance between samples with additional Ch and samples with additional Na at identical LutAO7 to NaS18 ratios. Even at very low LutAO7 to NaS18 ratios, the samples with additional Ch were only slightly bluish transparent, while the solutions with additional Na were nontransparent and white.

The same striking difference was found for 0.05 wt% NaS18 solutions with additional Ch<sub>4</sub>EDTA and Na<sub>4</sub>EDTA without LutAO7. The sample with additional Na was nontransparent and white after cooling for several days at 4 °C and after stirring for 2 d at 25 °C. But the sample with additional Ch was always transparent and bluish. Probably, with increasing ratio of Ch to Na, the system's behavior changes from that of pure NaS18 to the one of the pure ChS18. For pure ChS18, at low concentrations, also a bluish and transparent solution was obtained after stirring for 2 d at 25 °C (see section 4.3.4 and **Figure 4-5**), which was attributed to the formation of a liquid crystalline phase. However, it is not sure that for the NaS18 plus Ch system this is the thermodynamically stable state, since the solutions were heated above  $T_{Kr}$  after

preparation. Possibly, the formation of this phase yielding a bluish solution is only kinetically stable and with time NaS18 crystals form leading to turbid solution.



**Figure 5-9:** Comparison of different samples containing 0.05 wt% NaS18,  $\text{Na}_4\text{EDTA}$  or  $\text{CH}_4\text{EDTA}$  and LutAO7 after stirring for 2 days at 25 °C. Grouped samples contain always nearly the same amount of NaS18 and LutAO7, but differ in  $\text{Na}_4\text{EDTA}$  and  $\text{CH}_4\text{EDTA}$ . The more translucent samples always contain  $\text{CH}_4\text{EDTA}$ . The bluish character of the samples decreases with increasing mass ratio of LutAO7 to NaS18, e. g. from 3 to 7. Sample 9 is as clear as water. Samples 3/13: LutAO7/NaS18 = 0.4; Samples 5/15: LutAO7/NaS18 = 0.8; Samples 7/15: LutAO7/NaS18 = 1.2; Samples 9/16: LutAO7/NaS18 = 1.6.

To sum up the results of this section and section 5.3.1.3, concerning surfactant solubility/ $T_{Kr}$ , it is possible to achieve the positive effects of pure ChSXX compared to pure NaSXX by adding a certain amount of Ch to aqueous solutions of NaSXX. These findings will be utilized in the experiments presented in the next section, since this allows us to use the positive effects of Ch without specially synthesizing the ChSXX surfactants. This can be an important point in possible future applications, since formulations can be based on the common and well available NaSXX surfactants and no new surfactant has to be synthesized and introduced into the market.

### 5.3.2 Experiments in hard water

Hard tap water causes significant problems in laundry applications. It contains polyvalent Ca and Mg ions, which heavily interact with simple surfactants like alkyl sulfates or soaps. The formed crystals have a very low solubility in water at room temperature, what is illustrated by very high  $T_{Kr}$  values of calcium alkyl sulfates<sup>5</sup> ( $\text{Ca}(\text{S12})_2 = 50$  °C;  $\text{Ca}(\text{S14})_2 = 71$  °C,  $\text{Ca}(\text{S16})_2 = 85$  °C). Simply speaking, as long as the washing solution contains "free" hard Ca and Mg ions, these ions will precipitate nearly all washing active alkyl sulfates from solution at room temperature. Therefore, to efficiently and effectively wash with alkyl sulfates at low temperatures, it is necessary to remove the hard ions from the washing solution, i.e. soften the water. This can be achieved by so-called builders. Such builders can be for example

sodium silicate, sodium carbonate, zeolites, polymers, citrate or EDTA. All of them have in common that they remove the hard ions from solution based on a specific mechanism. The builders used in this study, EDTA and citrate (see **Figure 5-10**), are chelating agents and remove hard ions from solution by forming water soluble chalet complexes. Builders are the second most important ingredient of a detergent and next to water softening, they have to fulfill many other functions like for example increasing the efficiency of the surfactant, exhibiting detergency performance itself, dispersing soils and preventing redeposition on clothes, providing alkalinity and being environmentally and economically practicable.<sup>15-17</sup> It must be noted that, from an environmental point of view, the poorly biodegradable EDTA was no good choice, but it was the only very strong chelating agent at hand. The use of some other strong and well biodegradable organic chelating agents, like methylglycinediacetic acid (MGDA, see **Figure 5-10**) would have been more suitable.<sup>18</sup>

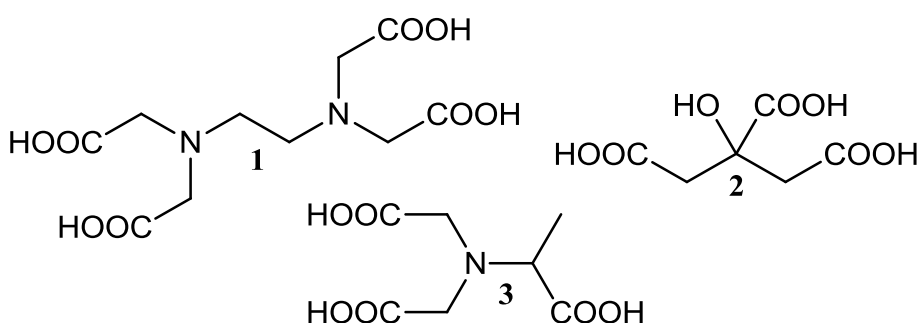


**Figure 5-10:** The chemical structures of ethylenediaminetetraacetic acid (EDTA) (1), citric acid (2) and methylglycinediacetic acid (MGDA) (3).

In detergent formulations, builders are commonly used as their Na salts, respectively the basic pH value necessary to deprotonate the builders' carboxylate groups is adjusted by Na salts. However, to benefit from the reduced  $T_{Kr}$  values of Ch or MeCh alkyl sulfates, it is crucial that no large amount of additional ions that would raise  $T_{Kr}$  of the alkyl sulfate are brought into the aqueous system (see section 5.3.1.2). Simply speaking, in common detergent formulations, the introduction of long chain Ch alkyl sulfates would be useless, since the  $T_{Kr}$ -reducing effect of Ch as counter ion instead of Na would be displaced by the high amount of Na introduced to the formulation by common Na builders. Considering this problem and the effect of Ch or MeCh on  $T_{Kr}$  of aqueous NaS16 and NaS18 solutions as shown in section 5.3.1.3, the idea of a "2 in 1"-builder was born. Such a "2 in 1"-builder shall consist of common builders already used in detergents only using Ch or MeCh as counter ion instead of Na. These builders should efficiently soften hard water and additionally decrease  $T_{Kr}$  of Na alkyl sulfates. As a consequence, common Na alkyl sulfates can be used as

surfactants and only Ch or MeCh builders have to be synthesized. If the free acid of the builder is available, this can easily be done by simple neutralization reactions.

In what follows, results of the experiments in hard water showing the improved performance of these "2 in 1"-builders compared to simple Na builders are presented. The experiments were only carried out with Ch, but MeCh is meant to show the same effects.

### 5.3.2.1 NaS16 plus additional builder

#### 5.3.2.1.1 Ch<sub>4</sub>EDTA/Na<sub>4</sub>EDTA

To show the "2 in 1"-builder effect for NaS16, samples with 0.05 wt% NaS16 and certain amounts of Ch<sub>4</sub>EDTA or Na<sub>4</sub>EDTA were prepared in hard water with 12.5 and 25 °d (Grad deutscher Härte). The ratio of EDTA to Ca ranged from 0 to 2 in steps of 0.25 for samples with Ch<sub>4</sub>EDTA and in steps of 0.5 for samples with Na<sub>4</sub>EDTA. The Ch or Na to S16 ratio was also determined by the ratio of EDTA to Ca, since EDTA was the only additional Ch or Na source. Note that the molecular amount of S16 equals the molecular amount of sodium introduced by NaS16. Water hardness, exact molecular ratios of EDTA to Ca and Ch or Na to S16 for each sample are given in **Table 5-1** for samples with Ch<sub>4</sub>EDTA and in **Table 5-2** for samples with Na<sub>4</sub>EDTA. The samples were analyzed by heating and stirring experiments.

Sample	°d	n(EDTA)/n(Ca)	n(Ch)/n(S16)	T <sub>Kr</sub> [°C]
green 1	12.50	0.00	0.00	> 75
green 2	12.45	0.26	1.61	> 75
green 3	12.41	0.53	3.21	> 75
green 4	12.37	0.72	4.32	73
green 5	12.33	1.00	6.04	24
green 6	12.28	1.28	7.72	17
green 7	12.22	1.59	9.58	16
green 8	12.14	2.07	12.31	15
green 9	25.00	0.00	0.00	> 75
green 10	24.81	0.27	3.24	> 75
green 11	24.64	0.52	6.23	> 75
green 12	24.45	0.79	9.53	75
green 13	24.29	1.04	12.35	20
green 14	24.11	1.31	15.42	15
green 15	23.91	1.61	18.89	15
green 16	23.58	2.13	24.23	15

**Table 5-1:** Water hardness and exact molecular ratios of EDTA to Ca and Ch to S16 of all samples that were prepared with 0.05 wt% NaS16 plus Ch<sub>4</sub>EDTA. Samples green 1 to 8 were prepared in water with 12.5 °d, samples green 9 to 16 in water with 25 °d and the molar ratio of EDTA to Ca increases with increasing number for each set. T<sub>Kr</sub> value of each sample is also listed.

Sample	°d	n(EDTA)/n(Ca)	n(Na)/n(S16)	T <sub>Kr</sub> [°C]
green 20	12.59	0.00	1.00	> 75
green 22	12.54	0.49	4.02	> 75
green 22	12.48	0.99	7.07	46
green 23	12.42	1.49	10.07	46
green 24	12.37	2.01	13.10	47
green 25	24.92	0.00	1.00	> 75
green 26	24.70	0.50	7.08	> 75
green 27	24.46	1.04	13.47	48
green 28	24.24	1.55	19.46	46
green 29	24.02	2.08	25.52	49

**Table 5-2:** Water hardness and exact molecular ratios of EDTA to Ca and Na to S16 of all samples that were prepared with 0.05 wt% NaS16 plus Na<sub>4</sub>EDTA. Samples green 20 to 24 were prepared in water with 12.5 °d, samples green 25 to 29 in water with 25 °d and the molar ratio of EDTA to Ca increases with increasing number for each set. T<sub>Kr</sub> value of each sample is also listed.

T<sub>Kr</sub> values for each sample are shown in **Figure 5-11**. Heating experiments were stopped at 75 °C and for samples that did not become clear below this temperature (EDTA to Ca ratio  $\leq 0.5$ ) T<sub>Kr</sub> was fixed at 85 °C. The results are perfectly in line with what would have been expected by considering the results in millipore water. EDTA is a very strong chelating agent and it can be assumed that it stoichiometrically removes Ca ions from the aqueous solution. Consequently, as soon as the ratio of EDTA to Ca is equal or bigger than one, the system should behave as in millipore water. And that is exactly what was found.

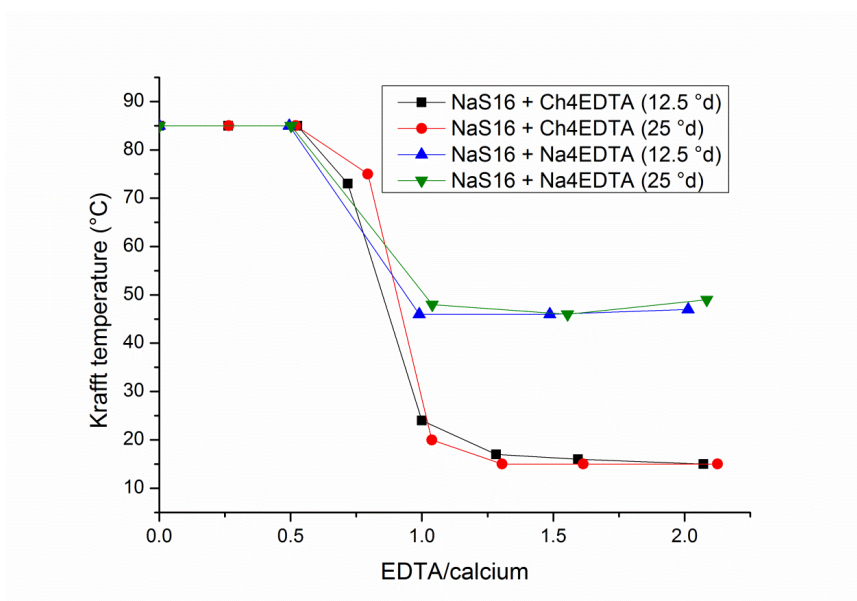


**Figure 5-11:** T<sub>Kr</sub> values of 0.05 wt% NaS16 samples plus Ch<sub>4</sub>EDTA or Na<sub>4</sub>EDTA in hard water plotted against the molecular ratio EDTA to Calcium. T<sub>Kr</sub> values of samples that were still turbid at 75 °C were fixed at 85 °C. ■ = NaS16 + Ch<sub>4</sub>EDTA at 12.5 °d, ● = NaS16 + Ch<sub>4</sub>EDTA at 25 °d, ▲ = NaS16 + Na<sub>4</sub>EDTA at 12.5 °d, ▼ = NaS16 + Na<sub>4</sub>EDTA at 25 °d.

As long as the ratio of EDTA to Ca is smaller than one,  $T_{Kr}$  is higher than 70 °C. This is due to the high  $T_{Kr}$  value of  $\text{Ca}(\text{S16})_2$ , which is 85 °C.<sup>5</sup>  $T_{Kr}$  values of 73 and 75 °C for the samples with  $\text{Ch}_4\text{EDTA}$  at a EDTA to Ca ratio of around 0.75 suggest a  $T_{Kr}$ -reducing effect probably caused by the increased Ch to Ca ratio. However, the effect is much less pronounced than for pure NaS16 (see section 5.3.1.3), since the actual Ch to Ca ratio of these samples was 10 and 15. Thus, it is impossible to significantly lower  $T_{Kr}$  of  $\text{Ca}(\text{S16})_2$  by adding reasonable amounts of Ch. This indicates much stronger binding of Calcium ions to alkyl sulfate micelles than for Na or Ch ions. This was also concluded by Klein et al.<sup>1</sup> from similar experiments with aqueous  $\text{ChS12/NaS12}$  solutions plus additional Calcium chloride. The results are independent from water hardness.

For ratios of EDTA to Ca equal or larger than one, nearly the same  $T_{Kr}$  values as in millipore water were measured for both the Ch and the Na system.  $T_{Kr}$  values of 0.05 wt% NaS16 plus  $\text{Na}_4\text{EDTA}$  are always slightly higher than 45 °C and remain constant even for very high ratios of sodium to S16. All samples with  $\text{Ch}_4\text{EDTA}$  show  $T_{Kr}$  values lower than 25 °C. This is in line with the results from section 5.3.1.3, since the ratio of Ch to S16 is always bigger than 4. For very high ratios of Ch to S16,  $T_{Kr}$  decreases up to 15 °C. Again, the results are independent of water hardness.

Stirring experiments were carried out with all samples, too. For a ratio of EDTA to Ca smaller than 1, all samples were nontransparent and white after stirring for 2 d at 25 °C, irrespective of the counter ion used. **Figure 5-12** shows the difference in appearance of similar samples, which only differ in  $\text{Ch}_4\text{EDTA}$  and  $\text{Na}_4\text{EDTA}$ , at EDTA to Ca ratios bigger than 1 and at 25 °d after stirring for 2 d at 25 °C. The samples with Ch builder became all as clear as water, while similar samples with Na builder were nontransparent and white. The same behavior was found at 12.5 °d water hardness (photo not shown).



**Figure 5-12:** Comparison of similar samples differing only in  $\text{Ch}_4\text{EDTA}$  and  $\text{Na}_4\text{EDTA}$  at 25 °d after stirring for 2 d at 25 °C. Samples green 13, 15 and 16 contain  $\text{Ch}_4\text{EDTA}$ , samples green 27, 28 and 29 contain  $\text{Na}_4\text{EDTA}$ . The ratio of EDTA to Ca was always  $\geq 1$ . The exact values and ratios are listed in Table 5-1 and Table 5-2.

To ensure that this concept also works for NaS16 plus additional Na ions in hard water, NaS16, NaCl and Ch<sub>4</sub>EDTA were mixed in hard water of 12.5 and 25 °d. The ratio of Na to S16 was adjusted to 3 and 5 by NaCl and the portion of Ch<sub>4</sub>EDTA was chosen so that the ratio of EDTA to Ca was always  $\geq 1$ . Water hardness, exact ratios of Na to S16, EDTA to Ca and Ch to Na are listed in **Table 5-3**. The samples were investigated by heating and stirring experiments.

Sample	°d	n(Na)/n(S16)	n(EDTA)/n(Ca)	n(Ch)/n(Na)	T <sub>Kr</sub>
20	12.20	3.00	1.02	2.02	30
21	12.15	3.03	1.28	2.50	27
22	12.11	3.12	1.54	2.92	24
23	24.21	3.15	1.03	3.87	25
24	24.04	3.16	1.30	4.85	21
25	23.86	3.04	1.58	6.04	21
26	12.20	5.02	1.02	1.21	33
27	12.15	5.37	1.29	1.42	31
28	12.11	4.98	1.54	1.82	28
29	24.21	4.94	1.03	2.46	26
30	24.04	4.96	1.30	3.05	23
31	23.86	5.03	1.58	3.60	23

**Table 5-3:** Water hardness and exact molecular ratios of EDTA to Ca, Na to S16 and Ch to Na of all samples with 0.05 wt% NaS16 plus additional Na and Ch<sub>4</sub>EDTA. T<sub>Kr</sub> value of each sample is also listed.

With regard to the experiments described above and in section 5.3.1.3, two assumptions can be made. First, NaS16 should behave like in millipore water, since the used amounts of EDTA should remove all Ca ions. Second, additional Na ions should also have no significant effect on T<sub>Kr</sub> and only the molecular ratio of Ch to Na should be important. As a consequence, plotting T<sub>Kr</sub> of all samples against the ratio of Ch to Na should give a curve as shown in **Figure 5-4**, irrespective of the ratio of Na to S16 or of EDTA to Ca. The resulting diagram is shown in **Figure 5-13**. The measured values fit very well to the curve measured for 0.1 wt% NaS16 in millipore water, which is drawn as a line for comparison reasons.

These results again show that EDTA efficiently removes all Ca ions from solution and that T<sub>Kr</sub> only depends on the ratio of Ch to Na, irrespective of the molar amount of S16 within the sample. Thus, the T<sub>Kr</sub>-increasing effect of small amounts of Na ions introduced to mixed NaS16 plus Ch aqueous systems from other sources can be displaced by increasing the amount of Ch salt within the aqueous system.

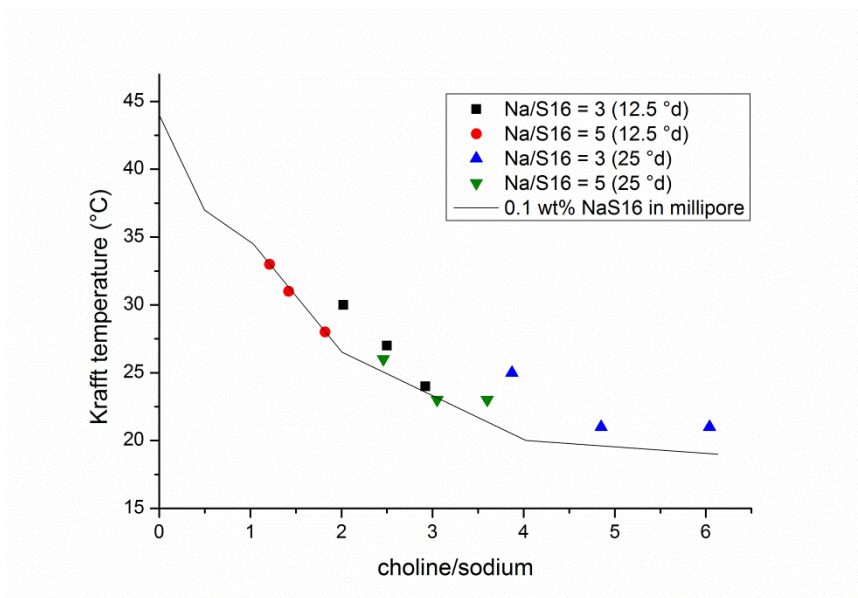


**Figure 5-13:** Plot of  $T_{Kr}$  against the ratio of Ch to Na for all samples listed in Table 5-3. Symbols represent the measured values. The continuous line represents the shape of the curve for 0.1 wt% NaS16 in millipore water. ■ = Na/S16 = 3 at 12.5 °d, ● = Na/S16 = 5 at 12.5 °d, ▲ = Na/S16 = 3 at 25 °d, ▼ = Na/S16 = 5 at 25 °d.

In stirring experiments for 2 d at 25 °C, all samples became clear as water except numbers 26 and 27, which remained markedly turbid. This is due to a too low ratio of Ch to Na and perfectly in line with what was found in millipore water. This observation indicates that a molecular ratio of Ch to Na of 1.82 is sufficient to reduce  $T_{Kr}$  of a 0.05 wt% NaS16 solution below 25 °C (see sample 28 in **Table 5-3**).

These findings reveal that, using the strong chelating agent EDTA plus Ch, it is possible to depress  $T_{Kr}$  of NaS16 below room temperature even in hard water. In this case,  $Ch_4EDTA$  acts as a "2 in 1"-builder. This effect cannot be observed for  $Na_4EDTA$ , for which  $T_{Kr}$  can only be reduced to the value of pure NaS16 by removing all hard water ions.

### 5.3.2.1.2 $Ch_3Cit/Na_3Cit$

Similar experiments as described in chapter 5.3.2.1.1 for 0.05 wt % NaS16 plus  $Ch_4EDTA$  or  $Na_4EDTA$  were carried out with  $Ch_3Cit$  or  $Na_3Cit$ . The preparation of the samples was the same except that the ratio of citrate to Ca varied from 0 to 5. Water hardness, exact ratios of citrate to Ca and Ch or Na to S16 for each sample are given **Table 5-4** for samples with  $Ch_3Cit$  and in **Table 5-5** for samples with  $Na_3Cit$ . The samples were analyzed by heating and stirring experiments.

Sample	°d	n(Cit)/n(Ca)	n(Ch)/n(S16)	T <sub>Kr</sub> [°C]
1	12.50	0.51	2.34	> 75
2	12.50	1.06	4.85	> 75
3	12.49	1.97	9.05	66
4	12.48	3.05	13.99	61
5	12.47	5.03	22.99	50
6	24.99	0.50	4.62	> 75
7	24.98	1.01	9.28	> 75
8	24.95	1.99	18.20	63
9	24.92	3.06	27.88	55
10	24.86	5.09	45.65	45

**Table 5-4:** Water hardness and exact molecular ratios of citrate to Ca and Ch to S16 of all samples prepared with  $\text{CH}_3\text{Cit}$ . Samples 1 to 5 were prepared in water with 12.5 °d, samples 6 to 10 in water with 25 °d and the molar ratio of citrate to Ca increases with increasing number for each set. T<sub>Kr</sub> value of each sample is also listed.

Sample	°d	n(Cit)/n(Ca)	n(Na)/n(S16)	T <sub>Kr</sub> [°C]
11	12.50	0.50	3.32	> 75
12	12.50	0.96	5.41	> 75
13	12.50	2.01	10.25	> 75
14	12.50	3.02	14.90	68
15	12.50	5.08	24.31	58
16	25.01	0.48	5.41	> 75
17	25.01	1.01	10.29	> 75
18	25.01	2.01	19.46	71
19	25.01	3.01	28.59	65
20	25.01	5.03	46.60	53

**Table 5-5:** Water hardness and exact molecular ratios of citrate to Ca and Na to S16 of all samples prepared with  $\text{Na}_3\text{Cit}$ . Samples 11 to 15 were prepared in water with 12.5 °d, samples 16 to 20 in water with 25 °d and the molar ratio of citrate to Ca increases with increasing number for each set. T<sub>Kr</sub> value of each sample is also listed.

In **Figure 5-14**, T<sub>Kr</sub> values of the samples are plotted against the ratio citrate to Ca. For all samples and citrate to Ca ratios  $\geq 2$ , T<sub>Kr</sub> decreases with increasing ratio of citrate to Ca. Comparing similar samples with  $\text{CH}_3\text{Cit}$  and  $\text{Na}_3\text{Cit}$ , T<sub>Kr</sub> values of samples with Ch are always around 10 °C lower. However, even at a citrate to Ca ratio of 5, T<sub>Kr</sub> of samples with Ch are still 45 and 50 °C and at a ratio of 1, none of the samples became clear below 75 °C. This is a huge difference compared to the samples with a ratio of EDTA to Ca  $\geq 1$  (see **Figure 5-11**). This can only be due to “free” Ca ions, since the ratio of Ch to Na was by far big enough to reduce T<sub>Kr</sub> of 0.05 wt% NaS16 to below 25 °C (see **Table 5-4**). T<sub>Kr</sub> values of the samples with  $\text{Na}_3\text{Cit}$  are also considerably higher than the value of pure NaS16. These results clearly show that citrate removes Ca ions much less from solution than EDTA, a fact already known in literature.<sup>15, 17</sup>

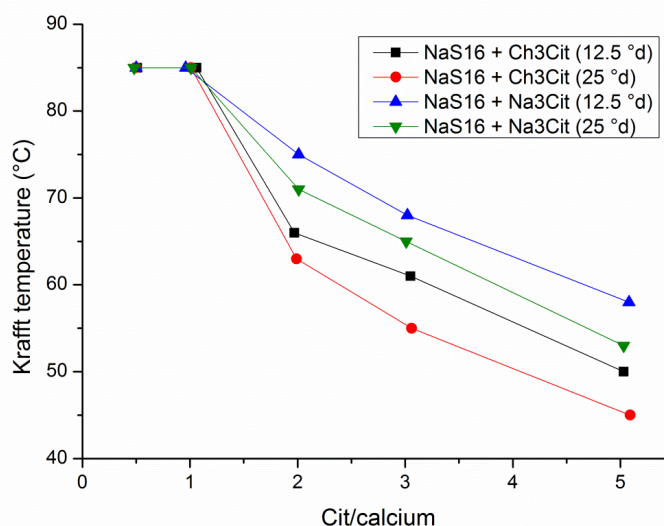


**Figure 5-14:**  $T_{Kr}$  values of 0.05 wt% NaS16 samples plus  $\text{Ch}_3\text{Cit}$  or  $\text{Na}_3\text{Cit}$  in hard water plotted against the ratio citrate to Ca.  $T_{Kr}$  values of samples that were still turbid at 75 °C were fixed at 85 °C. ■ = NaS16 +  $\text{Ch}_3\text{Cit}$  at 12.5 °d, ● = NaS16 +  $\text{Ch}_3\text{Cit}$  at 25 °d, ▲ = NaS16 +  $\text{Na}_3\text{Cit}$  at 12.5 °d, ▼ = NaS16 +  $\text{Na}_3\text{Cit}$  at 25 °d

Stirring experiments for 2 d at 25 °C were carried out, too. As expected, all samples with  $\text{Ch}_3\text{Cit}$  and  $\text{Na}_3\text{Cit}$  remained highly turbid and white.

It can be summarized that the weak chelating agent citrate is less appropriate to demonstrate the effect of a "2 in 1"-builder than the strong chelating agent EDTA. Although values for  $\text{Ch}_3\text{Cit}$  are around 10 °C lower than for comparable solutions with  $\text{Na}_3\text{Cit}$ , "free" Ca ions deteriorate the  $T_{Kr}$ -reducing effect of Ch by much stronger binding to the alkyl sulfate micelles than Na or Ch.

### 5.3.2.2 NaS18 plus LutAO7 and builder

#### 5.3.2.2.1 $\text{Ch}_4\text{EDTA}/\text{Na}_4\text{EDTA}$

In section 5.3.1.4, it was shown that a LutAO7 to ChS18 mass ratio of 1.4 is sufficient to reduce  $T_{Kr}$  of ChS18 below 25 °C in millipore water. The same value was found for aqueous solutions of NaS18 plus additional Ch with a Ch to Na ratio of 3. For NaS18, the mass ratio was considerably higher (2.4). Based on these findings, samples were prepared to show the "2 in 1"-builder effect in aqueous NaS18 plus LutAO7 systems in hard water.

Certain amounts of NaS18, LutAO7 and  $\text{Ch}_4\text{EDTA}$  or  $\text{Na}_4\text{EDTA}$  were mixed in hard water of 12.5 and 25 °d. All samples contained a total amount of surfactant NaS18 plus LutAO7 of 0.1 wt% and the mass ratio of Lut AO7 to NaS18 was chosen to be 1.5. The ratio of EDTA to Ca was adjusted from 0 to 1.5 in steps of 0.25. Water hardness, exact ratios of EDTA to Ca, Ch or Na to S18 and the mass ratio of LutAO7

to NaS18 for each sample are given in **Table 5-6** for samples with  $\text{CH}_4\text{EDTA}$  and in **Table 5-7** for samples with  $\text{Na}_4\text{EDTA}$ . The samples were analyzed by stirring experiments.

Sample	$^{\circ}\text{d}$	$n(\text{EDTA})/n(\text{Ca})$	$n(\text{Ch})/n(\text{S18})$	LutAO7/NaS18
green 30	12.43	0.00	0.00	1.49
green 31	12.33	0.51	4.15	1.65
green 32	12.29	0.78	6.34	1.56
green 33	12.24	1.02	8.32	1.67
green 33.5	12.20	1.29	10.45	1.51
green 34	12.16	1.54	12.43	1.50
green 35	24.85	0.00	0.00	1.50
green 36	24.50	0.51	8.28	1.50
green 37	24.32	0.78	12.51	1.51
green 38	24.14	1.04	16.33	1.47
green 39	23.78	1.59	24.64	1.48

**Table 5-6:** Water hardness and exact molecular ratios of EDTA to Ca, Ch to S18 and mass ratio of LutAO7 to NaS18 of all samples with  $\text{CH}_4\text{EDTA}$ . Samples green 30 to 34 were prepared in water with 12.5  $^{\circ}\text{d}$ , samples green 35 to 39 in water with 25  $^{\circ}\text{d}$  and the molar ratio of EDTA to Ca increases with increasing number for each set. The total amount of surfactant NaS18 plus LutAO7 was always 0.1 wt%.

Sample	$^{\circ}\text{d}$	$n(\text{EDTA})/n(\text{Ca})$	$n(\text{Na})/n(\text{S18})$	LutAO7/NaS18
green 40	12.37	0.51	5.22	1.55
green 41	12.34	0.77	7.31	1.53
green 42	12.31	1.01	9.26	1.52
green 42.5	12.28	1.28	11.34	1.55
green 43	12.25	1.53	13.44	1.51
green 44	24.62	0.50	9.17	1.52
green 45	24.51	0.77	13.58	1.50
green 46	24.40	1.01	17.40	1.52
green 47	24.17	1.56	25.90	1.50

**Table 5-7:** Water hardness and exact molecular ratios of EDTA to Ca, Na to S18 and mass ratio of LutAO7 to NaS18 of all samples with  $\text{Na}_4\text{EDTA}$ . Samples green 40 to 43 were prepared in water with 12.5  $^{\circ}\text{d}$ , samples green 44 to 47 in water with 25  $^{\circ}\text{d}$  and the molar ratio of EDTA to Ca increases with increasing number for each set. The total amount of surfactant NaS18 plus LutAO7 was always 0.1 wt%.

The appearance of the samples with  $\text{CH}_4\text{EDTA}$  builder after stirring for 2 d at 25  $^{\circ}\text{C}$  is shown in **Figure 5-15** (12.5  $^{\circ}\text{d}$ ) and **Figure 5-16** (25  $^{\circ}\text{d}$ ). Samples with a ratio of EDTA to Ca smaller than 1 were nontransparent and turbid. As soon as the ratio of EDTA to Ca was  $\geq 1$ , the samples were as clear as water. The only exception is green 33, which was visibly turbid. However, there is no reasonable explanation why sample green 38 was clear and green 33 not, since for both samples the ratio of EDTA to Ca is slightly higher than one and the ratio of Ch to S18 was much larger than 3. The samples only differed in the degree of water hardness. Possibly, the

much higher ratio of Ch to S18 or the much higher amount of ions in solution caused this difference. Nevertheless, as soon as the ratio of EDTA to Ca is 1.25, the samples were clear as water, irrespective of water hardness.

It should be noted that for ratios of EDTA to calcium  $< 1$  all samples were nontransparent and white after cooling. For ratios  $\geq 1$ , samples with  $\text{Na}_4\text{EDTA}$  were also nontransparent and white, but samples with  $\text{Ch}_4\text{EDTA}$  were only markedly turbid/bluish and translucent. Possible reasons for these differences have already been discussed in sections 5.3.1.4.



**Figure 5-15:** Appearance of samples with a mass ratio of LutAO7 to NaS18 of 1.5 and  $\text{Ch}_4\text{EDTA}$  at 12.5 °d after stirring for 2 d at 25 °C. Exact values and ratios are listed in Table 5-6.



**Figure 5-16:** Appearance of samples with a mass ratio of LutAO7 to NaS18 of 1.5 and  $\text{Ch}_4\text{EDTA}$  at 25 °d after stirring for 2 d at 25 °C. Exact values and ratios are listed in Table 5-6.

Samples with  $\text{Na}_4\text{EDTA}$  were all nontransparent and turbid and nearly no difference was observed for samples with a ratio of EDTA to Ca smaller than one or equal and larger than one. In **Figure 5-17**, this is shown for samples with  $\text{Na}_4\text{EDTA}$  at 12.5 °d.



**Figure 5-17:** Appearance of samples with a mass ratio of LutAO7 to NaS18 of 1.5 and Na<sub>4</sub>EDTA at 12.5 °d after stirring for 2 d at 25 °C. Exact values and ratios are listed in Table 5-7.

Considering the previous results, the findings could be expected. For ratios of EDTA to Ca equal or larger than one, EDTA removes all Ca ions and the samples behave like in millipore water. In millipore water, samples with a mass ratio of LutAO7 to NaS18 of 1.5 were turbid with additional Na<sub>4</sub>EDTA, but clear with Ch<sub>4</sub>EDTA. This is exactly what was found here.

It could be shown that, as soon as the ratio of EDTA to Ca is  $\geq 1$ , the use of Ch<sub>4</sub>EDTA lowers  $T_{Kr}$  of the mixed LutAO7 plus NaS18 surfactant system with a mass ratio of 1.5 below 25 °C, (only exception green 33). This was not possible with Na<sub>4</sub>EDTA. In this case, regarding the results in section 5.3.1.4, a LutAO7 to NaS18 ratio of at least 2.4 should be necessary to obtain clear solutions at 25 °C.

#### 5.3.2.2.2 Ch<sub>3</sub>Cit/Na<sub>3</sub>Cit

Nearly identical experiments, as described in section 5.3.2.2.1 for EDTA, were carried out with citrate.

Samples with a mass ratio of LutAO7 to NaS18 of 1.5 with a total surfactant concentration of LutAO7 plus NaS18 of 0.1 wt% were prepared in hard water of 12.5 and 25 °d. Again, the samples only differed in the builder, Ch<sub>3</sub>Cit and Na<sub>3</sub>Cit. The ratio of citrate to Ca was adjusted from 1 to 5. Water hardness, exact ratios of citrate to Ca, Ch or Na to S18 and the mass ratio of LutAO7 to NaS18 for each sample are given in **Table 5-8** for samples with Ch<sub>3</sub>Cit and in **Table 5-9** for samples with Na<sub>3</sub>Cit. The samples were analyzed by stirring experiments.

All samples remained nontransparent and turbid after stirring for 2 d at 25 °C, irrespective whether Ch<sub>3</sub>Cit or Na<sub>3</sub>Cit was used a builder. It was not possible to differentiate between samples with Ch builder or Na builder.

As for NaS16 systems in hard water (see section 5.3.2.1.2), the different observations for citrate and EDTA can be attributed to the much weaker Ca removing power of citrate compared to EDTA. “Free” Ca ions precipitate the alkyl sulfates and prevent the  $T_{Kr}$ -reducing effect of the Ch ions compared to Na ions.

Sample	°d	n(Cit)/n(Ca)	n(Ch)/n(S18)	LutAO7/NaS18
white 21	12.43	1.03	6.36	1.53
white 22	12.42	2.06	12.68	1.56
white 23	12.41	3.02	18.60	1.56
white 24	12.40	5.10	31.30	1.53
white 25	24.84	1.03	12.66	1.51
white 26	24.81	1.99	24.44	1.53
white 27	24.78	3.04	37.19	1.51
white 28	24.72	5.15	62.66	1.52

**Table 5-8:** Water hardness and exact molecular ratios of citrate to Ca, Ch to S18 and mass ratio of LutAO7 to NaS18 of all samples with  $\text{CH}_3\text{Cit}$ . Samples white 21 to 24 were prepared in water with 12.5 °d, samples white 25 to 28 in water with 25 °d and the molar ratio of citrate to Ca increases with increasing number for each set. The total amount of surfactant NaS18 plus LutAO7 was always 0.1 wt%.

Sample	°d	n(Cit)/n(Ca)	n(Na)/n(S18)	LutAO7/NaS18
white 31	12.44	1.03	7.39	1.50
white 32	12.43	2.02	13.45	1.57
white 33	12.43	3.03	19.72	1.53
white 34	12.44	5.02	32.02	1.51
white 35	24.87	1.01	13.51	1.50
white 36	24.87	2.03	26.07	1.51
white 37	24.87	3.03	38.41	1.52
white 38	24.87	5.04	63.04	1.55

**Table 5-9:** Water hardness and exact molecular ratios of citrate to Ca, Na to S18 and mass ratio of LutAO7 to NaS18 of all samples with  $\text{Na}_3\text{Cit}$ . Samples white 31 to 34 were prepared in water with 12.5 °d, samples white 35 to 38 in water with 25 °d and the molar ratio of citrate to Ca increases with increasing number for each set. The total amount of surfactant NaS18 plus LutAO7 was always 0.1 wt%.

## 5.4 Conclusion

It could be shown that the addition of Ch or MeCh to aqueous NaS16 or NaS18 solutions markedly decreases  $T_{Kr}$  of these surfactants in millipore water. The effect is very pronounced at low molecular ratios of Ch/MeCh to Na in solution and levels off at higher ones. As it is the case for the pure surfactants, MeCh turned out to be a bit more efficient and effective than Ch. Additional Na ions were found to have no positive effect on  $T_{Kr}$  of Na alkyl sulfates.

For aqueous NaS16 solutions, at molecular ratios of Ch/MeCh to Na in solution  $\geq 2$ , it was possible to reduce  $T_{Kr}$  from 44 °C to below room temperature. For NaS18, a Ch or MeCh to Na ratio of 2 is sufficient to nearly reach  $T_{Kr}$  of pure ChS18 or MeChS18, which is still considerably above room temperature.

Experiments with the nonionic alcohol ethoxylate surfactant LutAO7 pointed out that, compared to Na, the addition of Ch to mixed NaS18 plus LutAO7 surfactant systems heavily increases the solubility of this surfactant system in millipore water. At a

molecular ratio of Ch to Na of 3, a mass ratio of LutAO7 to NaS18 of 1.4 is sufficient to obtain clear solutions at 25 °C. For similar systems with additional Na ions, the mass ratio of LutAO7 to NaS18 has to be at least 2.4.

Further, it was also possible to achieve the same results in hard water. The only prerequisite was the removal of all hard Ca ions from solution by a strong builder. This was efficiently fulfilled by EDTA, while citrate proves to be less useful. By changing the counter ion of EDTA from Na to Ch, it was possible to create a "2 in 1" builder.  $\text{Ch}_4\text{EDTA}$  does not only efficiently remove Ca ions, but also introduces Ch ions that depress  $T_{\text{Kr}}$ , respectively increase solubility of the Na alkyl sulfates. According to these results, it is now possible to prepare clear and micellar aqueous solutions at low temperatures ( $< 25\text{ °C}$ ) on the basis of long chain Na alkyl sulfates by using adding a certain amount of Ch or MeCh salt. The results also indicate that only the actual ratio of Ch/MeCh to Na in solution determines  $T_{\text{Kr}}$ , irrespective of the molar amount of alkyl sulfate in solution. Thus, even if small amounts of Na ions exhibiting a  $T_{\text{Kr}}$ -increasing effect on the  $\text{NaSXX} + \text{Ch/MeCh}$  aqueous system are introduced from other sources, this effect can be displaced by simultaneously increasing the amount of Ch or MeCh. Consequently, it is not necessary to specially produce long chain Ch or MeCh alkyl sulfates and introduce them into the market, what could be linked to additional costs. This can be a big advantage when considering using the  $T_{\text{Kr}}$ -reducing effect of Ch and MeCh in a formulation. In the case of hard water, only Ch or MeCh builder have to be produced, which can easily be realized by neutralization of the acid form of the builder with Ch or MeCh hydroxide.

To sum up, Ch and MeCh are effective ions in reducing  $T_{\text{Kr}}$  of long chain Na alkyl sulfates. Best results are obtained at molecular ratios of Ch or MeCh to Na in solution  $\geq 2$ , but even smaller ratios show a distinct effect. The effects can also be realized in hard water, as soon as all hard Ca ions are removed by a strong builder. A very elegant way to use these findings in hard water is introduced by the "2 in 1"-builder-concept. This concept offers new possibilities to use highly surface active long chain Na alkyl sulfates at room temperature even in hard water, a fact that can be of particular interest for low temperature detergents.

## 5.5 Experimental

### 5.5.1 Chemicals

Sodium dodecyl sulfate (NaS12, AppliChem, > 99.8 %), sodium hexadecyl sulfate (NaS16, Alfa Aesar, > 99 %, LOT: 10167796), sodium octadecyl sulfate (NaS18, Alfa Aesar, > 98 %, LOT: 10176541), choline chloride (ChCl, Sigma, > 98 %), beta-methylcholine chloride (MeChCl, TCI, > 98 %), calcium chloride (Ca<sub>2</sub>Cl, Merck, anhydrous), sodium chloride (NaCl, analaR NORMAPUR, > 99.6 %), ethylenediaminetetraacetic acid (EDTA, Fluka, > 99.5 %), citric acid trisodium salt (Na<sub>3</sub>Cit, Sigma Aldrich, > 98 %) and tricholine citrate (Ch<sub>3</sub>Cit, Sigma Aldrich, ≈ 66 wt% in water) were used as received. Choline hydroxide solution (ChOH, ≈ 46.5 wt% in water) and beta-methylcholine hydroxide solution (MeChOH, ≈ 38.5 wt% in water) were provided by TAMINCO, Lutensol AO7 by BASF.

### 5.5.2 Sample preparation

Samples with surfactant and additional salts/builders and/or Lutensol AO7 were prepared as follows: the ingredients plus water were mixed in a vial und heated to some degrees above T<sub>Kr</sub> until a clear and homogeneous solution was obtained. The weight percent of surfactant and molar ratios of ions for each series of samples are given in the corresponding chapters. Afterwards the solution were cooled at around 4 °C and analyzed as described in section 5.5.3.

Many experiments were carried out at 0.1 wt% or close to 0.1 wt% surfactant, since this is the common concentration of surfactants inside a washing machine during the laundry process.

Aqueous stock solutions of and sodium/choline ethylenediaminetetraacetate (Na<sub>4</sub>EDTA/Ch<sub>4</sub>EDTA) were prepared by neutralizing EDTA with the necessary amount of substance of sodium hydroxide (NaOH, Merck TitriPur) or choline hydroxide (ChOH, TAMINCO).

Aqueous stock solutions of hard water were prepared with by dissolving CaCl<sub>2</sub> in millipore water. 1 °d corresponds to a Ca concentration of 0.1783 mM/l.

### 5.5.3 Determination of $T_{Kr}$

$T_{Kr}$  values were obtained by turbidity measurements with an automated home built apparatus as described in section 4.5.3.

Heating experiments were carried out in a water bath with a heating rate of about 1 °C/5 min. The samples were cooled for some days at 4 °C until some precipitate had formed or the samples were visibly turbid or bluish. In general, samples with additional Ch or MeCh ions were less turbid than similar samples containing only Na ions. However, all samples described in this chapter got at least well visibly bluish during cooling and could be properly analyzed. During heating, the samples were visually observed and  $T_{Kr}$  was taken as the temperature, from which on the surfactant solution was as clear as water.

Longtime stirring experiments were performed as follows: after cooling for several days at 4 °C, the samples were placed in a water bath and continuously stirred for 2 d at 25 °C. Then the appearance of the samples was visually analyzed.

## 5.6 Literature

1. Klein, R.; Kellermeier, M.; Touraud, D.; Müller, E.; Kunz, W., *J Colloid Interface Sci* **2013**, 392 (0), 274-280.
2. Lin, B.; McCormick, A. V.; Davis, H. T.; Strey, R., *J Colloid Interface Sci* **2005**, 291 (2), 543-549.
3. Yu, Z. J.; Zhang, X.; Xu, G.; Zhao, G., *J Phys Chem* **1990**, 94 (9), 3675-3681.
4. Klein, R.; Touraud, D.; Kunz, W., *Green Chem* **2008**, 10 (4), 433-435.
5. Shinoda, K.; Maekawa, M.; Shibata, Y., *J Phys Chem* **1986**, 90 (7), 1228-1230.
6. Hat, M.; Shinoda, K. z., *B Chem Soc JPN* **1973**, 46 (12), 3889-3890.
7. Irani, R. R., *J Chem Eng Data* **1962**, 7 (4), 580-581.
8. Irani, R. R.; Callis, C. F., *J Phys Chem* **1960**, 64 (11), 1741-1743.
9. Yoke, J. T., *J Phys Chem* **1958**, 62 (6), 753-755.
10. Lin, J. H.; Chen, W. S.; Hou, S. S., *J Phys Chem B* **2013**, 117 (40), 12076-12085.
11. Mitra, D.; Chakraborty, I.; Bhattacharya, S. C.; Moulik, S. P., *Langmuir* **2007**, 23 (6), 3049-3061.
12. Vlachy, N.; Jagoda-Cwiklik, B.; Vácha, R.; Touraud, D.; Jungwirth, P.; Kunz, W., *Adv Colloid Interface Sci* **2009**, 146 (1-2), 42-47.

13. Collins, K. D., *Methods* **2004**, 34 (3), 300-311.
14. Joshi, J. V.; Aswal, V. K.; Goyal, P. S., *J Phys Condens Matter* **2007**, 19 (19), 196219.
15. Yu, Y.; Zhao, J.; Bayly, A. E., *Chin J Chem Eng* **2008**, 16 (4), 517-527.
16. Bajpai, D.; Tyagi, V. K., *J Oleo Sci* **2007**, 56 (7), 327-40.
17. Smulders, E.; Rähse, W.; von Rybinski, W.; Steber, J.; Sung, E.; Wiebel, F., Detergent Ingredients. In *Laundry Detergents*, Wiley-VCH Verlag GmbH & Co. KGaA: 2003; pp 38-98.
18. Bretti, C.; Cigala, R. M.; De Stefano, C.; Lando, G.; Sammartano, S., *Fluid Phase Equilib* **2017**, 434, 63-73.



## **Chapter 6 Ethoxylated choline derivatives as counter ions for long chain alkyl sulfates and soaps**

### **6.1 Abstract**

In this chapter, which is the last one dealing with possible ways to decrease  $T_{Kr}$  of long chain surfactants and improving their water solubility at low temperatures, the effect of introducing flexible oxyethylene (EO) groups into the counter ion is investigated. This strategy was chosen, since it is well-known that chemical modification of alkyl sulfates or classical soaps by introducing EO groups between their polar head and their hydrophobic chain considerably reduces  $T_{Kr}$  of these surfactants compared to their chemically unmodified derivatives.<sup>1-4</sup> This part of the work was facilitated by BASF which kindly synthesized and provided ethoxylated choline derivatives  $ChEO_m$  (see **Figure 6-1**, 4).

$ChEO_2S18$  and  $ChEO_3S18$  were synthesized by ion exchange. Their  $T_{Kr}$  values, solubility behavior, cmc values as well as other physico-chemical parameters were determined by surface tension and solubility measurements and compared to  $ChS18$ . Further, the effect of additional  $ChEO_mCl$  on  $T_{Kr}$  of  $NaS16$  and  $NaS18$  was investigated. Next to this, aqueous solutions of choline, ethoxylated choline and sodium stearate ( $ChC18$ ,  $ChEO_mC18$  and  $NaC18$ ) with different molar excess of the respective base were prepared.  $T_{Kr}$  values and solubility behavior of these solutions were determined by solubility measurements and compared to each other. Further, these fatty acid solutions were subjected to simple foaming tests.

It could be shown that using  $ChEO_m$  as counter ion to  $S18$  considerably increases its solubility in water at room temperature compared to  $ChS18$ . Determined cmc values were also markedly lower. For the aqueous stearate systems, the same behavior was found. Compared to aqueous solutions of  $NaC18$ ,  $ChEO_m$  is much more efficient and effective in reducing  $T_{Kr}$  of this long chain soap than  $Ch$ . Finally, it will be shown that it is possible to produce very stable foams from  $ChEO_mC18$  solutions, whose time dependent behavior (foam volume and foam density) can be tuned by the ratio of organic  $ChEO_mOH$  base to  $C18$ .

## 6.2 Introduction

Next to changing the counter ion or addition of salt, which was already discussed in chapter 4 and 5, chemical modification of the surfactant itself is another possibility to affect  $T_{Kr}$  of a surfactant (see section 2.1.5.3). As it is the case when changing the counter ion from Na to bulky TAAs, these chemical modifications of the surfactant molecule are aimed at increasing the free energy of the surfactant's solid crystalline state.<sup>3, 5</sup>

A very effective way to increase the free energy of the solid crystalline state of long chain surfactants by chemical modification is the insertion of a polar group between the straight hydrophobic chain and the sulfate head group. Usually, these polar segments are oxyethylene (EO) or oxypropylene (PO) groups and their effect is illustrated by greatly depressed melting points and  $T_{Kr}$  values of the chemically modified surfactants compared to the unmodified ones.<sup>1, 3-5</sup> The effect can be achieved both for sodium alkyl sulfates<sup>1, 3, 6</sup> and sodium soaps<sup>2, 4</sup>. Our group could show that similar effects are observed when changing the alkyl moiety of sodium alkyl carboxylates to several oxyethylene groups. The resulting sodium 2,5,8,11-tetraoxatridecan-13-oate salt, shortly  $\text{Na}^+\text{TOTO}^-$ , was found to be a room temperature ionic liquid. This fact was attributed to the high flexibility of the polyoxyethylene chain.<sup>7-9</sup> In this work, the focus is on ethoxylated substances and the chemical structure of such an alcohol ether sulfate is shown in **Figure 6-1** on the left site. The effect of inserting ethylene ether groups into long chain sodium alkyl sulfates (NaS16 and NaS18) on  $T_{Kr}$  is shown in **Figure 6-2**. For both surfactants  $T_{Kr}$  decreases nearly linearly by addition of a further EO group with 2 EO groups being necessary to decrease  $T_{Kr}$  below room temperature for NaS16 and 4 EO groups for NaS18.

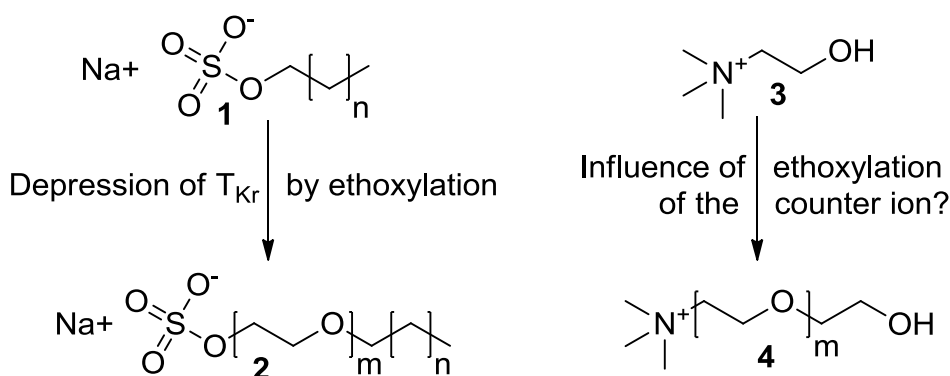


**Figure 6-1:** Molecular structures of sodium alkyl sulfate (1) and ethoxylated sodium alcohol ether sulfate (2) as well as choline (3) and an ethoxylated choline (4).  $n$  represents a certain amount of methylene groups,  $m$  a certain amount of oxyethylene groups.

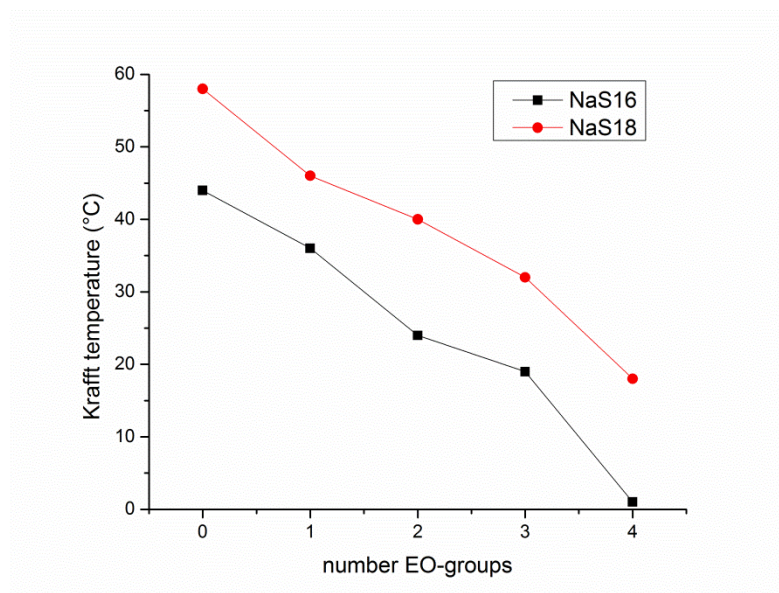


**Figure 6-2:** Dependence of  $T_{Kr}$  on the amount of oxyethylene groups inserted between the alkyl chain and the ionic head group for NaS16 (■) and NaS18 (●).  $T_{Kr}$  values are taken from reference 10.

The aim of this study was to investigate whether EO groups inserted in the structure of the counter ion have a similar  $T_{Kr}$ -reducing effect when inserted into the anionic surfactant molecule. This could be achieved by inserting EO groups into the ethanol moiety of the choline cation (see **Figure 6-1**, right). The work was part of a collaboration with BASF, which synthesized and provided these ethoxylated choline derivatives ( $\text{ChEO}_m$ ) as the chloride salt. It must be noted that, although lots of publications dealing with choline and different choline derivatives can be found in literature<sup>11-21</sup>, none was found using ethoxylated choline derivatives, which can therefore be regarded as a new class of molecules.  $\text{ChEO}_m$  can be regarded as very promising molecules as counter ions for long chain surfactants, since they combine a very unsymmetrical and bulky structure with the flexibility of an ethoxylated moiety in one molecule. These two features should strongly hamper surfactant crystallization and increase the free energy of the surfactant's solid state, which should lead to very low  $T_{Kr}$  values.

In this part of the work,  $\text{ChEO}_m\text{S18}$  ( $m = 2,3$ ) surfactants were prepared and their solubility behavior in water as well as their cmc values and some other physico-chemical properties were determined by solubility and concentration dependent surface tension measurements. The results will be compared to the results of  $\text{ChS18}$  and discussed with the increased bulkiness, molar mass and flexibility of the ethoxylated choline derivatives compared to simple choline. The effect of additional  $\text{ChEO}_m\text{Cl}$  ( $m = 1-3$ ) on  $T_{Kr}$  of aqueous NaS16 and NaS18 solutions was also investigated and compared to the one of  $\text{ChCl}$ .

Further, 0.1 and 1.0 wt% aqueous solutions of ChC18, ChEO<sub>m</sub>C18 and NaC18 with different ratios of the respective hydroxide base to C18 were prepared.  $T_{Kr}$  values and solubility behavior of these solutions were investigated by solubility measurements and compared to each other. The findings will again be explained by the difference in bulkiness and flexibility of the different counter ions. Unusual concentration dependent solubility results within these systems being contradictory to the Krafft theory are discussed by partial protonation of the C18 soap in solution as well as the complex concentration dependent phase behavior of soaps in dilute aqueous solutions. Finally, simple foaming tests were carried out with these soap solutions and the difference in foam behavior during aging will be related to the speed of formation of a highly viscous surface layer.

## 6.3 Results and discussion

First, the results with alkyl sulfates are presented and discussed. The discussion is quite condensed, since the general concepts applied are already discussed in detail in the two previous chapters.

Afterwards, the findings for the aqueous soap system will be discussed in detail.

### 6.3.1 Physico-chemical properties of ChEO<sub>m</sub>S18

#### 6.3.1.1 Solubility behavior and $T_{Kr}$

The solubility behavior of ChEO<sub>2</sub>S18 and ChEO<sub>3</sub>S18 was investigated identically to the ones of Ch and MeChS18 (see section 4.3.4). On the one hand,  $T_{Kr}$  was determined by turbidity measurements with a 1 wt% aqueous surfactant solution. On the other hand, the appearance of 0.02 wt%, 0.1 wt% and 1 wt% surfactant solutions was visually analyzed after stirring for 2 d at 25 °C.

The course of the turbidity curve of ChEO<sub>3</sub>S18 is illustrated in **Figure 6-3**. Strict evaluation of the turbidity curve of ChEO<sub>3</sub>S18 and taking  $T_{Kr}$  as the maximum value yields a value about 35 °C, which is around 15 °C smaller than the one of ChS18 and 10 °C than the one of MeChS18. However, the most striking difference is found when comparing the course of the turbidity curves for ChEO<sub>3</sub>S18, ChS18 and NaS18. The course of the curves for ChS18 and NaS18 were discussed in section 4.3.4 and are only shown for comparison reasons. The curve obtained for ChEO<sub>3</sub>S18 exhibits a value close to its maximum ( $T_{Kr}$ ) value after melting and the increase in turbidity from about 10 to 35 °C is very little. This suggests only low turbidity and nearly identical appearance of the 1 wt% ChEO<sub>3</sub>S18 solution from melting to  $T_{Kr}$ . The

turbidity curve measured for ChEO<sub>2</sub>S18 was nearly identical to the one shown for ChEO<sub>3</sub>S18 with a  $T_{Kr}$  value (maximum of the curve) of 43 °C.

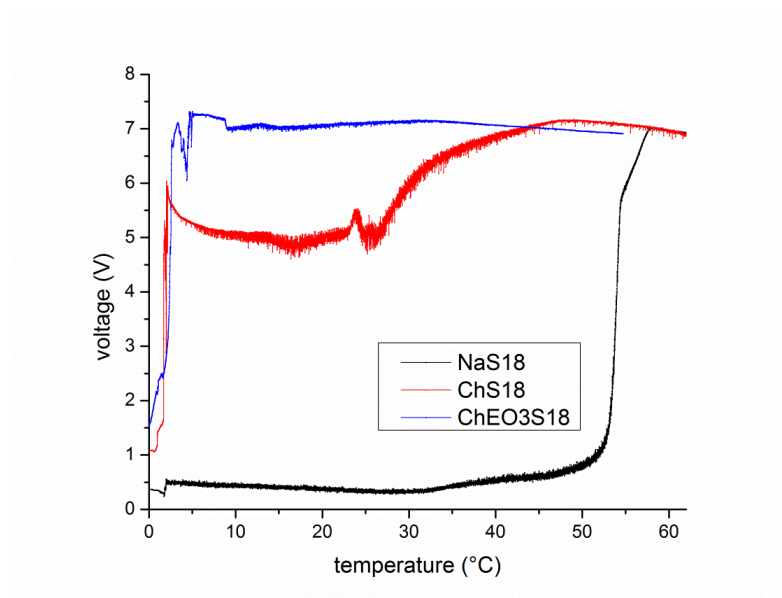


**Figure 6-3:** Comparison of the turbidity curves of aqueous solutions of 1 wt% NaS18, ChS18 and MeChS18 measured by a home-built apparatus. The transmittance of the samples, measured as the voltage  $V$ , is plotted against the temperature.

Concentration dependent (0.02/0.1/1.0 wt%) solubility experiments with NaS18, ChS18 and ChEO<sub>3</sub>S18 at 25 °C clearly reflect the differences illustrated by the turbidity curves. The appearance of the 1 wt% aqueous surfactant solution after stirring for 2 d at 25 °C are shown in **Figure 6-4**. Note that the samples were not heated above  $T_{Kr}$  before starting the experiment. Again, the solubility behavior for NaS18 and ChS18 is already discussed in detail in section 4.3.4. While the NaS18 sample is nontransparent white with some particles and the ChS18 one nontransparent turbid, birefringent and a bit viscous, the ChEO<sub>3</sub>S18 sample is highly transparent and only slightly turbid with some visible streaks. Identical experiments with 0.02 and 0.1 wt% ChEO<sub>3</sub>S18 samples yielded completely clear and water-like solutions.

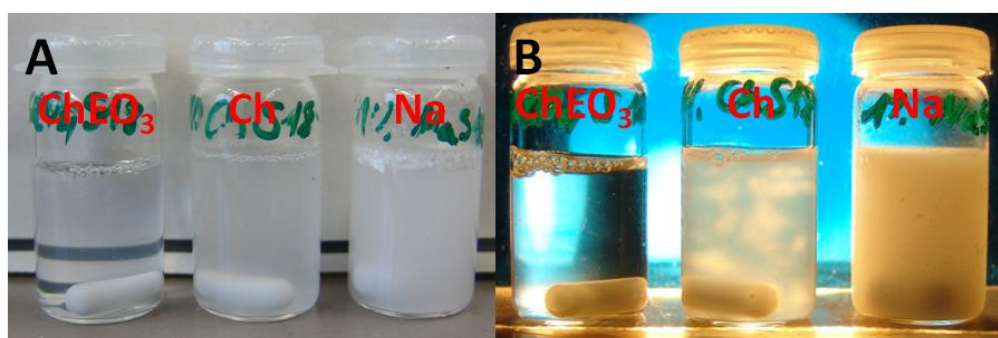


**Figure 6-4:** Photos of 1 wt% aqueous solution ChEO<sub>3</sub>S18, ChS18 and NaS18 after stirring for 2 d at 25 °C. Photo B was taken between crossed polarizers.

Clear solutions at 0.02 and 0.1 wt% ChEO<sub>3</sub>S18 suggest, as it is the case for ChS18 and MeCh18, a solubility behavior contradictory to the one expected from Krafft theory. However, for ChEO<sub>3</sub>S18, the slight turbidity as well as the observed streaks at 1wt% surfactant concentration could also be caused by some impurities, since the ChEO salts were not specially purified before usage. The significant difference in macroscopic appearance between 1 wt% aqueous ChEO<sub>3</sub>S18 and ChS18 solutions can possibly be explained by the increased bulkiness and the flexibility of the oxyethylene chain, which prevent the formation of a liquid crystalline phase in aqueous ChEO<sub>3</sub>S18 solutions at this surfactant concentration.

It must be noted that a significant drawback of reducing  $T_{Kr}$  by ethoxylation of the counter ion instead of the chemical modification of the alkyl sulfate surfactant could be the hard water stability. It was shown that the insertion of EO groups into the alkyl sulfates surfactant also heavily decreases  $T_{Kr}$  of Ca and Mg alkyl sulfates and thereby increases its stability in hard water.<sup>1, 3, 22, 23</sup> However, for the chemically unmodified alkyl sulfate plus ethoxylated counter ion system, Ca and Mg ions can still form crystals with the chemically unmodified alkyl sulfates that exhibit very high  $T_{Kr}$  values. Simple solubility experiments of 0.1 and 1 wt% ChEO<sub>3</sub>S18 in hard water of merely 3 °d water hardness and millipore water illustrated that problem. In millipore water, the solutions were clear (0.1 wt%) or slightly turbid (1 wt%), but in hard water the solutions were very turbid with some precipitate.

### 6.3.1.2 Cmc and other physico-chemical parameters derived from cmc measurements

The cmc values of ChEO<sub>2</sub>S18 and ChEO<sub>3</sub>S18 were determined by concentration dependent surface tension measurements and are listed in **Table 6-1**.

Surfactant	CMC [mM]
ChEO <sub>2</sub> S18	0.064 ± 0.000 (25°C)
ChEO <sub>3</sub> S18	0.057 ± 0.001 (25°C)
	0.066 ± 0.000 (40°C)

**Table 6-1:** Critical micellar concentration ChEO<sub>2</sub>S18 and ChEO<sub>3</sub>S18 at different temperatures. The values were obtained by surface tension measurements.

The cmc values of the ChEO<sub>m</sub>S18 surfactants are about 30 % smaller than the ones obtained for ChS18 and MeChS18 (see **Table 4-1**, section 4.3.2) with the value for ChEO<sub>3</sub>S18 being slightly lower than the one for ChEO<sub>2</sub>S18 at 25 °C. Markedly decreased cmc values for ChEO<sub>m</sub>S18 surfactants compared to ChS18/MeChS18 can be explained by mixed micellization with the larger ChEO<sub>m</sub> counter ion

containing strongly hydrated polar EO groups. As it is the case for nonionic alcohol ethoxylate surfactants, the EO moiety is likely to separate the ionic head groups at the micellar surface by simultaneously reducing the electrostatic interactions between them. This effect favors micellization, since less work is required to insert an ionic surfactant into this mixed micelle.<sup>24</sup> This decrease in the cmc value is in line with the effect observed for chemically modified sodium alkyl sulfates. In this case, the insertion of EO groups into the surfactant anion also leads to lower cmc values until the effects levels off at higher degrees of ethoxylation.<sup>10</sup> The slight increase in the cmc value for ChEO<sub>3</sub>S18 with increasing temperature was also found for ChS18 and is known from literature.<sup>5, 25</sup>

Further, the surface excess concentration  $\Gamma$ , the area per molecule at the surface  $A$  as well as the efficiency ( $pC_{20}$ ) and the effectiveness ( $\gamma_{cmc}$ ) of surface tension reduction were derived from surface tension data and are listed in **Table 6-2**. It should be mentioned that the change in surface tension with time before taking the  $\gamma$  value at a certain concentration always was  $< 0.05 \text{ mNm}^{-1}\text{min}^{-1}$ . Thus, the calculated parameters should all be very close to thermodynamic equilibrium values.

Surfactant	$\Gamma \cdot 10^6 [\text{mol/m}^2]$	$A [\text{\AA}^2]$	$pC_{20}$	$\gamma_{cmc} [\text{mN/m}]$
ChEO <sub>2</sub> S18	$2.18 \pm 0.03 (25^\circ\text{C})$	$76.04 \pm 0.87 (25^\circ\text{C})$	4.43 (25°C)	46.20 (25°C)
ChEO <sub>3</sub> S18	$1.97 \pm 0.07 (25^\circ\text{C})$	$84.51 \pm 2.91 (25^\circ\text{C})$	4.45 (25°C)	47.05 (25°C)
	$2.35 \pm 0.08 (40^\circ\text{C})$	$70.81 \pm 2.54 (40^\circ\text{C})$	4.47 (40°C)	43.90 (40°C)

**Table 6-2:** Surface excess concentration  $\Gamma$ , area per molecule at the surface  $A$ , efficiency of surface tension reduction  $pC_{20}$  and effectiveness in surface tension reduction  $\gamma_{cmc}$  of ChEO<sub>2</sub>S18 and ChEO<sub>3</sub>S18 at different temperatures. The values were obtained from surface tension measurements.

At 25 °C, the  $A$  value of ChEO<sub>3</sub>S18 is about  $11 \text{ \AA}^2$  bigger than the one obtained for ChEO<sub>2</sub>S18, which is about  $10 \text{ \AA}^2$  larger than the one of ChS18. Assuming a (at least partial) mixed S18/ChEO<sub>m</sub> surface layer with quite flexible EO groups, the measured  $A$  values are reasonable, since  $A$  values of simple nonionic alcohol ethoxylates increase in the same extent with one additional EO group.<sup>26, 27</sup> The effectiveness in surface tension reduction  $\gamma_{cmc}$  is quite similar for ChEO<sub>2</sub>S18 and ChEO<sub>3</sub>S18 and about 3-4 mN/m higher than for ChS18 (42.89 mN/m). The measured increase in  $A$  as well as in  $\gamma_{cmc}$  is also observed for chemically modified sodium alkyl ether sulfates, for which a higher the degree of ethoxylation resulted in larger the  $A$  and  $\gamma_{cmc}$  values.<sup>10</sup> The same is true for nonionic alcohol ethoxylates.<sup>26</sup> The decrease in  $A$  and in  $\gamma_{cmc}$  for ChEO<sub>3</sub>S18 when increasing the temperature from 25 to 40 °C was also observed for ChS18 and was already discussed in detail in section 4.3.3.

The efficiency in surface tension  $\text{pC}_{20}$  is more or is more or less equal for  $\text{ChEO}_2\text{S18}$  and  $\text{ChEO}_3\text{S18}$  irrespective of temperature and in good accordance with the values determined for  $\text{ChS18}$  and  $\text{MeChS18}$ .

### 6.3.2 Influence of $\text{ChEO}_m$ salts on $T_{\text{Kr}}$ of NaS16 and NaS18

In the previous chapter, it could be shown that the addition of Ch or MeCh salts can significantly reduce  $T_{\text{Kr}}$  of long chain sodium alkyl sulfate solutions.

In the following section, the effect of  $\text{ChEO}_m\text{Cl}$  ( $m = 1-3$ ) on  $T_{\text{Kr}}$  of aqueous 1 wt% NaS16 and NaS18 solution is shown. The ratio of  $\text{ChEO}_m$  to NaSXX was adjusted by adding a certain amount of  $\text{ChEO}_m\text{Cl}$  stock solution obtained by BASF and  $T_{\text{Kr}}$  was determined by turbidity measurements.

**Figure 6-5** illustrates the effect of  $\text{ChEO}_m$  ions on  $T_{\text{Kr}}$  of aqueous 1 wt% NaS16 solutions. The curves for ChS16 and MeChS16 are also shown for comparison reasons.

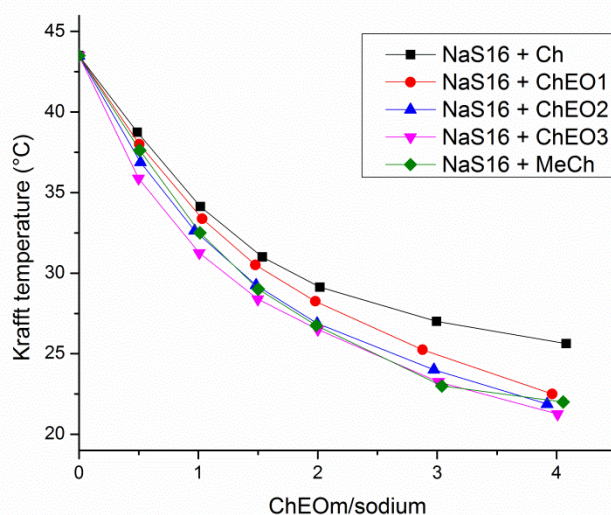


**Figure 6-5:** Influence of  $\text{ChEO}_m$  ions on  $T_{\text{Kr}}$  of aqueous 1 wt% NaS16 solutions. The curves were obtained by turbidity measurements:  $\blacksquare$  = NaS16 + ChCl,  $\bullet$  = NaS16 +  $\text{ChEO}_1\text{Cl}$ ,  $\blacktriangle$  = NaS16 +  $\text{ChEO}_2\text{Cl}$ ,  $\blacktriangledown$  = NaS16 +  $\text{ChEO}_3\text{Cl}$ ,  $\blacklozenge$  = NaS16 + MeChCl.

It is obvious that the effect of the  $\text{ChEO}_m$  ion is more or less independent of the degree of ethoxylation within the investigated range of  $m$ . Only at  $\text{ChEO}_m$  to Na ratios  $\leq 1$ ,  $\text{ChEO}_3$  seems to be a bit more efficient than the other ions. At higher ratios, the effect of  $\text{ChEO}_m$  on  $T_{\text{Kr}}$  is identical to the one of MeCh, and  $T_{\text{Kr}}$  of a 1 wt% NaS16 solution can be reduced below room temperature.

It must be noted that, up to a ratio of choline derivative to Na of 4, the course of turbidity curves for all NaS16 + Ch/MeCh/ $\text{ChEO}_m$  samples was very similar to the

one of pure NaS16 samples and a steep increase of the signal was observed within a few degrees. This indicates, that no complex (liquid crystalline) phases are formed within these systems.

The results of identical experiments carried out with aqueous 1 wt% NaS18 solutions are shown in **Figure 6-6**. Again, the curves show the same course for all organic ions. However,  $T_{Kr}$  of ChEO<sub>3</sub> samples is always about 8 °C lower than for MeCh or ChEO<sub>1</sub> irrespective of the ChEO<sub>m</sub> to Na ratio. Nevertheless, even for a ratio of ChEO<sub>3</sub> to Na of 4,  $T_{Kr}$  is still 15 °C above room temperature.

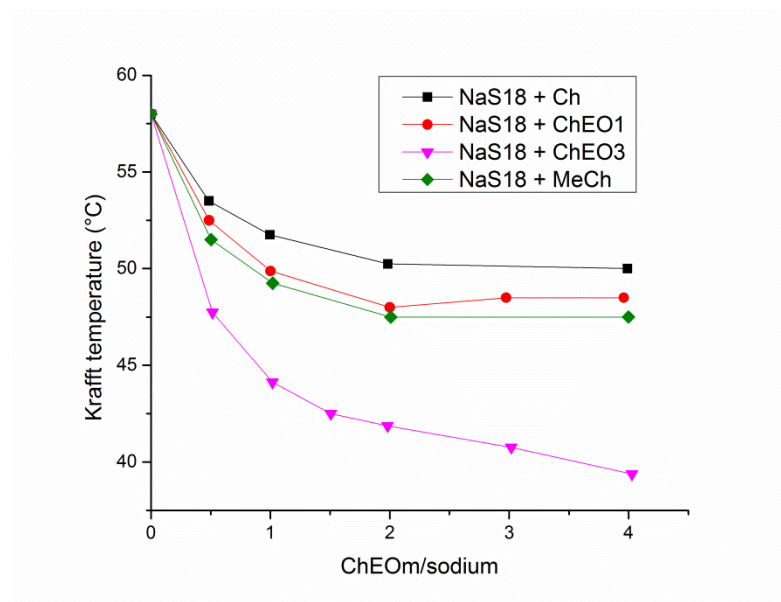


**Figure 6-6:** Influence of ChEO<sub>m</sub> ions on  $T_{Kr}$  of aqueous 1 wt% NaS18 solutions. The curves were obtained by turbidity measurements: ■ = NaS18 + ChCl, ● = NaS18 + ChEO<sub>1</sub>Cl, ▼ = NaS18 + ChEO<sub>3</sub>Cl, ◆ = NaS18 + MeChCl.

The striking difference of these NaS18 + Ch/MeCh/ChEO<sub>m</sub> systems gets obvious when analyzing the turbidity curves of the samples. For Ch, MeCh and ChEO<sub>1</sub>, with increasing ratio of choline derivative to Na the course of the turbidity curve changed from that of pure NaS18 to that of pure ChS18. However, in the case of ChEO<sub>3</sub>, the course remained similar to the one of pure NaS18. This is illustrated in **Figure 6-7**, which shows the turbidity curves of NaS18 plus Ch, ChEO<sub>1</sub> and ChEO<sub>3</sub> at a ratio of choline derivative to Na of 4. Comparing these curves to the ones of the pure S18 surfactants (see **Figure 6-3**) shows that only the curve with additional ChEO<sub>3</sub> is similar to the curve of pure NaS18, while the curves with additional Ch and ChEO<sub>1</sub> are very similar to the curves of pure ChS18 exhibiting different plateaus and a slow increase of the signal with temperature close to its maximum.

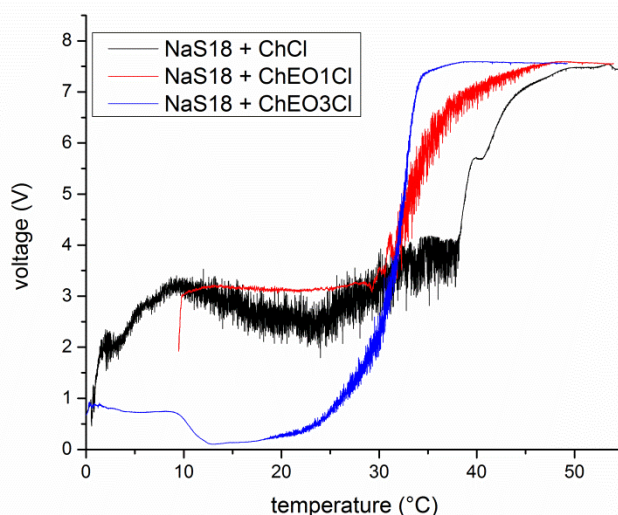


**Figure 6-7:** Comparison of the turbidity curves of aqueous 1wt% NaS18 solutions plus Ch, ChEO<sub>1</sub> and ChEO<sub>3</sub> measured by a home-built apparatus. The molecular ratio of choline derivative to Na was always 4. The transmittance of the samples, measured as the voltage V, is plotted against the temperature.

To check the difference in macroscopic phase behavior of NaS18 plus Ch and ChEO<sub>3</sub> system as indicated by turbidity measurements, different samples with NaS18 plus ChCl or ChEO<sub>3</sub>Cl were prepared with a choline derivative to Na ratio of 3. The NaS18 concentration was 0.02/0.05/0.1 and 1 wt%. The samples were heated above their  $T_{Kr}$ , cooled for several days at 4 °C and afterwards stirred for 1 d at 25 °C.

The great difference in appearance of the samples after stirring for 1 d at 25 °C is shown in **Figure 6-8**. The samples with additional Ch and NaS18 concentrations up to 0.1 wt% (samples 5 to 7) were homogeneously bluish/turbid and the turbidity increased with concentration of NaS18. Slewing of the samples between crossed polarizers showed weakly birefringent streaks. Sample 8 with Ch and a NaS18 concentration of 1 wt% was nontransparent turbid, exhibited an markedly increased viscosity and showed significant birefringence. In contrast, all samples with ChEO<sub>3</sub> contained some crystals and the amount of crystals increased with the surfactant concentration. This led to much more turbid solutions compared to identical samples with Ch. In contrast to sample 8, sample 12 was nontransparent white, low viscous and showed no birefringence (except for the crystals).

These findings are in line with the turbidity curves shown in **Figure 6-7**. It seems that the addition of Ch ions to NaS18 samples initiates the formation of a birefringent liquid crystalline phase and renders the appearance of the samples similar to the one of a pure aqueous ChS18 solution (see section 4.3.4). When adding ChEO<sub>3</sub> to NaS18 solutions, no birefringent liquid crystalline phase could be observed and

(NaS18) crystals precipitated from the solutions. These results also support the assumption that the increased bulkiness of the  $\text{ChEO}_3$  ion as well as the flexibility of its oxyethylene chain prevent the formation of a liquid crystalline phase with S18 for the investigated surfactant concentrations. However, it is possible that the observed birefringent liquid crystalline phases in samples of NaS18 plus Ch are not the thermodynamically stable state, since the solutions were heated above  $T_{\text{Kr}}$  after preparation. Thus, the formation of this phase could only be kinetically stable and with time, the NaS18 crystals will possibly precipitate from the solution.



**Figure 6-8:** Photos of aqueous NaS18 solution plus additional Ch or  $\text{ChEO}_3$  ions after stirring for 1 d at 25 °C. The molecular ratio of choline derivative to Na was always 3. Samples 5-8 contain additional Ch, the samples 9-12  $\text{ChEO}_3$  and the concentration of NaS18 increases from the left to the right (0.02(0.05/0.01 and 1 wt%).

### 6.3.3 $\text{ChEO}_m$ as counter ion of stearate

#### 6.3.3.1 $T_{\text{Kr}}$ and macroscopic appearance

So far, all experiments on reducing  $T_{\text{Kr}}$  of long chain surfactants by counter ion exchange, addition of organic salt or ethoxylation of the counter ion were focused on long chain alkyl sulfates. However, as already mentioned, similar effects can be found for soap surfactants.<sup>12, 28, 29</sup>

Simple sodium soaps can only be dissolved in water at room temperature up to a chain length of 12 C atoms ( $T_{\text{Kr}}(\text{NaC12}) = 25\text{ °C}$ ), since  $T_{\text{Kr}}$  values for longer chain homologues are considerably higher ( $\text{NaC14} = 45\text{ °C}$ ,  $\text{NaC16} = 60\text{ °C}$ ,  $\text{NaC18} = 71\text{ °C}$ ).<sup>28</sup> Klein et al.<sup>20</sup> could show that using Ch as counter ion of soaps reduces  $T_{\text{Kr}}$  of these surfactants to below room temperature up to a chain length of 16 C atoms ( $T_{\text{Kr}}(\text{ChC16}) = 12\text{ °C}$ ). Only for ChC18,  $T_{\text{Kr}}$  was 40 °C and markedly above room temperature. Further, Klein et al.<sup>30</sup> reported that the addition of excess ChOH to ChC18 solutions can considerably decrease  $T_{\text{Kr}}$  down to 14 °C at 100 % mol excess of ChOH.

To investigate the effect of ethoxylation of the Ch counter ion on  $T_{Kr}$  of long chain soaps, aqueous 0.1 and 1 wt%  $\text{ChEO}_2\text{C18}$ ,  $\text{ChEO}_3\text{C18}$  and  $\text{ChC18}$  solutions were prepared with varying excess of the respective base. Although Klein et al.<sup>30</sup> already did the same experiments for Ch, it was decided to repeat the experiments for better comparison, since so all samples were prepared from the same sample of stearic acid. No pure/solid C18 surfactants were synthesized and the test samples were prepared by mixing certain amounts of stearic acid (C18), aqueous organic base ( $\text{ChOH}$  or  $\text{ChEO}_m\text{OH}$ ) and water.  $T_{Kr}$  values were determined by turbidity measurements.

$T_{Kr}$  values of aqueous 1 wt% solutions of  $\text{ChEO}_2\text{C18}$ ,  $\text{ChEO}_3\text{C18}$  and  $\text{ChC18}$  in dependence of the ratio  $\text{ChEO}_m\text{OH}$  to C18 are shown in **Figure 6-9**. The  $T_{Kr}$  values of the pure surfactants, i.e.  $n(\text{ChEO}_m)/n(\text{C18}) = 1$ , are 44 °C for  $\text{ChC18}$ , 25 °C for  $\text{ChEO}_2\text{C18}$  and 29 °C for  $\text{ChEO}_3\text{C18}$ . Thus, applying the concept of counter ion exchange,  $\text{ChEO}_m$  have a much stronger ability to depress  $T_{Kr}$  of a 1 wt% aqueous  $\text{NaC18}$  solution than simple Ch and yield clear aqueous C18 solutions at room temperature. Considering theory, for the more bulky and more flexible  $\text{ChEO}_3$ , a lower value of  $T_{Kr}$  than for  $\text{ChEO}_2$  would be expected. This is probably the case and the slightly higher value can be explained by the presence of a small amount of weak amine bases (5-10 mol %) in the  $\text{ChEO}_3\text{OH}$  stock solution as indicated by the course of the acid base titration curves obtained for  $\text{ChEO}_3\text{OH}$  solutions. That means a 1 to 1 neutralization of C18 with  $\text{ChEO}_3\text{OH}$  corresponds to 90-95 % neutralization with strong  $\text{ChEO}_3\text{OH}$  base and to 5-10 % neutralization with weak amine bases. Between the weak amine bases and the weak acidic C18 soap, proton exchange can take place that increases the amount of protonated acid within the system. As discussed below, an increase in protonated C18 fatty acid is meant to raise  $T_{Kr}$  of the solution. For  $\text{ChEO}_2\text{OH}$  stock solutions, no sign of weak amine bases were found by acid base titration.

Further,  $T_{Kr}$  of the  $\text{ChEO}_2\text{C18}$  and  $\text{ChEO}_3\text{C18}$  system decreases significantly with increasing molar excess of organic base and a value of  $\text{ChEO}_m\text{OH}$  to C18 of 1.2 is enough to reduce  $T_{Kr}$  down to 0 °C. For the  $\text{ChC18}$  system, the decrease of  $T_{Kr}$  is less distinct and the curve indicates that a ratio of  $\text{ChOH}$  to C18 of about 1.3 is necessary to decrease  $T_{Kr}$  down to room temperature. The effect levels off at higher molar ratios and the minimum value of  $T_{Kr}$  at a molar ratio of 2 is 16 °C. Klein et al. reported nearly identical  $T_{Kr}$  values of pure  $\text{ChC18}$  (40 °C) and at a  $\text{ChOH}$  to C18 ratio of 2 (15 °C). However, in their experiments, excess of  $\text{ChOH}$  decreases  $T_{Kr}$  much more efficiently and a  $T_{Kr}$  value of 25 °C was already achieved at a molar ratio

of ChOH to C18 of 1.11. Probably, these differences can be attributed to different purities of the used C18 fatty acid.

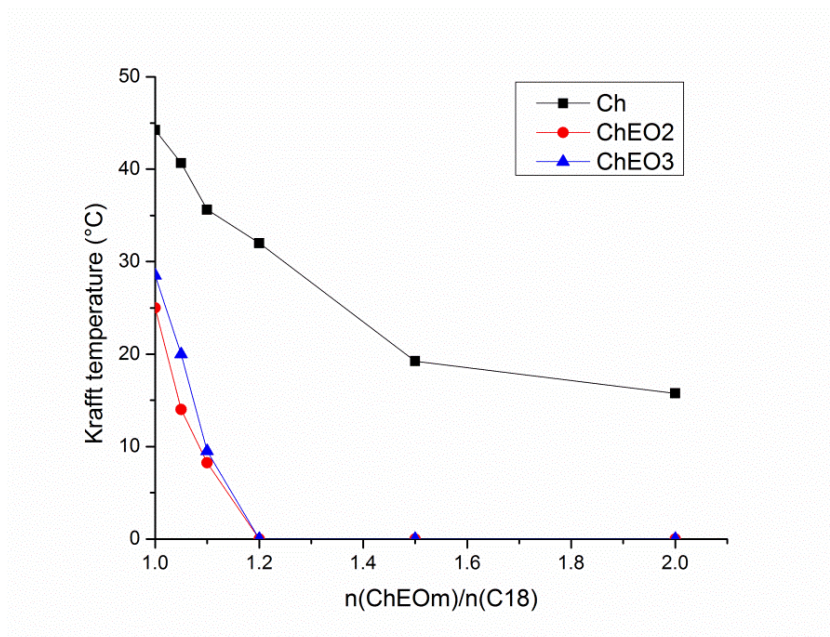


**Figure 6-9:**  $T_{Kr}$  value of aqueous 1 wt%  $\text{ChEO}_2\text{C18}$ ,  $\text{ChEO}_3\text{C18}$  and  $\text{ChC18}$  solutions in dependence of the molar ratio  $\text{ChEO}_m\text{OH}$  to C18. ■ = Ch, ● =  $\text{ChEO}_2$ , ▲ =  $\text{ChEO}_3$ .

The measured pH value of each sample as well its appearance after stirring for 1 d at 25 °C are listed for  $\text{ChEO}_2\text{C18}$  in **Table 6-3**, for  $\text{ChEO}_3\text{C18}$  in **Table 6-4** and for  $\text{ChC18}$  in **Table 6-5**. The visually observed macroscopic appearance of the samples is in perfect agreement with the measured  $T_{Kr}$  values. It must be noted that samples with  $T_{Kr}$  values below 25 °C were not completely clear as water and exhibited a marginal bluish character at closer inspection. Light microscope analysis at room temperature of the  $\text{ChC18}$  and  $\text{ChEO}_3\text{C18}$  samples at a ratio of base to C18 of 1 always showed defined and flat structures of different shape. Comparing the pH values of the different samples shows that for  $\text{ChEO}_2\text{C18}$  and  $\text{ChEO}_3\text{C18}$  clear solutions at room temperature can be obtained at pH values a bit lower than 10.5, for  $\text{ChC18}$  this is only possible at pH values larger than 11.5.

$\text{ChEO}_2\text{OH/C18}$	$T_{Kr}$ [°C]	Appearance at 25 °C	pH value
1/1	25	Very slightly bluish	10.44
1.05/1	14	Very slightly bluish	10.73
1.1/1	8	Very slightly bluish	10.94
1.2/1	<0	Very slightly bluish	11.17
1.5/1	<0	Very slightly bluish	n. m.
2/1	<0	Very slightly bluish	n. m.

**Table 6-3:**  $T_{Kr}$  value, macroscopic appearance at 25 °C and pH value for aqueous 1wt%  $\text{ChEO}_2\text{C18}$  solutions at different molar ratios of  $\text{ChEO}_2\text{OH}$  to C18.

ChEO <sub>3</sub> OH/C18	T <sub>Kr</sub> [°C]	Appearance at 25 °C	pH value
1/1	29	Slightly turbid	n. m.
1.05/1	20	Very slightly bluish	10.28
1.1/1	10	Very slightly bluish	10.69
1.2/1	<0	Very slightly bluish	11.02
1.5/1	<0	Very slightly bluish	n. m.
2/1	<0	Very slightly bluish	n. m.

**Table 6-4:** T<sub>Kr</sub> value, macroscopic appearance at 25 °C and pH value for aqueous 1 wt% ChEO<sub>3</sub>C18 solutions at different molar ratios of ChEO<sub>3</sub>OH to C18.

ChOH/C18	T <sub>Kr</sub> [°C]	Appearance at 25 °C	pH value
1/1	44	Nontransparent turbid	n. m.
1.05/1	41	Nontransparent turbid	n. m.
1.1/1	36	Very turbid	n. m.
1.2/1	32	Slightly turbid	11.45
1.5/1	19	Very slightly bluish	11.88
2/1	16	Very slightly bluish	12.17

**Table 6-5:** T<sub>Kr</sub> value, macroscopic appearance at 25 °C and pH value for aqueous 1 wt% ChC18 solutions at different molar ratios of ChOH to C18.

The same experiments were performed at 0.1 wt% surfactant concentration. The only difference was that the ratio of ChEO<sub>m</sub>OH to C18 ranged from 1 to 5. It must be noted that the turbidity curves for 0.1 wt% surfactant concentration were sometimes difficult to analyze due to the very low turbidity of these samples even at very low temperatures. As discussed in the next section, this can be attributed to the fact that these long chain soap solutions do not obey the Krafft theory and therefore only a very low amount of precipitates/additional phase is formed in these solutions.

The results for T<sub>Kr</sub> in dependence of the organic base to C18 ratio are shown in **Figure 6-10**. It is clearly obvious that T<sub>Kr</sub> of the pure ChEO<sub>m</sub>C18 and ChC18 are considerably larger at 0.1 wt% surfactant concentration than at 1 wt%. This fact is inconsistent with the phase rule for binary systems.<sup>31</sup> However, the same behavior is also described in literature<sup>32, 33</sup>, that at low soap concentrations, reducing the soap concentration results in higher "solubility temperatures". It can be explained by the partial protonation of the soap resulting in the corresponding less water-soluble fatty acid, which transforms the aqueous soap solution from a binary to a more complex system (see next section).<sup>31, 34</sup> The increase in "solubility temperature" with decreasing soap concentration was explained by a more prominent protonation of the soap in dilute solutions.<sup>33</sup> Thus, from a theoretical point of view, it is somehow wrong to use the expression "Krafft temperature" for the "solubility temperature" of dilute aqueous soap solutions. Nevertheless, in the following, since common practice in literature, the "solubility temperature" of dilute aqueous soap solutions will also be called T<sub>Kr</sub>. Further, these uncommon solubility behavior implies that comparing T<sub>Kr</sub>,

respectively the clearing temperature, of soap solutions is only reasonable at identical concentrations.

As for the 1 wt% systems,  $T_{Kr}$  is more efficiently reduced for  $\text{ChEO}_m\text{C18}$  than for Ch by increasing the molar ratio of organic base to C18. Thus, the ratio necessary to reduce  $T_{Kr}$  below room temperature is considerably smaller for  $\text{ChEO}_m\text{S18}$  (slightly smaller than 2) than for  $\text{ChC18}$  (slightly smaller than 5). For  $\text{ChEO}_m\text{S18}$ , at molar ratios of  $\text{ChEO}_m\text{OH}$  to C18  $\geq 3$ ,  $T_{Kr}$  was below  $0^\circ\text{C}$ .

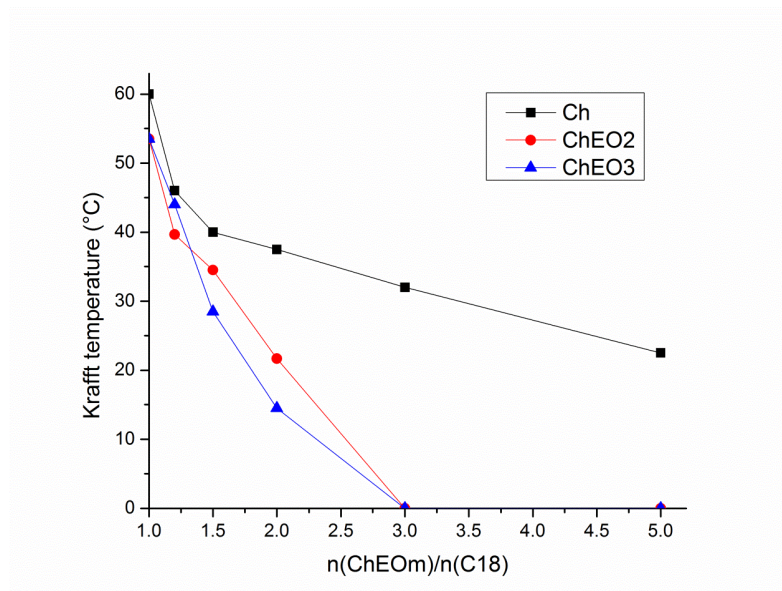


**Figure 6-10:**  $T_{Kr}$  value of aqueous 0.1 wt%  $\text{ChEO}_2\text{C18}$ ,  $\text{ChEO}_3\text{C18}$  and  $\text{ChC18}$  solutions in dependence of the molar ratio  $\text{ChEO}_m\text{OH}$  to C18. ■ = Ch, ● =  $\text{ChEO}_2$ , ▲ =  $\text{ChEO}_3$ .

The measured pH value of each sample as well its appearance after stirring for 1 at  $25^\circ\text{C}$  are listed for  $\text{ChEO}_2\text{C18}$  in **Table 6-6**, for  $\text{ChEO}_3\text{C18}$  in **Table 6-7** and for  $\text{ChC18}$  in **Table 6-8**. Again, the visually observed macroscopic appearance of the samples is in perfect agreement with the measured  $T_{Kr}$  values. As it is the case for the 1 wt % surfactant solutions, the minimum pH value to obtain clear and stable solution at room temperature is about 1 unit higher for  $\text{ChC18}$  ( $\approx 12$ ) than for  $\text{ChEO}_m\text{C18}$  (slightly higher than 11). The difference in macroscopic appearance between Ch and  $\text{ChEO}_m$  samples at low base to C18 ratios ( $\leq 1.2$ ) can probably be ascribed to the formation of a liquid crystalline phase within the Ch samples. The solutions were slightly turbid with some streaks and showed a slightly increased viscosity as well as weak birefringence between crossed polarizers. For the  $\text{ChEO}_m\text{C18}$  samples, always a white precipitate was observed that led to nontransparent and turbid solutions. The capability of Ch to provoke the formation of liquid crystalline phases was already suggested for S18 solutions, for which similar

observations were made (see 6.3.2, **Figure 6-8**). Since the samples were heated above  $T_{Kr}$  after preparation, it is not sure whether this liquid crystalline phase is thermodynamically stable or only kinetically.

ChEO <sub>2</sub> OH/C18	$T_{Kr}$ [°C]	Appearance at 25 °C	pH value
1/1	54	Nontransparent turbid	n. m.
1.2/1	40	Turbid	n. m.
1.5/1	35	Slightly turbid	n. m.
2/1	22	Very slightly bluish	11.29
3/1	<0	Very slightly bluish	11.59
5/1	<0	Very slightly bluish	n. m.

**Table 6-6:**  $T_{Kr}$  value, macroscopic appearance at 25 °C and pH value for aqueous 0.1 wt% ChEO<sub>2</sub>C18 solutions at different molar ratios of ChEO<sub>2</sub>OH to C18.

ChEO <sub>3</sub> OH/C18	$T_{Kr}$ [°C]	Appearance at 25 °C	pH value
1/1	54	Nontransparent turbid	n. m.
1.2/1	44	Turbid	n. m.
1.5/1	29	Slightly turbid	n. m.
2/1	15	Very slightly bluish	11.16
3/1	<0	Very slightly bluish	11.48
5/1	<0	Very slightly bluish	n. m.

**Table 6-7:**  $T_{Kr}$  value, macroscopic appearance at 25 °C and pH value for aqueous 0.1 wt% ChEO<sub>3</sub>C18 solutions at different molar ratios of ChEO<sub>3</sub>OH to C18.

ChOH/C18	$T_{Kr}$ [°C]	Appearance at 25 °C	pH value
1/1	60	Slightly turbid	n. m.
1.2/1	46	Slightly turbid	n. m.
1.5/1	40	Slightly turbid	n. m.
2/1	37	Slightly turbid	n. m.
3/1	32	Very slightly turbid	11.60
5/1	22	Very slightly bluish	12.00

**Table 6-8:**  $T_{Kr}$  value, macroscopic appearance at 25 °C and pH value for aqueous 0.1 wt% ChC18 solutions at different molar ratios of ChOH to C18.

Identical experiments with C18 and NaOH showed that it is not possible to decrease  $T_{Kr}$  of NaC18 below room temperature by increasing the ratio of NaOH to C18. This is illustrated in **Figure 6-11** for solutions of NaC18, ChC18 and ChEO<sub>3</sub>C18 at 0.1 wt% surfactant concentration at a molar ratio of base to C18 of 2. The photo was taken after stirring for 1 d at 25 °C. As already described above, the ChC18 solution was slightly turbid with streaks and the ChEO<sub>3</sub>C18 solution only very slightly bluish. In contrast, the solution with NaC18 contained a very big white and solid lump in a clear aqueous solution. For identical solutions with 1 wt% NaC18, the sample turned into a white solid mass. Similar results were obtained by Klein et al.<sup>30</sup>, who showed that the addition of excess NaOH to 1 wt% NaC12 solutions even slightly increases

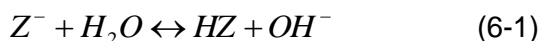
Possible reasons for the different behavior of ChEO<sub>m</sub>C18, ChC18 and NaC18 soap solutions when adding further hydroxide base will be discussed in detail in the next section.



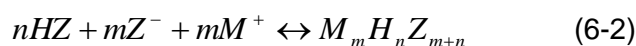
**Figure 6-11:** Photo of NaC18, ChC18 and ChEO<sub>3</sub>C18 at 0.1 wt% surfactant concentration and a molar ratio of base to C18 of 2. The samples were stirred for 1 d at 25 °C.

### 6.3.3.2 Complex phase behavior in dilute soap solutions and the importance of the counter ion

There are many papers that highlight the unusual behavior of dilute soap solutions when performing concentration dependent surface tension, conductivity or pH measurements.<sup>35-40</sup> This uncommon behavior of dilute aqueous soap solutions can be attributed to the hydrolysis reaction of the fatty acid in water (see equation 6-1). The related presence of more species in solution than the ionic surfactant differentiates aqueous soap solutions from common synthetic surfactant solutions with a strongly acidic head group, like alkyl sulfates and alkyl sulfonates.



Here  $Z^-$  represents the alkanoate anion and HZ the protonated fatty acid. Further, protonated fatty acid and alkanoate ions can form acid-soap complexes and crystals of various stoichiometry as depicted in equation 6-2, where  $M^+$  is the counter ion of the alkanoate anion.<sup>41</sup>



Both uncharged species, the fatty acid and the acid-soap complexes, are significantly less water-soluble than the charged alkanoate anion.<sup>35</sup> Due to the weak

acidic carboxylate group, the composition of dilute soap solutions is also heavily dependent on the pH value of the solution.

In 2007, Kralchevsky et al.<sup>35</sup> published a paper, in which they extended a theory of Lucassen<sup>40</sup> on the hydrolysis and precipitates in dilute aqueous soap solutions. In this outstanding paper, they combine theory with experimental results for NaC12 as well as NaC14 and are able to give reasonable explanations for many peculiar experimental results obtained for aqueous soap solutions. For better understanding of the complex phenomena in dilute aqueous soap solutions, it can be highly recommended to have a closer look at this publication.

For an aqueous NaC14 solution at 25 °C, they could show that the kind of precipitate present in solution depends heavily on the overall NaC14 concentration (see **Figure 6-12**). The increase in pH value with overall NaC14 concentration up to the formation of neutral soap (MZ) indicates that, although some precipitate is present in solution, more alkanoate anions dissolve until the pH value remains constant. This is merely based on the fact that different species are present in solution, of which the protonated fatty acid or the acid-soap complexes are present above their solubility limit, but not the alkanoate anion. The alkanoate ion reaches its solubility limit as soon as the pH value remains constant and precipitates as neutral soap. Comparing the maximum solubility of myristic acid to the NaC14 concentration at which fatty acid precipitation is observed indicates that only a low portion of the alkanoate anions are in the protonated state. Similar results were reported by Wen et al.<sup>37</sup>.

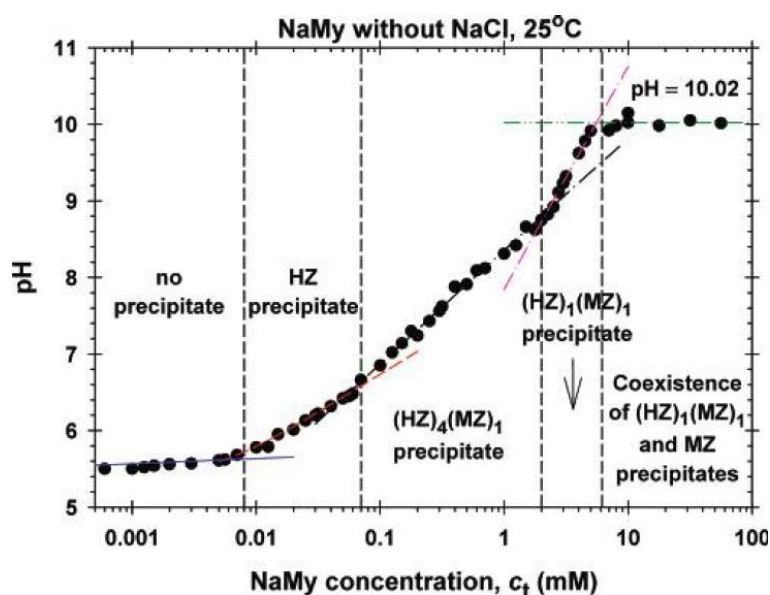


**Figure 6-12:** The pH value of an aqueous NaC14 solution plotted against the concentration of the soap. The concentration ranges for different precipitates are depicted by the dashed vertical lines. HZ is the protonated fatty acid,  $(\text{HZ})_n(\text{MZ})_m$  acid-soap complexes and MZ the neutral soap. The figure is taken from reference 35.

Further, Kralchevsky and co-worker could relate this concentration dependent formation of specific precipitates to the course of concentration dependent surface tension or conductivity measurements. The presence of different plateaus in concentration dependant surface tension measurements, a behavior uncommon for synthetic surfactants, can now be explained by the concentration dependent formation of different fatty acid precipitates. In other words, at each plateau another nonionic and highly surface active species is adsorbed at the surface. This is illustrated for the aqueous system NaC14 plus 10 mM NaCl at 25 °C in **Figure 6-13**.

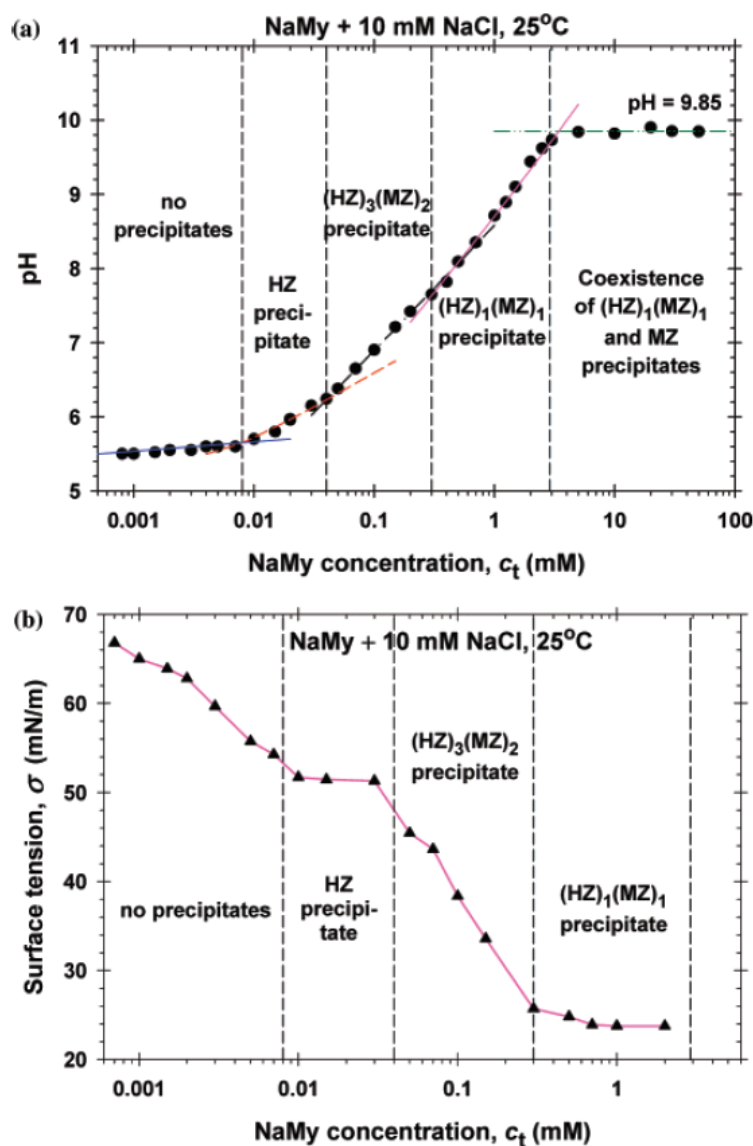


**Figure 6-13:** (a) The pH value of an aqueous NaC14 solution plus 10 mM NaCl plotted against the concentration of the soap. The concentration ranges for different precipitates are depicted by the dashed vertical lines. HZ is the protonated fatty acid,  $(HZ)_n(MZ)_m$  acid-soap complexes and MZ the neutral soap. (b) Comparison of the experimental surface tension isotherm with the precipitation zones determined from the pH data. The figure is taken from reference 35.

Moreover, the often reported knick, i.e. the change in the slope at 6-7 mM NaC14 found in concentration dependent conductivity measurements can now be related to the maximum solubility of NaC14 in water. In former publications, plateaus in surface tension isotherms or such knicks in conductivity data were often taken as the cmc value of the respective soap.

Another important, respectively the most important fact concerning this thesis shown in Kralchevsky's work is that the addition of an excess amount of NaOH can considerably simplify the phase behavior of the NaC14 solution at 25 °C. The excess amount of NaOH increases the pH value and prevents the formation of protonated fatty acid. Therefore, with increasing overall NaC14 concentration only neutral soap precipitates as soon as its solubility limit is reached.

Finally, it must be noted that the calculated precipitation zones of different fatty acid crystals agreed very well with the experimental observation, i.e. the macroscopic appearance of the solution. Further, the precipitation of different fatty acid crystals could be proven by microscopy, since the shape of the crystals in solution varied with the overall NaC14 concentration in solution.

Considering the complex concentration dependence formation of precipitates in dilute aqueous soap solutions, another explanation than more prominent fatty acid hydrolysis with lower soap concentration as suggested by McBain<sup>33</sup> seems reasonable for the observed unusual concentration dependent solubility behavior in water. It is likely that the structurally different crystal precipitates exhibit a different solubility in water with the ones formed at lower overall soap concentration possessing a higher solubility temperature.

Transferring these findings to the results presented in the previous section, the differences in the behavior of NaC18 and ChC18/ChEO<sub>m</sub>C18 solutions can reasonably be explained with regard to the structure of the counter ion. Calculations and experiments done by Kralchevsky et al.<sup>35</sup> and Lucassen<sup>40</sup> showed that the concentration ranges of different fatty acid precipitates are shifted to lower concentrations by increasing the fatty acid chain length and the salt content of the system. Therefore, the molar concentration of C18 in the 0.1 and 1 wt% test solutions should be far above the concentration, for which precipitates are predicted in NaC18 solutions at room temperature. It must be pointed out that the calculation and the experiments of Kralchevsky et al. and Lucassen were only performed and proven for sodium and potassium soaps.

The discussion will be made for the 1 wt% C18 systems, since the general idea should also be valid for the 0.1 wt% surfactant solutions. It must be noted that only

the general differences found for the different counter ions can be addressed. It is nearly impossible (without very extensive and time consuming structural analysis) to make some assumptions or predictions on the precipitates/additional phases formed in solution that were turbid at room temperature. As shown by Kralchevsky et al.<sup>35</sup>, even the dilute NaC14 solution exhibit a very complex phase behavior. The use of organic counter ions as well as the addition of excess base can further complicate the concentration dependent phase behavior of the dilute soap solutions.

Let us first consider the NaC18 system. Since even NaC14 neutral soap has only a solubility of about 6 mM in water at 25 °C (see **Figure 6-12**), it is a reasonable assumption that the one of NaC18 is considerably smaller. Therefore, an aqueous 1 wt% NaC18 solutions ( $c \approx 33$  mM) turns into a solid white mass due to the large amount of neutral soap precipitate. Kralchevsky et al.<sup>35</sup> found the same macroscopic appearance for larger concentrations of NaC14 at 25 °C. For the NaC18 systems, excess of base has no effect on the macroscopic appearance of the solutions, since only the formation of acid-soap crystals is prevented, but the little soluble neutral Na soap can still be formed. The well-known salting out effect of additional sodium ions in solution should further reduce the solubility of the neutral soap within these systems. This was also shown by Kralchevsky et al.<sup>35</sup>. The increase in  $T_{Kr}$  of 1 wt% aqueous NaC12 solutions with increasing ratio of NaOH to C12 as reported by Klein et al.<sup>30</sup> also strongly support the presented discussion for the NaC18 system.

For the Ch and ChEO<sub>m</sub> ions, the situation changes drastically. This can be explained by the bulky structure of the organic ions preventing the formation of neutral soap at 25 °C, since they are meant to increase the free energy of the neutral soap's solid crystalline state. This is proven by the fact that it is possible to depress  $T_{Kr}$  to below 0 °C by increasing the ratio of ChEO<sub>m</sub> base to C18 and thereby preventing the formation of protonated fatty acid. In this case, the soap solution can be regarded as a simple binary ionic surfactant-water system and the same arguments are valid that are used throughout the thesis to explain the heavily reduced  $T_{Kr}$  values for Ch or ChEO<sub>m</sub> alkyl sulfates compares to their Na homologues. The fact that it is not possible to depress  $T_{Kr}$  of ChC18 down to 0 °C could possibly be again ascribed to the formation of liquid crystalline phases, since directly after melting at 1 °C, all ChC18 solutions were highly viscous and exhibited a similar appearance like 1 wt% ChS18 solutions at room temperature (see section 4.3.4). Precipitates in solutions below a certain ratio of ChOH or ChEO<sub>m</sub>OH to C18 (for ChEO<sub>m</sub> below room temperature!) can be attributed to the formation of fatty acid or acid-soap crystals due to the presence of some hydrolyzed soap within these solutions. Possibly, even some more complex lamellar phases could be present. Such lamellar phases with

the bilayer in a rigid gel state were reported by Arnould et al.<sup>42</sup> in aqueous 1 wt% ChC14 solutions at a ratio of ChOH to C14 smaller than 1. Lower solubility temperatures of these crystals/structures for the ChEO<sub>m</sub> systems compared to the Ch system at identical ratio of base to C18 can again be ascribed to the more bulky and flexible structure of the counter ion. First, this fact renders the formation of acid-soap crystals or rigid lamellar phases less favorable compared to the micellar state. Secondly, the larger and more flexible counter ion possibly enables a larger share of protonated fatty acid to be solubilized in the micellar aggregates.

For the 0.1 wt% solutions, the same general discussion can be applied. Higher  $T_{Kr}$  values at similar ratios of organic base to C18 than for the 1 wt% systems are possibly due to structurally different and less soluble precipitates/additional phases than in the 1 wt% systems.

To conclude, ChEO<sub>m</sub> as counter ion to C18 considerably reduces  $T_{Kr}$  of aqueous 1 wt% soap solutions compared NaC18 and clear solutions could be obtained for the pure surfactant (ratio base to C18 = 1) at room temperature. By increasing the molar ratio of ChEO<sub>m</sub>OH to C18 it is even possible to reduce  $T_{Kr}$  down to 0 °C. ChEO<sub>m</sub> were also found to be more efficient and effective than Ch. The same general behavior was found for 0.1 wt% soap solutions, however, measured  $T_{Kr}$  values were considerably higher than for 1 wt% soap solutions with identical ratio of base to C18. Probably, this can be ascribed to the complex concentration dependent phase behavior of dilute aqueous soap solutions. The presented results could be explained by an increase in bulkiness and flexibility of the counter ion from Na over Ch to ChEO<sub>m</sub>.

#### 6.3.4 Foaming properties of aqueous ChEO<sub>m</sub>C18 solutions

Liquid foams are a dispersion of gas bubbles in a liquid phase. Foams cannot be produced in a pure liquid, some surface-active material, e.g. surfactants or particles, has to be present. Due to their high interfacial free energy, all foams are thermodynamically unstable.<sup>43</sup>

Two quite easily noticeable and more or less extreme structures can be described in liquid foam systems. In freshly prepared systems, sphere foam is produced consisting of small and roughly spherical bubbles that are separated by thick films of the liquid. In this state, the foam can be regarded as a dilute dispersion of bubbles in the liquid. With increasing time, the film walls drain and the structure of the foam gradually transform into polyhedral gas cells with thin and flat liquid film walls. Here,

the liquid phase forms a network of interconnected channels, whose junction points are known as plateau borders. In a foam column (or a vial after shaking), these different foam structures may occur with time due to the drainage of the liquid into the bottom solution (see **Figure 6-14**). Usually, the foam collapses from the top to the bottom, since the thin liquid walls in the polyhedral foam are less resistant towards rupture by vibration, shock or temperature gradient.<sup>43</sup>

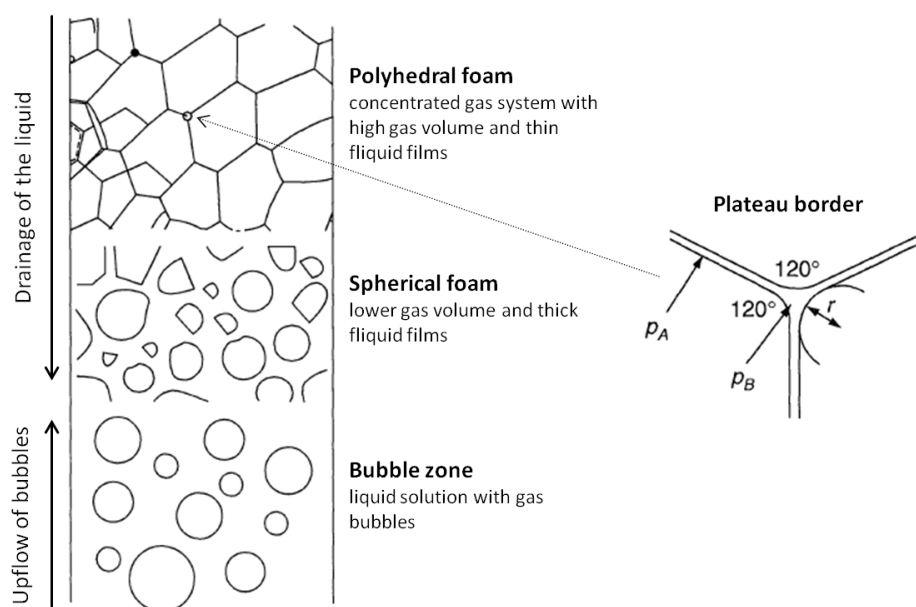


**Figure 6-14:** Area of different foam structures occurring in a foam column during formation and drainage of the foam (left). The right illustration shows the structure of a plateau border, where  $p_B$  is smaller than  $p_A$  and leads to a flow of the liquid from the centre of the film towards the plateau border. This figure is based on reference 43.

There exist various theories and connected mechanism that are used to explain foam stability. In this context, high viscosities of the liquid phase as well as the surface layer are meant to give stable foams. A high surface viscosity, which is achieved by a very tightly packed monolayer with strong cohesive interactions, dampens the film deformation prior to film rupture. Further, it is also a measure of energy dissipation in the surface layer. A high viscosity of the liquid phase retards the drainage phenomena.<sup>43</sup>

#### 6.3.4.1 Visual observations and dependence of foam stability on the ratio organic base to C18

The foaming properties of  $\text{ChEO}_m\text{C18}$ ,  $\text{ChC18}$  and  $\text{NaC12}$  solutions were investigated by simple shaking tests according the following procedure: 6 g of the test solution were filled into a vial with a volume of around 30 ml and heavily shaken

by hand for 15s. Afterwards, the vials were stored at room temperature and the quality of the foam was evaluated by visual observation.

The experiments were performed for 0.1 and 1 wt%  $\text{ChEO}_2\text{C18}$ ,  $\text{ChEO}_3\text{C18}$  and  $\text{ChC18}$  with different ratios of  $\text{ChEO}_m\text{OH}/\text{ChOH}$  to C18, which were the same as for the  $T_{\text{Kr}}$  measurements. The general findings were always the same and the foam stability was heavily dependent on the ratio of organic base to C18. Further, an aqueous solution of 1 wt% NaC12, the longest sodium soap that can be dissolved in water at room temperature, was investigated for comparison reasons. In the following, the results of the foaming of aqueous 1 wt%  $\text{ChEO}_3\text{C18}$  solutions will be discussed in detail. Foams being stable for several days will be denoted stable foams, whereas foams that are only stable for some hours will be denoted unstable foams.

The appearance of shaken aqueous 1 wt%  $\text{ChEO}_3\text{C18}$  solutions at different ratios of base to C18 (1.05/1; 1.1/1 and 1.2/1) after different times of aging are shown in **Figure 6-15**.

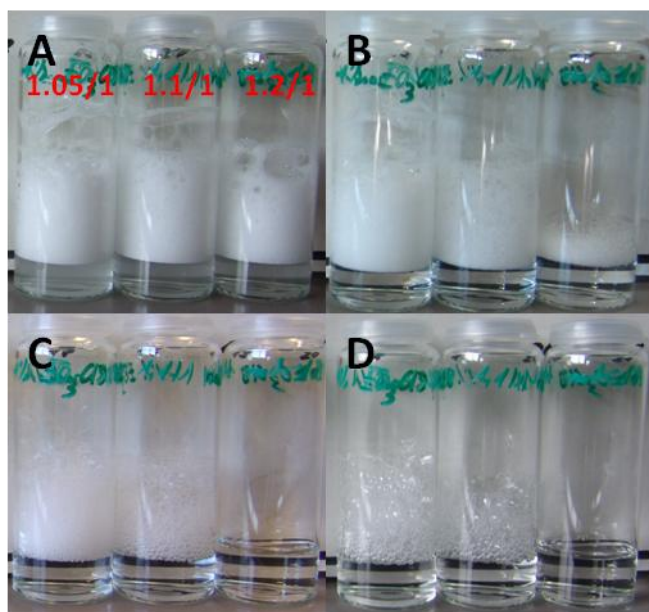


**Figure 6-15:** Time dependent appearance of aqueous 1 wt%  $\text{ChEO}_3\text{C18}$  solutions at different ratios of  $\text{ChEO}_3\text{OH}$  to C18 after shaking. The red numbers indicate the ratio of organic base to C18. Time of aging: A = 0 min, B = 45 min, C = 1 d, D = 7 d.

Immediately after shaking (photo A in **Figure 6-15**), the samples looked identical with more or less the same foam volume and density. During aging, heavy differences in foam stability between the samples were observed. For the 1.2/1 sample, the foam volume and density markedly decreased within the first hour and after 1 d the foam was gone (see photos B and C in **Figure 6-15**). The two other

samples behaved very similarly and after 1 d, the foam volume was nearly as big as the initial one after shaking. A small difference between the samples was found regarding the development of the foam density within the first day. The 1.05/1 sample kept the initial foam density for at least 4 h, while for the 1.1/1 sample a decrease in foam density, expressed by larger gas bubbles, was already observed after 45 min. After 1 d, the foam density of the 1.1/1 sample was markedly lower than the one of the 1.05/1 as illustrated in photo C in **Figure 6-15**. After 7 d of aging, the foam volume was still close to the initial one after shaking, but now in both samples the foam density was quite low and the polyhedral form of the liquid film was well observed (see photo D in **Figure 6-15**). Foaming tests with aqueous 1 wt%  $\text{ChEO}_3\text{C18}$  solutions at other base to C18 ratios (1/1; 1.5/1 and 2/1) were also carried out. The 1/1 sample, which was turbid at room temperature, also gave stable foams similar to the ones of the 1:05/1 and 1.1/1 samples, but the foam volume was decreased. Possibly, this can be attributed to the precipitate. The two solutions with a higher ratio of base to C18 behaved identically to the 1.2/1 system.

Aqueous 1 wt%  $\text{ChEO}_2\text{C18}$  samples showed the same behavior (foam volume and foam stability) as presented for the  $\text{ChEO}_3\text{C18}$  systems except that the border between stable and unstable foams is shifted to lower ratios of base to C18. That means, the (clear) 1/1  $\text{ChEO}_2\text{C18}$  solution behaves like the 1.05/1  $\text{ChEO}_3\text{C18}$  solution, the 1.05/1 like the 1.1/1 and the 1.1/1 like the 1.2/1 one. Probably, this is, like the slight difference in  $T_{\text{Kr}}$  values, again due to the small amount of weak amine bases in the  $\text{ChEO}_3\text{C18}$  systems. Considering the pH value of the different samples, the similarity between the samples can be understood. The samples exhibiting similar foam stability possess nearly identical pH values (compare **Table 6-3** and **Table 6-4**). The importance of the pH value in the foam stability of these systems will be explained in detail in the proposed mechanism that leads to the observed foam stability in dependence of the ratio of base to C18, respectively of the pH value.

For both  $\text{ChEO}_2\text{C18}$  and  $\text{ChEO}_3\text{C18}$ , in aqueous 0.1 wt% solutions the same dependence of foam stability on the ratio of organic base to C18 is found. In these systems, the transition from stable to unstable foams is from an organic base to C18 ratio of 2/1 to 3/1. For the turbid systems with a ratio of 1/1, 1.2/1 and 1.5/1 stable foams were also obtained, but the foam volume was smaller than for the clear 2/1 system.

For both aqueous 1 wt% and 0.1 wt%  $\text{ChC18}$  solutions, it was not possible to obtain stable foams for solutions being clear at room temperature ( $T_{\text{Kr}} \leq \text{room temperature}$ ). The evolution of the foam with time for the aqueous 1 wt%  $\text{NaC12}$  sample is shown in **Figure 6-16**. Directly after shaking, the foam volume was considerably larger than

for the  $\text{ChEO}_m\text{C18}$  samples and the whole vial was filled with dense foam (see photo A in **Figure 6-16**). Probably, this can be attributed to faster adsorption kinetics of the shorter C12 molecule at newly generated surfaces compared to the C18 soap.<sup>44</sup> However, the foam is much less stable than the stable ones obtained for different  $\text{ChEO}_m\text{C18}$  samples. After 45 min of aging, although the foam volume remained constant, the foam was much less dense than immediately after preparation and the polyhedral form of the gas bubbles could clearly be observed (see photo B in **Figure 6-16**). After 4 h of aging, the foam volume nearly halved and the foam density was similar to the one of stable  $\text{ChEO}_m\text{C18}$  foams after 7 d of aging. The foam was nearly completely destroyed after 1 d of aging (see photo C in **Figure 6-16**).



**Figure 6-16:** Time dependent appearance of an aqueous 1 wt% NaC12 solution after shaking. Time of aging: A = 0 min, B = 45 min, C = 4 h, D = 1 d.

To conclude, for aqueous  $\text{ChEO}_2\text{C18}$  and  $\text{ChEO}_3\text{C18}$  systems at 0.1 and 1 wt% surfactant concentration, it is possible to generate stable foams from solutions being clear at room temperature ( $T_{\text{Kr}} \leq \text{room temperature}$ ). The same is not possible for aqueous NaC12 systems. The findings show that the stability of the foams is heavily dependent on the ratio of organic base to C18. Further, the results suggest that within the area of stable foams, the behavior of the foam during aging (foam volume and foam density) can be tailor made by careful tuning of the ratio of organic base to C18, respectively the pH value.

#### 6.3.4.2 Time dependent surface tension measurements and a possible mechanism for the formation of stable foams

Time dependant surface tension measurements were carried out for all solutions that were investigated on their foaming properties by using the pendant drop technique. In all cases, it was possible to relate the time dependence of the surface tension to foam stability. In general, the results of the surface tension measurements were well

reproducible. Only solutions that were clear at room temperature were measured to avoid problems with the pendant drop apparatus.

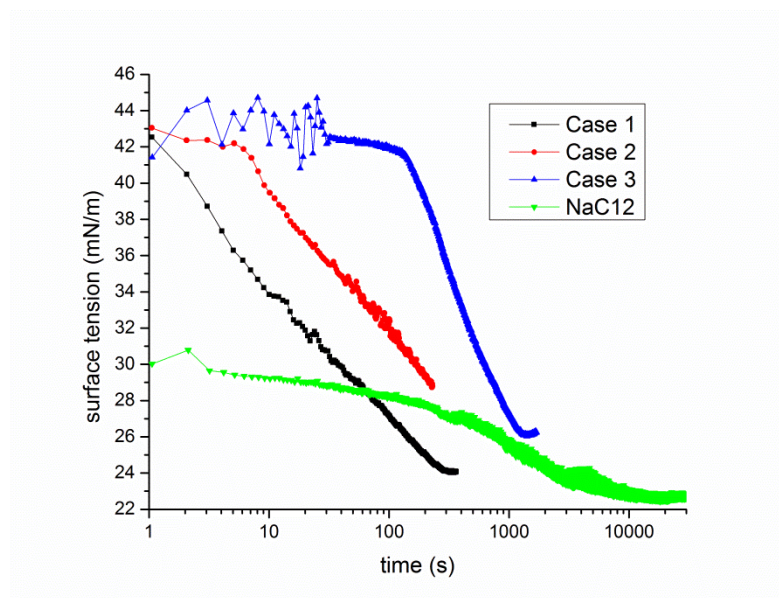


**Figure 6-17:** Time dependence of the surface tension for selected aqueous  $\text{ChEO}_2\text{C18}$  and  $\text{ChEO}_3\text{C18}$  solutions. Case 1 (■), case 2 (●) and case 3 (▲) are related to the differences in foam stability in dependence of the measured curve and explained below. The time dependent surface tension of an aqueous 1 wt% NaC12 solution is also given (▼).

In **Figure 6-17** 3 different cases for the time dependence of the surface tension of aqueous 0.1 and 1 wt%  $\text{ChEO}_m\text{C18}$  solution are illustrated. Each measurement started around  $44 \pm 2$  mN/m and showed a minimum at about  $26 \pm 2$  mN/m. Each case could be directly linked to the foam stability of the respective solution. It must be noted that the different cases are surely not as sharply separated as it will be discussed here. The differences between the investigated ratios of organic base to C18 were very large and more precise and detailed experiments would certainly show a gradual transition between each case. However, based on the results of the time dependent surface tension and foaming tests, each investigated sample could be assigned to one of the following cases:

- Case 1: The surface tension decreases linearly without exhibiting a plateau at the beginning. Here, the most stable foams were observed that kept their initial volume and density for hours. This was only found for 1 wt%  $\text{ChEO}_2\text{C18}$  1/1 and  $\text{ChEO}_3\text{C18}$  1.05/1.
- Case 2: The surface tension remains stable for 3 - 15 s before it decreases linearly. Here, somewhat less stable foams than in case 1 were observed. These foams also keep nearly their initial volume for

days, but they show an decreased density (increased bubbles) within the first hours of aging. This was the case for the 1 wt%  $\text{ChEO}_2\text{C18}$  1.05/1 and the  $\text{ChEO}_3\text{C18}$  1.1/1 samples as well as both 0.1 wt%  $\text{ChEO}_2\text{C18}$  and  $\text{ChEO}_3\text{C18}$  solutions at a ratio of 2/1.

- Case 3 + 4: Here, the surface tension remains constant for at least 20 s before it decreases linearly. The higher the ratio of organic base to C18, respectively the pH value, the longer the surface tension remained constant. However, as already mentioned, the foam stability of these solutions were identically worse than for solutions belonging to case 1 or 2.

Considering the discussion on the complex phase behavior in dilute soap solutions in section 6.3.3.2, it is very hard to compare the results on surface tension measurements of different aqueous soap solutions. The soap (anion + cation), the applied concentration as well as additional salt can heavily affect the measured surface tension value due to the many chemically different precipitates that can occur and influence the surface tension value. Nevertheless, in literature, similar time dependence of the surface tension of dilute soap solution was reported.<sup>35, 38, 39</sup> This change in surface tension with time was explained by continuing adsorption and monolayer reorganization. Further, low surface tension values of dilute soap solutions were explained by surface layers that do not only contain deprotonated soap molecules, but also protonated soap as well as acid-soap complexes.<sup>35, 36</sup> Based on these findings, a possible explanation for the obtained surface tension data as well as the related foam stability will be given.

The fact that the initial surface tension value for each  $\text{ChEO}_m\text{C18}$  solution measured is more or less the same ( $\approx 44 \pm 2$  mN/m) suggests that the initial surface adsorption, respectively the surface packing is independently from the pH value, respectively the ratio of organic base to C18. Further, the same is true for the final packing at the surface, which is indicated by identical minimum values for each sample ( $\approx 25 \pm 2$  mN/m). The only difference is the extent of the plateau of constant surface tension until the onset of surface tension decrease, which ranges from 0 s for 1 wt%  $\text{ChEO}_2\text{C18}$  1/1 to above 1000 s for 1 wt%  $\text{ChEO}_3\text{C18}$  2/1. In other words, the higher the pH value, the longer it takes until the surface tension value starts to change significantly. Considering the pH dependence of the state of the carboxylate group (protonated  $\leftrightarrow$  deprotonated) of the C18 soap, which has already been discussed in detail throughout this thesis, the following explanation for the measured time

dependent surface tension and the related foam stability of these samples is proposed: the initial surface tension value of about 44 mN/m can possibly be attributed to an initial adsorption of deprotonated C18 soap, which should be in large excess in solution compared to the protonated C18 fatty acid. In this state, the negatively charged head groups repel each other leading to a loosely covered surface with a comparable low surface viscosity (see **Figure 6-18**, left).

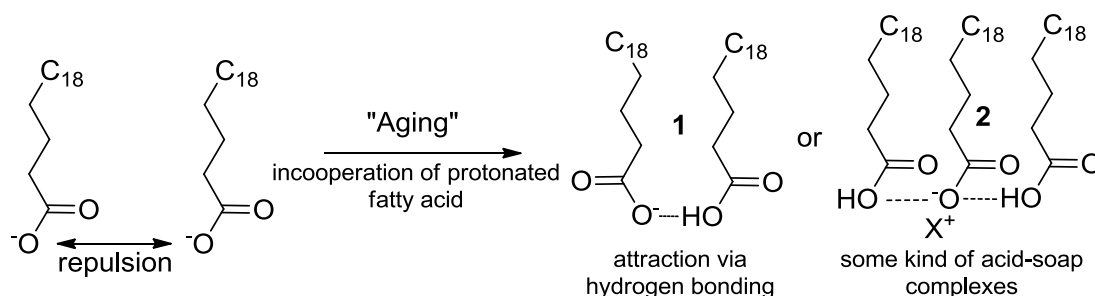


**Figure 6-18:** Possible molecular structure and ordering at the surface of the molecules in ChEO<sub>m</sub>C18 solutions at a surface tension around 44 nN/m (left site) and around 25 nN/m (right site).

It is impossible to predict what exactly happens on a molecular level as soon as the surface tension abruptly decreases, but the pH dependence strongly suggests the involvement of protonated fatty acid. The following two scenarios are possible: in the first one, protonated fatty acid being already present in solution diffuses to the interface. The amount of fatty acid in solution should be reduced by increasing the pH value and therefore it takes longer until the necessary amount of protonated fatty acid to cause surface tension reduction is present in the surface layer. The second possible scenario would be that the protonated fatty acid is directly formed in the surface layer due to the negative surface charge density and the related attraction of H<sup>+</sup> ions. Again, the higher the pH value the lower the H<sup>+</sup> ions concentration and the longer it would take to form a certain amount of fatty acid (for detailed discussion see section 2.4.4). It is also possible that both mechanisms occur simultaneously.

The slight decrease in surface tension during the first plateau and the abrupt decrease at around 42 mN/m (observed for every curve belonging to case 3) suggests that a minimum amount of fatty acid has to be present in the surface layer until a more distinct effect sets in. Whether a stable network of hydrogen bonds between protonated and deprotonated fatty acids (see **Figure 6-18**, 1) or the formation of any kind of acid-soap complexes (see **Figure 6-18**, 2) in the surface layer is responsible for the decrease in surface tension during aging is only speculative. It is even possible that some completely different pH dependent change in the molecular structure of the surface layer takes place. Independent of the surface layer structure actually formed, the C18 molecules should be more densely

packed than in the case of almost complete deprotonation of the surface layer. This is indicated by the considerably lower surface tension value and schematically illustrated in **Figure 6-18**.

The difference in foam stability between the three cases can now be explained by the formation of a tightly packed surface layer that exhibits a high surface viscosity.<sup>43</sup> The decrease in surface tension is also likely to stabilize the foam. However, these effects only work, if the change in surface ordering of the molecules starts within a certain time range ( $< 15$  s). If it takes too long (case 3), probably the structure of the foam changes too heavy within the first minute(s) and the stabilization effect cannot be obtained.

The time dependent surface tension of an aqueous 1 wt% NaC12 solution is also shown in **Figure 6-17**. It is shifted to significantly lower surface tension values than the samples of ChEO<sub>m</sub>C18 belonging to case 3, but it exhibits the same course. Nearly identical foam stabilities of the NaC12 and the unstable ChEO<sub>m</sub>C18 samples suggest that a change in molecular ordering at the surface, which possibly leads to an increased surface viscosity, is more important for foam stability than low surface tensions. However, the lower initial surface tension ( $\approx 30$  mN/m) of the 1 wt% NaC12 sample possibly leads to the higher foam volume compared to all ChEO<sub>m</sub>C18 samples.

## 6.4 Conclusion

It could be shown that ChEO<sub>m</sub>S18 ( $m = 2,3$ ) surfactants show an improved water solubility compared to ChS18 or NaS18 at room temperature. Other than for the latter ones, an aqueous 1 wt% solution of ChEO<sub>3</sub>S18 was highly translucent with a waterlike viscosity. 0.02 and 0.1 wt% aqueous ChEO<sub>m</sub>S18 solutions were even as clear as water. The markedly difference in macroscopic appearance at 1 wt% compared to ChS18 could be explained by the assumption that the more bulky and flexible ChEO<sub>m</sub> counter ion prevents the formation of liquid crystalline phases. Stirring experiments at 25 °C with NaS18 plus additional Ch or ChEO<sub>3</sub> support these assumption. Moreover, cmc values of ChEO<sub>m</sub>S18 at 25 °C are distinctly lower than the one of ChS18. A significant drawback of introducing the oxyethylene groups into the counter ion instead of chemically modification of the alkyl sulfate surfactant is the maintained sensitivity to hard water ions of the chemically unmodified surfactant.

Further, It was possible to reduce  $T_{Kr}$  of NaS16 (44 °C) below room temperature by the addition of ChEO<sub>m</sub>Cl ( $m = 1-3$ ). The different ethoxylated choline derivatives

showed nearly the same effect and were slightly more efficient and effective than simple choline. For NaS18 solutions, ChEO<sub>3</sub> was found to be more efficient and effective than Ch or ChEO<sub>1</sub>, but the lowest obtained  $T_{Kr}$  value was still far above room temperature ( $\approx 40\text{ }^{\circ}\text{C}$ ).

Aqueous 1 wt% solutions of pure ChEO<sub>m</sub>C18 ( $m = 2,3$ ) exhibited  $T_{Kr}$  values around room temperature, which is much smaller than the values for ChS18 ( $44\text{ }^{\circ}\text{C}$ ) and NaC18 ( $71\text{ }^{\circ}\text{C}$ ). By increasing the amount of organic base to C18,  $T_{Kr}$  of the ChEO<sub>m</sub>C18 solutions was more efficiently and effectively reduced than for the ChC18 system. For the ChEO<sub>m</sub>C18 systems, it was even possible to reduce  $T_{Kr}$  to below  $0\text{ }^{\circ}\text{C}$ , while for ChC18 the lowest  $T_{Kr}$  value achieved for the investigated ratios was  $16\text{ }^{\circ}\text{C}$ .  $T_{Kr}$  of an NaC18 solution could not be depressed below room temperature. The significant differences in  $T_{Kr}$  values of the pure surfactants as well as the different behavior with increasing ratio of base to C18 could be explained by partial protonation of the C18 soap in solution as well as the difference in bulkiness and flexibility of the counter ions. For the 0.1 wt% systems, the same general results were obtained. However,  $T_{Kr}$  values at identical ratios of base to C18 were considerably higher. This concentration dependent solubility behavior is contradictory to Krafft theory and was explained by the complex phase behavior of soaps in dilute aqueous solutions.

Finally, it was possible to produce very stable foams from ChEO<sub>m</sub>C18 solutions that were clear at room temperature. The behavior of these foams during aging (foam volume and foam density) could be controlled by the ratio of organic base to C18. Time dependent surface tension measurements suggested that the speed of formation of a newly structured and probably highly viscous surface layer is responsible for the observed differences in stability.

To sum up, by using ethoxylated choline derivatives as counter ions of long chain C18 alkyl sulfate or soap, it is possible to obtain highly translucent (S18) or completely clear (C18) aqueous solutions at 1 wt% surfactant concentration at room temperature. By reducing the surfactant concentration down to 0.1 wt% even completely clear solutions can be obtained for ChEO<sub>m</sub>S18. For ChEO<sub>m</sub>C18 systems, slightly increasing the ratio of organic base to C18 yields  $T_{Kr}$  values even below  $0\text{ }^{\circ}\text{C}$ . These significant differences in water solubility at low temperatures compared to the respective common sodium surfactants opens new opportunities of using these long chain C18 surfactants in many low-temperature applications. This area is currently dominated by short chain (C12 and C14) surfactants due to the low solubility of longer chain surfactants with conventional alkali counter ions. Next to expected reductions of the amount of surfactant in certain applications due to an increased

surface activity and decreased cmc values of longer chain surfactants, an increased usage of long chain C18 surfactants is particularly interesting for the European market and should be desired from a economical, agricultural as well as environmental point of view. On the one hand, these long chain surfactants could be oleochemically prepared from common oils produced from plants harvested in Europe, like rapeseed, olive or sunflower oil, which contain mainly saturated and unsaturated C18 fatty acids.<sup>45-48</sup> On the other hand, by increasing the demand for C18 surfactants due to partial replacement of shorter chain homologues in different applications, the value of the European oils would rise and the imports of oils for oleochemical purposes containing short chain fatty acids, like coconut or palm kernel oil, into the EU could be reduced.<sup>46</sup>

At last, it must be noted that in the near future comprehensive toxicity and biodegradability tests have to be performed to make sure that the usage ethoxylated choline derivatives in surfactants is both safe for humans and the environment.

## 6.5 Experimental

### 6.5.1 Chemicals

Sodium octadecyl sulfate (NaS18, Alfa Aesar, > 98 %, LOT: 10176541), sodium laurate (NaC12, 99-100 %, Sigma) and stearic acid (C18,  $\geq$  98.5 %, Sigma) were used as received. Sodium hydroxide solution (NaOH) was bought from Merck, TitriPur and choline hydroxide solution (ChOH,  $\approx$  46.5 wt% in water) was provided by TAMINCO. ChEO<sub>m</sub> (m =1-3) was provided as the chloride salt in aqueous solutions by BASF.

The main component of each ChEO<sub>m</sub>Cl stock solution was determined by mass spectroscopy. Further, the concentration of quaternary ammonium ion in mol ChEO<sub>m</sub>Cl per gram stock solution was determined by <sup>1</sup>H-NMR experiments using an internal standard. The amount of solid content (determined by BASF), the determined concentration of ChEO<sub>m</sub>Cl as well as the solid content of ChEO<sub>m</sub>Cl (calculated by multiplying the ChEO<sub>m</sub>Cl concentration with the respective molar weight) are listed in **Table 6-9**. Comparing the amount of overall solid content to the content of ChEO<sub>m</sub>Cl shows that the solutions are considerably impure.

Substance	c [mol/g solution]	wt % ChEO <sub>m</sub> Cl	wt % total
ChEO <sub>1</sub> Cl	0.00204	37.5	40.0
ChEO <sub>2</sub> Cl	0.00152	34.6	40.0
ChEO <sub>3</sub> Cl	0.00119	32.3	39.0

**Table 6-9:** Concentration of ChEO<sub>m</sub>Cl per gram stock solution, wt % ChEO<sub>m</sub>Cl and total wt % of solid content for aqueous stock solutions of ChEO<sub>m</sub>Cl.

ChEO<sub>m</sub>OH stock solutions were obtained from ChEO<sub>m</sub>Cl stock solutions by ion exchange using the strong basic ion exchanger III (OH<sup>-</sup> form) from Merck. The ion exchanger was first rinsed with 2 M NaOH to ensure complete loading and afterwards with millipore water until the effluent had a pH around 7. Then, a 0.1 M ChEO<sub>m</sub>Cl solution slowly passed the column at ambient temperature. The amount of used ChEO<sub>m</sub>Cl was around 1/4 of the maximum exchange capacity. Almost complete exchange of Cl<sup>-</sup> against OH<sup>-</sup> was checked by adding 1 M silver nitrate (AgNO<sub>3</sub>) solution after acidifying the ChEO<sub>m</sub>OH solution with nitric acid.

## 6.5.2 Surfactant synthesis

ChEO<sub>2</sub>S18 and ChEO<sub>m</sub>S18 was prepared identically to ChS18 and MeChS18 as described in section 4.5.2. The only difference was that the ion exchanger was loaded with a ChEO<sub>m</sub>OH solution (c ≈ 0.09 mM/g solution) and the amount of ChEO<sub>m</sub>OH was around 3 times the maximum exchange capacity of the ion exchanger. The surfactants were obtained as a white and slightly sticky solid.

Purity of the surfactants was checked by <sup>1</sup>H NMR and <sup>13</sup>C NMR in CDCl<sub>3</sub> and electron spray mass spectroscopy (ES-MS). Mass spectroscopy was carried out with an Agilent Q-TOF 6540 UHD instrument. NMR spectra were recorded on a Bruker Advance 300 spectrometer at 300 MHz and tetramethylsilane as internal standard.

*ChEO<sub>2</sub>S18:*

**<sup>1</sup>H-NMR** (300 MHz, CDCl<sub>3</sub>, 25 °C, TMS): δ = 0.87 (t, 3H; CH<sub>2</sub>CH<sub>3</sub>), 1.25 (m, 30H; CH<sub>2</sub>CH<sub>2</sub>CH<sub>3</sub>), 1.65 (quin, 2H; CH<sub>2</sub>CH<sub>2</sub>SO<sub>4</sub><sup>-</sup>), 3.33 (s, 9H; N(CH<sub>3</sub>)<sub>3</sub>), 3.58-3.75 (m, 10H; N(CH<sub>3</sub>)<sub>3</sub>CH<sub>2</sub>, CH<sub>2</sub>OH and CH<sub>2</sub>CH<sub>2</sub>OCH<sub>2</sub>), 4.00 (m, 4H; CH<sub>2</sub>SO<sub>4</sub><sup>-</sup> and N(CH<sub>3</sub>)<sub>3</sub>CH<sub>2</sub>CH<sub>2</sub>)

**<sup>13</sup>C-NMR** (300 MHz, CDCl<sub>3</sub>, 25 °C, TMS): δ C= 14.16 (CH<sub>2</sub>CH<sub>3</sub>), 22.72 (CH<sub>2</sub>CH<sub>3</sub>), 25.87 (CH<sub>2</sub>CH<sub>2</sub>CH<sub>3</sub>), 29.39-29.74 (CH<sub>2</sub>CH<sub>2</sub>), 31.95 (CH<sub>2</sub>CH<sub>2</sub>SO<sub>4</sub><sup>-</sup>), 54.50 (N(CH<sub>3</sub>)<sub>3</sub>), 61.43 (CH<sub>2</sub>OH), 65.29 (N(CH<sub>3</sub>)<sub>3</sub>CH<sub>2</sub>), 65.81 (N(CH<sub>3</sub>)<sub>3</sub>CH<sub>2</sub>CH<sub>2</sub>), 68.23 (CH<sub>2</sub>SO<sub>4</sub><sup>-</sup>), 70.27-70.32 (OCH<sub>2</sub>CH<sub>2</sub>O), 72.38 (CH<sub>2</sub>CH<sub>2</sub>OH)

**ES-MS (Agilent):** m/z (+p): 192.16 [ $M^+$ ]; (p-): 349.24 [ $M^-$ ]

*ChEO<sub>3</sub>S18:*

**<sup>1</sup>H-NMR** (300 MHz, CDCl<sub>3</sub>, 25 °C, TMS):  $\delta$  = 0.87 (t, 3H; CH<sub>2</sub>CH<sub>3</sub>), 1.24 (m, 30H; CH<sub>2</sub>CH<sub>2</sub>CH<sub>3</sub>), 1.65 (quin, 2H; CH<sub>2</sub>CH<sub>2</sub>SO<sub>4</sub><sup>-</sup>), 3.34 (s, 9H; N(CH<sub>3</sub>)<sub>3</sub>), 3.56-3.76 (m, 14H; N(CH<sub>3</sub>)<sub>3</sub>CH<sub>2</sub>, CH<sub>2</sub>OH and CH<sub>2</sub>CH<sub>2</sub>OCH<sub>2</sub>), 4.00 (m, 4H; CH<sub>2</sub>SO<sub>4</sub><sup>-</sup> and N(CH<sub>3</sub>)<sub>3</sub>CH<sub>2</sub>CH<sub>2</sub>)

**<sup>13</sup>C-NMR** (300 MHz, CDCl<sub>3</sub>, 25 °C, TMS):  $\delta$  C= 14.16 (CH<sub>2</sub>CH<sub>3</sub>), 22.72 (CH<sub>2</sub>CH<sub>3</sub>), 25.87 (CH<sub>2</sub>CH<sub>2</sub>CH<sub>3</sub>), 29.39-29.74 (CH<sub>2</sub>CH<sub>2</sub>), 31.95 (CH<sub>2</sub>CH<sub>2</sub>SO<sub>4</sub><sup>-</sup>), 54.50 (N(CH<sub>3</sub>)<sub>3</sub>), 61.37 (CH<sub>2</sub>OH), 65.19 (N(CH<sub>3</sub>)<sub>3</sub>CH<sub>2</sub>), 65.73 (N(CH<sub>3</sub>)<sub>3</sub>CH<sub>2</sub>CH<sub>2</sub>), 68.20 (CH<sub>2</sub>SO<sub>4</sub><sup>-</sup>), 69.97-70.49 (OCH<sub>2</sub>CH<sub>2</sub>O), 72.39 (CH<sub>2</sub>CH<sub>2</sub>OH)

**ES-MS (Agilent):** m/z (+p): 236.19 [ $M^+$ ]; (p-): 349.24 [ $M^-$ ]

### 6.5.3 Sample preparation

Samples with NaS16 or NaS18 plus ChEO<sub>m</sub>Cl were prepared as follows: the sodium surfactant, the ChEO<sub>m</sub>Cl stock solution and water were mixed in a vial und heated to some degrees above  $T_{Kr}$  until a clear and homogeneous solution was obtained. Then, the samples were frozen at - 20 °C and analyzed by turbidity measurements or stirring experiments. The exact molar ratios of ChEO<sub>m</sub> to NaSXX are given in the respective section.

Aqueous solutions of ChC18, ChEO<sub>2</sub>C18 and ChEO<sub>3</sub>C18 were prepared by mixing defined amounts of C18, organic base stock solution and water in a vial. The samples were heated above the clearing temperature until a clear and homogeneous solution was obtained. Then, the samples were frozen at - 20 °C and analyzed by turbidity measurements or stirring experiments. The exact molar ratios of organic base to C18 are given in the respective section.

### 6.5.4 Determination of $T_{Kr}$

$T_{Kr}$  values were measured with a home-built apparatus as described in section 4.5.3.

## 6.5.5 Surface tension measurements

### 6.5.5.1 Du Noüy ring technique

Concentration dependent surface tension measurements were carried out with a Krüss Tensiometer (model K100 MK2). The exact procedure of the measurement as well as analysis of the obtained curves was done as described in section 4.5.4.

### 6.5.5.2 Pendant drop technique

Time dependent surface tension isotherms were obtained by a profile analysis tensiometer (PAT-1M, SINTERFACE Technologies, Berlin), which was used in the pendant drop configuration. The schematic setup for the pendant drop method is shown in **Figure 6-19**.

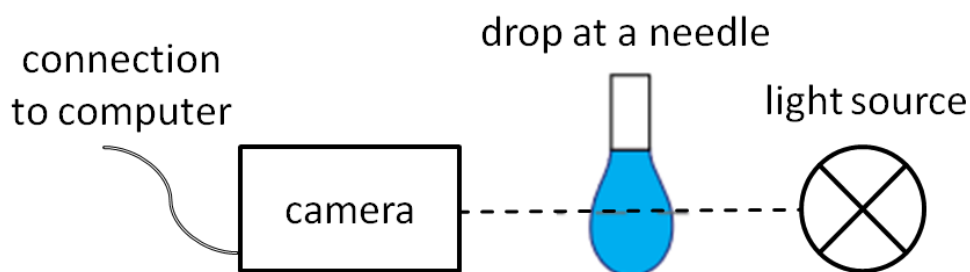


**Figure 6-19:** Simple schematic setup of the pendant drop technique.

The tensiometer delivers surface tension values according to the Young-Laplace equation:

$$\gamma \left( \frac{1}{R_1} + \frac{1}{R_2} \right) = \Delta P \quad (1-6)$$

In equation 1-6,  $\gamma$  denotes the active surface tension,  $R_1$  and  $R_2$  the respective radii of curvature and  $\Delta P$  the Laplace pressure across the interface. Further,  $\Delta P$  can be written as the sum of the pressure difference in a reference plane  $\Delta P_0$  and the hydrostatic pressure  $\Delta \rho g z$ :

$$\Delta P = \Delta P_0 \pm \Delta \rho g z \quad (2-6)$$

here,  $\Delta \rho$  is the difference in mass density of air and the aqueous phase,  $g$  the gravitational acceleration,  $z$  the vertical distance from the reference plane. The

reference plane is usually set at the apex, since there is  $R_1 = R_2$  due to axial symmetry of the droplet and further calculations are simplified. The pear-like shape of the droplet results from the interplay between surface tension forces, which try to minimize the surface area and realize a spherical shape of the drop, and gravitational forces, which stretch the droplet from its spherical shape. Images of the hanging drop are captured by a camera and analyzed by algorithms for contour tracing. Afterwards, a computer software fits the Young-Laplace equation, using  $\gamma$  as a fit parameter, to get a curve that corresponds to the experimentally obtained coordinates of the drop meniscus.<sup>49</sup> Drop formation was controlled by a computer controlled syringe pump that was connected to a stainless steel capillary with a diameter of 2 mm. All measurements were carried out at ambient temperature ( $\approx 23$  °C). For each measurement, the drop volume was 12  $\mu\text{l}$  to ensure both accuracy of the data and preventing the drop from tearing off.

### 6.5.6 Foaming tests

The foam behavior of the respective aqueous solutions was investigated by simple shaking test according to the following procedure: 6 g of the test solution were filled into a vial with a volume of around 30 ml and heavily shaken by hand for 15s. Afterwards, the vials were stored at room temperature and the quality of the foam (foam volume and foam density) was evaluated by visual observation.

## 6.6 Literature

1. Domingo, X., Alcohol and Alcohol Ether Sulfates. In *Anionic Surfactants: Organic Chemistry*, Stache, H., Ed. Marcel Dekker: 1996; Vol. 56, pp 223-312.
2. Czichocki, G.; Holzbauer, H. R.; Martens, C., *Lipid / Fett* **1992**, 94 (2), 66-73.
3. Schwuger M, J., Interfacial and Performance Properties of Sulfated Polyoxyethylenated Alcohols. In *Structure/Performance Relationships in Surfactants*, Rosen, M. J., Ed. American Chemical Society: 1984; Vol. 253, pp 3-26.
4. Shinoda, K.; Minegishi, Y.; Arai, H., *J Phys Chem* **1976**, 80 (18), 1987-1988.
5. Lindman, B., Physico-Chemical Properties of Surfactants. In *Handbook of Applied Surface and Colloid Chemistry (Volume 1)*, Holmberg, K., Ed. Wiley: 2002; pp 421-443.
6. Weil, J. K.; Bistline, R. G.; Stirton, A. J., *J Phys Chem* **1958**, 62 (9), 1083-1085.
7. Klein, R.; Zech, O.; Maurer, E.; Kellermeier, M.; Kunz, W., *J Phys Chem B* **2011**, 115 (29), 8961-8969.

8. Zech, O.; Hunger, J.; Sangoro, J. R.; Iacob, C.; Kremer, F.; Kunz, W.; Buchner, R., *Phys Chem Chem Phys* **2010**, 12 (42), 14341-14350.
9. Zech, O.; Kellermeier, M.; Thomaier, S.; Maurer, E.; Klein, R.; Schreiner, C.; Kunz, W., *Chem - Eur J* **2009**, 15 (6), 1341-1345.
10. Domingo, X., Alcohol and Alcohol Ether Sulfates. In *Anionic Surfactants: Organic Chemistry*, Stache, H., Ed. Marcel Dekker: 1996; pp 223-312.
11. Ferreira, R.; Garcia, H.; Sousa, A. F.; Guerreiro, M.; Duarte, F. J. S.; Freire, C. S. R.; Calhorda, M. J.; Silvestre, A. J. D.; Kunz, W.; Rebelo, L. P. N.; Silva Pereira, C., *RSC Adv* **2014**, 4 (6), 2993-3002.
12. Klein, R.; Kellermeier, M.; Touraud, D.; Müller, E.; Kunz, W., *J Colloid Interface Sci* **2013**, 392 (0), 274-280.
13. Isik, M.; Gracia, R.; Kollnus, L. C.; Tomé, L. C.; Marrucho, I. M.; Mecerreyes, D., *ACS Macro Lett* **2013**, 2 (11), 975-979.
14. Stolte, S.; Steudte, S.; Areitioaurtena, O.; Pagano, F.; Thöming, J.; Stepnowski, P.; Igartua, A., *Chemosphere* **2012**, 89 (9), 1135-1141.
15. Liu, Q.-P.; Hou, X.-D.; Li, N.; Zong, M.-H., *Green Chem* **2012**, 14 (2), 304-307.
16. Costa, A. J. L.; Soromenho, M. R. C.; Shimizu, K.; Marrucho, I. M.; Esperança, J. M. S. S.; Lopes, J. N. C.; Rebelo, L. P. N., *ChemPhysChem* **2012**, 13 (7), 1902-1909.
17. Aparicio, S.; Atilhan, M.; Khraisheh, M.; Alcalde, R., *J Phys Chem B* **2011**, 115 (43), 12473-12486.
18. Petkovic, M.; Ferguson, J. L.; Gunaratne, H. Q. N.; Ferreira, R.; Leitao, M. C.; Seddon, K. R.; Rebelo, L. P. N.; Pereira, C. S., *Green Chem* **2010**, 12 (4), 643-649.
19. Yu, Y.; Lu, X.; Zhou, Q.; Dong, K.; Yao, H.; Zhang, S., *Chem - Eur J* **2008**, 14 (35), 11174-11182.
20. Klein, R.; Touraud, D.; Kunz, W., *Green Chem* **2008**, 10 (4), 433-435.
21. Fukaya, Y.; Iizuka, Y.; Sekikawa, K.; Ohno, H., *Green Chem* **2007**, 9 (11), 1155-1157.
22. Shinoda, K.; Maekawa, M.; Shibata, Y., *J Phys Chem* **1986**, 90 (7), 1228-1230.
23. Hato, M.; Tahara, M.; Suda, Y., *J Colloid Interface Sci* **1979**, 72 (3), 458-464.
24. Scamehorn, J. F., An Overview of Phenomena Involving Surfactant Mixtures. In *Phenomena in Mixed Surfactant Systems*, Scamehorn, J. F., Ed. American Chemical Society: 1986; Vol. 311, pp 1-27.
25. Kronberg, B.; Castas, M.; Silvestroni, R., *J Dispersion Sci Technol* **1994**, 15 (3), 333-351.

26. Myers, D., Fluid Surfaces and Interfaces. In *Surfactant Science and Technology*, John Wiley & Sons, Inc.: 2005; pp 80-106.
27. Rosen, M. J., Reduction of Surface and Interfacial Tension by Surfactants. In *Surfactants and Interfacial Phenomena*, John Wiley & Sons, Inc.: 2004; pp 208-242.
28. Lin, B.; McCormick, A. V.; Davis, H. T.; Strey, R., *J Colloid Interface Sci* **2005**, 291 (2), 543-549.
29. Zana, R., *Langmuir* **2004**, 20 (14), 5666-5668.
30. Klein, R.; Kellermeier, M.; Drechsler, M.; Touraud, D.; Kunz, W., *Colloids Surf A Physicochem Eng Asp* **2009**, 338 (1-3), 129-134.
31. Laughlin, R. G., Phase Diagrams and the Phase Rule. In *The Aqueous Phase Behaviour of Surfactants*, Academic Press: 1994; pp 67-101.
32. Klein, R., Dissertation. Universität Regensburg: 2011.
33. McBain, J.; Sierichs, W., *J Am Oil Chem Soc* **1948**, 25 (6), 221-225.
34. Laughlin, R. G., The Characteristic Features of Surfactant Phase Behavior In *The Aqueous Phase Behaviour of Surfactants*, Academic Press: 1994; pp 102-154.
35. Kralchevsky, P. A.; Danov, K. D.; Pishmanova, C. I.; Kralchevska, S. D.; Christov, N. C.; Ananthapadmanabhan, K. P.; Lips, A., *Langmuir* **2007**, 23 (7), 3538-3553.
36. Wen, X.; Lauterbach, J.; Franses, E. I., *Langmuir* **2000**, 16 (17), 6987-6994.
37. Wen, X.; Franses, E. I., *J Colloid Interface Sci* **2000**, 231 (1), 42-51.
38. Wen, X.; McGinnis, K. C.; Franses, E. I., *Colloids Surf A Physicochem Eng Asp* **1998**, 143 (2-3), 371-380.
39. Coltharp, K. A.; Franses, E. I., *Colloids Surf A Physicochem Eng Asp* **1996**, 108 (2), 225-242.
40. Lucassen, J., *J Phys Chem* **1966**, 70 (6), 1824-1830.
41. Lynch, M. L., *Curr Opin Colloid Interface Sci* **1997**, 2 (5), 495-500.
42. Arnould, A.; Perez, A. A.; Gaillard, C.; Douliez, J.-P.; Cousin, F.; Santiago, L. G.; Zemb, T.; Anton, M.; Fameau, A.-L., *J Colloid Interface Sci* **2015**, 445, 285-293.
43. Pugh, R. J., Foams and Foaming. In *Handbook of Applied Surface and Colloid Chemistry (Volume 2)*, Holmberg, K., Ed. Wiley: 2002; pp 23-43.
44. Schmiedel, P.; von Rybinski, W., Applied Theory of Surfactants. In *Chemistry and Technology of Surfactants*, Blackwell Publishing Ltd: 2007; pp 46-90.
45. Przybylski, R., Canola/Rapeseed Oil. In *Vegetable Oils in Food Technology*, Gunstone, F. D., Ed. Wiley-Blackwell: 2011; pp 107-136.
46. Gunstone, F. D., Production and Trade of Vegetable Oils. In *Vegetable Oils in Food Technology*, Gunstone, F. D., Ed. Wiley-Blackwell: 2011; pp 1-24.

47. Grompone, M. A., Sunflower Oil. In *Vegetable Oils in Food Technology*, Gunstone, F. D., Ed. Wiley-Blackwell: 2011; pp 137-167.
48. Boskou, D., Olive Oil. In *Vegetable Oils in Food Technology*, Gunstone, F. D., Ed. Wiley-Blackwell: 2011; pp 243-271.
49. Berry, J. D.; Neeson, M. J.; Dagastine, R. R.; Chan, D. Y. C.; Tabor, R. F., *J Colloid Interface Sci* **2015**, *454*, 226-237.



## **Chapter 7 Laundry detergency tests at room temperature**

### **7.1 Abstract**

In the last decades, subjects like energy consumption and sustainability are important issues in the evaluation of processes or products due to an increased public environmental awareness. For machine laundry washing, the energy consumption mainly depends on the washing temperature during the process.<sup>1</sup> Thus, to meet consumers demand for high performance detergency products and simultaneously fulfill environmental energy saving demands, it is necessary to develop detergent formulations being highly efficient at ambient temperatures.

There exist many studies that, if used under the right conditions, detergency power of ionic surfactants increases with increasing hydrophobic chain length of the surfactant.<sup>2-5</sup> However, the use of common sodium long chain alkyl sulfates in modern laundry detergent formulations, which are meant to work from ambient to elevated temperatures, is restricted by their low solubility at moderate temperatures.

Therefore, the important findings on improving the solubility, respectively reducing  $T_{Kr}$  of long chain alkyl sulfates presented in the chapters 4-6 were applied to formulate complex aqueous detergent systems containing long chain alkyl sulfates in millipore and in hard water. The formulations were based on the standard detergent formulation used by BASF, in which the alkyl ether sulfate was replaced by NaS12, NaS16 or NaS18. The detergency power of these detergent solutions was tested for two cotton textiles with different soils at room temperature and compared to the original formulation and Persil Universalpulver from Henkel.

Unfortunately, no statement about the effect of long chain alkyl sulfates on detergency power could be made. For the first textile investigated, a standardized cotton fabric soiled with sebum and pigment,  $\Delta E$  values were too small and identical for all investigated systems. For the second textile, a cotton fabric that was soiled in the lab with a mixture of palmitic acid and Sudan Black B, inconsistencies in the results and uncertainties in the evaluation methods allowed no proper statements.

## 7.2 Introduction

The main share ( $\approx 50\%$ ) of the global surfactant consumption is made up by the household cleaning sector and laundry detergents contribute by far for the largest portion of this domestic cleaning products market.<sup>6-8</sup> In 2015, the global domestic cleaning products market was estimated to be worth 100 billion dollars per year.<sup>6</sup> In 2016, The EU market value of laundry care was 13.5 billion dollars and constituted 47.3 % market share in household care.<sup>9</sup>

The first known washing detergent was soap. In 1907, Henkel introduced the first heavy-duty detergent containing soap and so-called builders. In 1932, the first synthetic detergent based on anionic fatty alcohol sulfates was introduced also by Henkel. A few years later, nonionic surfactants were used for the first time in laundry detergents. In the following decades, lots of research on laundry detergents was carried out and new surfactants and builder systems as well as additional ingredients, like soil antiredeposition agents, enzymes, bleaches or optical brighteners were introduced into detergent formulations.<sup>10</sup> These developments were mainly caused by environmental legislation, progress in washing technology and consumer habits.<sup>10, 11</sup> Modern laundry detergents are very complex formulations and consist of up to 20 individual components, of which each has very specific functions during the washing process.<sup>3, 11</sup> Laundry detergent composition and the share of certain ingredients in the final formulation can vary heavily between different continents due to different washing habits and washing machines used.<sup>3, 11-13</sup>

Surfactants are by far the most important laundry detergent ingredients and comprise as much as 15 to 40 % of the total laundry detergent formulation.<sup>11</sup> In modern detergent formulations mixtures of anionic and nonionic surfactants are used to strengthen their cleaning performance by synergisms. Here, anionic surfactants are the most important surfactant class and are used in superior amounts than nonionic ones in common laundry detergents.<sup>3, 6, 14</sup> In industrial countries, typical anionic surfactants used in laundry detergents are linear alkyl benzene sulfonates (LABS), alkyl sulfates (AS), alkyl ether sulfates (AES) or  $\alpha$ -methyl ester sulfonate (MES). Typical nonionic ones are fatty alcohol ethoxylates (AE), alkylpolyglycosides (APG), methyl ester ethoxylates (MEE) or alkylamine oxides (AAO). The chemical structures of these surfactants are shown in **Figure 7-1**.

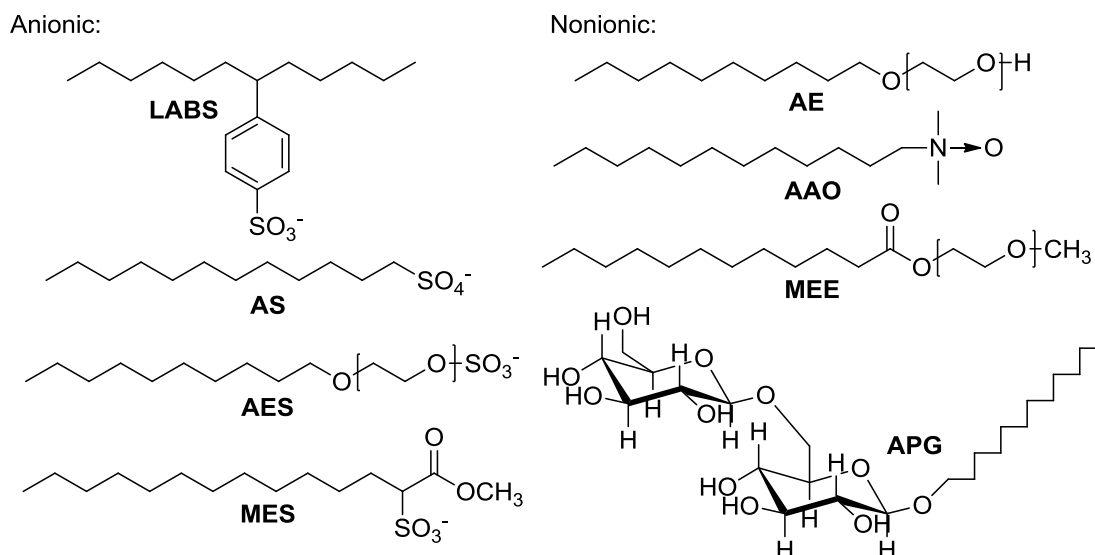


**Figure 7-1:** Chemical structures of anionic (left) and nonionic (right) surfactants used in laundry detergent formulations: linear alkyl benzene sulfonates (LABS), alkyl sulfates (AS), alkyl ether sulfates (AES),  $\alpha$ -methyl ester sulfonate (MES), fatty alcohol ethoxylates (AE), alkylamine oxides (AAO), methyl ester ethoxylates (MEE) and alkylpolyglycosides (APG).

For sodium alkyl sulfates, it was shown that detergency increases with increasing number of C atoms in the straight surfactant chain.<sup>2, 4, 5</sup> However, due to the high  $T_{\text{Kr}}$  values of NaS16 or NaS18, these experiments were all performed at high temperatures ( $\approx 60^\circ\text{C}$ ), since optimum detergency is generally achieved by the longest straight-chain surfactants being sufficiently soluble in the cleaning solution under use conditions.<sup>2</sup> Another advantage of longer chain alkyl sulfates, next to an increase in detergency, is the great reduction of the amount of surfactant being necessary to achieve significant deterative properties compared to shorter chain ones.<sup>4, 5</sup>

Solving the solubility problem of long chain alkyl sulfates at ambient temperatures, which is now possible (see Chapter 4 to Chapter 6), the detergency results at high temperatures also render these surfactants promising ingredients for highly efficient low temperature laundry detergents. Low temperature washing is desired from an environmental point of view, since the energy consumption during the wash process mainly depends on the washing temperature.<sup>1</sup> It could be shown that reduction of the wash temperature from 60 to 30  $^\circ\text{C}$  led to a decrease in energy consumption of roughly 60 % and from 40 to 30  $^\circ\text{C}$  of about 30 %.<sup>15</sup>

In this part of the work, the design of the surfactant solutions subjected to detergency tests at room temperature was driven by two aspects. First, the influence of the alkyl sulfate's hydrophobic chain length on detergency performance at room temperature should be investigated. Secondly, the effect of Ch and ChEO<sub>3</sub> as simple on-top additives to a basic detergent formulation should be checked.

Therefore, detergent solutions based on a standard surfactant formulation given by BASF plus additional builder were prepared in millipore and hard water. The four investigated surfactant mixtures were LABS/AE plus AES or NaS12 or NaS16 or NaS18. The used builders were  $\text{Ch}_4\text{EDTA}$ ,  $(\text{ChEO}_3)_4\text{EDTA}$  and  $\text{Na}_4\text{EDTA}$ . In all samples containing Ch or  $\text{ChEO}_3$ , the molecular ratio of Ch or  $\text{ChEO}_3$  to Na was between 2.5 and 4 to take advantage of the solubility increasing, respectively  $T_{\text{Kr}}$  reducing effect of additional Ch or  $\text{ChEO}_3$  on long chain sodium alkyl sulfates. These effects are discussed in detail in chapterChapter 5 andChapter 6. The detergency tests were also carried out with Persil Universalpulver from Henkel for comparison reasons.

The used textiles were a standardized cotton being already soiled with sebum plus pigment and a cotton textile, which was soiled in our lab by a mixture of palmitic acid plus Sudan Black B.

Detergency performance was evaluated by photospectrometrical color measurements and by determination of the removed percentage of soil by weighing (only for the cotton oiled in our lab).Unfortunately, no statements on the difference in detergency performance of the different systems could be made. Detergency tests with the standardized soiled cotton gave too low and similar  $\Delta E$  values for each system investigated. For the cotton textile soiled in our lab, inconsistencies in the results and uncertainties in the evaluation methods allowed no proper statements.

At the end, the shortcomings of evaluating textiles soiled in the lab by photospectrometrical and weighing methods will be discussed and a new general approach to evaluate detergency performance is proposed.

Unlike in all other chapters, the preparation and composition of the detergent solution and the washing procedure will be described first. Afterwards, the results will be presented and discussed.

## **7.3 Experimental**

It must be noted that this part of the thesis was also conducted as part of a collaboration with BASF and some specifications and system parameters were prescribed by BASF due to internal results or experience.

### **7.3.1 Preparation of the detergent solutions**

The preparation of the detergent solutions was quite complex, since many parameters had to be adjusted that were related to each other. The most important

points and difficulties are explained in detail in the following to allow easy reproduction of the samples.

The general procedure of sample preparation could be separated into two steps and was slightly different for samples with AES or NaSXX. For samples with AES, in step 1, a stock solution with a total surfactant concentration of 0.1 wt % (equal mass share of each surfactant) was prepared by dissolving the calculated amount of the surfactant stock solutions in millipore water or hard water of 14 °d at room temperature. Afterwards, in step 2 a certain amount of the respective builder stock solution and NaOH or HCl were added and the sample was heated to 60 °C for 1 h to ensure complete dissolution of all ingredients. For samples with NaSXX, the procedure slightly deviates. Here the first stock solution was prepared only with LABS and AE (0.067 wt% total surfactants!) and the calculated amount of NaSXX was added with the builder and NaOH or HCl. All samples became clear at 60 °C. The detergency tests were carried out the next day after stirring at room temperature over night.

All prepared detergent solution are based on a standard surfactant formulation given by BASF. This initial formulation contains equal amounts (wt%) of anionic linear alkylbenzene sulfonate (LABS), nonionic alcohol ethoxylate (AE) and anionic alkyl ether sulfate (AES). LABS was purchased from SIGMA (technical grade, 81.1 %), AE (Lutensol AO7, C13-15EO7) and AES (Texapon N70, C12EO2SO<sub>4</sub>Na) were provided by BASF. Since LABS and AE are the most common anionic and nonionic surfactants in laundry detergents, it was decided to replace AES by NaS12 or NaS16 or NaS18. The same sodium alkyl sulfate samples were used as for experiments in chapterChapter 4. Consequently, identical detergency tests were always conducted with four different surfactant composition differing only in one surfactant component: 1. LABS/AE/AES; 2. LABS/AE/NaS12; 3. LABS/AE/NaS16; 4. LABS/AE/NaS18. The total surfactant concentration in the final solutions was chosen close to 0.1 wt%, since this is the common surfactant concentration of the washing liquor in a washing machine. For sample preparation, LABS, EA and AES were used as 10 wt% stock solutions, NaSXX surfactants were used in the pure powder form.

To take advantage of the "2 in 1"-builder-concept introduced in Chapter 5 and to check the effect of Ch and ChEO<sub>3</sub> as on-top additives, it was necessary to introduce certain amounts of Ch or ChEO<sub>3</sub> ions into the detergent solution. This was achieved by addition of the respective EDTA builders. The amount of builder was chosen so that the ratio of Ch or ChEO<sub>3</sub> to Na in the final formulation was between 2.5 and 4, since for these ratios the  $T_{Kr}$  reducing effects on NaS16 and NaS18 were nearly constant and close to its maximum value (see chapter 5.3.1.3 and 6.3.2). Identical

samples were prepared with Na builder for comparison reasons. Note that the molar amount of builder used was always the same irrespective of the nature of its counter ion or composition of the surfactant system. This led to the differences in the molar ratio of Ch,  $\text{ChEO}_3$  or Na introduced by the builder to Na introduced by other components for different samples, since the latter, which was caused by LABS, AES, NaSXX and added NaOH, varied for each builder plus surfactant composition. Although a constant molar ratio of Ch,  $\text{ChEO}_3$  or Na introduced by the builder to Na introduced by other components for each sample would have been desired for better comparison reasons, these deviations had to be accepted due to preparation conditions. Adjustment of this ratio (by using the same builder stock solutions) would have changed the final surfactant concentration and water hardness for each sample. Stock solutions of the EDTA builders ( $\text{Ch}_4\text{EDTA} = 1.4 \text{ wt\%}$ ,  $(\text{ChEO}_3)_4\text{EDTA} = 2.5 \text{ wt\%}$  and  $\text{Na}_4\text{EDTA} = 0.75 \text{ wt\%}$ ) were obtained by neutralization of EDTA by the respective hydroxide base in millipore water.  $\text{ChOH}$  was obtained by TAMINCO and  $\text{ChEO}_3\text{OH}$  from the  $\text{ChEO}_3\text{Cl}$  stock solution as described in section 6.5.1. The mass shares of the different builder stock solutions was chosen to obtain nearly identical molar concentrations, since the addition of the builder stock solutions to the surfactant stock solution prepared in step 1 reduced the final amount of surfactant and water hardness by dilution effects.

Further, each surfactant plus builder system was prepared in millipore water and hard water. The water hardness in the final solutions was chosen to be  $3.5^\circ\text{d}$ , since washing tests at BASF are usually carried out with some remaining water hardness. Hard water was prepared by dissolving calcium chloride  $\times 2 \text{ H}_2\text{O}$  and magnesium chloride  $\times 6 \text{ H}_2\text{O}$  in millipore water with a molar ratio of Ca to Mg of 2. The initial water hardness (Ca + Mg) of the water used for the preparation of the samples in step 1 was  $14^\circ\text{d}$ . This value was determined by the added molar amounts of EDTA builder (assuming that one EDTA molecule removes one hard water ion from solution) and the accompanying dilution effect (see above).

At last, the pH value had to be adjusted to about  $10.4 (\pm 0.1)$ . This was necessary, since detergent solutions of Persil Universalpulver in millipore or hard water, which were prepared for comparison reasons, always gave this pH value. For samples prepared with millipore water, the pH had to be slightly decreased by the addition of 1 M HCl. For solutions prepared with hard water, it had to be increased by the addition of 1 M NaOH. The required amount of base or acid was only dependent on the nature of the builder and was identical for the different surfactant systems. Note that the amount of added NaOH considerably changes the ratio of Ch or  $\text{ChEO}_3$  to

Na within these systems, while HCl has no effect on other important parameters than pH value.

The important parameters of each final detergent solution for the experiments with cotton that was soiled with palmitic acid are shown in the following tables. The caption of the **Table 7-1** to **Table 7-8** only contains the surfactant system, since the parameter have the same meaning for each system: °d = water hardness;  $n(\text{countBui})/n(\text{Na})$  = the molar ratio of the counter ions of the builder introduced to the sample to the Na ions originating from other Na ions; LABS [wt%], AE [wt%] and NaSXX [wt%]: mass share of the respective surfactant.

Some further statements on the difference in the depicted parameters for each detergent solution should help to reproduce the different solutions if necessary. (1) Total surfactant concentration lower than 0.1 wt% reflects the dilution effect by the builder stock solutions. Identical values for each sample irrespective of the builder is due to the addition of nearly identical volumes of the different builder stock solutions (2) Heavily differing  $n(\text{countBui})/n(\text{Na})$  ratios reflect the fact that the same molar amount of builder was added to each solution irrespective of the nature of the counter ion. For millipore water systems, the different values for different surfactant compositions are due to different molar masses of the Na containing surfactants. Different values at one surfactant composition for different builders in hard water systems are caused by different amounts of NaOH necessary to adjust the pH value. (3) The difference in  $n(\text{countBui})/n(\text{Na})$  for identical surfactant plus builder systems in hard and millipore water is a measure for the amount of added NaOH, since the addition of HCl to the millipore systems has no influence on this value. (4) Constant  $n(\text{countBui})/n(\text{Na})$  values for identical surfactant compositions in millipore water, which vary only in the builder, as well as constant water hardness of around 3.60 for each sample with hard water also reflect the addition of identical molar amounts of builder to each sample.

Builder	°d	$n(\text{countBui})/n(\text{Na})$	LABS [wt%]	AE [wt%]	NaS12 [wt%]
Ch <sub>4</sub> EDTA	-	3.37	0.0306	0.0306	0.0307
ChEO <sub>3</sub> <sub>4</sub> EDTA	-	3.37	0.0306	0.0306	0.0308
Na <sub>4</sub> EDTA	-	3.37	0.0306	0.0306	0.0307

**Table 7-1:** LABS/AE/NaS12 in millipore water.

Builder	°d	$n(\text{countBui})/n(\text{Na})$	LABS [wt%]	AE [wt%]	NaS12 [wt%]
Ch <sub>4</sub> EDTA	3.60	2.80	0.0306	0.0307	0.0311
ChEO <sub>3</sub> <sub>4</sub> EDTA	3.59	2.47	0.0306	0.0308	0.0308
Na <sub>4</sub> EDTA	3.60	2.90	0.0306	0.0307	0.0307

**Table 7-2:** LABS/AE/NaS12 in hard water.

Builder	°d	n(countBui)/n(Na)	LABS [wt%]	AE [wt%]	NaS16 [wt%]
Ch <sub>4</sub> EDTA	-	3.70	0.0307	0.0306	0.0307
ChEO <sub>3</sub> EDTA	-	3.69	0.0308	0.0306	0.0307
Na <sub>4</sub> EDTA	-	3.67	0.0307	0.0306	0.0311

Table 7-3: LABS/AE/NaS16 in millipore water.

Builder	°d	n(countBui)/n(Na)	LABS [wt%]	AE [wt%]	NaS16 [wt%]
Ch <sub>4</sub> EDTA	3.57	3.05	0.0306	0.0307	0.0307
ChEO <sub>3</sub> EDTA	3.58	2.64	0.0306	0.0308	0.0308
Na <sub>4</sub> EDTA	3.72	3.12	0.0306	0.0308	0.0302

Table 7-4: LABS/AE/NaS16 in hard water.

Builder	°d	n(countBui)/n(Na)	LABS [wt%]	AE [wt%]	NaS18 [wt%]
Ch <sub>4</sub> EDTA	-	3.85	0.0306	0.0306	0.0307
ChEO <sub>3</sub> EDTA	-	3.85	0.0307	0.0306	0.0308
Na <sub>4</sub> EDTA	-	3.84	0.0306	0.0306	0.0307

Table 7-5: LABS/AE/NaS18 in millipore water.

Builder	°d	n(countBui)/n(Na)	LABS [wt%]	AE [wt%]	NaS18 [wt%]
Ch <sub>4</sub> EDTA	3.58	3.15	0.0306	0.0306	0.0307
ChEO <sub>3</sub> EDTA	3.60	2.71	0.0306	0.0306	0.0308
Na <sub>4</sub> EDTA	3.59	3.24	0.0306	0.0306	0.0307

Table 7-6: LABS/AE/NaS18 in hard water.

Builder	°d	n(countBui)/n(Na)	LABS [wt%]	AE [wt%]	AES [wt%]
Ch <sub>4</sub> EDTA	-	3.87	0.0306	0.0306	0.0306
ChEO <sub>3</sub> EDTA	-	3.87	0.0306	0.0307	0.0306
Na <sub>4</sub> EDTA	-	3.87	0.0306	0.0306	0.0306

Table 7-7: LABS/AE/AES in millipore water.

Builder	°d	n(countBui)/n(Na)	LABS [wt%]	AE [wt%]	AES [wt%]
Ch <sub>4</sub> EDTA	3.57	3.15	0.0306	0.0306	0.0309
ChEO <sub>3</sub> EDTA	3.57	2.71	0.0307	0.0307	0.0310
Na <sub>4</sub> EDTA	3.56	3.25	0.0306	0.0306	0.0309

Table 7-8: LABS/AE/AES in hard water.

Detergency solutions of Persil Universalpulver from Henkel were prepared as follows: 1.08 g Persil was added to 250 g millipore or hard water of 14 °d and dissolved under stirring for 30 min. Afterwards, the solution were immediately used for detergency tests. The calculation of the mass share of Persil were based on dosage recommendations for medium water hardness, medium degree of soiling and a water volume of 15 l during the washing process in the washing machine.

## **7.3.2 Detergency tests**

### **7.3.2.1 Setup and procedure**

Detergency tests were carried out with a quite simple setup, which is shown in **Figure 7-2**. The soiled textile was fixed with clip and immersed into the detergent solution. Mechanical energy was provided by a magnetic stirrer. There was no temperature control and all experiment were carried out at ambient temperature (20 - 25 °C).

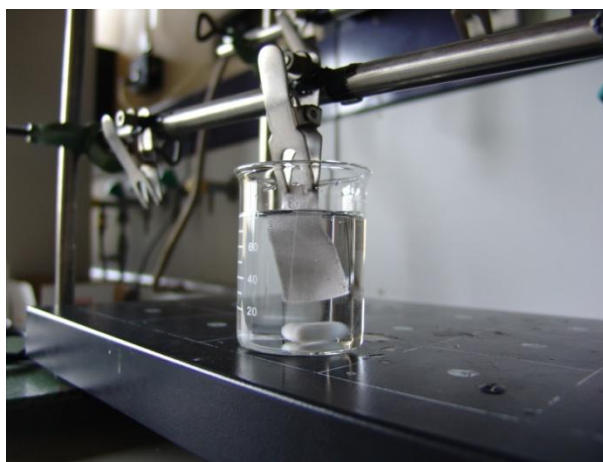


**Figure 7-2:** Photo of the simple setup for the detergency tests.

The exact washing procedure was the following: 80 mL of the washing solution was placed in a 100 mL beaker and the soiled textile (5 x 2 cm), which was fixed by a clip, was immersed into the solution without contacting the magnetic stirrer. The magnetic stirrer was about 2 cm long and the operating speed was 300 rpm. The washing time was 20 min. Then, the detergent solution was replaced by 80 mL millipore water and the same procedure was repeated again for 20 min. Afterwards, the wet textiles were dried over night at ambient conditions.

Identical experiments (detergent solution plus soiled textile) were carried out three times to ensure the reproducibility of the measurements.

### **7.3.2.2 Evaluation by photometric**

The detergency performance of the different solutions was evaluated by measuring the color of the textile stripes with a spectrophotometer (Elrepho SE 071 from Lorentzen and Wettre). The standardized light D65 was used as light source and the software L&W Elrepho Colour Brightness was taken for data recording. The measurements gave a, b and L values for each stripe before and after the washing procedure. The a and b values correspond to the colorfulness, which increases with

increasing absolute values of a and b. The L value is a measure of brightness (see **Figure 7-3**).<sup>16, 17</sup> The color difference  $\Delta E = E_A - E_B$  was obtained by calculating the E value before ( $E_B$ ) and after ( $E_A$ ) washing according to equation 1-7. The larger the  $\Delta E$  value, the larger the color difference and the better the detergency performance of the respective surfactant solution.

$$E = \sqrt{L^2 + a^2 + b^2} \quad (1-7)$$

After soiling and washing, all textile stripes were dried at ambient conditions over night to ensure comparability of the data. To prove equal soiling of the used textiles as well as to allow reasonable statistical treatment of the data, for each textile stripe (5 x 2 cm) L, a and b values of 10 different points were measured before and after the washing process. The standard deviation was of L, a and b was always < 0.5 for the WfK textile and always < 1 for the Swissatest textile soiled in the lab and therefore neglected in further statistics.

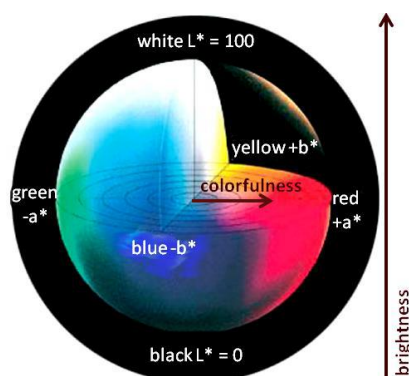


**Figure 7-3:** The L, a and b color system, in which a and b correspond to the colorfulness and L to the brightness. The picture is taken from reference 17.

### 7.3.2.3 Soiled textiles

Detergency tests were carried out with two differently soiled cotton textiles.

The first textile was WfK 10D obtained by WfK Testgewebe GmbH. This cotton textile was already soiled with a mixture of black pigment and sebum and was used as received. Sebum is a fatty mixture secreted by skin and contains triglycerides (25-35 %), diglycerides (6-10 %), free fatty acids (22-27 %), wax and sterol esters (20-22 %), squalene (10-15 %), sterol (2-5 %) and paraffin (0.5-1.5 %). For this textile, detergency tests were only performed in hard water. Before washing, the different textile stripes exhibited E values of  $70 \pm 0.5$ .

The second textile was a non-soiled white cotton textile purchased from Swissatest Tesmaterialien GmbH (article 211). The textile was soiled with palmitic acid colored with 2 % of the black dye Sudan Black B (SigmaAldrich). Sudan Black B is a lysochromic and fat soluble azo dye (see **Figure 7-4**), which is often used in microscopy experiments as staining agent for lipids or triglycerides.<sup>18</sup>

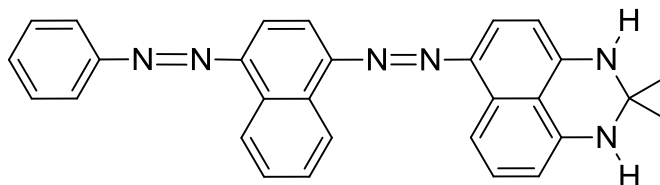


**Figure 7-4:** Molecular structure of Sudan Black B.

The palmitic acid/Sudan Black mixture was liquefied and homogenized at 67 °C, then 15 drops of this solution were added to 10 mL Chloroform under rapid stirring. This solution could be used to equally soil 6 textile stripes (5 x 2 cm) by slow dipping. The soiled stripes were stored at ambient conditions over night to allow complete evaporation of the chloroform before photospectrometrical analysis or weighing. For this textile, the degree of soiling  $X_S$  was calculated for each stripe with equation 2-7:

$$X_S = \frac{m_{AS} - m_{BS}}{m_{AS}} \quad (2-7)$$

where  $m_{AS}/m_{BS}$  is the mass of the stripe after and before soiling with the palmitic acid/Sudan Black B mixture.  $X_S$  was between 3 and 4.7 % for all stripes subjected to detergent tests. The photospectrometrically determined E values for different stripes before washing were nearly independent of  $X_S$  and more less constant ( $64 \pm 1.5$ ). The E value of the unsoiled textile was about 87.

Moreover, the percentage of soil displacement  $P_s$  was calculated for the Swissatest textile stripes according to equation 3-7:

$$P_S = \frac{m_{AS} - m_{AW}}{m_{AS} - m_{BS}} \quad (3-7)$$

where  $m_{AW}$  is the mass of the textile stripe after washing. Of course, the masses were obtained for the dried textile stripes. In general, the higher the value of  $P_s$ , the better the detergency performance is. The values will be presented and discussed in the next section.

## 7.4 Results and discussion

In the following, since all detergent solutions contain equal amounts of LABS and AE, only the third surfactant part and the respective builder will be used to discuss the different samples.

### 7.4.1 Macroscopic appearance of the detergent solutions

In this section, the macroscopic appearance of the detergent solutions before being used for detergency experiments, e.g. after 1 d at room temperature, is shortly presented. Note that the solutions could only have been kinetically stable.

Samples with NaS12 and AES were as clear as water in millipore and hard water irrespective of the builder used.

Samples with NaS16 were as clear as water when millipore water was used and showed some precipitate leading to turbid solutions when hard water was used. Again, the results were irrespective of the builder used.

All samples with NaS18 showed some precipitate and were non-transparent turbid when prepared in hard water. In millipore water, the sample with Na builder was non-transparent turbid with some precipitate, whereas the samples with Ch and  $\text{ChEO}_3$  builder were as clear as water.

It is well-known that the addition of well water-soluble surfactants can improve the solubility, respectively can decrease  $T_{\text{Kr}}$  of other surfactants in the respective mixture. This effect is observed for the NaS16 solutions in millipore water plus Na builder, since  $T_{\text{Kr}}$  of pure NaS16 is far above room temperature (44 °C). For the NaS18 sample plus Na builder in millipore water, this effect is not sufficient to reduce  $T_{\text{Kr}}$  of NaS18 to below room temperature and (NaS18) precipitate is formed. Clear solutions of NaS18 plus Ch or  $\text{ChEO}_3$  builder in millipore water illustrate the  $T_{\text{Kr}}$  reducing effect of additional Ch or  $\text{ChEO}_3$  ions on NaS18 as shown in previous chapters. Of course, this effect is also active in the NaS16 systems, but not observed at room temperature due to the  $T_{\text{Kr}}$  reducing effects of the other surfactants (LABS and AE).

The formation of precipitate in NaS16 and NaS18 solutions prepared in hard water, probably caused by  $\text{Ca}(\text{SXX})_2$  crystals, irrespective of the builder used, illustrates an important fact already underlined in chapterChapter 5: the "2in1"-builder-concept can only operate efficiently, if the builder removes all hard water ions.

Solutions of Persil Universalpulver were slightly turbid with some large solid particles both in millipore and hard water.

## **7.4.2 Detergency tests on cotton at room temperature**

Textile properties, nature of the soil, water quality, detergent composition and washing technique are important factors, to which the detergency performance is very sensitive. The term washing technique comprises the washing time, amount and kind of mechanical input and the wash temperature.<sup>19</sup> Therefore, extreme attention was paid to conduct the experiments as identically as possible for each solution investigated. This includes preparation of the detergent solutions, soiling of the textile as well as the washing and evaluation procedure. Some further general statements on the washing process are given in chapter 2.1.6.

### **7.4.2.1 WfK 10D**

As already mentioned, the WfK 10D product is a standardized cotton textile soiled by a mixture of sebum and black pigment. No information was available on the chemical composition of the artificial sebum used to soil the cotton. Considering the common composition of humans sebum<sup>20</sup>, to a rough estimate the soil can be regarded as a viscous oil plus solid pigments. Possibly, there are even some fatty crystalline parts present. Therefore, mainly liquid soil removal processes should be important, since it is also known that particulate soil is often fixed on the fabric with an oil casing.<sup>20</sup> However, considering the results, this is only of minor importance. In hard water, for all tested solutions the detergency performance was negligible and  $\Delta E$  about 2 were found. This value is too small to perceive some change in color by visual observation. As a general rule, to speak about improvement in detergency, the difference in the  $\Delta E$  value between two samples should be at least 5. Therefore, all tested solutions can be regarded as equally bad.

For AES and NaS12 solutions, the results are shown in **Figure 7-5**, for NaS16 and NaS18 solutions in **Figure 7-6**. The  $\Delta E$  value of Persil Universalpulver is added to each figure for comparison reasons. The standard deviations for the 3 measurements was always below 0.15 and could be neglected.

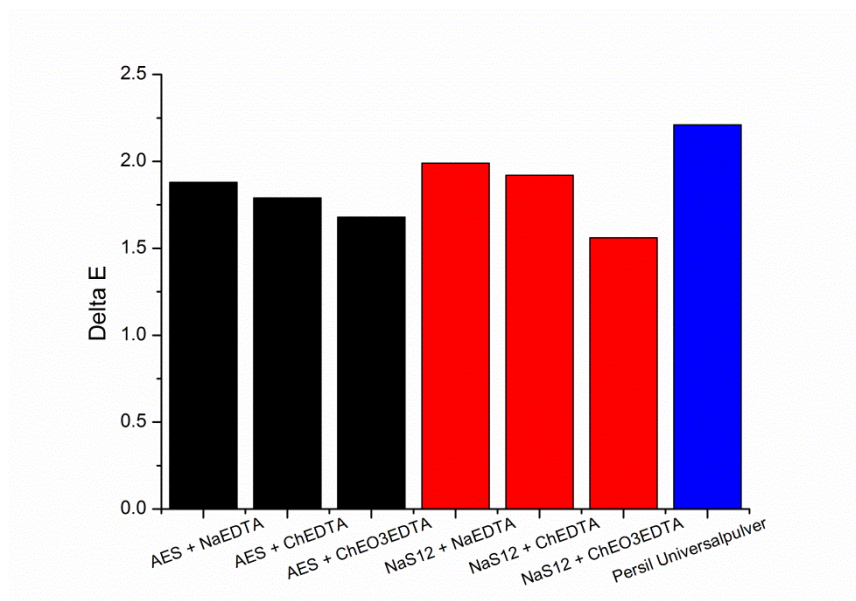


**Figure 7-5:**  $\Delta E$  values of AES(Black) and NaS12(red) plus different builders as well as Persil Universalpulver(blue) in hard water for WfK 10D.

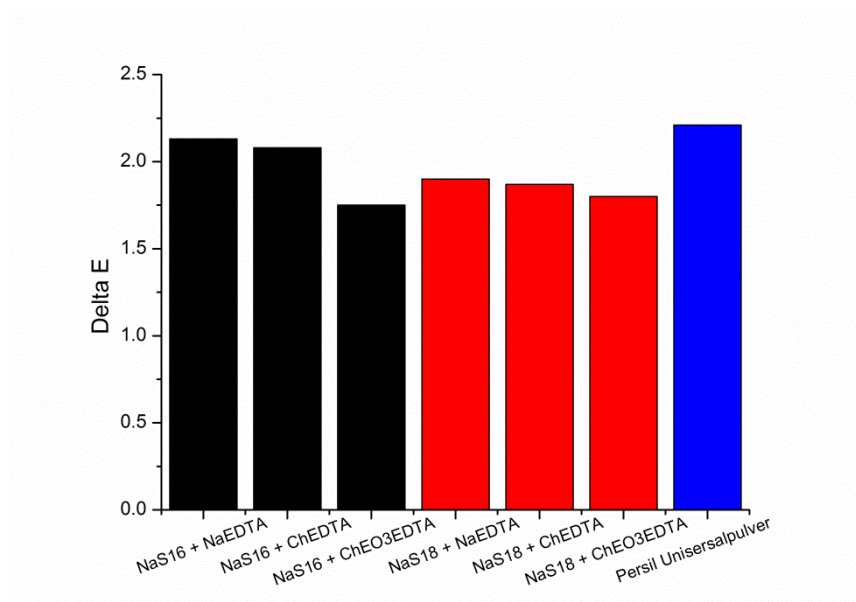


**Figure 7-6:**  $\Delta E$  values of NaS16(Black) and NaS18(red) plus different builders as well as Persil Universalpulver(blue) in hard water for WfK 10D.

The most astonishing finding of these experiments is the fact that even Persil Universalpulver, which is a heavy-duty washing powder that also contains bleaches enzymes and optical brighteners<sup>21</sup>, has nearly no detergency effect.

According to experts from BASF in field of detergency, this can be due to the nature of the soiled textile. Many standardized soiled textiles are designed to sensitively reveal differences in detergency performance at elevated temperatures ( $> 40\text{ }^{\circ}\text{C}$ ), whereas at room temperature nearly no detergency effect can be observed.

#### 7.4.2.2 **Swissatest cotton soiled with palmitic acid/Sudan Black B**

In this case, the soil composition is well-known and is expected to be a crystalline palmitic acid matrix with minor amounts of Sudan Black B. Therefore, mechanisms of solid soil removal should be of major importance. However, the case is not that easy, since fatty acid is no particulate inorganic mineral soil and can also be molecularly dissolved in the washing liquor in its protonated or deprotonated form at sufficiently high pH values. Further, there are also studies that solid organic soils can be liquefied by penetration of surfactants from the cleaning solution and removed by mechanism usually observed for liquid soil.<sup>2</sup>

Palmitic acid was chosen as soil, since it was thought to be a promising candidate to obtain positive effects of added Ch or ChEO<sub>3</sub> compared to Na. The dissolution of palmitic acid in its deprotonated form should be preferred in the detergent solutions containing Ch and ChEO<sub>3</sub> builders due to the increased solubility of ChC16 compared to NaS16. Next to this dissolution-detergency effect, the dissolved soap could act as a surfactant and contribute to the solution's detergency power.

For each solution, the standard deviation of the  $\Delta E$  value presented in the following figures was always < 1 and therefore neglected. The results for pure millipore and hard water (14 °d) as well as Persil Universalpulver in millipore and hard water are shown in Figure 7-7. The  $\Delta E$  value of the Persil solution was around 8 for both millipore and hard water and a change in the color intensity of the stripes could be observed with the naked eye.

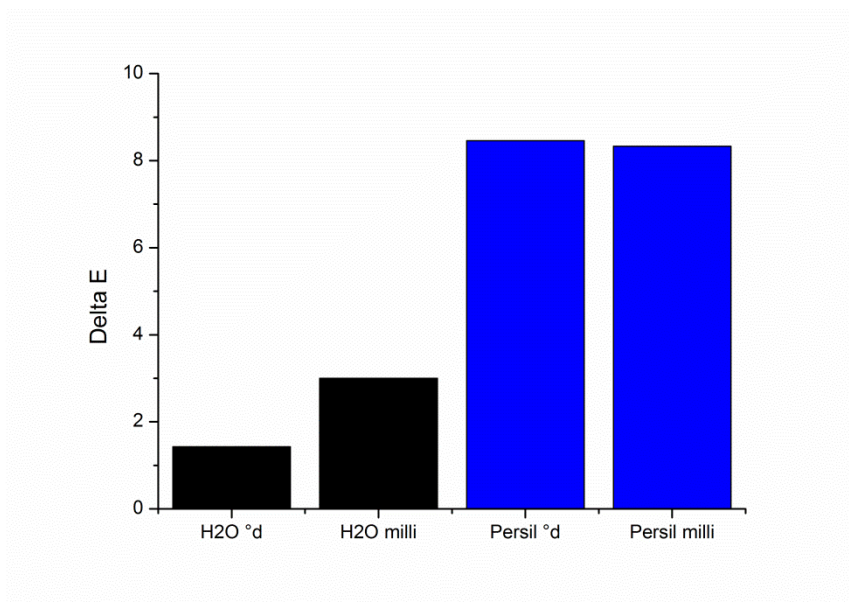


**Figure 7-7:**  $\Delta E$  values of millipore and hard water (14 °d) as well as Persil Universalpulver in millipore and hard water for cotton soiled with palmitic acid/Sudan Black.

The values for EAS (**Figure 7-8**), NaS12 (**Figure 7-9**), NaS16 (**Figure 7-10**) and NaS18 (**Figure 7-11**) are shown below.

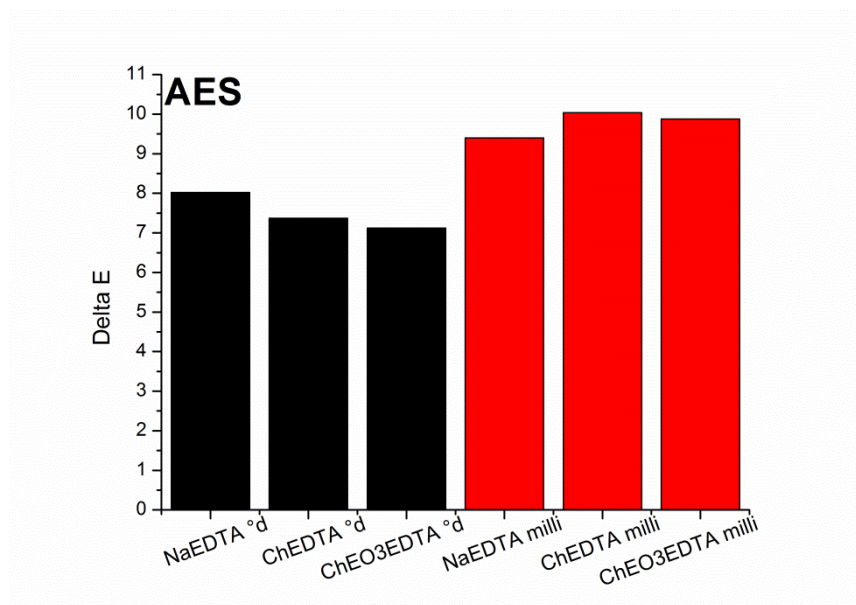


**Figure 7-8:**  $\Delta E$  values of EAS solutions plus different builders in hard water (black) and millipore water (red) for cotton soiled with palmitic acid/Sudan Black.

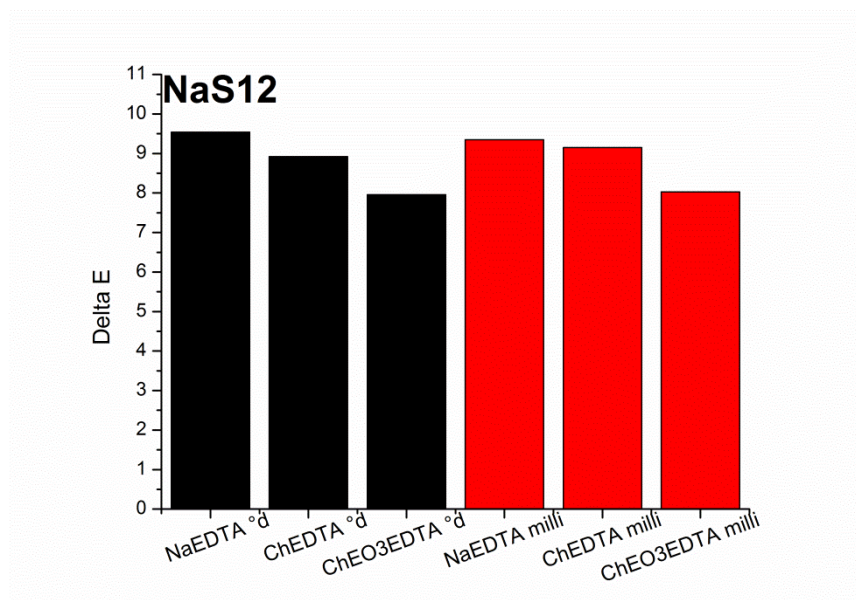


**Figure 7-9:**  $\Delta E$  values of NaS12 solutions plus different builders in hard water (black) and millipore water (red) for cotton soiled with palmitic acid/Sudan Black.

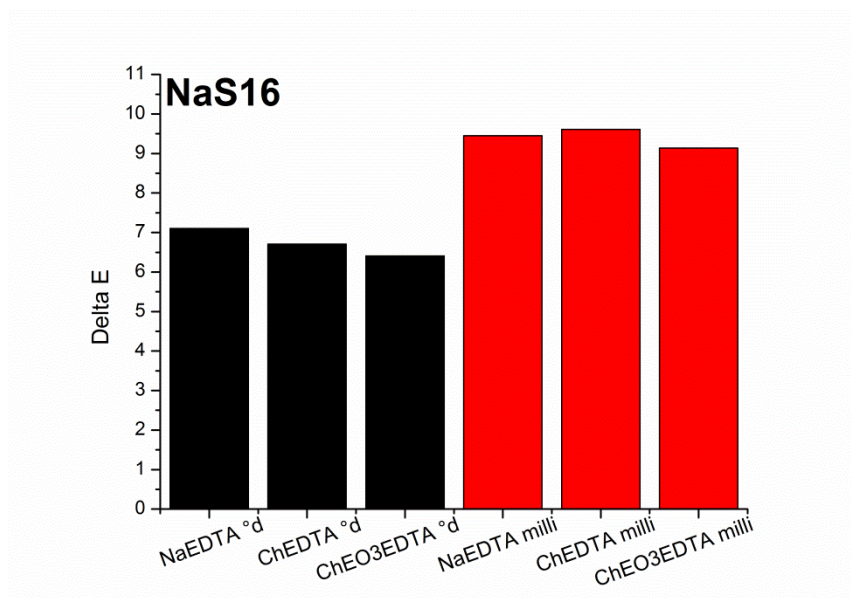


**Figure 7-10:**  $\Delta E$  values of NaS16 solutions plus different builders in hard water (black) and millipore water (red) for cotton soiled with palmitic acid/Sudan Black.

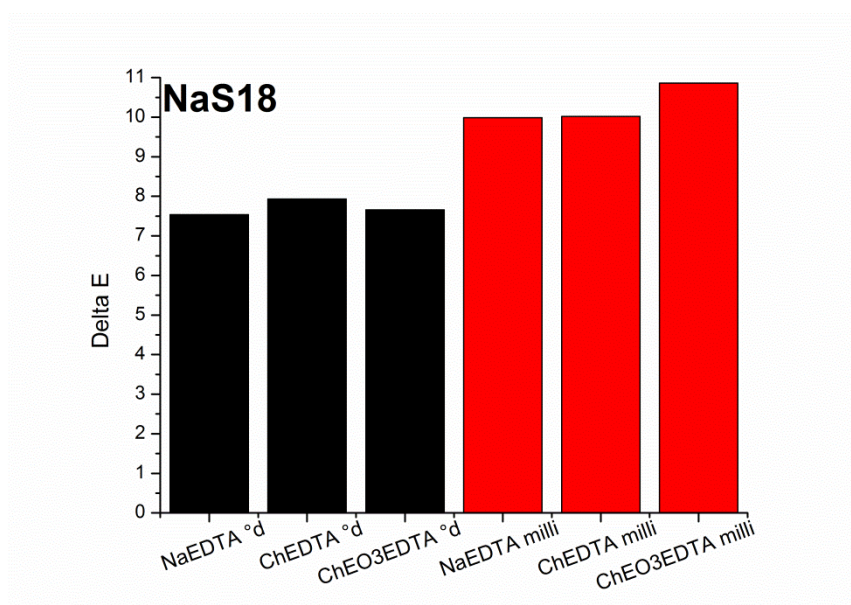


**Figure 7-11:**  $\Delta E$  values of NaS18 solutions plus different builders in hard water (black) and millipore water (red) for cotton soiled with palmitic acid/Sudan Black

The general findings of these washing tests by simply analyzing the measured  $\Delta E$  values are the following: (1) more or less all surfactants exhibit equal detergency performance and show  $\Delta E$  values close to the ones of Persil Universalpulver. Although the results suggest worse detergency for AES, NaS16 and NaS18 in hard water than in millipore, the difference in  $\Delta E$  is still small ( $< 3$ ) and almost within the standard deviation. (2) Identical values for each surfactant system in hard and in millipore water reveal that Ch or ChEO<sub>3</sub> as an on-top additive has no observable effect on detergency.

To allow appropriate evaluation of the detergency performance of different solutions, the measured  $\Delta E$  should be directly proportional to the percentage of soil displacement  $P_s$ . The  $P_s$  values for the different solutions are shown from **Figure 7-12** to **Figure 7-16**. Unfortunately most values for AES plus  $\text{Na}_4\text{EDTA}$ ,  $\text{Ch}_4\text{EDTA}$  and  $(\text{ChEO}_3)_4\text{EDTA}$  as well as NaS12 plus  $\text{Na}_4\text{EDTA}$  and  $\text{Ch}_4\text{EDTA}$  in hard water were lost and no values are shown in the respective figures. However, the few values being still available show small negative  $P_s$  values similar to the ones for the system NaS12 plus  $(\text{ChEO}_3)_4\text{EDTA}$  (see **Figure 7-14**). The very low standard deviations for each sample show the reliability of the data. Further, washing experiments with unsoiled stripes in water showed negligible changes in the weight of the stripes before and after the procedure. Therefore, changes in weight due to the loss of textile material (fluffs) during the experiment are also negligible.

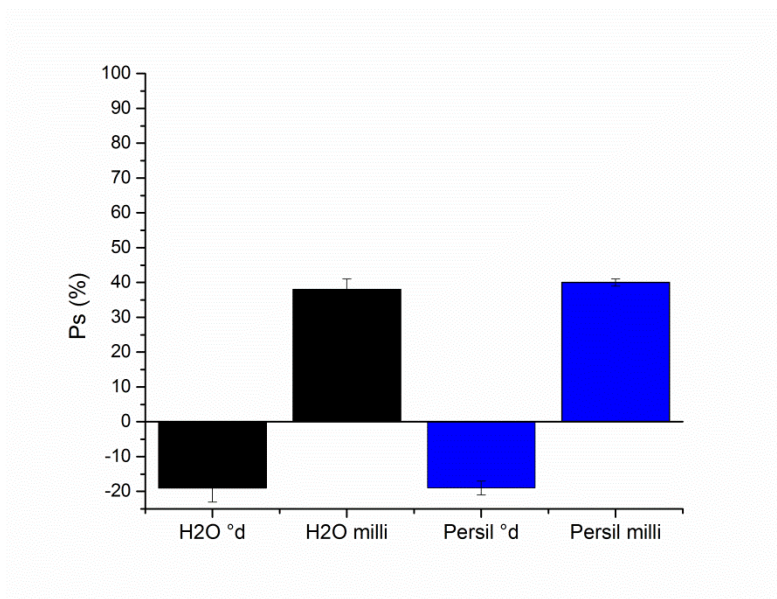


**Figure 7-12:** Percentage of soil displacement  $P_s$  for millipore water and Persil in millipore water for cotton soiled with palmitic acid/Sudan Black.

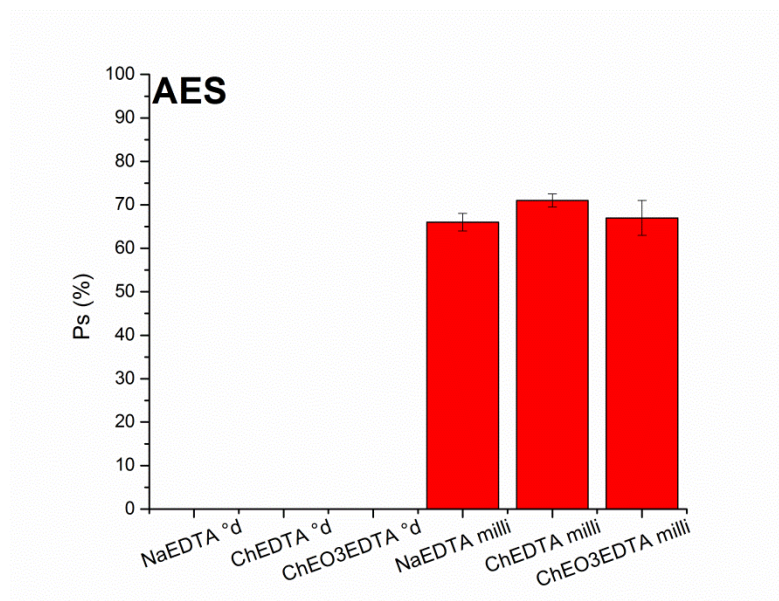


**Figure 7-13:** Percentage of soil displacement  $P_s$  for AES solutions plus different builders in millipore water for cotton soiled with palmitic acid/Sudan Black. Unfortunately, the values for hard water experiments were lost.

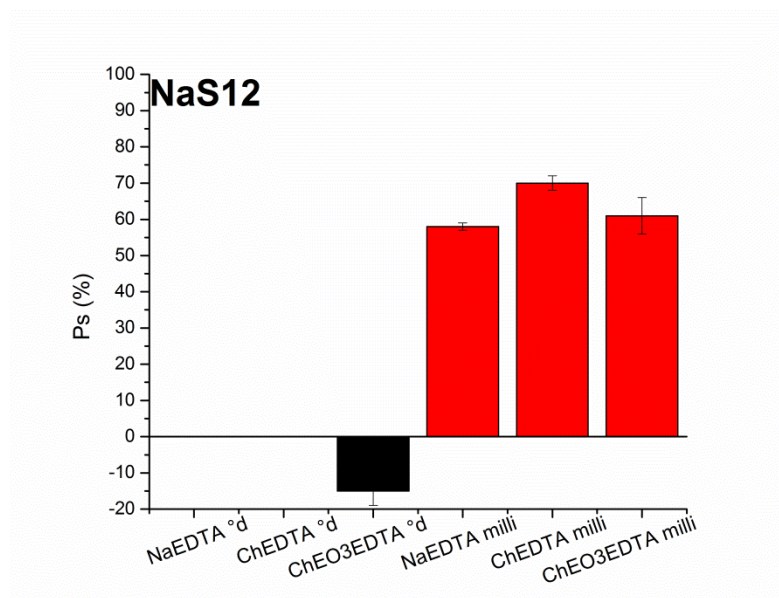


**Figure 7-14:** Percentage of soil displacement  $P_s$  for NaS12 solutions plus different builders in millipore water for cotton soiled with palmitic acid/Sudan Black. Unfortunately, the values for hard water experiments were lost.

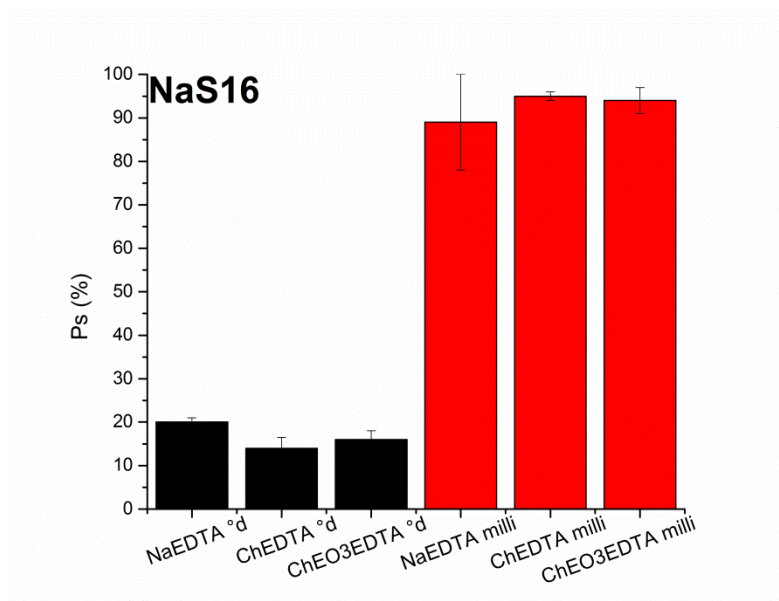


**Figure 7-15:** Percentage of soil displacement  $P_s$  for NaS16 solutions plus different builders in millipore and hard water for cotton soiled with palmitic acid/Sudan Black.

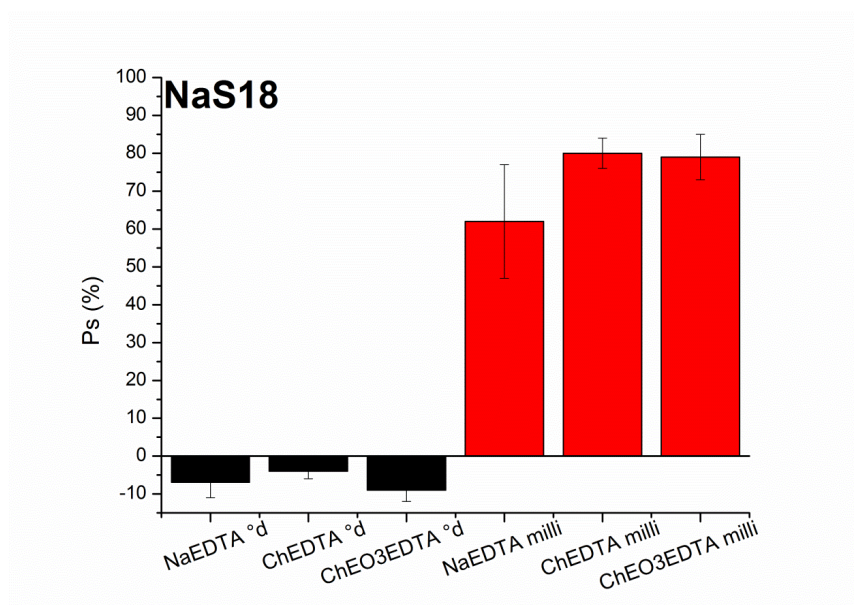


**Figure 7-16:** Percentage of soil displacement  $P_s$  for NaS18 solutions plus different builders in millipore and hard water for cotton soiled with palmitic acid/Sudan Black.

Evaluation of the  $P_s$  data of the different solutions must be divided into solutions prepared in hard and in millipore water. For millipore water systems, the results suggest best detergency for NaS16 systems with values of nearly 100 %. The values for NaS18 ( $\approx 80$  %) or AES and NaS12 (both  $\approx 60$ -70 %) systems are considerably lower. Pure water and Persil show the lowest values with about 40 %. These marked differences in  $P_s$  should also be reproduced in the  $\Delta E$  values. However, this is not the case, since for all solutions (except pure water) nearly identical  $\Delta E$  values (8-10) are found.

For hard water systems, considerably lower values, and sometimes even negative, can be explained by adsorption of material from the detergent solution onto the textile. But again, NaS16 systems show the best values among these solutions with positive  $P_s$  values of about 15 %. Again, these differences are not reflected by the  $\Delta E$  values, which are again more or less identical for all hard water samples.

These discrepancies in determining detergency performance either by measuring the  $\Delta E$  values or calculating the  $P_s$  values led to closer evaluation of these two methods. It was concluded that both methods exhibit considerable weaknesses and are inappropriate to determine detergency performance.

Let us first consider the photospectrometrical evaluation. Here, the main issue is that the  $E$  values and therefore the  $\Delta E$  values are mainly caused by the amount of dye (Sudan Black B) on the textile stripe, and not by the actual soil (palmitic acid). The two major problems are: (1) it is not known, whether the dye is uniformly removed from the textile as the actual palmitic acid soil or shows a stronger binding to the textile. This could lead to the scenario that nearly all palmitic acid is removed from the textile, but a considerable amount of dye is still adhered to the textile surface. In this case,  $\Delta E$  values would not reflect the removal of the actual palmitic acid soil. (2) it is not known, whether  $E$  is linearly dependent on the amount of dye adsorbed or even small amounts of dye cause a strong decrease in  $E$ , which quickly levels off. In this case, also no proper evaluation of detergency performance would be possible, since large differences in soil removal (palmitic acid plus Sudan Black in equal amounts) would hardly cause differences in  $\Delta E$  values. Whether these requirements are fulfilled for commercially available standardized soiled textiles, is an interesting question.

The main problem of the evaluation by weighing is the possible adsorption of different substances from the detergent solutions, which can considerably affect the results. This fact renders this method useless for quantitative valuation of detergency performance. However, for quite similar systems, e.g. clear solutions of AES, NaS12, NaS16 and NaS18 (except solutions plus NaEDTA) in millipore water, the trends should be reliable. The same is true for hard water systems.

To sum up, both methods exhibit too many uncertainties and weaknesses to allow proper evaluation of the detergency performance. Considering the possible problems for the two applied methods, it seems difficult or nearly impossible to solve the problems. For example, it will not be possible to prevent the adsorption of material from the detergent solution onto the textile. This is a central part of the washing

process. Further, even if for a certain soil plus dye system, equal removal from a certain textile is proven (probably by elaborate and time consuming work), this has to be done again for each soil/dye/textile system as soon as one component is changed.

Therefore, new methods of determining the detergency performance should be used. Probably, the best solution, which would give nice quantitative results, would be the following general procedure: (1) Soil the textile without dye. (2) Determine the amount of soil on the substrate. This can easily be done by weighing. (3) Perform the washing tests. (4) Dissolve the remaining amount of soil in an appropriate solvent and determine the remaining amount. (5) Determine the detergency performance by the percentage of removed soil. The crucial point will be a specific determination of the soil component in step 4, since material adsorbed onto the textile from the surfactant solution during the washing process could also be dissolved in the solvent.

It should be a future project to investigate the detergency performance at room temperature of the all solutions prepared in this study according to this new procedure. Above all in millipore water systems, where all solutions were completely clear (except NaS18 + NaEDTA), the effect of longer alkyl chains on the detergency performance in this mixed surfactant system can be well investigated. From an academic point view, it would even be more favorable to start by investigating the individual components, i.e. start by comparing pure Ch, ChEO<sub>3</sub> and Na alkyl sulfates with different chain lengths and adjust, respectively improve the detergent composition step by step based on previous results.

## **7.5 Conclusion**

Unfortunately, the aim of this study could not be fulfilled, since the overall results of the washing tests allow no precise statement.

The standardized cotton soiled with sebum and pigment from WfK Testgewebe GmbH proved to be useless to investigate at room temperature. The photospectrometrically obtained  $\Delta E$  values, even for Persil Universalpulver, were too small and nearly identical for all investigated systems.

Discrepancies between different methods for the evaluation of the washing tests with cotton soiled with palmitic acid plus Sudan Black B made the relevance of the data doubtful. Consequently, these tests gave also no reliable data on the detergency performance of the different investigated systems.

Closer evaluation of the photospectromerical ( $\Delta E$ ) and the weighing ( $P_s$ ) method revealed explicit uncertainties and weaknesses of these methods for determining the detergency performance. Therefore, a new general approach for determining detergency performance, which is meant to overcome the revealed problems, was suggested.

## 7.6 Literature

1. Pakula, C.; Stamminger, R., *Energ Effic* **2010**, 3 (4), 365-382.
2. Rosen, M. J., Detergency and Its Modification by Surfactants. In *Surfactants and Interfacial Phenomena*, John Wiley & Sons, Inc.: 2004; pp 353-378.
3. Smulders, E.; Rähse, W.; von Rybinski, W.; Steber, J.; Sung, E.; Wiebel, F., Detergent Ingredients. In *Laundry Detergents*, Wiley-VCH Verlag GmbH & Co. KGaA: 2003; pp 38-98.
4. Domingo, X., Alcohol and Alcohol Ether Sulfates. In *Anionic Surfactants: Organic Chemistry*, Stache, H., Ed. Marcel Dekker: 1996; pp 223-312.
5. Preston, W. C., *J Phys Colloid Chem* **1948**, 52 (1), 84-97.
6. Smallwood, P., Global Cleaning Trends and their Effect on Surfactant Choice. In *CESIO 10th World Surfactant Congress*, Istanbul, 2015.
7. Karsa, D. R.; Houston, J., What are Surfactants? In *Chemistry and Technology of Surfactants*, Farn, R. J., Ed. Blackwell Publishing Ltd: 2007; pp 1-23.
8. Huber, L.; Nitschke, L., Environmental Aspects of Surfactants. In *Handbook of Applied Surface and Colloid Chemistry (Volume 1)*, Holmberg, K., Ed. Wiley: 2002; pp 509-536.
9. A.I.S.E., Activity and Sustainability Report 2016-17. 2017.
10. Smulders, E.; Rähse, W.; von Rybinski, W.; Steber, J.; Sung, E.; Wiebel, F., Historical Review. In *Laundry Detergents*, Wiley-VCH Verlag GmbH & Co. KGaA: 2003; pp 1-6.
11. Scheibel, J. J., *J Surfact Deterg* **2004**, 7 (4), 319-328.
12. Smulders, E.; Rähse, W.; von Rybinski, W.; Steber, J.; Sung, E.; Wiebel, F., Washing Machines and Wash Programs (Cycles). In *Laundry Detergents*, Wiley-VCH Verlag GmbH & Co. KGaA: 2003; pp 220-238.
13. Smulders, E.; Rähse, W.; von Rybinski, W.; Steber, J.; Sung, E.; Wiebel, F., Household Laundry Products. In *Laundry Detergents*, Wiley-VCH Verlag GmbH & Co. KGaA: 2003; pp 98-120.
14. Yu, Y.; Zhao, J.; Bayly, A. E., *Chin J Chem Eng* **2008**, 16 (4), 517-527.
15. Laitala, K.; Boks, C.; Klepp, I. G., *Int J Consum Stud* **2011**, 35 (2), 254-264.

16. Pauler, N., *Paper Optics - optical and colour science in the pulp and paper industry*. AB Lorentzen & Wettre: Schweden, 2012.
17. Pauler, N., *Optische Eigenschaften von Papier*. AB Lorentzen & Wettre: Schweden, 2012.
18. Sabnis, R. W., *Handbook of biological dyes and stains: synthesis and industrial applications*. John Wiley & Sons: 2010.
19. Smulders, E.; Rähse, W.; von Rybinski, W.; Steber, J.; Sung, E.; Wiebel, F., Physical Chemistry of the Washing Process. In *Laundry Detergents*, Wiley-VCH Verlag GmbH & Co. KGaA: 2003; pp 7-38.
20. Venkatesh, G. M.; Dweltz, N. E.; Madan, G. L.; Alurkar, R. H., *Text Res J* **1974**, *44* (5), 352-362.
21. [http://henkel-businessline.de/persil\\_tp\\_universal\\_pulver.php](http://henkel-businessline.de/persil_tp_universal_pulver.php). (accessed 27.7.2017).

## Chapter 8 Summary

In accordance with the design of the main part of this thesis, this chapter will also be divided into two parts. First, a summary of the results of the work with aqueous solutions of long chain soaps plus Rebaudioside A (Chapter 3) is presented. Afterwards, the results of the work with choline derivatives as counter ions of long chain alkyl sulfates and long chain soaps (Chapter 4 to Chapter 7) are summarized. In addition, at the end of each part, possible further experiments based on the ones presented in this thesis are proposed.

*Part 1 (Chapter 3):* The surfactant-like behavior of Rebaudioside A (RebA), a natural and non-caloric high efficiency sweetener, was confirmed by determining its cmc value by concentration dependent surface tension and DLS measurements. Thus, RebA can be regarded as a true bio-surfactant.

Then, the influence of different amounts of the bio-surfactant RebA on the aqueous phase behavior of long chain soaps was investigated at different pH values, by adding a certain amount of HCl.

For aqueous systems of 1 wt% sodium oleate (NaOl) plus RebA, the formation of mixed aggregates was verified by a downward shift of the acid-base titration curves with increasing amount of RebA and the accompanied decrease in the  $pK_a$  value of NaOl. Visual observation as well as turbidity measurements showed that, for certain initial mass ratios of NaOl to RebA, highly translucent and macroscopically stable solutions can be obtained at even neutral pH value. It turned out that these solutions are stable at room temperature for more than 50 days. For pure NaOl solutions, this is not possible due to turbidity and macroscopic phase separation of respective solutions at pH values  $< 10$ . Phase contrast and freeze etching electron microscopy showed much smaller structures in stable NaOl plus RebA systems at neutral pH values than in comparable NaOl systems without RebA. Although the pictures obtained from microscopy allow no exact determination of the structure of the mixed NaOl/oleic acid(OA)/RebA aggregates at neutral pH values, it was assumed that they exhibit a lamellar structure. The change in macroscopic appearance as well as the formation of smaller structures and a reduced size distribution in the mixed NaOl/RebA system compared to the pure NaOl system was explained by the incorporation of RebA into the NaOl/OA structures and the formation of a hydrogen bond network between the NaOl/OA head groups and the hydroxyl groups of RebA at the surface of the mixed aggregate. This is for the first time that such

concentrations of a long chain soap are really solubilised in water at neutral pH values and at room temperature with the long chain soap being the main component of the system. Further, the system (water, NaOI and RebA) is fully composed of natural and edible substances. These findings open new fields to use aqueous NaOI solutions in food or cosmetic applications, since RebA can overcome the soapy taste of NaOI by its high sweetening capacity and the neutral pH value of the soap solution is meant to diminish irritancy problems in cosmetics often being caused by the high inherent pH values of simple aqueous soap solutions.

These findings for the mixed NaOI/RebA system were also applied to aqueous solutions of choline omega-3-fatty acids (Ch $\omega$ -3-FA), which made it possible to prepare translucent and stable solutions of Ch $\omega$ -3-FA plus RebA at a pH value of 7.5 and at room temperature.

Unfortunately, it turned out that the effect of RebA on the appearance of aqueous long chain soap solutions can only be observed, if the temperature exceeds the chain melting temperature of the fatty acid and acid soap crystals. This was proven by temperature dependent experiments with aqueous sodium dodecanoate (NaC<sub>12</sub>) plus RebA systems. As a consequence, at room temperature, the positive effects of RebA on the pH stability of long chain soaps can only be used for unsaturated long chain soaps.

Some interesting continuative experiments based on the results presented in this thesis in Chapter 3 are:

1. A detailed and time dependent study on the microscopic phase behavior of the mixed NaOI/RebA system in dependence of the pH value, respectively amount of added HCl, using scattering methods and cryo-TEM to undoubtedly elucidate the structure of the mixed NaOI/Oa/RebA aggregates as well as the role of RebA within these complex systems.
2. Identical experiments with other (natural and edible) molecules exhibiting a similar structure like RebA to investigate whether this stabilizing effect can also be obtained with further molecules. An interesting group of molecules could be saponins, for example.
3. Attempts to formulate aqueous food or cosmetic products based on the system long chain soap plus RebA at neutral pH values.

4. Attempts to realize the concept also for long chain saturated soaps exhibiting a chain melting temperature of the fatty acid and acid soap crystals above room temperature by introducing a further compound into the system. This will be a very challenging task and important points, which have to be considered, are mentioned in section 3.4.

*Part 2 (Chapter 4 to Chapter 7):* Choline alkyl sulfates (ChSXX) and beta-methylcholine alkyl sulfates (MeChSXX) with alkyl chains ranging from 12 to 18 C atoms have been synthesized and characterized in various aspects (Chapter 4). The same was done for ethoxylated choline octadecyl sulfate (ChEO<sub>2</sub>S18 and ChEO<sub>3</sub>S18) (Chapter 6). In contrast to their Na homologues, ChSXX and MeChSXX are well soluble in water at room temperature up to a chain length of 16 C atoms, which enables the application of the desirable long chain derivatives at ambient temperature. Krafft temperatures ( $T_{Kr}$ ) of ChS18 and MeChS18 were markedly above room temperature. MeCh proved to be slightly more effective in increasing the solubility of long chain alkyl sulfates compared to Ch, which can be seen by faintly reduced Krafft temperatures ( $T_{Kr}$ ). Lower  $T_{Kr}$  values of Ch and MeCh alkyl sulfates compared to their Na homologues are due to the unsymmetrical and bulky structure of the organic Ch and MeCh ions, which hinders the formation of a regular crystalline packing and thereby decrease  $T_{Kr}$ . For S18, both Ch and MeCh surfactants exhibited a solubility behavior different to the one of NaS18 and incompatible with the usually observed Krafft phenomena for aqueous surfactant solutions. Based on temperature dependent turbidity curves as well as visual observation, this behavior was attributed to concentration dependent formation of liquid crystalline phases in the aqueous ChS18 or MeChS18 solutions. ChEO<sub>m</sub>S18 showed an considerably increased solubility compared to ChS18 or MeChS18 and highly translucent aqueous solutions of 1 wt % surfactant were obtained. This fact was explained by the assumption that the increased bulkiness and flexibility of ChEO<sub>m</sub> compared to Ch or MeCh prevent the formation of liquid crystalline phases. Cmc values for Ch, MeCh and ChEO<sub>m</sub> alkyl sulfates were found to be markedly lower than for their Na homologues and to decrease with increasing size of the organic counter ion (Na > Ch > MeCh > ChEO<sub>2</sub> > ChEO<sub>3</sub>). This beneficial effect of lower cmc values was discussed by mixed micellization between the alkyl sulfate surfactant and the organic counter ion.

Experiments with aqueous NaS16 solutions plus Ch, MeCh or ChEO<sub>m</sub> salts showed the possibility to reduce  $T_{Kr}$  of NaS16 from 44 °C to below room temperature in millipore water by adjusting a certain molecular ratio of choline derivative to Na in the aqueous surfactant solution (Chapter 5 and Chapter 6). For NaS18,  $T_{Kr}$  could only be

decreased below room temperature by adding Ch, if a certain amount of non ionic alcohol ethoxylate surfactant was also present within the mixed system (Chapter 5). Based on the results in millipore water, a "2 in 1"-builder concept was developed, which allows the usage of the  $T_{Kr}$ -reducing effect of additional Ch, MeCh or  $ChEO_m$  ions on NaSXX surfactants also in hard water (Chapter 5). The only prerequisite was the removal of all hard water ions, which could be achieved by combining  $T_{Kr}$ -reducing Ch cations with the strong water softening anion EDTA resulting in the "2 in 1" builder  $Ch_4EDTA$ , which fulfills two functions. On the one hand, the Ch ions reduce  $T_{Kr}$  of the NaSXX surfactant, on the other hand, EDTA softens the water. The possibility to decrease  $T_{Kr}$  of common long chain Na alkyl sulfates below room temperature by simply adding Ch or Ch derivative ions, demonstrates that it is not necessary to specially produce long chain Ch, MeCh or  $ChEO_m$  alkyl sulfates and introduce them into the market, what would be linked to additional costs. This can be a big advantage when considering using the  $T_{Kr}$ -reducing effect of Ch, MeCh or  $ChEO_m$  in a formulation. In the case of hard water, only "2 in 1"-builders have to be produced, which can easily be realized by neutralization of the acid form of the builder with Ch, MeCh or  $ChEO_m$  hydroxide.

Further, aqueous solutions of 0.1 and 1 wt% of choline stearate ( $ChC_{18}$ ) and  $ChEO_m$  ( $m = 2,3$ ) stearate ( $ChEO_mC_{18}$ ) were prepared with different molar excess of the respective hydroxide base (Chapter 6). As it is the case for S18,  $ChEO_m$  were also more effective than Ch in increasing the solubility of C18. It was found that the clearing temperature (temperature, from which on the solution is as clear as water) for aqueous solutions of 1 wt %  $ChEO_mC_{18}$  is around room temperature, while the one for  $ChC_{18}$  is markedly higher (44 °C). For  $ChEO_mC_{18}$  systems, it was even possible to obtain clear solutions at 0 °C by adding a small excess molar amount of  $ChEO_mOH$  (< 20 %). To obtain clear solutions of  $ChC_{18}$  at room temperature, an excess molar amount of  $ChOH$  of around 40 % was necessary. The lowest possible clearing temperature of  $ChC_{18}$  solutions at 100 % molar excess of  $ChOH$  was 16 °C. For NaS18 solutions, it was not possible to obtain clear solutions at room temperature by using molar excess of NaOH. The great difference in the behavior of NaC18 as well as  $ChC_{18}$  and  $ChEO_mC_{18}$  with increasing ratio of hydroxide base to C18 could be explained by partial protonation of the C18 soap in solution as well as the difference in bulkiness and flexibility of the counter ions. For the 0.1 wt% systems, the same general results were obtained. However, the clearing temperature at identical ratios of base to C18 were considerably higher. This concentration dependent solubility behavior is contradictory to Krafft theory and was explained by the complex phase behavior of soaps in dilute aqueous solutions due to

partial protonation. Finally, highly stable foams were prepared from aqueous 0.1 and 1 wt % ChEO<sub>m</sub>C18 solutions being clear and stable at room temperature (Chapter 6). The behavior of these foams during aging (foam density and foam volume) could be controlled by the ratio of organic base to C18.

To sum up, the use of Ch, MeCh and ChEO<sub>m</sub> as counter ions for long chain alkyl sulfates or long chain soaps can considerably increase the solubility of these long chain surfactants compared to their Na homologues. Especially for C18 and S18 surfactants, ChEO<sub>m</sub> are much more efficient than Ch or MeCh and highly translucent aqueous solutions with 1 wt % surfactant can be prepared at room temperature. Similar effects are obtained when adding these ions to aqueous solutions of long chain Na alkyl sulfates. These significant differences in water solubility at low temperatures compared to the respective common Na surfactants open new opportunities of using these long chain surfactants (16 and 18 C atoms) in many low-temperature applications, an area currently being dominated by short chain (C12 and C14) surfactants due to the low solubility of longer chain surfactants with conventional alkali counter ions. Next to expected reductions of the amount of surfactant in certain applications due to an increased surface activity and decreased cmc values of longer chain surfactants, an increased usage of long chain surfactants with 18 C atoms is of particular interest for the European market and should be desired from an economical, agricultural as well as environmental point of view. Such long chain surfactants could be oleochemically prepared from common oils produced from plants harvested in Europe, like rapeseed, olive or sunflower oil, which contain mainly saturated and unsaturated C18 fatty acids.

Attempts to investigate the effect of Ch or ChEO<sub>m</sub> ions as on-top additives as well as the influence on surfactant's hydrophobic chain length on the detergency power of a standard surfactant solution at room temperature failed (Chapter 7). Experiments with a standardized cotton textile soiled with pigment and sebum gave too low  $\Delta E$  values. For detergency tests with a cotton fabric that was soiled in the lab with a mixture of palmitic acid and Sudan Black B, inconsistencies in the results and uncertainties in the evaluation methods allowed no proper statements.

Interesting continuative experiments based on the results presented in this thesis in Chapter 3 to Chapter 7 are:

1. Establishing a phase diagram for ChS18 and/or MeChS18 in water at low surfactant concentrations at room temperature to check the assumptions made in this work based on turbidity curves and visual observations (section 4.3.4). The concentration dependent microscopic phase behavior of the

surfactant should be investigated by scattering methods and electron microscopy. Further, temperature dependent measurements should also be carried out for some concentrations.

2. Establishing a temperature dependent phase diagram of ChC18 or ChEO<sub>m</sub>C18 in water at very low surfactant concentrations. These surfactants seem to be well appropriate to investigate the uncommon concentration dependent solubility behavior of soaps in aqueous solutions at moderate temperatures. The study should include methods to determine the crystal or liquid crystal structure of the observed precipitates below the clearing temperature at each concentration to verify the assumptions made in this work (section 6.3.3.2).
3. Performing comprehensive toxicity and biodegradability tests of the ChEO<sub>m</sub> surfactants.
4. Development of a reliable method for laundry detergency tests similar to the procedure suggested at the end of section 7.4.2.2.

## List of figures

<b>Figure 2-1:</b> Outlook on global surfactant demand taken from reference 17. Abbreviations: LABS: linear alkylbenzene sulfonate, MES: methyl ester sulfonate, AS: fatty alcohol sulfate, FES: fatty alcohol ether sulfate, AE: alcohol ethoxylate, APE: alkylphenol ethoxylate. ....	10
<b>Figure 2-2:</b> The ionic surfactant choline hexadecyl sulfate as an example for the general structure of a surfactant. ....	11
<b>Figure 2-3:</b> Simple scheme of the production of nonionic and anionic surfactants derived from natural oils. The figure is based on reference 10. ....	14
<b>Figure 2-4:</b> left: primary and ultimate biodegradation of linear alkyl sulfate; right: primary degradation step for linear alkylbenzene sulfonate. Based on schemes from reference 30. ....	21
<b>Figure 2-5:</b> left: schematic illustration of the attractive forces acting on a molecule in the bulk and at the surface; right: schematic illustration of the different attractive forces leading to an interfacial tension between two liquids. The figures are based on reference 45. ....	28
<b>Figure 2-6:</b> Schematic illustration of the general course of the surface tension $\gamma$ of an aqueous solution vs. log of the surfactant concentration in the bulk. $C_{20}$ represents the surfactant concentration needed to decrease $\gamma$ by 20 mN/m, CMC is the critical micellar concentration. ....	29
<b>Figure 2-7:</b> Simple model of a spherical micelle of an anionic surfactant. The curved lines represent the surfactant's hydrophobic group, the small spheres the counter ion and the big spheres the anionic head groups. The small hooks illustrate water molecules. The extent of the hydrophobic core, the palisade layer and the outer polar layer are also shown. The lower graph represent the course of the permittivity from the interior core to bulk water. The figure is based on reference 57. ....	33

- Figure 2-8:** Schematic variation of different physico-chemical properties of aqueous surfactant solutions with increasing surfactant concentration. The cmc range is illustrated by the colored area. The figure is based on reference 49. ....34
- Figure 2-9:** Temperature-dependence of the cmc, monomer solubility and total solubility of a surfactant. The intersection of the surfactant monomer solubility curve and the cmc curve is referred to the Krafft temperature ( $T_{Kr}$ ). The figure is based on reference 4. ....37
- Figure 2-10:** Schematic illustration of the two main mechanism of liquid soil removal from flat surfaces. (1): “emulsification” mechanism. (2): “roll-up” mechanism. This figure is based on reference 82. ....41
- Figure 2-11:** Different stages during the “roll-up” mechanism. (1): initial situation before surfactant adsorption. (2): situation during surfactant adsorption,  $\gamma_{sc}$  and  $\gamma_{oc}$  decrease. (3): the oil is droplet is completely lifted off from the surface. ....41
- Figure 2-12:** The two main mechanism for anionic (left) and nonionic surfactants (right) in reducing the adhesion (Van der Waals) forces between a solid particle and a substrate.  $\pi_p$  denotes the splitting pressure of the surfactant layer on the particle and  $\pi_s$  splitting pressure of the surfactant layer on the substrate. ....43
- Figure 2-13:** Typical ordering of anions and cations in the "Hofmeister series". This figure is based on reference 84. ....45
- Figure 2-14:** Left: Division of alkali ions and halide ions into strongly hydrated kosmotropes (above the line) and weakly hydrated chaotropes (below the line). The medium-sized zwitterion in the left illustration represents a water molecule. Ion sizes are drawn true to scale. Right: It is shown that ions have to be similar in size to form inner sphere ion pairs. This figure is based on reference 90. ....47
- Figure 2-15:** Ordering of anionic surfactant head groups and some important cations from hard to soft, according to Collins’ “law of matching water affinities”. The green arrows represent strong ion interactions, the red ones weak interactions. This figure is based on reference 85.....49
- Figure 2-16:** The structure of the biological ion choline, a vital amine. ....51

- Figure 2-17:** Reaction scheme of the industrial synthesis of choline from trimethylamine and ethylene oxide. This scheme is taken from reference 101. .... 51
- Figure 2-18:** Structures of the most important molecules, for which choline acts as a precursor in human metabolism. This figure is based on reference 109..... 53
- Figure 2-19:** The molecular structures of beta-methylcholine (left) and ethoxylated choline (right). .... 54
- Figure 2-20:** Typical curves obtained for acidic titration of alkali soaps above the cmc and the formed aggregates within certain zones. The left curve is for temperatures higher than  $T_m$ , the right one for temperatures lower than  $T_m$ . The diagrams are based on data from references 166, 167, 171, 172..... 67
- Figure 3-1:** Comparison of the chemical structures of rebaudioside A (1) and stevioside (2). .... 85
- Figure 3-2:** Aqueous solutions of RebA after different times of aging at room temperature. Photo A was taken 0.5 h after preparation, B after 1 d, C after 14 d and D after 75 d. The concentration increases from left to right (0.2, 0.4, 0.6, 0.8, 1.0 and 4.0 wt%). .... 87
- Figure 3-3:** Plot of the surface tension  $\sigma$  versus the  $\ln$  of RebA concentration. The cmc for each curve is defined by the intersection of the two linear parts of the curve as it is illustrated. .... 89
- Figure 3-4:** Evolution of the correlation functions from DLS measurements of aqueous RebA solutions at different concentrations. ► = 0.8wt%. ◄ = 0.6 wt%, ◆ = 0.4 wt%, ■ = 0.2 wt%, ▲ = 0.1 wt%. .... 90
- Figure 3-5:** Typical curves obtained for acidic titration of alkali soaps above the cmc and the formed aggregates within certain zones. The left curve is for temperatures higher than  $T_m$ , the right one for temperatures lower than  $T_m$ . The diagrams are based on data from references 1, 19, 20, 55. .... 91
- Figure 3-6:** Titration curves of 1 wt% NaOI solutions with different amounts of RebA at 25 °C. The solutions were titrated with 0.2 M HCl and the pH was measured after

7 d of aging at room temperature. The added amount of RebA in wt% is: ■ = 0, ● = 0.2, ▲ = 0.4, ▼ = 0.6, ◆ = 0.8, ◀ = 1.0, ▶ = 2.0. .... 95

**Figure 3-7:** Plot of the determined  $\text{apK}_A$  values of an aqueous 1 wt% NaOI solution versus the concentration of RebA present in solution. .... 96

**Figure 3-8:** Photos of aqueous 1 wt% NaOI solutions with different amount of RebA after 21 days of aging. All samples have been shaken before taking the photo. The amounts of RebA are in wt%: A = 0.0, B = 0.2, C = 0.4, D = 0.6, E = 0.8, F = 1.0, D = 2.0. The neutralization state  $\Theta_P$  is given on the bottom of the figure and increases from left to right. Samples on a vertical line possess the same  $\Theta_P$  (deviation < 0.01) and can be directly compared. .... 98

**Figure 3-9:** Absorbance of aqueous 1 wt% NaOI solutions at 350 nm with varying amounts of RebA at different neutralization states  $\Theta_P$  after 21 days of aging. The legend and the units also apply to the small inset, which is a magnification at low absorbance. Note that all solutions were shaken before measuring to obtain homogenous solutions if phase separation already took place. The added amount of RebA in wt% is: ■ = 0, ● = 0.2, ▲ = 0.4, ▼ = 0.6, ◆ = 0.8, ◀ = 1.0, ▶ = 2.0. .... 99

**Figure 3-10:** Absorbance of aqueous NaOI/RebA solutions with an initial ratio NaOI to RebA of 1.25 at 350 nm and at different neutralization states  $\Theta_P$  after 21 days of aging. The initial concentrations of NaOI were 2.5 (▼), 1 (▲), 0.5(●) and 0.25 (■) wt%. Note that all solutions were slewed before measuring to obtain homogenous solutions if phase separation took place. .... 102

**Figure 3-11:** Phase-contrast microscopy of aqueous 1 wt% NaOI solutions without (A – D) and with 0.8wt% RebA (E – H) at different values of  $\Theta_P$  and several days after preparation. The scale bar always represents 20  $\mu\text{m}$ . (A)  $\Theta_P = 0.28$ : Uni- and multilamellar vesicular structures, elongated lamellar structures as well as threadlike structures could be seen; (B) and (C)  $\Theta_P = 0.47$ : The same structures as in picture A were present. However, the amount of lamellar structures was much higher. Long threadlike structures covered almost the whole photos. (D)  $\Theta_P = 0.56$ : Shiny oil-like-droplets were present in solution. The other spherical structures were also meant to be oil-like, but they were not focused. E)  $\Theta_P = 0.28$ : big multilamellar vesicular structures being partly aggregated were the main structure; (F)  $\Theta_P = 0.48$ : small “black dots” and small threadlike structures were observed. In the middle one bigger lamellar structure is visible (G) and (H) both  $\Theta_P = 0.57$ : in picture G the same

structures as in picture F can be seen. Picture H shows that also some bigger phase dark multilamellar structures could be found..... 104

**Figure 3-12:** FE-TEM pictures of 1 wt% NaOI solutions without and with 0.8 wt% RebA at identical  $\Theta_P$  values (0.47/0.48). Replica for pictures A, B and C were prepared directly after preparation of the samples. Replica for picture D were prepared 6 weeks after preparation of the sample. (A) pure NaOI solution directly after preparation; (B) and (C): 1 wt% NaOI + 0.8 wt% RebA directly after preparation; the streaks are artefacts from freeze etching; (D): 1 wt% NaOI + 0.8 RebA six weeks after preparation..... 106

**Figure 3-13:** Composition of samples in the mixed NaOI/RebA systems. The mass ratio of OA to oleate is plotted against the mass ratio of RebA to oleate for each system with 1 wt% NaOI and 0-2 wt% RebA. The masses of oleate, OA and RebA within each sample were calculated. Each inclined line represents one NaOI/RebA system with a certain initial ratio of NaOI to RebA. The initial ratio decreases from left to right. The figure is valid for samples after 21 days of aging.  $m(\text{OA})/m(\text{Oleate}) = 0.5$  corresponds to a neutralization state  $\Theta_P$  of 0.33 and  $m(\text{OA})/m(\text{Oleate}) = 2$  to  $\Theta_P$  of 0.67. The marked area shows the compositions of stable solutions, where the dotted part is estimated. The dashed horizontal line marks  $m(\text{OA})/m(\text{Oleate}) = 1$ . ■ denotes unstable samples and ● stable ones..... 111

**Figure 3-14:** Absorbance of aqueous solutions with 1 wt% NaOI and 0.8 wt% RebA at 350 nm at different neutralization states  $\Theta_P$  after different time of aging (■ = 0 d, ● = 1 d, ▲ = 4 d, ◆ = 15 d, ◀ = 30 d, ▶ = 59 d, ▼ = 100 d). The legend and the units also apply to the small inset, which is a magnification at low absorbance. Note that all solutions were slewed before measuring to obtain homogenous solutions if phase separation took place..... 115

**Figure 3-15:** Titration curves of 1 wt% NaC12 solutions without (■) and with 1.16 wt% of RebA (●) at 25 °C. The solutions were titrated with 0.2 M HCl and the pH was measured seven days after preparation..... 117

**Figure 3-16:** Absorbance of aqueous 1 wt% NaC12 solutions at 350 nm without (■ at 25 °C, ● at 45 °C) and with 1.16 wt% RebA (▲ at 25 °C, ▼ at 45 °C) at different neutralization states  $\Theta_P$  after seven days of aging. The measurements were performed at 25 °C and 45 °C. Note that all solutions were slewed before measuring to obtain homogenous solutions if phase separation took place. .... 119

**Figure 3-17:** Photos of aqueous 1 wt% NaC12 solutions without (A) and with (B) 1.16 wt% RebA after stirring for 2h at 45 °C. The neutralization state  $\Theta_P$  is given on the bottom of the figure and increases from left to right. Samples on a vertical line possess the same  $\Theta_P$  (deviation < 0.01) and can be directly compared. .... 119

**Figure 3-18:** Photo of aqueous 2 wt% choline fatty acid carboxylate solutions (1.2 wt% choline  $\omega$ -3-FAs) with different amounts of RebA and a pH value of 7.5 after 3 h hours of aging. Sample 1 contained no RebA, from sample 2 - 7 the concentration of RebA increased. .... 121

**Figure 3-19:** The problems in usage of long chain soaps as basis of aqueous formulations for application in food or cosmetics and possible green ways to overcome them. The red part is the contribution of the work presented in this chapter. .... 123

**Figure 4-1:** The molecular structures of an alkyl sulfate (1), choline (2) and beta-methylcholine (3). .... 137

**Figure 4-2:** Comparison of the Krafft temperatures of sodium(■), choline(●) and beta-methylcholine(▲) alkyl sulfates with a Carbon atom chain length of 12, 16 and 18. The value for NaS12 is taken from reference 1. The dashed horizontal line represents room temperature (25 °C). .... 139

**Figure 4-3:** Comparison of the turbidity curves of NaS18, ChS18 and MeChS18 measured by a home-built apparatus. The transmittance of the samples, measured as the voltage V, is plotted against the temperature. .... 145

**Figure 4-4:** Photos of 1 wt% aqueous solution of NaS18 and ChS18 after stirring for 1d at 25 °C. Photo B was taken between crossed polarizers. Photo C shows the phase separation of a 1 wt% ChS18 solution after several days of aging at room temperature. .... 147

**Figure 4-5:** Appearance of aqueous MeChS18 solutions with different concentrations after stirring for 2 d at 25 °C. MeChS18 concentrations: 1 = 0.02 wt%, 2 = 0.1 wt%, 3 = 0.2 wt%, 4 = 1 wt%. .... 148

**Figure 4-6:** Surface tension versus  $\ln(c)$  plots for choline alkyl sulfates (ChSXX). ▲ = ChS12 at 25 °C, ■ = ChS16 at 25 °C, ● = ChS18 at 25 °C, ○ = ChS18 at 40 °C. .... 266

For ChS12, the two linear parts of the curve necessary to determine the cmc are fitted and the cmc is given by their intersection. .... 154

**Figure 4-7:** Surface tension versus  $\ln(c)$  plots for beta-methylcholine alkyl sulfates (MeChSXX).  $\blacktriangle$  = MeChS12 at 25 °C,  $\blacksquare$  = MeChS16 at 25 °C,  $\bullet$  = MeChS18 at 40 °C. .... 155

**Figure 4-8:** Plotting the specific conductivity  $\kappa$  in S/cm against the surfactant concentration in mmol/l for ChS12 at 25 °C (A), ChS16 ( $\blacktriangle$ ) and MeChS16 ( $\blacksquare$ ) at 25 °C (B) as well as ChS18 ( $\blacktriangle$ ) and MeChS18 ( $\blacksquare$ ) at 50 °C (C). .... 156

**Figure 5-1:** Influence of additional Na ions on  $T_{Kr}$  of aqueous 1 wt% solutions of ChS18. .... 165

**Figure 5-2:** Influence of Ch and MeCh on  $T_{Kr}$  of aqueous NaS16 solutions. The curves were obtained by turbidity measurements (1 wt%) and heating experiments (0.1 wt%).  $\blacksquare$  = 1 wt% NaS16 + ChCl,  $\bullet$  = 0.1 wt% NaS16 +  $\text{Ch}_3\text{Cit}$ ,  $\blacktriangle$  = 1 wt% NaS16 + MeChCl,  $\blacktriangledown$  = 0.1 wt% NaS16 + ChCl. .... 166

**Figure 5-3:** Influence of Ch and MeCh on  $T_{Kr}$  of aqueous NaS18 solutions. The curves were obtained by turbidity measurements (1 wt%) and heating experiments (0.1 wt%).  $\blacksquare$  = 1 wt% NaS18 + ChCl,  $\bullet$  = 0.2 wt% NaS18 +  $\text{Ch}_3\text{Cit}$ ,  $\blacktriangle$  = 1 wt% NaS18 + MeChCl,  $\blacktriangledown$  = 0.1 wt% NaS18 + ChCl. .... 167

**Figure 5-4:** Influence of Ch on  $T_{Kr}$  of aqueous 0.1 wt% NaS16 solutions at different Na to S16 ratios. The curves were obtained by heating experiments. The ratio sodium to S16 is:  $\blacksquare$  = 1,  $\bullet$  = 3,  $\blacktriangle$  = 5,  $\blacktriangledown$  = 10. .... 167

**Figure 5-5:** Photo of the series 0.1 wt% NaS16 plus Ch with additional Na after stirring for 1 d at 25 °C. The ratio of Na to S16 is 10 and the ratio of Ch to Na is: 13 = 0.0, 14 = 0.52, 15 = 1.0, 16 = 1.98, 17 = 3.97, 18 = 5.98. .... 168

**Figure 5-6:** Photo of 0.1 wt% NaS16 plus different amounts of MeCh chloride after stirring for 1 d at 25 °C. The ratio of MeCh to Na is: 21 = 0.0, 22 = 0.62, 23 = 1.02, 24 = 1.93, 25 = 3.76, 26 = 5.91. .... 168

**Figure 5-7:** Comparison of different samples containing 0.05 wt% NaS16 without and with  $\text{Na}_4\text{EDTA}$  or  $\text{Ch}_4\text{EDTA}$  after stirring for 1 d at 25 °C. Sample 20 = 0.05 wt%

NaS16, sample 21 = NaS16 +  $\text{CH}_4\text{EDTA}$  ( $\text{Ch}/\text{NaS16} = 3$ ) and sample 23 = NaS16 +  $\text{Na}_4\text{EDTA}$  ( $\text{Na}/\text{S16} = 4$ ). ..... 169

**Figure 5-8:** Photo of 1 wt% NaS18 (left) and ChS18 (right) plus additional LutAO7. The mass ratio of LutAO7 to surfactant was always around 1.4..... 172

**Figure 5-9:** Comparison of different samples containing 0.05 wt% NaS18,  $\text{Na}_4\text{EDTA}$  or  $\text{CH}_4\text{EDTA}$  and LutAO7 after stirring for 2 days at 25 °C. Grouped samples contain always nearly the same amount of NaS18 and LutAO7, but differ in  $\text{Na}_4\text{EDTA}$  and  $\text{CH}_4\text{EDTA}$ . The more translucent samples always contain  $\text{CH}_4\text{EDTA}$ . The bluish character of the samples decreases with increasing mass ratio of LutAO7 to NaS18, e. g. from 3 to 7. Sample 9 is as clear as water. Samples 3/13: LutAO7/NaS18 = 0.4; Samples 5/15: LutAO7/NaS18 = 0.8; Samples 7/15: LutAO7/NaS18 = 1.2; Samples 9/16: LutAO7/NaS18 = 1.6. .... 173

**Figure 5-10:** The chemical structures of ethylenediaminetetraacetic acid (EDTA) (1), citric acid (2) and methylglycinediacetic acid (MGDA) (3). .... 174

**Figure 5-11:**  $T_{\text{Kr}}$  values of 0.05 wt% NaS16 samples plus  $\text{CH}_4\text{EDTA}$  or  $\text{Na}_4\text{EDTA}$  in hard water plotted against the molecular ratio EDTA to Calcium.  $T_{\text{Kr}}$  values of samples that were still turbid at 75 °C were fixed at 85 °C. ■ = NaS16 +  $\text{CH}_4\text{EDTA}$  at 12.5 °d, ● = NaS16 +  $\text{CH}_4\text{EDTA}$  at 25 °d, ▲ = NaS16 +  $\text{Na}_4\text{EDTA}$  at 12.5 °d, ▼ = NaS16 +  $\text{Na}_4\text{EDTA}$  at 25 °d. .... 176

**Figure 5-12:** Comparison of similar samples differing only in  $\text{CH}_4\text{EDTA}$  and  $\text{Na}_4\text{EDTA}$  at 25 °d after stirring for 2 d at 25 °C. Samples green 13, 15 and 16 contain  $\text{CH}_4\text{EDTA}$ , samples green 27, 28 and 29 contain  $\text{Na}_4\text{EDTA}$ . The ratio of EDTA to Ca was always  $\geq 1$ . The exact values and ratios are listed in Table 5-1 and Table 5-2. .... 177

**Figure 5-13:** Plot of  $T_{\text{Kr}}$  against the ratio of Ch to Na for all samples listed in Table 5-3. Symbols represent the measured values. The continuous line represents the shape of the curve for 0.1 wt% NaS16 in millipore water. ■ =  $\text{Na}/\text{S16} = 3$  at 12.5 °d, ● =  $\text{Na}/\text{S16} = 5$  at 12.5 °d, ▲ =  $\text{Na}/\text{S16} = 3$  at 25 °d, ▼ =  $\text{Na}/\text{S16} = 5$  at 25 °d. .... 179

**Figure 5-14:**  $T_{\text{Kr}}$  values of 0.05 wt% NaS16 samples plus  $\text{CH}_3\text{Cit}$  or  $\text{Na}_3\text{Cit}$  in hard water plotted against the ratio citrate to Ca.  $T_{\text{Kr}}$  values of samples that were still

turbid at 75 °C were fixed at 85 °C. ■ = NaS16 + Ch<sub>3</sub>Cit at 12.5 °d, ● = NaS16 + Ch<sub>3</sub>Cit at 25 °d, ▲ = NaS16 + Na<sub>3</sub>Cit at 12.5 °d, ▼ = NaS16 + Na<sub>3</sub>Cit at 25 °d..... 181

**Figure 5-15:** Appearance of samples with a mass ratio of LutAO7 to NaS18 of 1.5 and Ch<sub>4</sub>EDTA at 12.5 °d after stirring for 2 d at 25 °C. Exact values and ratios are listed in Table 5-6..... 183

**Figure 5-16:** Appearance of samples with a mass ratio of LutAO7 to NaS18 of 1.5 and Ch<sub>4</sub>EDTA at 25 °d after stirring for 2 d at 25 °C. Exact values and ratios are listed in Table 5-6..... 183

**Figure 5-17:** Appearance of samples with a mass ratio of LutAO7 to NaS18 of 1.5 and Na<sub>4</sub>EDTA at 12.5 °d after stirring for 2 d at 25 °C. Exact values and ratios are listed in Table 5-7..... 184

**Figure 6-1:** Molecular structures of sodium alkyl sulfate (1) and ethoxylated sodium alcohol ether sulfate (2) as well as choline (3) and an ethoxylated choline (4). n represents a certain amount of methylene groups, m a certain amount of oxyethylene groups..... 192

**Figure 6-2:** Dependence of  $T_{Kr}$  on the amount of oxyethylene groups inserted between the alkyl chain and the ionic head group for NaS16 (■) and NaS18 (●).  $T_{Kr}$  values are taken from reference 10..... 193

**Figure 6-3:** Comparison of the turbidity curves of aqueous solutions of 1 wt% NaS18, ChS18 and MeChS18 measured by a home-built apparatus. The transmittance of the samples, measured as the voltage V, is plotted against the temperature..... 195

**Figure 6-4:** Photos of 1 wt% aqueous solution ChEO<sub>3</sub>S18, ChS18 and NaS18 after stirring for 2 d at 25 °C. Photo B was taken between crossed polarizers..... 195

**Figure 6-5:** Influence of ChEO<sub>m</sub> ions on  $T_{Kr}$  of aqueous 1 wt% NaS16 solutions. The curves were obtained by turbidity measurements: ■ = NaS16 + ChCl, ● = NaS16 + ChEO<sub>1</sub>Cl, ▲ = NaS16 + ChEO<sub>2</sub>Cl, ▼ = NaS16 + ChEO<sub>3</sub>Cl, ◆ = NaS16 + MeChCl. .... 198

**Figure 6-6:** Influence of  $\text{ChEO}_m$  ions on  $T_{Kr}$  of aqueous 1 wt% NaS18 solutions. The curves were obtained by turbidity measurements: ■ = NaS18 + ChCl, ● = NaS18 +  $\text{ChEO}_1\text{Cl}$ , ▼ = NaS18 +  $\text{ChEO}_3\text{Cl}$ , ◆ = NaS18 + MeChCl..... 199

**Figure 6-7:** Comparison of the turbidity curves of aqueous 1wt% NaS18 solutions plus Ch,  $\text{ChEO}_1$  and  $\text{ChEO}_3$  measured by a home-built apparatus. The molecular ratio of choline derivative to Na was always 4. The transmittance of the samples, measured as the voltage V, is plotted against the temperature.....200

**Figure 6-8:** Photos of aqueous NaS18 solution plus additional Ch or  $\text{ChEO}_3$  ions after stirring for 1 d at 25 °C. The molecular ratio of choline derivative to Na was always 3. Samples 5-8 contain additional Ch, the samples 9-12  $\text{ChEO}_3$  and the concentration of NaS18 increases from the left to the right (0.02(0.05/0.01 and 1 wt%)).....201

**Figure 6-9:**  $T_{Kr}$  value of aqueous 1 wt%  $\text{ChEO}_2\text{C18}$ ,  $\text{ChEO}_3\text{C18}$  and ChC18 solutions in dependence of the molar ratio  $\text{ChEO}_m\text{OH}$  to C18. ■ = Ch, ● =  $\text{ChEO}_2$ , ▲ =  $\text{ChEO}_3$ .....203

**Figure 6-10:**  $T_{Kr}$  value of aqueous 0.1 wt%  $\text{ChEO}_2\text{C18}$ ,  $\text{ChEO}_3\text{C18}$  and ChC18 solutions in dependence of the molar ratio  $\text{ChEO}_m\text{OH}$  to C18. ■ = Ch, ● =  $\text{ChEO}_2$ , ▲ =  $\text{ChEO}_3$ .....205

**Figure 6-11:** Photo of NaC18, ChC18 and  $\text{ChEO}_3\text{C18}$  at 0.1 wt% surfactant concentration and a molar ratio of base to C18 of 2. The samples were stirred for 1 d at 25 °C.....207

**Figure 6-12:** The pH value of an aqueous NaC14 solution plotted against the concentration of the soap. The concentration ranges for different precipitates are depicted by the dashed vertical lines. HZ is the protonated fatty acid,  $(\text{HZ})_n(\text{MZ})_m$  acid-soap complexes and MZ the neutral soap. The figure is taken from reference 35.....208

**Figure 6-13:** (a) The pH value of an aqueous NaC14 solution plus 10 mM NaCl plotted against the concentration of the soap. The concentration ranges for different precipitates are depicted by the dashed vertical lines. HZ is the protonated fatty acid,  $(\text{HZ})_n(\text{MZ})_m$  acid-soap complexes and MZ the neutral soap. (b) Comparison of the

experimental surface tension isotherm with the precipitation zones determined from the pH data. The figure is taken from reference 35. .... 209

**Figure 6-14:** Area of different foam structures occurring in a foam column during formation and drainage of the foam (left). The right illustration shows the structure of a plateau border, where  $p_B$  is smaller than  $p_A$  and leads to a flow of the liquid from the centre of the film towards the plateau border. This figure is based on reference 43..... 213

**Figure 6-15:** Time dependent appearance of aqueous 1 wt% ChEO<sub>3</sub>C18 solutions at different ratios of ChEO<sub>3</sub>OH to C18 after shaking. The red numbers indicate the ratio of organic base to C18. Time of aging: A = 0 min, B = 45 min, C = 1 d, D = 7 d. ... 214

**Figure 6-16:** Time dependent appearance of an aqueous 1 wt% NaC12 solution after shaking. Time of aging: A = 0 min, B = 45 min, C = 4 h, D = 1 d. .... 216

**Figure 6-17:** Time dependence of the surface tension for selected aqueous ChEO<sub>2</sub>C18 and ChEO<sub>3</sub>C18 solutions. Case 1 (■), case 2 (●) and case 3 (▲) are related to the differences in foam stability in dependence of the measured curve and explained below. The time dependent surface tension of an aqueous 1 wt% NaC12 solution is also given (▼)..... 217

**Figure 6-18:** Possible molecular structure and ordering at the surface of the molecules in ChEO<sub>m</sub>C18 solutions at a surface tension around 44 nN/m (left site) and around 25 nN/m (right site). .... 219

**Figure 6-19:** Simple schematic setup of the pendant drop technique. .... 225

**Figure 7-1:** Chemical structures of anionic (left) and nonionic (right) surfactants used in laundry detergent formulations: linear alkyl benzene sulfonates (LABS), alkyl sulfates (AS), alkyl ether sulfates (AES),  $\alpha$ -methyl ester sulfonate (MES), fatty alcohol ethoxylates (AE), alkylamine oxides (AAO), methyl ester ethoxylates (MEE) and alkylpolyglycosides (APG). .... 233

**Figure 7-2:** Photo of the simple setup for the detergency tests. .... 239

**Figure 7-3:** The L, a and b color system, in which a and b correspond to the colorfulness and L to the brightness. The picture is taken from reference 17..... 240  
271

<b>Figure 7-4:</b> Molecular structure of Sudan Black B. ....	241
<b>Figure 7-5:</b> $\Delta E$ values of AES(Black) and NaS12(red) plus different builders as well as Persil Universalpulver(blue) in hard water for WfK 10D. ....	244
<b>Figure 7-6:</b> $\Delta E$ values of NaS16(Black) and NaS18(red) plus different builders as well as Persil Universalpulver(blue) in hard water for WfK 10D. ....	244
<b>Figure 7-7:</b> $\Delta E$ values of millipore and hard water (14 °d) as well as Persil Universalpulver in millipore and hard water for cotton soiled with palmitic acid/Sudan Black. ....	245
<b>Figure 7-8:</b> $\Delta E$ values of EAS solutions plus different builders in hard water (black) and millipore water (red) for cotton soiled with palmitic acid/Sudan Black. ....	246
<b>Figure 7-9:</b> $\Delta E$ values of NaS12 solutions plus different builders in hard water (black) and millipore water (red) for cotton soiled with palmitic acid/Sudan Black. .	246
<b>Figure 7-10:</b> $\Delta E$ values of NaS16 solutions plus different builders in hard water (black) and millipore water (red) for cotton soiled with palmitic acid/Sudan Black. .	247
<b>Figure 7-11:</b> $\Delta E$ values of NaS18 solutions plus different builders in hard water (black) and millipore water (red) for cotton soiled with palmitic acid/Sudan Black ..	247
<b>Figure 7-12:</b> Percentage of soil displacement $P_s$ for millipore water and Persil in millipore water for cotton soiled with palmitic acid/Sudan Black. ....	248
<b>Figure 7-13:</b> Percentage of soil displacement $P_s$ for AES solutions plus different builders in millipore water for cotton soiled with palmitic acid/Sudan Black. Unfortunately, the values for hard water experiments were lost. ....	249
<b>Figure 7-14:</b> Percentage of soil displacement $P_s$ for NaS12 solutions plus different builders in millipore water for cotton soiled with palmitic acid/Sudan Black. Unfortunately, the values for hard water experiments were lost. ....	249
<b>Figure 7-15:</b> Percentage of soil displacement $P_s$ for NaS16 solutions plus different builders in millipore and hard water for cotton soiled with palmitic acid/Sudan Black. ....	250

<b>Figure 7-16:</b> Percentage of soil displacement $P_s$ for NaS18 solutions plus different builders in millipore and hard water for cotton soiled with palmitic acid/Sudan Black.	
.....	250



## List of tables

<b>Table 2-1:</b> Structures of some important ionic, nonionic and zwitterionic head groups. ....	13
<b>Table 3-1:</b> Range of $\Theta_P$ and pH for which different phases are present in an aqueous 1 wt% solution of NaOl. The values are rounded.....	92
<b>Table 3-2:</b> Characteristics of aqueous NaOl/RebA mixtures investigated in this study. $\Delta\Theta_P$ stable/ $\Delta$ pH stable stands for the range of $\Theta_P$ /pH, over which stable and highly translucent solutions were obtained, $\Theta_{oil}$ for the neutralization state, from which an oil phase was present in solution. The values were measured after 21 days of aging.....	108
<b>Table 4-1:</b> Critical micellar concentration and micelle ionization degree $\alpha$ of choline and beta-methylcholine alkyl sulfates at different temperatures in comparison to respective sodium alkyl sulfates. The values were obtained by surface tension <sup>a</sup> and conductivity <sup>b</sup> measurements or taken from literature. ....	140
<b>Table 4-2:</b> Surface excess concentration $\Gamma$ , area per molecule at the surface $A$ , efficiency of surface tension reduction $pC_{20}$ and effectiveness in surface tension reduction $\gamma_{cmc}$ of choline and beta-methylcholine alkyl sulfates at different temperatures in comparison to respective sodium alkyl sulfates. The values were obtained from surface tension measurements or taken from literature. ....	143
<b>Table 4-3:</b> Slope $S_1$ and $S_2$ obtained from fitting of the linear parts in the specific conductivity $\kappa$ versus concentration $c$ plots for choline and beta-methylcholine alkyl sulfates.....	157
<b>Table 5-1:</b> Water hardness and exact molecular ratios of EDTA to Ca and Ch to S16 of all samples that were prepared with 0.05 wt% NaS16 plus Ch <sub>4</sub> EDTA. Samples green 1 to 8 were prepared in water with 12.5 °d, samples green 9 to 16 in water with 25 °d and the molar ratio of EDTA to Ca increases with increasing number for each set. $T_{Kr}$ value of each sample is also listed. ....	175

**Table 5-2:** Water hardness and exact molecular ratios of EDTA to Ca and Na to S16 of all samples that were prepared with 0.05 wt% NaS16 plus Na<sub>4</sub>EDTA. Samples green 20 to 24 were prepared in water with 12.5 °d, samples green 25 to 29 in water with 25 °d and the molar ratio of EDTA to Ca increases with increasing number for each set. T<sub>Kr</sub> value of each sample is also listed. .... 176

**Table 5-3:** Water hardness and exact molecular ratios of EDTA to Ca, Na to S16 and Ch to Na of all samples with 0.05 wt% NaS16 plus additional Na and Ch<sub>4</sub>EDTA. T<sub>Kr</sub> value of each sample is also listed. .... 178

**Table 5-4:** Water hardness and exact molecular ratios of citrate to Ca and Ch to S16 of all samples prepared with Ch<sub>3</sub>Cit. Samples 1 to 5 were prepared in water with 12.5 °d, samples 6 to 10 in water with 25 °d and the molar ratio of citrate to Ca increases with increasing number for each set. T<sub>Kr</sub> value of each sample is also listed. .... 180

**Table 5-5:** Water hardness and exact molecular ratios of citrate to Ca and Na to S16 of all samples prepared with Na<sub>3</sub>Cit. Samples 11 to 15 were prepared in water with 12.5 °d, samples 16 to 20 in water with 25 °d and the molar ratio of citrate to Ca increases with increasing number for each set. T<sub>Kr</sub> value of each sample is also listed. .... 180

**Table 5-6:** Water hardness and exact molecular ratios of EDTA to Ca, Ch to S18 and mass ratio of LutAO7 to NaS18 of all samples with Ch<sub>4</sub>EDTA. Samples green 30 to 34 were prepared in water with 12.5 °d, samples green 35 to 39 in water with 25 °d and the molar ratio of EDTA to Ca increases with increasing number for each set. The total amount of surfactant NaS18 plus LutAO7 was always 0.1 wt%. .... 182

**Table 5-7:** Water hardness and exact molecular ratios of EDTA to Ca, Na to S18 and mass ratio of LutAO7 to NaS18 of all samples with Na<sub>4</sub>EDTA. Samples green 40 to 43 were prepared in water with 12.5 °d, samples green 44 to 47 in water with 25 °d and the molar ratio of EDTA to Ca increases with increasing number for each set. The total amount of surfactant NaS18 plus LutAO7 was always 0.1 wt%. .... 182

**Table 5-8:** Water hardness and exact molecular ratios of citrate to Ca, Ch to S18 and mass ratio of LutAO7 to NaS18 of all samples with Ch<sub>3</sub>Cit. Samples white 21 to 24 were prepared in water with 12.5 °d, samples white 25 to 28 in water with 25 °d and the molar ratio of citrate to Ca increases with increasing number for each set. The total amount of surfactant NaS18 plus LutAO7 was always 0.1 wt%. .... 185

<b>Table 5-9:</b> Water hardness and exact molecular ratios of citrate to Ca, Na to S18 and mass ratio of LutAO7 to NaS18 of all samples with Na <sub>3</sub> Cit. Samples white 31 to 34 were prepared in water with 12.5 °d, samples white 35 to 38 in water with 25 °d and the molar ratio of citrate to Ca increases with increasing number for each set. The total amount of surfactant NaS18 plus LutAO7 was always 0.1 wt%.....	185
<b>Table 6-1:</b> Critical micellar concentration ChEO <sub>2</sub> S18 and ChEO <sub>3</sub> S18 at different temperatures. The values were obtained by surface tension measurements. ....	196
<b>Table 6-2:</b> Surface excess concentration $\Gamma$ , area per molecule at the surface A, efficiency of surface tension reduction $pC_{20}$ and effectiveness in surface tension reduction $\gamma_{cmc}$ of ChEO <sub>2</sub> S18 and ChEO <sub>3</sub> S18 at different temperatures. The values were obtained from surface tension measurements. ....	197
<b>Table 6-3:</b> $T_{Kr}$ value, macroscopic appearance at 25 °C and pH value for aqueous 1wt% ChEO <sub>2</sub> C18 solutions at different molar ratios of ChEO <sub>2</sub> OH to C18.....	203
<b>Table 6-4:</b> $T_{Kr}$ value, macroscopic appearance at 25 °C and pH value for aqueous 1 wt% ChEO <sub>3</sub> C18 solutions at different molar ratios of ChEO <sub>3</sub> OH to C18.....	204
<b>Table 6-5:</b> $T_{Kr}$ value, macroscopic appearance at 25 °C and pH value for aqueous 1 wt% ChC18 solutions at different molar ratios of ChOH to C18. ....	204
<b>Table 6-6:</b> $T_{Kr}$ value, macroscopic appearance at 25 °C and pH value for aqueous 0.1wt% ChEO <sub>2</sub> C18 solutions at different molar ratios of ChEO <sub>2</sub> OH to C18.....	206
<b>Table 6-7:</b> $T_{Kr}$ value, macroscopic appearance at 25 °C and pH value for aqueous 0.1 wt% ChEO <sub>3</sub> C18 solutions at different molar ratios of ChEO <sub>3</sub> OH to C18.....	206
<b>Table 6-8:</b> $T_{Kr}$ value, macroscopic appearance at 25 °C and pH value for aqueous 0.1 wt% ChC18 solutions at different molar ratios of ChOH to C18.....	206
<b>Table 6-9:</b> Concentration of ChEO <sub>m</sub> Cl per gram stock solution, wt % ChEO <sub>m</sub> Cl and total wt % of solid content for aqueous stock solutions of ChEO <sub>m</sub> Cl. ....	223
<b>Table 7-1:</b> LABS/AE/NaS12 in millipore water. ....	237
<b>Table 7-2:</b> LABS/AE/NaS12 in hard water.....	237

<b>Table 7-3:</b> LABS/AE/NaS16 in millipore water.....	238
<b>Table 7-4:</b> LABS/AE/NaS16 in hard water. ....	238
<b>Table 7-5:</b> LABS/AE/NaS18 in millipore water.....	238
<b>Table 7-6:</b> LABS/AE/NaS18 in hard water. ....	238
<b>Table 7-7:</b> LABS/AE/AES in millipore water.....	238
<b>Table 7-8:</b> LABS/AE/AES in hard water. ....	238

## List of publications

Marcus, J.; **Wolfrum, S.**; Touraud, D.; Kunz, W., Influence of high intensity sweeteners and sugar alcohols on a beverage microemulsion, *J Colloid Interface Sci* **2015**, 460, 105-112.

**Wolfrum, S.**; Marcus, J.; Touraud, D.; Kunz, W., A renaissance of soaps? — How to make clear and stable solutions at neutral pH and room temperature, *Adv Colloid Interface Sci* **2016**, 236, 28-42.



## List of poster presentations

- |         |  |
|---------|--|
| 09/2013 | <b>46th biennial meeting of the German Colloid Society</b> , Paderborn (Germany)<br>"Choline alkyl sulfates - New promising green surfactants"               |
| 07/2016 | <b>Formula VIII</b> , Barcelona (Spain)<br>"Clear food solutions of Rebaudioside A and Sodium Oleate at neutral pH"  |
| 05/2017 | <b>International Symposium on Green Chemistry 2017</b> , La Rochelle (France)<br>"Clear solutions of Rebaudioside A and Sodium Oleate at neutral pH"         |
| 09/2017 | <b>31st Conference of the European Colloid and Interface Science</b> , Madrid (Spain)<br>"Clear solutions of Rebaudioside A and Sodium Oleate at neutral pH" |



## **Eidesstattliche Erklärung**

Ich erkläre hiermit an Eides statt, dass ich die vorliegende Arbeit ohne unzulässige Hilfe Dritter und ohne Benutzung anderer als der angegebenen Hilfsmittel angefertigt habe; die aus anderen Quellen direkt oder indirekt übernommenen Daten und Konzepte sind unter Angabe des Literaturzitats gekennzeichnet.

Weitere Personen waren an der inhaltlich-materiellen Herstellung der vorliegenden Arbeit nicht beteiligt. Insbesondere habe ich hierfür nicht die entgeltliche Hilfe eines Promotionsberaters oder anderer Personen in Anspruch genommen. Niemand hat von mir weder unmittelbar noch mittelbar geldwerte Leistungen für Arbeiten erhalten, die im Zusammenhang mit dem Inhalt der vorgelegten Dissertation stehen.

Die Arbeit wurde bisher weder im In- noch im Ausland in gleicher oder ähnlicher Form einer anderen Prüfungsbehörde vorgelegt.

Regensburg, den 30.8.2017

---

Stefan Wolfrum